



Hydrodynamic Shear Sensitivity of Suspension Cultured Plant Cells

by

WONG Vai Tak Victor

Thesis submitted for the degree of
Doctor of Philosophy


in

The University of Adelaide
Department of Chemical Engineering
Faculty of Engineering

July 2001

This work contains no material which has been accepted for the award of any other degree or diploma in any university or other tertiary institution and, to the best of my knowledge and belief, contains no material previously published or written by another person, except where due reference has been made in the text.

I give consent to this copy of my thesis, when deposited in the University Library, being available for loan and photocopying.

SIGNED : 

DATE : 18/7/2001

ACKNOWLEDGMENTS

I would like to acknowledge the invaluable contributions of several individuals and organisations towards this work. Firstly, I would like to thank my supervisors Dr David Williams, Dr Christopher Colby and Dr David Saint for their guidance and encouragement throughout the project, and for taking the time to edit this thesis and suggest useful changes. I would also like to thank Prof Eric Dunlop for his advice and help in the early periods of the project.

I am grateful to Mr Chris Mansell for his help with setting up the Plant Cell Culture laboratory and for his technical assistance, as well as to Mrs Mary Barrow and Mrs Elaine Minerds for their wonderful secretarial support. I am particularly indebted to the departmental workshop staff, especially Mr Peter Kay, for providing their practical expertise in the construction of the novel Couette viscometer. I would also like to thank Dr Joe Wiskich and Mz Lidia Mischis of the Department of Environmental Biology at The University of Adelaide, for the loan of the DO probes and their invaluable advice regarding the oxygen uptake rate measurements.

Financial support for this work was provided by an Australian Research Council grant. I am grateful for their award of a postgraduate scholarship and for contributing towards the operating expenses incurred.

I would like to thank my fellow postgraduate students within the Department of Chemical Engineering for their camaraderie and discussion. Being an overseas student in a foreign land, the emotional support of friends, both in and outside the university, was essential for getting through difficult periods during the project. Although I cannot name everyone, I would especially like to thank Rev. Father Maurice Shinnick.

Finally, I would like to express my deepest, heartfelt thanks to my parents, for their support and encouragement throughout my life. Their unconditional support during my education has been invaluable and it is to them that I would like to dedicate the spirit of this work.

SUMMARY

There is growing interest in the industrial cultivation of plant cells in bioreactors for the production of valuable bio-products, including drugs, food flavours and dyes. However, some types of plant cells are sensitive to hydrodynamic shear stresses present in commercial bioreactors, which may significantly inhibit cell growth and product expression achievable. Recent studies have shown that various chemical compounds that disrupt cellular ion-signalling pathways may alleviate similar inhibitory effects on whole plants caused by mechanical and osmotic stresses. This thesis investigates whether the same compounds might also alleviate the negative effects of fluid shear stress on suspension cultured plant cells. The ultimate goals behind this work are: (i) to consider whether the addition of these compounds or other measures could be used to improve the productivity and performance of suspension cultured plant cells grown in industrial bioreactors; and (ii) elucidate the biochemical mechanisms that cause a biological response to fluid shear in suspension cultured plant cells.

The effects of four chemical compounds on the biological response of *Daucus carota* (carrot) cells exposed to laminar shear in a Couette viscometer were studied. The four compounds were: ruthenium red, an intracellular Ca^{2+} channel blocker; verapamil, a voltage-operated Ca^{2+} channel blocker; 5-nitro-2,3-phenylpropylaminobenzoic acid (NPPB), a Cl^- channel blocker; and N-(6-aminohexyl)-5-chloro-1-napthalene-sulfonamide (W7), a calmodulin inhibitor. These compounds have previously been shown to alleviate the effects of mechanical and osmotic stresses in whole plants. The carrot cultures were subjected to defined, controlled and reproducible laminar shear stresses in a novel Couette viscometer with O_2 -permeable walls. The Couette viscometer was designed with the aid of mathematical modelling to ensure sufficient oxygenation. The carrot cells were exposed to different levels of shear stress in the viscometer (38-100 N/m^2) and shake flasks in factorial experiments designed to establish the effects of the chemicals on various indicators of biological response. The indicators used were mitochondrial activity, coupled and uncoupled oxygen uptake rate (OUR) and membrane integrity. Additional experiments were conducted in shake flasks over 24 hours to study the effect of long-term exposure of these chemicals on the biological response of the carrot cells in low fluid shear

conditions. Patch-clamp studies were also performed separately to monitor changes in ion channel behaviour in response to cell membrane stretching, since membrane stretching caused by fluid shear forces may significantly affect the activity of ion channels involved in the signalling process.

Results from the factorial experiments found that only W7 and ruthenium red were able to mitigate the negative effects of fluid shear on the carrot cells. W7 reduced the effect of shear on the coupled OUR of the carrot cells by approximately 50%, while ruthenium red almost eliminated the effect of shear on mitochondrial activity. However, shake flask experiments suggest that long-term exposure of the carrot cells to ruthenium red inhibits mitochondrial activity by approximately 50%, counteracting the protective effect observed against fluid shear.

The patch-clamp measurements found multiple channels on the cell membrane. One of the channels was likely a Cl^- channel but no sensitivity to membrane stretching was detected for this channel. The other channels could not be identified due to their infrequent appearance in the patches, which could not always be successfully patch-clamped.

The above results imply that calmodulin and calcium are involved in mediating the biological response of carrot cells to shear. Furthermore, addition of chemicals that suppress calmodulin activity (W7) and/or reduce calcium (ruthenium red) in the cytoplasm of the plant cells could be used to diminish stress effects on OUR (W7) and increase mitochondrial activity (ruthenium red), which could prevent fluid shear from inhibiting the growth rate of the cells in suspension cultures, but only where such chemicals are not toxic to the plant cell itself (ruthenium red). An alternative approach to chemical addition could be to reduce expression of calmodulin and/or activity of calcium channels by genetic engineering. These findings affect our current understanding of the biochemical mechanism by which plant cells perceive and respond to fluid shear forces.

TABLE OF CONTENTS

Chapter 1	Introduction	1
1.1	Background	1
1.2	Purpose of study	4
1.3	Organization of thesis	5
Chapter 2	Literature Review	8
2.1	Shear sensitivity of plant cell cultures	8
2.2	Biological indicators of shear effects	12
2.3	Shear devices	17
2.4	Mechano-sensitivity of plants	20
2.5	Ion channels in mechanical signal transduction	22
2.6	Conclusions	25
Chapter 3	Methodology	27
3.1	Shear viscometer based investigations	28
3.2	Patch-clamp investigations	31
Chapter 4	Experimental Apparatus	32
4.1	Shear device configuration	33
4.2	Considerations for Couette viscometer	35
4.3	Range of shear stress	35
4.4	Flow stability	41
4.5	Oxygen transfer	44
4.5.1	Introduction	44
4.5.2	Mathematical model	45
4.5.3	Model solution - Numerical solution strategy	50

4.5.4	Model parameters	52
4.5.5	Simulation results	54
4.5.6	Alternative viscometer design	56
4.6	Temperature control	60
4.7	Sterility	63
4.8	Description of apparatus	64
Chapter 5	Experimental Methods	67
5.1	Cell culture and medium	67
5.2	Chemicals	68
5.3	Viscometer shear tests	68
5.3.1	Sample preparation	68
5.3.2	Shear tests in viscometer	68
5.3.3	Biological assays	70
5.3.3.1	Mitochondrial activity	70
5.3.3.2	Membrane integrity	71
5.3.3.3	Dissolved oxygen measurement and calculation of oxygen uptake rate	71
5.3.3.4	Regrowth ability	72
5.3.3.5	Precautions to limit variability in assay results	73
5.4	Patch-clamping	74
5.4.1	Protoplast isolation for patch-clamping	74
5.4.2	Solutions for patch-clamping	75
5.4.3	Patch formation and clamping	75
5.4.4	Data acquisition and analysis	77

Chapter 6	Factorial Design and Statistical Analysis Methods	78
6.1	Definitions	79
6.2	The half-fraction factorial design, 2^{5-1}	81
6.3	Statistical analysis methods	84
6.3.1	Normal scores plot of effects	84
6.3.2	Analysis of variances and F-tests	85
6.3.3	Analysis of residuals	86
Chapter 7	Preliminary Studies	88
7.1	Comparison of growth in shake flasks at different speeds	89
7.2	Comparison of DO in viscometers	93
7.3	Shear tests in oxygen-permeable viscometer	96
7.3.1	Effect of shear on biological response	96
7.3.2	Kinetics of cell damage	108
7.3.3	Variation of biological activity with energy dissipation in the viscometer	112
7.3.4	Comments on coupled OUR	114
7.3.5	Correlation between mitochondrial activity and uncoupled OUR	117
7.4	Discussion	119
Chapter 8	Results and Discussion	124
8.1	Effects of ion channel blockers and calmodulin inhibitor	125
8.1.1	Effects on coupled OUR	125
8.1.2	Effects on uncoupled OUR	138
8.1.3	Effects on mitochondrial activity	145
8.1.4	Effects on membrane integrity	150
8.1.5	Summary of effects for factorial experiments	153
8.1.6	Effects of long-term exposure	155
8.2	Patch-clamp investigations	157

8.3 Discussion	163
8.3.1 Effects of ion-signalling disruption on biological response to shear	163
8.3.2 Implications for industrial plant cell culturing	167
8.3.3 Possible mechanism for perception and response to fluid shear by plant cells	170
Chapter 9 Conclusions	174
Appendix A Wild Carrot Medium formulation	178
Appendix B Yate's Algorithm	179
Appendix C Statistical analysis of factorial design experimental results	181
Appendix D Publications List	186
Nomenclature	187
References	191

LIST OF FIGURES

Figure	Title	Page
4-1	Relationship between shear stress and shear rate for pre-screened carrot cultures ($< 263 \mu\text{m}$), cell density = 0.05 g/ml (FW).....	36
4-2	Schematic diagram of annular gap section in a Couette viscometer	38
4-3	Variation of mean shear stress with the rotational speed of the outer bowl in Couette viscometers of different gap widths	41
4-4	Variation of critical speed with Couette gap width for different apparent viscosities.	43
4-5	Schematic diagram of oxygen transfer in annular gap of the Couette viscometer.....	46
4-6	Variation in model solution with number of internal collocation points, N at a simulation time of 1800 s	55
4-7	Simulated variation in dissolved oxygen concentration axial profile with time, $N=9$, conventional Couette design	55
4-8	Variation in model solution with number of internal collocation points for the oxygen-permeable Couette viscometer at a simulation time of 1800 s	59
4-9	Simulated variation in dissolved oxygen concentration radial profile with time, $N=9$, oxygen-permeable Couette viscometer	59
4-10	Schematic of heat transfer across viscometer gap.....	61

Figure	Title	Page
4-11	Variation of temperature at surface of inner bob with average shear stress for different gap widths	62
4-12	Photograph of oxygen-permeable Couette viscometer and schematic of inner bob-outer bowl section	65
5-1	Main components of patch-clamp set-up.....	75
6-1	Plot of response data for Table 1 example.....	80
6-2	An example of a normal scores plot of effects.....	85
7-1	Comparison of dry weight accumulation in carrot cultures grown in shake flasks agitated at either 100 or 150 rpm. Speed increased on day 3 as indicated by the arrow. Values shown are the mean of 2 replicates. Error bars indicate standard error.	90
7-2	Comparison of fresh weight accumulation in carrot cultures grown in shake flasks agitated at 100 or 150 rpm. Speed increased on day 3 as indicated by the arrow. Values shown are the mean of 2 replicates. Error bars indicate standard error.....	91
7-3	Comparison of membrane integrity of carrot cultures grown in shake flasks agitated at 100 or 150 rpm. Speed increased in day 3 as indicated by the arrow. Values shown are the mean of 2 replicates.....	92
7-4	Comparison of DO level in viscometer with oxygen-impermeable steel bowl and oxygen-permeable ceramic bowl. Viscometer gap width is approximately 1000 μm and 600 μm for the steel and ceramic bowl respectively	95

Figure	Title	Page
7-5	Absolute values for (A) coupled OUR, (B) uncoupled OUR, (C) mitochondrial activity and (D) membrane integrity of carrot cultures sheared at 57.3 N/m ² (open circles) and controls (closed circles)	97
7-6	Effect of hydrodynamic shear in the oxygen-permeable viscometer on the mitochondrial activity of carrot cultures.....	99
7-7	Effect of hydrodynamic shear in the oxygen-permeable viscometer on the uncoupled OUR of carrot cultures	99
7-8	Effect of hydrodynamic shear in the oxygen-permeable viscometer on the membrane integrity of carrot cultures.....	100
7-9	Effect of hydrodynamic shear in the oxygen-permeable viscometer on the coupled OUR of carrot cultures	100
7-10	Effect of hydrodynamic shear on the biological activity of carrot cultures at a shear stress of 57 N/m ²	102
7-11	Effect of hydrodynamic shear on the biological activity of carrot cultures at a shear stress of 6 N/m ²	102
7-12	Effect of hydrodynamic shear on the biological activity of carrot cultures at a shear stress of 74 N/m ²	103
7-13	Digital images of aggregates in agarose. Images shown are of cells sheared at 57 N/m ² for 8 h. (a) Day 0, immediately after shearing (b) Day 5.....	105
7-14	Size distribution of aggregates immediately (i.e. Day 0) after shearing at 57 N/m ² for 8 h	106
7-15	Comparison of cumulative frequencies of aggregate sizes on Day 0 for Control cells and cells sheared at 57 N/m ² for 8 h.....	106

Figure	Title	Page
7-16	Comparison of cumulative frequencies of aggregate sizes on Day 5 for Control cells and cells sheared at 57 N/m ² for 8 h.....	107
7-17	Comparison of estimated volume increase for Control cells and cells sheared at 57 N/m ² for 8 h	107
7-18	Variation of relative mitochondrial activity of sheared cells with exposure time. Lines are for first-order model fitted to the experimental data	109
7-19	Variation of relative uncoupled OUR of sheared cells with exposure time	109
7-20	Variation of relative membrane integrity of sheared cells with exposure time. Lines are for first-order model fitted to the experimental data.....	110
7-21	Variation of first order decay constant with average laminar shear stress for different biological activities	110
7-22	Variation of mitochondrial activity, coupled and uncoupled OUR and membrane integrity with the cumulative energy dissipated on the carrot cells in the oxygen-permeable Couette viscometer.	113
7-23	Typical profile of coupled OUR of sheared and control cells after sheared cells were removed from the viscometer. See Section 5.3.3 for experimental details.....	115
7-24	Comparison of coupled/uncoupled OUR ratio of control and sheared cultures.....	116

Figure	Title	Page
7-25	Uncoupled OUR versus mitochondrial activity for sheared cultures. Linear regression was forced through origin. $y = 0.172x$, $R^2 = 0.847$	118
8-1	Coupled OUR of sheared cells for factorial runs at 38 N/m ²	127
8-2	Coupled OUR of sheared cells for factorial runs at 100 N/m ² ...	127
8-3	Normal scores plot of main effects and interactions of Coupled OUR response for sheared cultures. The letters 'a, b, c, d, e' refer to the effect of W7, Ruthenium red, Verapamil, NPPB and shear level respectively	130
8-4	Plot of main effects on coupled OUR of sheared cells for (a) W7 and (b) shear.....	132
8-5	'W7 x shear' interaction for coupled OUR of sheared cells.....	132
8-6	Normal scores plot of residuals between actual and predicted coupled OUR response for sheared cells.	135
8-7	Residuals vs predicted value of coupled OUR response for sheared cells.....	136
8-8	Normal scores plot of main effects and interactions of coupled OUR response for Control+ cells.....	136
8-9	Normal scores plot of main effects and interactions of uncoupled OUR response for sheared cells. The letters 'a, b, c, d, e' refers to W7, Ruthenium red, Verapamil, NPPB and shear level respectively	138
8-10	Normal scores plot for residuals of uncoupled OUR response for sheared cells	140

Figure	Title	Page
8-11	Residuals vs predicted value of uncoupled OUR for sheared cells	140
8-12	Residuals vs each of the factors for the uncoupled OUR response of sheared cells. (a) W7, (b) Ruthenium red, (c) Verapamil, (d) NPPB and (e) Shear level	141
8-13	Main effects on uncoupled OUR response of sheared cells for (a) W7 and (b) NPPB	142
8-14	‘W7 x NPPB’ interaction for uncoupled OUR of sheared cells ..	142
8-15	Normal scores plot of main effects and interactions of uncoupled OUR response for Control+ cells	143
8-16	‘W7 x NPPB’ interaction for uncoupled OUR of Control+ cells	144
8-17	Normal scores plot for mitochondrial activity effects. The letters ‘a, b, c, d, e’ refer to the effect of W7, Ruthenium red, Verapamil, NPPB and shear level respectively.....	147
8-18	Main effects on mitochondrial activity of sheared cells for (a) W7 and (b) Ruthenium red	147
8-19	Normal scores plot of main effects and interactions of mitochondrial activity response for Control+ cells. The letter ‘a’ refers to W7.	149
8-20	Main effect of W7 on mitochondrial activity of Control+ cells	149
8-21	Normal scores plot of main effects and interactions of membrane integrity response for sheared cell. Letter ‘e’ refers to the main effect of shear level	150

Figure	Title	Page
8-22	Plot of main effect on membrane integrity of sheared cells for shear level	152
8-23	Normal scores plot of main effects and interactions of membrane integrity response for Control+ cells.	152
8-24	Mitochondrial activity of 14 day carrot cultures after shearing at 100 or 150 rpm for 24 h.	155
8-25	Effect of W7 dosage on growth of carrot cells in shake flasks (100 rpm, 27°C). Filter-sterilised W7 was added on day 2 as indicated by the arrow	156
8-26	(a) to (c) Current-time profiles for carrot protoplasts, cell attached configuration, clamped at 0, -20 and -40 mV respectively. (d) to (f) are the respective current amplitude histograms	158
8-27	(a) Current-time profile for carrot, cell attached configuration, as a voltage ramp from -25mV to 75 mV was applied. (b) Corresponding current-voltage (I/V) curve derived from difference between open and close current traces	158
8-28	(a) Current-time profile for carrot, inside-out configuration, as a voltage ramp from -100 mV to 30 mV was applied. (b) Corresponding current-voltage (I/V) curve derived from difference between open and close current traces	159
8-29	(a) Current-time profile for <i>Nicotiana plumbaginifolia</i> , inside-out configuration, as a voltage ramp from -100 mV to 100 mV was applied. (b) Corresponding current-voltage (I/V) curve derived from difference between open and close current traces	160

Figure	Title	Page
8-30	Multiple channels in a single patch. (a) Current-time profile. (b) Amplitude histogram. Carrot protoplast, cell attached, clamped at 0mV	160
8-31	Effect of increased suction pressure on channel activity of carrot protoplasts in the cell attached configuration. (a) no suction applied. (b) 40 cmH ₂ O suction applied through pipette tip	162
8-32	Schematic of proposed model for reception and transduction of fluid shear stimuli in plant cells. CaM refers to calmodulin. WML refers to wall-to-membrane linkers. TML refers to transmembrane-linkers.....	173
C-1	Normal scores plot for residuals of mitochondrial activity response for sheared cells	183
C-2	Normal scores plot for residuals of membrane integrity response for sheared cells	185

LIST OF TABLES

Table	Title	Page
2-1	Biological indicators used to study shear effects in plant cell suspension cultures	13
2-2	Apparatus used in defined flow field studies of plant cell suspension cultures	18
3-1	Relationship between aims of study and methodology for the channel blocker/shear viscometer investigations	29
4-1	Comparison of capillary and Couette shear devices	33
4-2	Principal model parameters and assumed values for model simulation of a conventional Couette viscometer	53
4-3	Principal model parameters and assumed values for model simulation of alternative Couette viscometer	58
4-4	Dimensions of oxygen-permeable viscometer	66
5-1	Concentration and function of blockers used in factorial experiment.....	70
6-1	System response at various levels of dummy factors A and B ..	79
6-2	A full 2^5 factorial design	82
6-3	The 2^{5-1} factorial design.....	83
6-4	Analysis of variance for example shown in Figure 6-2	86
7-1	Range of values observed for biological indicators in controls during shear tests.....	96

Table	Title	Page
7-2	Correlation coefficients (R^2) for first order model of biological activity of sheared cells.....	111
7-3	R and R^2 values for linear regressions between mitochondrial activity, uncoupled OUR and membrane integrity.....	118
8-1	Biological response (% Control -) of sheared carrot cultures in factorial design experiment.....	126
8-2	Treatment combinations in the selected factorial runs. A tick indicates the inclusion of the chemical in that run. Factorial runs where the coupled OUR response of sheared cells was lower than the response when no blocker treatment was used are marked with an asterisk (*).....	128
8-3	Estimates of effects and sum of squares of the coupled OUR response of sheared cells for the factorial experiment. The letters 'a, b, c, d, e' refer to the effect of W7, Ruthenium red, Verapamil, NPPB and shear level respectively. The combination 'ab' refers to the two-factor interaction between W7 and Ruthenium red.	129
8-4	Analysis of variance for coupled OUR response of sheared cultures. A and E refer to W7 and shear respectively, while AE refers to the 'W7 x shear' interaction	133
8-5	Analysis of variance for coupled OUR response of Control+ cells. AD and ABD refer to the 'W7 x NPPB' two-factor interaction, and the 'W7 x Ruthenium red x NPPB' three-factor interaction respectively.....	137

Table	Title	Page
8-6	Estimates of effects and sum of squares of the uncoupled OUR response of sheared cells for the factorial experiment. The letters 'a, b, c, d, e' refers to the effect of W7, Ruthenium red, Verapamil, NPPB and shear level respectively.....	139
8-7	Estimates of effects and sum of squares of the mitochondrial activity response of sheared cells for the factorial experiment. The letters 'a, b, c, d, e' refer to the effect of W7, Ruthenium red, Verapamil, NPPB and shear level respectively.....	146
8-8	Estimates of effects and sum of squares of the membrane integrity response of sheared cells for the factorial experiment. The letters 'a, b, c, d, e' refer to the effect of W7, Ruthenium red, Verapamil, NPPB and shear level respectively.....	151
8-9	Summary of factorial experiment results. Cells were sheared in the viscometer (38 or 100 N/m ²) or maintained in shake flasks (100 rpm) for 1 h. 'n.e.' denotes no significant effect (5% level of significance)	154
8-10	Nernst potential for various ions.....	159
A-1	Formulation of wild carrot medium.....	178
B-1	Yate's algorithm for the Coupled OUR (% control-) data.....	179
C-1	Analysis of variance for uncoupled OUR response of sheared cultures. A and D refers to W7 and NPPB respectively, while AD refers to the 'W7 X NPPB' interaction	181
C-2	Analysis of variance for uncoupled OUR response of Control+ cultures. A and D refers to W7 and NPPB respectively, while AD refers to the 'W7 X NPPB' interaction	182

Table	Title	Page
C-3	Analysis of variance for mitochondrial activity response of sheared cultures. A and B refers to W7 and ruthenium red respectively	182
C-4	Analysis of variance for mitochondrial activity response of Control+ cultures	184
C-5	Analysis of variance for membrane integrity response of sheared cultures.....	184



CHAPTER 1

INTRODUCTION

1.1 Background

Plants provide the biotechnology industry with an exciting source of valuable bio-products, including pharmaceuticals, food flavours and dyes. It has been estimated that a quarter of all prescription drugs in the US are of plant origin (Curtin, 1983), while oriental cultures have a long tradition of using plant-based medicines. In many of these cases, the complexity of the plant-derived molecules precludes chemical synthesis or expression through recombinant microbial systems. It is therefore necessary to achieve commercial production through native or genetically modified field-grown plants or plant cell cultures grown in industrial bioreactors. From a commercial perspective, there are considerable advantages in growing plant cells as cultures in bioreactors over field-grown plants. For instance, plant cell cultures are not as susceptible to the vagaries of disease, weather and political control, thus ensuring a more steady supply. By avoiding long lag times between planting and harvesting, plant cell cultures enable companies to adapt quickly to meet market demands. For example, consider Taxol, a chemotherapeutic drug obtained from the Pacific Yew Tree (Payne *et al.*, 1991). The bark of a 200-year old tree is only sufficient to provide a single dose of the drug. For this reason, traditional agricultural production cannot be expanded fast enough to meet demands for the drug. However, despite these potential benefits, commercial processes utilising plant cell cultures have been, to date, limited to high-value bio-products exceeding US\$1000/kg because industrial plant cell culture is expensive (Payne *et al.*, 1987). Various economic analyses of industrial processes based on plant cell cultures have highlighted culture productivity as a major bottleneck to widespread commercialisation of this technology (Kieran *et al.*, 1997, and references therein). The low productivity of plant cell culture systems is, in turn, linked to its poor scalability from laboratory to industrial conditions (Kieran *et al.*, 1997).

One of the major obstacles to the scale up of plant cell cultures is the sensitivity of plant cells to the fluid shear stresses generated in industrial bioreactors (Prokop and Bajpai, 1992). This causes many cell lines that perform well under shake flask conditions to falter when cultivated in bioreactors, resulting in either slow cell growth or a loss in productivity.

Early studies have largely assumed that the effect of shear stresses on plant cell cultures during scale up was caused by physical damage to the cell, leading to lysis and cell death (for example, see Wagner and Vogelmann, 1977). However, recent studies (Rosenberg, 1989; Takeda *et al.*, 1994) have shown that fluid shear affects key metabolic functions in cultured plant cells well before physical damage occurs. These “sub-lytic” effects can dramatically reduce the cell growth and product expression achievable in the high shear environments present in commercial bioreactors (Dunlop *et al.*, 1994; Kieran *et al.*, 2000).

Previous attempts to circumvent the problem of shear sensitivity have focused on reducing the level of shear stress in the bioreactor, for example, by decreasing the impeller speed and aeration rate or using different impeller designs (Hooker *et al.*, 1990; Leckie *et al.*, 1991) or novel reactor configurations (Singh and Curtis, 1994). However, bioreactors require sufficient levels of agitation to maintain plant cell aggregates in suspension and provide adequate oxygen transfer from the gas to the liquid phase. Therefore, lowering the impeller speed or aeration rate in an effort to avoid shear damage can cause other problems by introducing mass transfer limitations and mixing problems. Novel reactor designs, such as the immobilised cell reactor (Doran, 1993), are also unlikely to be used for large scale processes as there is a lack of experience in the scale up of these designs compared to conventional stirred-tank reactors. In general, all of these approaches have met with limited success and even then, the results have been highly specific to the bioreactor configuration and cell line used. Ideally, if the robustness of cultured plant cells can be improved by alleviating the negative effects of fluid shear stresses on cell growth and product expression, then more industrially favoured bioreactor designs and wider ranges of operating conditions can be used.

Unfortunately, there is currently no known method for alleviating the fluid shear sensitivity of cultured plant cells largely because the biological mechanism responsible for sub-lytic effects is still poorly understood. However, observations from studies on

the sensitivity of whole plants and tissues to mechanical stimulation (which occurs in nature in the form of rain, wind or touch) suggests a promising approach to understanding fluid shear sensitivity in cultured plant cells and the possibility of attenuating sub-lytic effects.

Whole plants and tissues have long been known to exhibit specific responses to mechanical stimulation (Mitchell, 1996). For example, plants subjected to rain, wind or touch stimulation develop shorter but thicker stems to adapt to the environmental assault (Braam and Davis, 1990). Other responses include increased respiration (Uritani and Asahi, 1980) and production of activated oxygen species (Low and Merida, 1996). Individual plant cells have also been shown to be sensitive to mechanical stimuli, exhibiting preferential orientation in cell growth in response to mechanical loading (Lynch and Lintilhac, 1997) as well as many of the same responses observed in plant tissues (Cazalé *et al.*, 1998; Yahraus *et al.*, 1995). It is widely acknowledged that plant cells have evolved sophisticated mechanisms for sensing and transducing mechanical signals into biological responses within the cell. Although the details of the signalling mechanisms are still not clearly understood, ion channels (particularly Ca^{2+} and Cl^- channels) and ion-binding regulatory proteins (e.g. calmodulin) are known to play a crucial role in the signal transduction process (Barbier-Brygoo *et al.*, 2000; Bush, 1995). More importantly, disruption of the signal transduction process by chemical compounds which act specifically on ion channels or ion-binding proteins have been shown to suppress the mechanosensitive response in whole plants. For example, inhibitors of calmodulin have been found to partly attenuate the touch-induced growth inhibition of soybean plants (Jones and Mitchell, 1989). Other examples found in the literature will be discussed in the next chapter. These results suggest that disruption of the ion signalling process may be a possible approach to attenuating sub-lytic shear sensitivity in industrial plant cell culturing. To investigate the efficacy of this approach, it is necessary to first study the effects of these compounds on the biological response of cultured plant cells subjected to controlled levels of fluid shear stress.

1.2 Purpose of study

The purpose of this work is to establish if disruption of the ion signalling process by specific chemical compounds would have a significant effect on the sub-lytic response of cultured plant cells to fluid shear stresses and to elucidate the mechanism behind these effects. Four chemical compounds were studied and the biological responses of *Daucus carota* (carrot) cells exposed to well-defined laminar shear were monitored. Carrot was selected for investigation because it is a commonly used species for plant cell culture studies (for example McCabe *et al.*, 1997; Thuleau *et al.*, 1993). The cell line also exhibits stable growth and properties in suspension culture. The four compounds investigated were ruthenium red, an intracellular Ca^{2+} channel blocker, verapamil, a voltage-operated Ca^{2+} channel blocker, 5-nitro-2,3-phenylpropylaminobenzoic acid (NPPB), a Cl^- channel blocker and N-(6-aminohexyl)-5-chloro-1-naphthalene-sulfonamide (W7), a calmodulin inhibitor. The ability of these compounds to modulate the response of plant cells to a variety of external stimuli, including mechanical stimulation and changes in osmotic pressure, have been demonstrated in previous studies. The ultimate goals behind this work are: (i) to consider if the addition of these compounds or other measures could be used to improve the productivity and performance of plant cell cultures grown in industrial bioreactors and (ii) elucidate the mechanism by which fluid shear forces are perceived and transduced within the cell by identifying potential key ion channels involved in the process. Knowledge of the signalling mechanism could be exploited to select or genetically engineer robust cell lines.

Since fluid shear forces may cause stretching of the cell membrane, they can significantly affect the activity of ion channels located in the cell membrane. Certain ion channels in plant cells have been shown to be activated by membrane stretch and have been proposed to mediate the signalling processes for mechanical stimuli (Falke *et al.*, 1988). Knowledge of how ion channels in cultured plant cells respond to membrane stretching will help to further our understanding of the signalling mechanism. Therefore, in addition to experimentation using the four chemical compounds, studies were conducted using the patch-clamp technique to investigate the changes in ion channel activity in response to stretching of the cell membrane. The patch-clamp technique involves direct measurements of ion channel currents across the membrane of

an individual cell. It can, therefore, provide important insights into ion channel behaviour that could be used to verify and expand on the results of the blocker treatment experiments.

1.3 Organisation of thesis

Chapter 2 begins by reviewing the findings of previous studies into the shear sensitivity of cultured plant cells, particularly focusing on the sub-lytic response to shear, which has been observed in a number of recent studies but is still poorly understood. In the review, we will also compare the relative merits of various biological response indicators and shear devices with a view to selecting suitable indicators and a shear device to be used in this work. In the remainder of the chapter, the proposition that the effects of fluid shear on the biological response of suspension cultured plant cells could be alleviated through disruption of the ion-signalling pathway will be developed. Firstly, the evidence of mechanosensitivity in whole plants and individual plant cells will be examined and the close parallel between the effects of mechanical stimulation in whole plants and the fluid shear sensitivity of cultured plant cells will be highlighted. Next, the central role of Ca^{2+} and Cl^- channels and Ca^{2+} -binding calmodulin in mechanical signal transduction and osmoregulation will be discussed. In particular, the effects of various channel blockers and inhibitors on the mechanosensitive response will be reviewed.

Based on the issues highlighted in the literature review and the evidence for attenuation of the effects of mechanosensitivity in whole plants by channel blockers and inhibitors, the methodology that was developed to study the sub-lytic shear sensitivity of cultured plant cells will be described in Chapter 3.

Chapter 4 is devoted to the design and construction of the custom-built experimental apparatus used in this work. A novel shear viscometer was constructed in this study to overcome some of the deficiencies present in commercial viscometers. Various factors that were taken into consideration in designing the viscometer will be discussed and analysed with the aid of mathematical models. These factors include the viscometer configuration, the range and stability of the shear field and the provision of sufficient oxygen to the cells during the shear run. As oxygen is an important requirement, particular emphasis was placed on providing sufficient oxygen to the cells.

A finite element method was used to model the oxygen transfer in a typical impermeable Couette viscometer and in the novel oxygen-permeable viscometer. The results of the two models will be compared.

Chapter 5 then describes the experimental methods used in this work, including the various biological assays and the patch-clamp technique as well as the precautions undertaken to limit variability in the assay results.

The experimental plan for studying the effects of the various channel blockers and inhibitor was based on the statistical factorial-design. This experimental design was adopted because it allowed both the main effects of each chemical as well as the interaction between the various factors to be determined. The experimental design technique will be described in Chapter 6, along with the statistical methods used to analyse the results.

Chapter 7 presents the results of preliminary investigations in shake flasks and the novel shear viscometer to characterise and quantify the sub-lytic effects that are observed in the carrot cultures. The relative effects of shear on different biological indicators will be compared and the kinetics of cell damage evaluated. The possible correlation between the various biological response indicators will also be discussed. This part of the work also helps to establish the critical shear stress levels at which different sub-lytic effects occur in the carrot cultures, which in turn enables suitable levels to be selected for the subsequent factorial-design experiments.

The main results of the factorial-design experiments to investigate the effects of the various chemical compounds and the patch clamp studies to monitor ion channel activity are presented in Chapter 8. The results of the factorial experiments will be subjected to statistical analysis to test their statistical significance. The significant effects on each biological indicator will then be compared and the implications of these results on our understanding of how fluid shear forces are perceived by plant cells, as well as their potential applications to improve the performance of industrial plant culturing, will be discussed. Based on the results of this work and of other published studies, a possible mechanism by which plant cells perceive and respond to fluid shear forces will also be proposed.

Finally, the main findings of this work will be summarised in the concluding chapter and recommendations for further research proposed.

CHAPTER 2

LITERATURE REVIEW

2.1 *Shear sensitivity of plant cell cultures*

There is much interest in utilising plant cell cultures for the production of valuable plant-derived compounds. This can be seen in the large number of reports on attempts to cultivate suspension cultured plant cells in laboratory or pilot-scale bioreactors. Unfortunately, the success of these attempts has been mixed, with almost all reporting a significant reduction in culture performance (in terms of cell growth and production of the desired compound) upon scaling-up from shake flasks to bioreactors. A recent example is the production of ginseng saponin, a highly valued medicinal compound in oriental countries, from *Panax notoginseng* cultures in stirred bioreactors (Zhong *et al.*, 2000). The maximum cell density attained in the stirred tank reactors with either a turbine impeller or a novel centrifugal impeller was only 22.7 and 26.0 g/l (dry weight) respectively, compared to 28.9 g/l in shake flask cultures. At the same time, saponin productivity fell from 34 mg/(l day) in the shake flask to 21 and 29 mg/(l day) in the respective bioreactors.

The dramatic reduction in culture performance upon scale up could be due to a number of factors, such as mass transfer limitation of nutrients or oxygen (Wagner and Vogelmann, 1977) or the influence of the gas composition in the headspace above the culture liquid (Pan *et al.*, 2000). However, it is widely recognised that the sensitivity of plant cells to hydrodynamic shear forces is a major factor contributing to the productivity loss. For example, Wongsamuth and Doran (1997) observed a drop in specific growth rates of *Atropa belladonna* from 0.21 day⁻¹ to 0.13 day⁻¹ when the stirrer speed in the stirred-tank fermenter was increased from 400 to 1000 rpm. Similarly, Chen and Huang (2000) found that the growth rate of *Stizolobium hassjoo* cells cultivated in a 7 l stirred tank bioreactor decreased for impeller speeds above 300 rpm.

The final cell concentration dropped from 21.5 g/l at 300 rpm to about 12 g/l at 500 rpm, with a concomitant reduction in L-dopa content.

However, the shear sensitivity of different cell lines seems to exhibit a considerable amount of variation. For instance, Wagner and Vogelmann (1977) found that even mild mechanical agitation resulted in complete disruption of *Catharanthus roseus* cells by the fifth day of cultivation in a supposedly low-shear airlift reactor. In contrast, Meijer *et al.* (1994) found that *C. roseus* cultures grew equally well in stirred tank bioreactors at impeller speeds of either 252 or 1002 rpm. Allan *et al.* (1988) reported the gradual development of shear tolerance in a *Picrasma quassioides* line after 2 years of cultivation and minor changes in subculture methods. Unfortunately, none of these reports provided satisfactory explanations for the large variation in shear sensitivity observed between various cell lines and even within the same species, although some researchers have linked it to culture age, history and maintenance conditions (Meijer *et al.*, 1994; Scragg *et al.*, 1988). The development of shear tolerance in certain cell lines (Allan *et al.*, 1988) could not be explained and the outcome appeared more fortuitous than planned. Indeed, the suggested link between shear tolerance and culture age appears to be refuted by the same authors who proposed it (Scragg *et al.*, 1988). Clearly, a better understanding of the effects of hydrodynamic shear on plant cell growth and function is needed to develop a more rational approach to overcoming the problem of shear sensitivity in large-scale plant cell culturing.

Early studies on shear sensitivity in plant cells have mainly attributed the loss in cell growth and production to increased lysis or damage to the cell wall and membrane caused by the harsh shearing environment (for example, see Hooker *et al.*, 1990; Markx *et al.*, 1991; Wagner and Vogelmann, 1977). The relatively large size of plant cells, the tendency to aggregate due to incomplete division of the cell wall, the presence of a large vacuole and a brittle cellulosic cell wall have all been cited as possible reasons for plant cells being especially susceptible to disruption by fluid shear forces (Mandels, 1972; Meijer *et al.*, 1993).

However, recent studies have shown that fluid shear can have subtle effects on cell function at a level of shear stress well below that required to cause cell lysis. For example, Dunlop *et al.* (1994) reported that when *Daucus carota* cells were subjected to laminar shear in a Couette viscometer, a hierarchy in response could be observed, with

regrowth ability and mitochondrial activity being affected well before damage to membrane integrity and cell lysis occurred. Similarly, Takeda *et al.* (1994) found that the DNA and ATP content as well as the mitochondrial activity of *Eucalyptus perriniana* cells decreased at a much faster rate compared to membrane integrity damage as the agitation rate of the stirred tank reactor was raised. Other subtle effects of shear on plant cells include shear-induced increases in respiration rate (Keßler *et al.*, 1997b), changes in cell wall composition (Tanaka *et al.*, 1988) and alterations in the proportion of cells in the various phases within the reproductive growth cycle (Yanpaisan *et al.*, 1998). Although these reports help to identify some of the effects of sub-lytic levels of shear on plant cell metabolism and reproductive growth, the underlying mechanism that causes these effects is still unknown. Nonetheless, these reports bring to light the intimate and complex interactions between fluid shear forces and the physiology of suspended plant cells, which have been largely ignored in early studies.

In contrast to plant cell cultures, sub-lytic effects have long been recognised in animal cell cultures and much more is known about their mechanism and effects. For example, animal cells respond to sub-lytic levels of hydrodynamic shear stress by altering cell metabolism and gene expression (Nollert *et al.*, 1991), inducing apoptotic pathways (Al-Rubeai *et al.*, 1995) or expressing specific enzymes (Mufti and Shuler, 1995). The mechanisms underlying these effects have been shown to involve intracellular Ca^{2+} (Aloi and Cherry, 1996), arachidonic acid (Mufti and Shuler, 1996) and Ah receptors (Mufti *et al.*, 1995). Suppression of shear-induced apoptotic pathways has been found to enhance the performance of mammalian cell cultures (Tey *et al.*, 2000). In comparison, sub-lytic effects in microbes do not appear to be a dominant factor. Although the metabolite production and morphology of some yeasts and fungi have been reported to be affected by the agitation speed of the reactor, it has been difficult to conclusively prove, under the reported conditions, that these effects were directly due to shear and not sub-optimal mixing (Merchuk, 1991). The susceptibility of plant and animal cells to sub-lytic levels of shear could stem from the fact that both these cells occur naturally as a part of highly organised tissues or organs, whereas microbes exist as freely suspended single organisms in nature, very similar to *in vitro* cultivation conditions (Kieran *et al.*, 2000).

The current approach towards scale-up of plant cell cultures has been based on previous experience with fermentation of micro-organisms. However, as noted above, there are significant differences between micro-organisms and plant cells in suspension culture. The impact of these biological differences is reflected in the complex and subtle interaction between fluid shear forces and plant cell growth and metabolism. In the design and optimisation of bioreactors for large scale plant cell culturing, biochemical engineers not only need to avoid conditions of cell lysis due to mechanical disruption, it is also critical to account for sub-lytic effects of fluid shear forces (Merchuk, 1991). It has been suggested that sub-lytic effects, not lysis, may ultimately dominate the kinetics of growth and metabolite production in plant cell cultures (Kieran *et al.*, 2000; Namdev and Dunlop, 1995).

It should be noted that the above discussion, as well as the scope of this thesis, focuses mainly on the effects of hydrodynamic shear stress on cell growth. The ultimate goal of most industrial plant cell culture processes is to maximise product yield, since plant cell culture processes are rarely used solely for the production of cell biomass. Cell growth is one of two main factors that determine product yield, the other being the specific productivity of the cells. To maximise product yield, both cell growth and specific productivity have to be optimised. As commonly practised in the microbial fermentation and cell culture industries, bio-pharmaceutical companies utilise extensive strain-selection programs to isolate strains or cell-lines that are able to express high levels of the product of interest (i.e. high specific productivity). This strain-selection stage is usually conducted at a laboratory scale, in shake flasks or Petri dishes. While selection for strains with high product expression is relatively straightforward, it is often much more difficult to select for strains that will grow well under bioreactor conditions without actually scaling up and cultivating each strain in bioreactors. This difficulty is compounded in the case of plant cell cultures by the current lack of understanding of the biochemical mechanisms underlying the shear sensitivity of suspension cultured plant cells. Hence, while current strain-selection programs can be applied to isolate cell lines with high product expression levels, such programs cannot be easily applied to select for cell lines that will grow well in bioreactor conditions. There have been suggestions that environmental stresses (including shear stresses) may enhance specific productivity at the expense of cell growth (private communication). In this case, the negative effects of

shear stress on cell growth would be the limiting factor in maximising final product yield. Taken together, these observations indicate that while it is important to account for the effects of hydrodynamic shear on both cell growth and product expression, understanding the effects of shear stress on cell growth appear to be more critical at present.

2.2 Biological indicators of shear effects

A number of biological indicators have been used to quantify the effects of shear in plant cell cultures. A selection of indicators used is summarised in Table 2-1. A more comprehensive list has been compiled by Kieran and co-workers (Kieran *et al.*, 1997; Kieran *et al.*, 2000).

While measurements of biomass accumulation and metabolite production are important to assess the overall effect of shear on plant cell culture performance, these indicators provide little information about the mechanism for cell damage.

Measurement of regrowth potential has been used to quantify the effect of shear on the viability of the cell, defined as the ability to grow and divide when placed under favourable conditions. The assessment of regrowth potential after shear exposure can be carried out in either shake flasks (Scragg *et al.*, 1988; Takeda *et al.*, 1994) or agar plates (Rosenberg, 1989). Rosenberg (1989) found that the regrowth potential of carrot cells was very sensitive to shear exposure in a Couette viscometer, with reductions in regrowth potential occurring well before any effects on membrane integrity or cell lysis could be observed. In contrast, there have been reports that fluid shear does not affect the regrowth ability of *C. roseus* (Scragg *et al.*, 1988) or *C. tinctorius* (Takeda *et al.*, 1994) cells compared to other damage indicators.

Table 2-1: Biological indicators used to study shear effects in plant cell suspension cultures (adapted from list compiled by Kieran *et al.* (1997) with additional information by present author)

System response	Parameter measured	Reference
Growth	Biomass accumulation	(Meijer <i>et al.</i> , 1994)
	Regrowth potential	(Rosenberg, 1989; Scragg <i>et al.</i> , 1988; Takeda <i>et al.</i> , 1994)
Membrane integrity	Dye staining	(Kieran <i>et al.</i> , 1995; Rosenberg, 1989)
	Dielectric permittivity	(Markx <i>et al.</i> , 1991)
Release of intracellular components	Protein release	(Meijer <i>et al.</i> , 1994)
	Organic carbon release	(Meijer <i>et al.</i> , 1994)
	Phenolics release	(Hooker <i>et al.</i> , 1989)
	Esterase release	(Steward <i>et al.</i> , 1999)
Changes in morphology / aggregation patterns	Aggregate size / shape	(Kieran <i>et al.</i> , 1995)
	Cake filtration properties	(Wongsamuth and Doran, 1997)
Changes in metabolism	Oxygen uptake rate	(Keßler <i>et al.</i> , 1997b)
	Mitochondrial activity (TTC reduction)	(Hooker <i>et al.</i> , 1989; Rosenberg, 1989; Zhong <i>et al.</i> , 1994)
	ATP concentration	(Takeda <i>et al.</i> , 1998)
	NAD(P)H	(Takeda <i>et al.</i> , 1998)
	Cell wall composition	(Tanaka <i>et al.</i> , 1988)
	Cell cycle activity	(Yanpaisan <i>et al.</i> , 1998)
	Metabolite production	(Rodriguez-Monroy and Galindo, 1999; Zhong <i>et al.</i> , 2000)
	Acid phosphatase activity	(Keßler <i>et al.</i> , 1997a)

Regrowth studies are often lengthy and inconvenient due to the slow growth rate of plant cells and the susceptibility to contamination. To overcome the problem of contamination, Rosenberg (1989) incorporated antibiotics into the agar medium used for regrowth assessment. However, it is not known if antibiotics would place additional selection pressure on the already shear-weakened cells, although there have been reports that some antibiotics (e.g. carbenicillin) can have inhibitory effects on plant tissue growth (Sarma *et al.*, 1995).

Another commonly used method to assess cell damage is to monitor the membrane integrity of the cell. Membrane integrity is frequently determined using staining techniques, such as fluorescein diacetate (Widholm, 1972) or Evan's blue (e.g. Kieran *et al.*, 1995). The proportion of cells with intact membranes is usually determined through microscopic counting, though image analysis software can be used to facilitate the process (Steward *et al.*, 1999). Membrane integrity has also been measured by dielectric spectroscopy (Markx *et al.*, 1991), although this method may be affected by changes in cell size during the cultivation period (Kieran *et al.*, 2000). Several authors have noted that membrane integrity is less sensitive to mild hydrodynamic shear compared to other biological indicators (Dunlop *et al.*, 1994; Takeda *et al.*, 1998; Wongsamuth and Doran, 1997).

Measurement of the amount of intracellular compounds released into the surrounding medium has also been used to indicate damage by lysis or changes to the cell wall permeability following shear exposure. Increasing shear exposure has led to a rise in the concentration of phenolics (Hooker *et al.*, 1989), protein (Meijer *et al.*, 1994) and esterase (Steward *et al.*, 1999) in the extracellular medium. This method can be used to assess shear damage to the physical structure of the cell but may not be suitable for monitoring sub-lytic effects.

Morphological variations and changes in aggregate size distribution are commonly measured to monitor shear effects on cell size, shape and aggregation patterns. Sub-lytic levels of shear stress are known to affect the shape of cultured animal cells (Prokop and Bajpai, 1992), although the effect on plant cells is less dramatic (Kieran *et al.*, 1995). The effect of hydrodynamic shear on the average aggregate size appears to differ between different cell lines and shearing devices, with an increase observed in some

systems (Wagner and Vogelmann, 1977) and a decrease in others (Scragg *et al.*, 1988; Wongsamuth and Doran, 1997).

Monitoring changes in cellular metabolism has proven to be very useful in quantifying sub-lytic shear effects in both plant and animal cells (Kieran *et al.*, 2000). As shown in Table 2-1, an extensive array of assays has been used to probe the effects of fluid shear on various aspects of the metabolic pathway. A commonly used assay to determine the mitochondrial activity of plant cells is based on a method originally proposed by Towill and Mazur (1975). It involves incubating a culture of plant cells for 18 h or more in the presence of 2,3,5-triphenyl tetrazolium chloride (TTC) and recording the absorbance of the formazan produced. Reduction of the tetrazolium salt to formazan is thought to occur via the electron transport process in the inner membrane of the mitochondria of living cells (Towill and Mazur, 1975). A number of studies have found that mitochondrial activity is very sensitive to hydrodynamic shear (Hooker *et al.*, 1989; Rosenberg, 1989; Takeda *et al.*, 1994; Zhong *et al.*, 1994), especially in comparison to membrane integrity. The method was originally proposed as a viability assay for plant cells, since living cells require a functioning mitochondria to survive. However, a recent study suggests that formazan production is dependent on the metabolic state of the cell, which is expected to fluctuate in the normal course of the cell growth cycle (Keßler and Furusaki, 1997). Thus, it is important to interpret TTC results with caution. The electron transport process in the mitochondria makes use of a variety of enzymes and co-factors, which are in turn activated by other signalling processes upstream (Alberts *et al.*, 1994c). When any of these enzymes or co-factors are damaged by processes triggered by fluid shear stresses, electron transport in the mitochondria is affected. Instead of considering TTC reduction as an indication of general cell viability, a more cautious interpretation is to consider it as an indication of oxidative electron transport (i.e. mitochondrial) activity (Rosenberg, 1989).

Measurement of oxygen uptake rate (OUR) is a convenient method to quantify the effect of hydrodynamic shear on the metabolic activity of plant cell cultures. Fluid shear has been found to increase the specific OUR of various plant cell cultures (Ho *et al.*, 1995; Keßler *et al.*, 1997b; Scragg *et al.*, 1988). Ho *et al.* (1995) suggested that this increase in OUR could be due to an increase in the maintenance energy requirements of stressed cells, but did not explain the mechanism for this effect. The OUR is

determined by monitoring the rate of change in dissolved oxygen (DO) in a plant cell culture. Measurement of DO levels can be easily carried out in bioreactor cultures using standard DO electrodes. However, elaborate precautions must often be taken to ensure that no air bubbles are present in the bioreactor (Keßler *et al.*, 1997b). On the other hand, most viscometers used in shear sensitivity studies are too small to accommodate a standard DO electrode. An alternative method to determine OUR is to take a sample of the sheared culture and measure the rate of DO consumption in a shake flask equipped with a standard DO probe or in a purpose built DO electrode chamber. Zhang *et al.* (1999) has made effective use of the latter technique to determine the effect of a herbicide on suspension cultures of tobacco cells and mitochondria. This method has the additional advantage of enabling uncoupling agents to be added to determine the *uncoupled OUR*. The oxygen uptake of a cell is linked to the electron transport process occurring within the inner mitochondrial membrane. This electron transport process is dependent on the electrochemical proton (H^+) gradient across the membrane, which is in turn linked to ATP synthesis in the cell (Alberts *et al.*, 1994c). Effectively, electron transport and oxygen uptake is *coupled* to ATP synthesis. If more ATP is required, the electron transport rate increases. As ATP accumulates, the H^+ gradient levels off and electron transport slows accordingly. Uncoupling agents (eg. dinitrophenol, salicylamide) are lipid-soluble weak acids that act as H^+ carriers. When an uncoupling agent is added, electron transport continues at a rapid rate but no H^+ gradient is produced, and ATP synthesis is halted. Once free from the feedback inhibitory influence of ATP synthesis, electron transport progresses at the maximal rate and there is a substantial increase in oxygen uptake by the mitochondria. In essence, the uncoupled OUR measures the maximum respiration rate that can be achieved by a cell. To date, there has been no study into the effect of hydrodynamic shear on the uncoupled OUR of plant cells.

2.3 Shear devices

Most shear sensitivity studies fall into one of two classes, depending on the prevailing hydrodynamic environment.

The first class of shear sensitivity studies are carried out in bench-scale bioreactors. The bioreactors used include the conventional stirred tank configuration (Ho *et al.*, 1995) or airlift configuration (Wagner and Vogelmann, 1977). The duration of shear exposure ranges from a day (Takeda *et al.*, 1994) to the entire period of the growth cycle (Ho *et al.*, 1995). Very often, the effect of varying levels of hydrodynamic shear on the biomass accumulation and production of secondary metabolites are monitored in these studies (Chen and Huang, 2000; Zhong *et al.*, 2000), although more subtle metabolic responses can also be measured (Takeda *et al.*, 1998). The intensity of the shear field in a stirred tank is varied either by changing the speed of the impeller (Chen and Huang, 2000) or the type of impeller used (Hooker *et al.*, 1990). In airlift reactors, the intensity of mixing is varied by changing the aeration rates. However, increased aeration can cause other non-shear related effects, such as gas-stripping of dissolved carbon dioxide and other gaseous components, leading to reduced growth and production (Hegarty *et al.*, 1986). As bioreactors are normally designed for extended sterile operation, the effect of long-term exposure to a high shear environment can be readily investigated in these devices. This may be useful to test the scale-up potential of a cell line. However, it is very difficult to quantify the magnitude of shear stresses that cells experience in a bioreactor because the flow field is transient, non-homogeneous and anisotropic (Hua *et al.*, 1993). Another problem is the difficulty in uncoupling shear effects from mass transfer effects by varying the stirrer speed alone as the mass transfer coefficient is closely related to the agitation/aeration level in the bioreactor. Moreover, culture properties such as pH and viscosity vary continuously throughout the course of the cultivation cycle, compounding the difficulty in quantifying the shear stress at a particular time. In these studies, the intensity of the flow field can often only be expressed in terms of the impeller speed. Otherwise, empirical correlations have to be used to estimate the power input and energy dissipation rate (Ho *et al.*, 1995; Wongsamuth and Doran, 1997). Most of these correlations are highly system-specific, thus limiting comparison across different reactor geometries.

Table 2-2: Apparatus used in defined flow field studies of plant cell suspension cultures.

Flow regime	Apparatus	Reference
Laminar	Couette viscometer	(Rosenberg, 1989)
	Rotating wall vessel	(Sun and Linden, 1999)
Turbulent	Submerged jet	(MacLoughlin <i>et al.</i> , 1998)
	Haake rotoviscometer	(Rosenberg, 1989)
Mixed/Transitional	Coutte-type	(Hooker <i>et al.</i> , 1989)
	Recirculating flow capillary	(Kieran <i>et al.</i> , 1995)

The second class of shear studies overcomes some of the shortcomings associated with bioreactor-based studies. In these studies, plant cell cultures are subjected to well-defined shear fields, usually in purpose-built shear devices. Shear exposure times can range from a few seconds (Kieran *et al.*, 1995) to around 15 hours (Hooker *et al.*, 1989). Table 2-2 lists some of the devices that have been used to generate well-defined laminar or turbulent shear fields. As these devices are seldom designed for extended sterile operation, experimental runs rarely last longer than a day. Hence, these devices cannot be used to determine long-term biological responses like changes in specific growth rates. On the other hand, nutritional and culture properties like pH and viscosity are likely to remain uniform during the shear testing period. There has been a very small number of reports of cell growth measurements carried out in custom-built bioreactors with well-defined shear fields, usually based on the Couette concentric cylinder configuration (e.g. Sun and Linden, 1999). Unfortunately, these studies report optimal growth only at extremely low rotational speeds, corresponding to levels of shear stress which are not representative of those prevailing in industrial bioreactors.

The mechanism by which laminar and turbulent fluid shear damages suspension cultured plant cells is still poorly understood. Nonetheless, it has been proposed that turbulent shear causes damage mainly via collision between the energetic turbulent eddies and the plant cell aggregates. This proposition is based on the concept of Kolmogoroff turbulent eddy size. It is assumed that suspended particles which are considerably smaller than the Kolmogoroff length scale will be harmlessly entrained,

whereas eddies which are of comparable size to the suspended cells would cause the most damage (Papoutsakis, 1991). On the other hand, laminar flow is thought to affect cell aggregates by stretch and distortion due to the velocity differential.

The hydrodynamics of laminar flow are much better established and characterised compared to turbulent flow (Bird *et al.*, 1960; Taylor, 1936; Wilkinson, 1960). Laminar shear devices are commonly used in animal cell studies (Frangos *et al.*, 1988; Nollert *et al.*, 1991) and have also been adopted in plant cell studies (Rosenberg, 1989; Zhong *et al.*, 1994). The well-defined characteristics of laminar flow helps to simplify the analysis of shear effects on the metabolic response of the cells. There are also other reasons why studying the effect of laminar shear on plant cell cultures is important. Plant cell suspension cultures become very viscous at the high cell densities required for industrial production (Scragg, 1995). Thus, in large-scale bioreactor vessels, flow in the bulk of the fluid away from the impeller or sparger would be likely to approach laminar conditions. There is also a growing interest in the use of novel bioreactor designs for the cultivation of shear sensitive cell lines (Doran, 1993). In some of these designs, laminar flow plays a significant role in the hydrodynamics of the bioreactor broth (Millward *et al.*, 1994; Millward *et al.*, 1996). For example, the vortex wave membrane bioreactor makes use of laminar flow to achieve adequate mixing while avoiding high shear stresses (Millward *et al.*, 1996).

The two most commonly used devices for subjecting cell suspensions to laminar shear stresses are capillary flow (see references within Kieran *et al.*, 1995) and Couette (for example Rosenberg, 1989; Zhong *et al.*, 1994) systems. Another shear configuration, flow through parallel-plates, has also been used for animal cell cultures but tends to be more suited for anchorage-dependent cells (Frangos *et al.*, 1988). Couette-type devices are more popular in studies involving plant cell suspension cultures than capillary flow devices as they are able to subject cells to continuous shearing over extended periods, whereas capillary-based systems require multiple passes through the shearing section to extend the shear exposure period. The relative merits of the Couette and capillary flow systems will be discussed further in Chapter 4. Couette viscometers have been used for shear sensitivity studies involving cultured plant cells (Hooker *et al.*, 1989; Rosenberg, 1989; Zhong *et al.*, 1994), enzymes (Thomas *et al.*, 1979) and red blood cells (Joshi *et al.*, 1996). However, conventional Couette

viscometers are normally designed for rheological measurements involving non-living samples. When the investigation involves living cells, additional factors need to be considered. In particular, the provision of sufficient oxygen to the cells during shearing might be difficult to achieve in conventional Couette viscometers. There have been no studies into the possible effects of oxygen starvation on cells exposed to shear in closed viscometers to date, although, the appearance of purpose-built, oxygen permeable shear devices (Sun and Linden, 1999; Wudtke and Schugerl, 1987) demonstrates that at least some researchers have recognised this potential problem.

2.4 *Mechano-sensitivity of plants*

From the above discussion, it is clear that hydrodynamic shear forces affect suspension cultured plant cells at both the physical and physiological level. While severe levels of shear can result in cell lysis and damage to the ultrastructure of the cell, mild levels of shear can perturb the metabolic balance of the cell and trigger a cascade of biochemical reactions which ultimately leads to changes in growth and cellular activity. Unfortunately, an understanding of how and why mild fluid shear elicits a range of physiological changes in plant cells is still very poor. Nevertheless, a review of the literature reveals a strong parallel between the effects of fluid shear on suspension cultured plant cells, and mechanical stresses on whole plants and tissues. Although this connection has been largely unexplored, a careful examination may be beneficial to elucidating the mechanism underlying the sub-lytic response. It may also suggest a new approach to overcoming the problem of sub-lytic shear sensitivity in plant cell cultures.

The susceptibility of plants to mechanical stresses from the environment has long been recognised. The inability of plants to change location when confronted with environmental stresses has led to the evolution of complex mechanisms to sense and adapt to various stresses in order to maximise their potential for survival. Thigmomorphogenesis refers to alterations in plant growth and development because of non-injurious mechanical stimulation of the plant by touch (Jaffe, 1973). For example, plants exposed to wind stimulation show stunted vertical growth and thicker stems, leading to stiffening of the tissues (Telewski and Jaffe, 1986). It has been suggested that this may be an adaptive response, as shorter and sturdier plants are less likely to be damaged by the wind (Telewski and Jaffe, 1986). Controlled application of mechanical

stress, by either shaking or touching, also has the same growth-inhibiting effect. For example, Braam and Davis (1990) subjected two-week-old *Arabidopsis thaliana* plants to touch stimulation, twice daily for three weeks. The touch-stimulated plants had shorter petioles, showed delayed bolting and developed shorter bolts compared to the unstimulated plants. Similarly, Jaffe (1973) found that a rubbing stimulus applied to the stem significantly retarded the growth of a variety of plant species. When the stimulus was discontinued after 7 days, normal growth resumed in these plants. There are numerous other examples where controlled application of mechanical stress has led to changes in plant growth and these have been reviewed by Mitchell (1996). The broad similarity of these effects on whole plants to the sub-lytic responses of plant cell cultures to fluid shear is striking.

Apart from effects on plant growth, mechanical stress has also been found to increase the respiratory and metabolic activity of plant tissues. When sweet potato root tissues were mechanically cut into slices, an increase in the rate of respiration was observed. This increased respiration in wounded tissues is termed wound respiration (Uritani and Asahi, 1980). Similarly, infection with pathogens also elicits an increase in respiration rate, termed infection-induced respiration (Uritani and Asahi, 1980). In both cases, the stimulation in respiration is accompanied by increased carbohydrate catabolism to supply more ATP and for precursor production for the formation of secondary products (Uritani and Asahi, 1980). This enhanced respiration has been linked to wound healing processes such as lignin formation, as well as defence reactions against pathogen attack. Such defence reactions include production of phytoalexins, which are antibiotics against penetrating parasites, and localised cell death of the infected areas, known as the hypersensitive response (Uritani and Asahi, 1980). Interestingly, suspension cultured plant cells have also been found to show increased oxygen uptake rates in response to mild hydrodynamic shear (e.g. Keßler *et al.*, 1997b).

An early indication of the hypersensitive response is the production and release of activated oxygen species, such as the superoxide anion and H_2O_2 . This phenomenon is termed the oxidative burst. Oxidative burst has been reported in whole plants subjected to mechanical wounding and pathogen attack (Uritani and Asahi, 1980). A similar phenomenon has also been reported in suspension cultured plant cells. For instance, increased production of H_2O_2 in suspension cultured plant cells has been observed in

response to hydrostatic pressure (Schreck *et al.*, 1996), changes in osmotic pressure of the medium (Cazalé *et al.*, 1998; Yahraus *et al.*, 1995) and mechanical stimulation (Cazalé *et al.*, 1998).

Although one must be cautious in applying results observed in whole plants and tissues to undifferentiated plant cell cultures, the striking similarity between the sensitivity of whole plants to mechanical stress and that of plant cells to fluid shear stress is strongly suggestive. Furthermore, mechanically induced physiological responses in suspension cultured plant cells have also been reported. The oxidative burst phenomenon previously discussed is one example (Schreck *et al.*, 1996). Another is the increase in intracellular calcium following mechanical perturbation of suspended plant cells (Haley *et al.*, 1995; Takahashi *et al.*, 1997). A recent report on the effect of mechanical loading on the growth and division of single cells (Lynch and Lintilhac, 1997) further supports the proposition that individual plant cells and aggregates are sensitive to mechanical signals. Lynch and Lintilhac (1997) observed that when controlled mechanical loads were applied to tobacco protoplasts embedded in agarose blocks, cells preferentially divided either parallel or perpendicular to the principal stress tensors. The authors suggest that the preferential orientation of the newly formed cell wall in relation to the direction of the applied stress indicate that the perception of mechanical stress is a characteristic of individual plant cells.

Unfortunately, the mechanism by which environmental signals, such as rain, wind and touch, are received and transduced within the plant cell is not fully understood. However, it is known that ion channels and ion-binding regulatory proteins play a central role in the signal transduction mechanism.

2.5 Ion channels in mechanical signal transduction

Ion channels are pores that span the plasma membrane and various intracellular membranes. They enable the rapid channelling of specific ions to appropriate locations within the cell, which in turn triggers a cascade of events resulting in modification of cellular activity or gene expression, leading to a biological response. These pores show ion selectivity and open in response to a specific stimulus. The main types of stimuli that are known to open ion channels include a change in the voltage across the membrane (voltage-operated channels) or the binding of a ligand (ligand-operated

channels). However, of particular interest to the transduction of mechanical signals are stretch-operated channels, which open in response to mechanical stress. Such stretch-operated channels have been found in both animal and plant cells. In plant cells, they have been identified in both the plasma membrane (Cosgrove and Hedrich, 1991; Ding and Pickard, 1993a; Falke *et al.*, 1988) and the membranes surrounding intracellular organelles (Alexandre and Lassalles, 1991). The identification and characterisation of many ion channels have been largely facilitated by the development of the patch-clamp technique (Hamill *et al.*, 1981). Although technically demanding, this technique enables the direct measurement of currents flowing through single ion channels. Through analysis of the current-voltage profile of the patch-clamp recordings, information about the ion selectivity and the type of stimuli that activates the channel can be obtained.

Of the many ion channels found in plant cells, Ca^{2+} channels and anion channels have been identified as key components in the signal transduction pathways of many types of stimuli. Ca^{2+} channels, along with Ca^{2+} -activated regulatory proteins such as calmodulin, play pivotal roles in the intracellular signalling pathway of plant cells (Bush, 1995; Zielinski, 1998). A number of studies have demonstrated the involvement of Ca^{2+} and calmodulin in mediating the response of plant cells to mechanical stimulation. For instance, Knight *et al.* (1992) studied the effect of wind stimulation on cytosolic calcium levels $[\text{Ca}^{2+}]_i$ using *Nicotiana plumbaginifolia* plants which had been genetically transformed to express aequorin. These plants emit blue light in response to increases in $[\text{Ca}^{2+}]_i$. It was found that wind-induced plant motion causes $[\text{Ca}^{2+}]_i$ to increase immediately and transiently, with the magnitude of the increase dependent on the strength of the wind stimuli. At the same time, wind stimulation inhibited the growth of the plants by about 30%. Application of ruthenium red, a putative blocker of mitochondrial and endoplasmic reticulum Ca^{2+} channels, eliminated the wind-induced $[\text{Ca}^{2+}]_i$ increase.

Braam and Davis (1990) also demonstrated the involvement of Ca^{2+} in mechanosensitivity in experiments with *A. thaliana* plants subjected to rain, wind and touch stimulation. They found that these mechanical stimuli induced the expression of calmodulin and calmodulin-related genes, while inhibiting the growth of the plants. Similar effects have also been noted in soybean plants (Jones and Mitchell, 1989).

Jones and Mitchell (1989) observed that application of calmodulin inhibitors partially reduced the growth inhibition caused by mechanical stress on soybean seedlings. Wallace *et al.* (1984) reported a rapid increase in γ -aminobutyric acid (GABA) in the leaves of soybean seedlings in response to mechanical wounding. The increase in GABA was found to be activated by a Ca^{2+} -calmodulin mediated pathway that could be fully inhibited by the calmodulin inhibitor, W7 (Snedden *et al.*, 1995). Apart from these examples, Ca^{2+} and calmodulin have also been implicated in the touch-sensitive response of a variety of other plant species, including mung beans (Botella and Arteca, 1994), *Bryonia dioica* (Galaud *et al.*, 1993) and potatoes (Takezawa *et al.*, 1995).

Verapamil, a blocker of voltage-operated Ca^{2+} channels, has been shown to suppress the effects of mechanical damage on the biological response of lemon seedlings (Castañeda and Pérez, 1996). Castañeda and Pérez (1996) demonstrated that the increase in phenylalanine ammonia-lyase activity produced by wounding of lemon seedlings could be completely suppressed by verapamil. Verapamil has also been shown to attenuate shear-induced reductions in NAD(P)H levels in eucalyptus cultures (Takeda *et al.*, 1998).

A Ca^{2+} -selective channel that is activated by mechanical stretching of the plasma membrane has been identified in onion cells (Ding and Pickard, 1993a). The activity of this channel is sensitive to temperature (Ding and Pickard, 1993b) and pH (Ding *et al.*, 1993). It exhibits enhanced mechanosensitive activity as the temperature is lowered from 25°C to 6°C, with activity falling at temperatures slightly above 25°C, although higher temperatures could not be studied because of the instability of the cell patches at high temperatures (Ding and Pickard, 1993b). Similarly, lowering the pH from 7.2 to 4.5 reduces the mechanosensitive activity of this channel (Ding *et al.*, 1993).

Anion channels are involved in cell signalling, osmoregulation, plant nutrition and metabolism (Barbier-Brygoo *et al.*, 2000). Stretch-activated Cl^- channels have been identified in *Vicia faba* guard cells (Cosgrove and Hedrich, 1991) and cultured tobacco cells (Falke *et al.*, 1988). These channels are thought to be involved in the regulation of cell volume and turgor pressure (Cosgrove and Hedrich, 1991) and in response to changes in the osmotic pressure of the environment (Falke *et al.*, 1988). Application of the Cl^- channel blocker, NPPB, has been found to strongly inhibit anion channels in

Vicia faba guard cells reported to be involved in osmoregulation (Schroeder *et al.*, 1993). The involvement of anion channels in osmoregulation may be particularly relevant to the perceived sensitivity of plant cells to fluid shear forces. For example, Namdev and Dunlop (1995) proposed a model for plant cell growth which suggests that changes in cell turgor through interference with osmoregulation and cell wall composition could lead to increased sensitivity to fluid shear forces. They reported studies on yeast cells which showed that significant variations in cell size, wall strength, turgor pressure and elastic modulus of the cell wall accompanied high levels of turbulent shearing in a chemostat. They maintained that these results strongly suggested a link between the interference of osmoregulation and wall rheology by the fluid shear stresses and the production of various sub-lytic effects.

2.6 Conclusions

The discussion in Section 2.1 highlighted the present lack of understanding of the cause of shear sensitivity in plant cell culture systems. Previous approaches to overcoming the shear sensitivity of plant cell cultures, for example by reducing the intensity of mixing or using low-shear bioreactors, have met with limited success. Moreover, these approaches do not address the issue of the sub-lytic response observed in a number of studies. One promising solution to the problem is to attenuate the negative effects of sub-lytic shear sensitivity to enable plant cells to withstand the high shear environment present in industrial bioreactors. As discussed in Sections 2.4 and 2.5, there is a substantial body of evidence to suggest that this may be achieved by disrupting the ion-signalling pathway within plant cells through various ion channel blockers and protein inhibitors. Although the effects of these chemicals have previously been demonstrated on whole plants subjected to mechanical or osmotic stresses, their effects on the fluid shear sensitivity of cultured plant cells is still relatively unknown.

In Section 2.3, a number of shear devices used in previous studies have been discussed. Conventional bioreactors have poorly defined, non-homogeneous shear fields, which make it difficult to determine the shear stresses to which the plant cells have been exposed. On the other hand, conventional viscometers and other similar devices designed for non-biological samples are able to generate known, controllable and reproducible shear fields but may not be suitable for shear testing on living cells,

especially in terms of providing sufficient oxygen to the cells during the shear exposure period. This factor has not been adequately addressed in previous studies involving viscometers.

In the next chapter, the methodology developed to address these issues and to study the effects of ion channel blockers and calmodulin inhibitors on the shear responses of cultured plant cells will be outlined.

CHAPTER 3

METHODOLOGY

From the survey of the current literature presented in the previous chapter, the following issues have been identified:

- Sub-lytic shear effects

There is currently no direct solution to overcoming sub-lytic shear sensitivity in plant cell cultures. This is mainly because of a lack of understanding of the cellular mechanisms underlying sub-lytic effects. However, a promising approach is suggested by the effectiveness of certain ion channel blockers and calmodulin inhibitors at attenuating the mechanosensitive response of whole plants and isolated plant cells. The purpose of the work reported here is to establish if these chemicals would have a similar effect on the sub-lytic response of plant cells to fluid shear.

- Hydrodynamic stress signal transduction

Current understanding of the mechanism by which mechanical or hydrodynamic stress signals are perceived and transduced within the plant cell is still very poor. In this work, ion channel blockers that are known to target specific ion channels were used to help in the identification of potential key components in the signalling pathway. In addition, patch-clamping of protoplasts isolated from the cultured plant cells was attempted to study the behaviour of ion channels in response to stretching of the cell membrane.

- Oxygen limitation in shear viscometers

Conventional Couette-type viscometers can be used to generate well-defined laminar shear fields, but may become oxygen limited after long exposure times, especially for designs with small gap widths. In this study, finite element techniques were used to model the oxygen transfer in a conventional Couette-type viscometer. The model suggests that oxygen limitation may occur in a conventional Couette during the shear testing period. Hence, a novel Couette that can generate defined, controlled and reproducible laminar flow fields while providing sufficient oxygenation of the cultures had to be constructed.

The channel blocker/shear viscometer studies and the patch clamp investigations are described in detail in the following sections.

3.1 *Shear viscometer based investigations*

To examine the effect of ion channel blockers on the sub-lytic response of cultured plant cells, the cellular response of a given cell line to a defined level of fluid shear stress in the absence of any blockers must first be characterised and quantified. This requires a suitable cell line with stable properties that will exhibit sub-lytic effects at practical levels of shear stresses, as well as a device which can generate a well-defined shear field while providing sufficient oxygen to the cells during shear testing. The specific aims for this part of the work, based on the requirements outlined above, are summarised in Table 3-1, along with the methodology.

Table 3-1: Relationship between aims of study and methodology for the channel blocker/shear viscometer investigations

Specific Aim	Method
1. Construct a laminar shear device with sufficient oxygen supply to cells during shear period.	<ul style="list-style-type: none"> a. Determine rheological properties of carrot culture. b. Finite element modelling of oxygen transfer in a typical Couette viscometer. c. Design and construct a O₂ permeable Couette viscometer. d. Finite element modelling of oxygen transfer in O₂ permeable viscometer. e. Compare the rate of DO decrease between oxygen permeable and impermeable viscometer.
2. Determine if sub-lytic effect on cell growth can be observed in carrot cell line..	<ul style="list-style-type: none"> a. Conduct preliminary investigations on shake flask cultures.
3. Quantify the biological response to laminar shear.	<ul style="list-style-type: none"> a. Conduct a series of randomised shear runs on the carrot cells in the oxygen permeable viscometer over a range of shear stresses and shear exposure periods, monitoring a range of biological activities.
4. Determine the effect of various blockers and inhibitors on the biological response to laminar shear and any interactions between the blocker treatments	<ul style="list-style-type: none"> a. Conduct a set of factorial designed experiments involving 2 Ca²⁺ channel blockers, a Cl⁻ channel blocker and a calmodulin inhibitor on cells sheared at 2 shear stress levels in the Couette. b. Conduct a parallel set of experiments involving the same blockers on shake flask cultures
5. Determine the effect of prolonged exposure to the various blockers on cell growth and function.	<ul style="list-style-type: none"> a. Expose shake flask cultures to compounds for 1 to 16 days and monitor cell growth (16 days) and mitochondrial activity (1 day).

Various laminar shear devices were compared with a view to selecting a suitable device for the present work. A Couette configuration was found to be adequate. However, preliminary calculations suggested that conventional Couette designs may not be able to supply sufficient oxygen to the plant cells during shear-testing. Detailed modelling using a finite element technique confirmed our preliminary calculations. Hence, a novel oxygen-permeable Couette was designed and constructed to allow adequate oxygenation of the cells during shear testing. Experimental verification of the model results was performed by comparing the rate of decrease in dissolved oxygen in the oxygen-permeable Couette versus a similar impermeable Couette.

To determine if sub-lytic effects could be observed in the carrot (*Daucus carota*, wild type) cell line maintained in our laboratory, preliminary investigations were conducted in shake flasks to monitor the growth rate and membrane integrity of the carrot cultures agitated at different shaker speeds.

To quantify the effects of shear on the biological response and to determine the critical shear levels at which different effects are observed, a series of randomised shear runs was conducted on the carrot cell cultures in the oxygen-permeable viscometer. Five biological indicators were monitored: mitochondrial activity, coupled and uncoupled oxygen uptake rate (OUR), membrane integrity and regrowth ability. Previous studies have only reported the effect of shear on the coupled OUR. However, it is important to determine if changes in the OUR are due to a change in the maximal metabolic (respiratory) capacity of the cell (ie. uncoupled OUR), or a change in the cell's utilisation of its existing metabolic capacity. This will help in understanding how hydrodynamic shear affects the energy conversion processes within the cell. A range of shear stress levels (6 to 100 N/m²) and shear periods (up to 8 hours) were used to obtain a set of graphs that characterised the biological response of the carrot cells to the level of shear.

Next, the effects of different ion channel blockers and a calmodulin inhibitor on the shear response of the carrot cells were evaluated. A factorial-designed set of experiments was planned and conducted. Factorial designed experiments have the advantage of economising on the number of experimental runs required to determine a statistically valid result. It also enables the determination of interaction effects between the various factors under study. Two suitable shear stress levels were selected based on

the results of the earlier viscometer runs. Four different blockers/inhibitors were studied (see Section 2.5): ruthenium red, an intracellular Ca^{2+} channel blocker, verapamil, a voltage-operated Ca^{2+} channel blocker, 5-nitro-2,3-phenylpropylaminobenzoic acid (NPPB), a Cl^- channel blocker and N-(6-aminohexyl)-5-chloro-1-naphthalene-sulfonamide (W7), a calmodulin inhibitor. The results from these factorial experiments were then statistically analysed to determine the significant effects.

Finally, to determine the effects of prolonged exposure to these chemical compounds on plant cell growth and function, carrot shake flask cultures were exposed to the compounds for periods ranging from 1 to 16 days.

3.2 Patch-clamp investigation

The aim of the patch-clamp investigation was to study the activity of ion channels of cultured plant cells in response to membrane stretching. Fluid shear forces acting on suspended cells would cause stretching of the cell membranes. It was envisaged that specific ion channels would be activated or show increased activity when the cell membrane was stretched by the fluid shear forces. The ion selectivity of the “shear-sensitive” ion channel and the mechanism of activation (eg. stretch-operated or voltage-operated) would help in the elucidation of the signal transduction pathway that leads to sub-lytic effects. The proposed experimental scheme is as follows:

1. Identify any ion channels in the plasma membrane of protoplasts isolated from the cultured plant cells.
2. Monitor ion channel activity in response to suction applied through the patch-clamp pipette to determine if ion channel sensitive to membrane stretching.

CHAPTER 4

EXPERIMENTAL APPARATUS

To investigate the effect of hydrodynamic shear on suspension cultured plant cells, it is necessary to devise a suitable experimental apparatus that will subject the suspended cells to a range of defined, controlled and reproducible shear fields. In Chapter 2, a number of shear devices for generating defined flow fields in shear sensitivity studies were discussed. Two common configurations for subjecting cell suspensions to laminar shear stresses were identified: (i) flow through capillary tubes (see references within Kieran *et al.*, 1995) and (ii) rotating concentric cylinders or Couettes (for example, Rosenberg, 1989; Zhong *et al.*, 1994).

In this chapter, the relative merits of these two configurations are compared with a view to selecting a suitable configuration for the present experimental work. This is followed by a detailed discussion of the various factors that were considered when designing the viscometer for use with live carrot cells. In particular, a substantial part of this discussion is devoted to the need for adequate oxygenation of the cells during shear testing. Finally, a description of the experimental apparatus and construction procedure is given.

4.1 Shear device configuration

Table 4-1 summarises some of the features of the capillary and Couette shear devices.

Table 4-1: Comparison of capillary and Couette shearing devices.

	Capillary	Couette
Shear stress profile	Varies from 0 at center of tube to maximum at tube wall	Varies slightly across annular gap.
Shear exposure time	Depends on length of capillary tube	Not limited by design
Auxiliary equipment required (e.g. pumps, holding reservoirs)	Yes	No
Volume of suspension required	large (~100 ml)	small (~20 ml)
Continuous sampling	Yes	No
Shearing mode	Intermittent	Continuous

The velocity profile for fully developed laminar flow in a capillary tube is parabolic. The shear stress varies linearly with the radial distance, ranging from zero at the center of the tube to a maximum along the tube wall. The flow pattern in a Couette gap follows a simple circular fluid flow (Bird *et al.*, 1960). The shear rate produced in the fluid at a particular speed also varies slightly across the annular gap. For a rotating outer bowl and a stationary inner bob, the maximum shear stress occurs along the surface of the inner bob and the minimum at the surface of the outer cup. However, a constant shear rate approximation is usually adequate (Thomas *et al.*, 1979). In a capillary-based system, the period of time for which the cell suspensions are exposed to defined shear stresses for a single pass through the capillary is limited by the length of the capillary tube. To extend the shear exposure time, multiple passes through the tubes are needed. However, the shear experience of the suspended cells in multiple passes is intermittent instead of continuous. Moreover, re-circulation of the culture fluid requires

a variety of auxiliary equipment, such as pumps, connecting tubes and holding reservoirs. This means that cell suspensions would be exposed not only to the hydrodynamic shear in the capillary section, but also to the effects of pumping and flow through the auxiliary devices. To quantify the effects of the auxiliary devices alone, control experiments are often conducted by removing the capillary tube section. However, the absence of the shearing section might alter the back pressure on the remainder of the system and thus control runs may not be representative of the actual auxiliary effects. This was highlighted in a study by Kieran *et al.* (1995) where a capillary tube was used to generate turbulent flow. On the other hand, cell suspensions can be easily subjected to continuous defined shearing over extended periods in the Couette configuration without the need for auxiliary fittings. The capillary-based system also requires a sizeable volume of culture to ensure continuous flow through the system of pumps and fittings. In contrast, the volume of culture required for a Couette viscometer is comparatively small, as it only needs to fill the annular gap.

One advantage of the capillary system is that it allows samples of the test culture to be removed after each pass through the shearing section without affecting the hydrodynamic environment, provided the total volume of culture is large enough. Repeated sampling from the Couette annular gap could lead to the creation of a free surface between fluid and the wall of the inner bob at high shear rates as the fluid is propelled outwards by the centrifugal force. This will significantly alter the hydrodynamic environment in the annular gap. Drawn samples could be replaced with fresh medium to maintain the volume in the Couette, but would lead to gradual dilution of the test culture. Alternatively, a single shear stress-shear period combination can be tested at a time. The shear effects can then compared to a low-shear control culture maintained for the same period (e.g. in a shake flask).

From the comparison of the characteristics of these two configurations, the Couette was considered to be more suitable than the capillary system for subjecting cell suspensions to continuous, defined laminar flow fields. Thus, the Couette configuration was selected for the present experimental work.

4.2 Considerations for Couette viscometer

Although the Couette configuration is commonly used in shear sensitivity studies, details of the equipment design are rarely reported. In the present study, a Couette viscometer was specially constructed for subjecting plant cell suspension cultures to varying levels of well-defined laminar shear stresses. The decision to construct our own Couette viscometer was prompted by the results of finite element modelling studies to calculate the dissolved oxygen level in the annular gap during the shear testing period. The modelling studies suggested that conventional Couette viscometers originally designed for rheological measurements might not be suitable for use with living biological samples, particularly in terms of providing sufficient oxygenation of the cells suspended in the annular gap. In the design of the novel Couette viscometer, the following factors were taken into consideration:

- range of shear stress achievable
- stability of the flow field
- adequate oxygenation of the plant cells
- temperature control
- sterile operation

Each of these factors is discussed in detail in the following sections.

4.3 Range of shear stress

The rheological properties of the culture fluid has an important impact on the range of shear stresses that can be achieved in the Couette viscometer, as well as on the temperature rise due to shearing and the stability of the flow field. The most important rheological property that needs to be determined is the relationship between the shear stress and the shear rate for the culture.

Samples of 14-day carrot cultures, pre-screened to exclude aggregates larger than 263 μm and adjusted to a cell density of 0.05 g/ml (Fresh weight) with fresh culture medium, were placed in a Haake viscometer (Rotovisco RV100, bob-cup configuration) and the torque produced at varying rotational speeds recorded. The choice of using 14-

day cultures and pre-screening the cultures was based on considerations to limit the variability of TTC assay results (see Section 5.3.3.5). The experimental procedures for screening the cell cultures and adjusting the cell density will be explained in Section 5.3.1. Measurements were carried out at 27°C. The torque and speed readings were then converted to the respective shear stress and shear rate based on correlations provided by the manufacturer. Figure 4-1 shows the typical variation between the shear stress and shear rate for the pre-screened carrot cultures. Due to the low viscosity of the culture fluid, very high rotational speeds could not be tested in the Haake as the high speeds would cause splattering of the test sample and non-laminar flow.

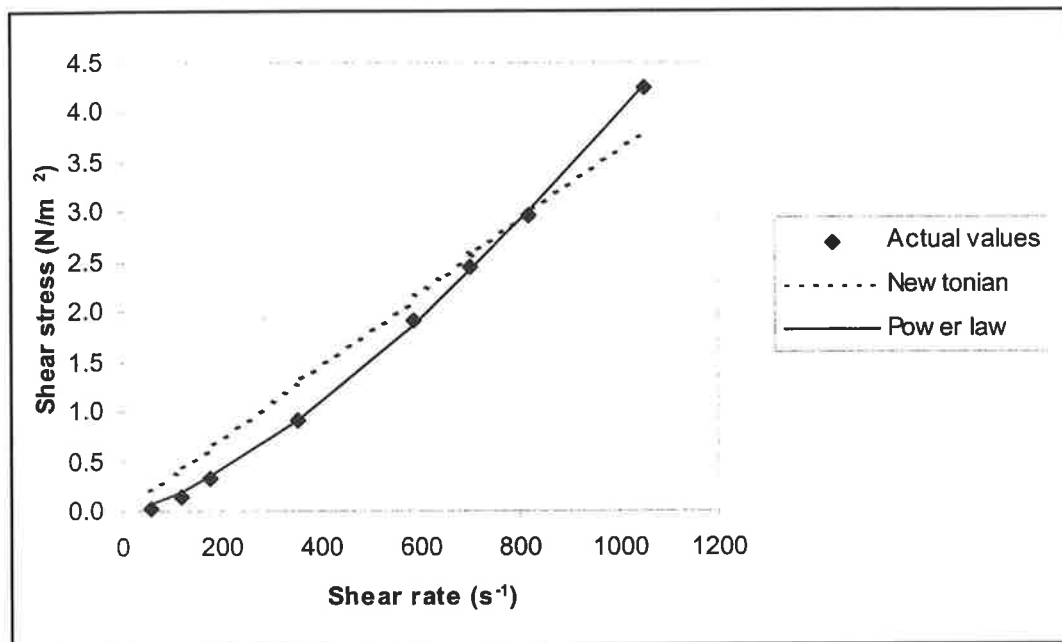


Figure 4-1: Relationship between shear stress and shear rate for pre-screened carrot cultures (< 263 μm), cell density = 0.05 g/ml (FW).

Figure 4-1 shows that a power-law expression gave the best fit of the data. The relationship between shear stress (τ) and shear rate ($\dot{\gamma}$) for a power-law fluid is given by:

$$\tau = k(\dot{\gamma})^n \quad (\text{Eq 4-1})$$

where k and n are experimentally determined parameters.

Figure 4-1 includes a curve representing the power-law relationship with the following parameters:

$$k = 0.000253 \text{ N s}^n/\text{m}^2$$

$$n = 1.399 \text{ (-)}$$

Since the power law index (n) is fairly close to one, the deviation from Newtonian behaviour (where $n=1$) is relatively mild in this case. Figure 4-1 also includes a line representing a Newtonian relationship fitted to the actual values using the least-squares method. The corresponding viscosity assuming a Newtonian relationship was 0.0036 Pa s.

The shear rate in a Couette viscometer varies with the radial position in the annular gap. The relationship between shear rate and the angular velocity of the Couette for a power-law fluid can be derived as follows (Wilkinson, 1960):

Consider a section through the Couette of unit height, as shown in Figure 4-2. Let the torque per unit height of liquid be G .

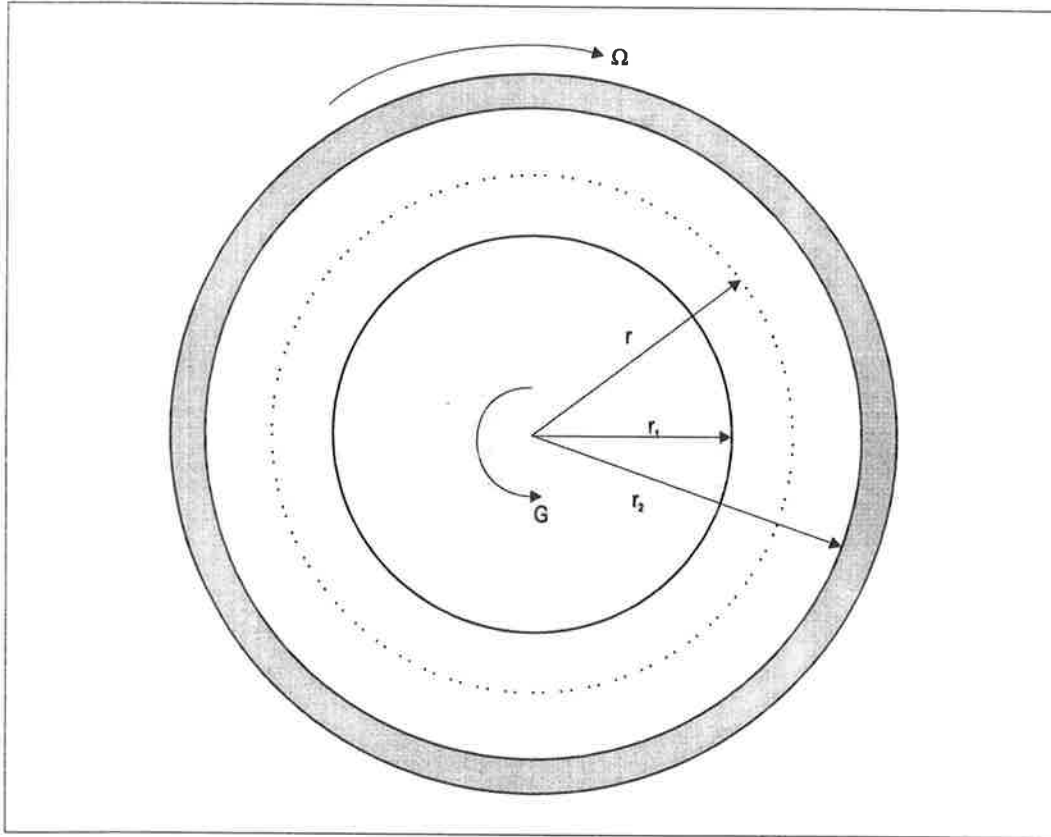


Figure 4-2: Schematic diagram of annular gap section in a Couette viscometer.

The shear stress at radius r is given by

$$\tau(r) = \frac{G}{2\pi r^2} \quad (\text{Eq 4-2})$$

The shear rate is calculated from

$$\dot{\gamma} = r \frac{d\Omega}{dr} \quad (\text{Eq 4-3})$$

Rearranging Equation 4-1, we obtain

$$\dot{\gamma} = \left(\frac{\tau}{k} \right)^{1/n} \quad (\text{Eq 4-4})$$

Substituting τ in Equation 4-4 with Equation 4-2, we get,

$$\dot{\gamma} = \left(\frac{G}{2\pi r^2 k} \right)^{1/n} \quad (\text{Eq 4-5})$$

Therefore, combining Equations 4-3 and 4-5

$$r \frac{d\Omega}{dr} = \left(\frac{G}{2\pi r^2 k} \right)^{1/n} \quad (\text{Eq 4-6})$$

For the case where the inner bob ($r = r_1$) is stationary while the outer bowl ($r = r_2$) is rotating with angular velocity, Ω , Equation 4-6 can be integrated to obtain

$$\begin{aligned} \int_0^{\Omega} d\Omega &= \int_{r_1}^{r_2} \left(\frac{G}{2\pi r^2 k} \right)^{1/n} \frac{dr}{r} \\ \Omega &= \frac{n}{2} \left(\frac{G}{2\pi k} \right)^{1/n} \left[\left(\frac{1}{r_1^2} \right)^{1/n} - \left(\frac{1}{r_2^2} \right)^{1/n} \right] \end{aligned} \quad (\text{Eq 4-7})$$

Equation 4-7 gives a relation between the angular velocity, Ω and the torque, G . By substituting for G in this equation with Equation 4-5, we get

$$\begin{aligned} \Omega &= \frac{n}{2} (r^2 \dot{\gamma}^n)^{1/n} \left[\left(\frac{1}{r_1^2} \right)^{1/n} - \left(\frac{1}{r_2^2} \right)^{1/n} \right] \\ \dot{\gamma} &= \frac{2\Omega}{n \left[\left(\frac{1}{r_1} \right)^{2/n} - \left(\frac{1}{r_2} \right)^{2/n} \right] r^{2/n}} \end{aligned} \quad (\text{Eq 4-8})$$

Thus, for a given angular velocity, the shear rate at radius r can be calculated from Equation 4-8. The corresponding shear stress can then be determined from Equation 4-1. Wilkinson (1960) suggests that a mean shear rate and stress can be conveniently calculated at the geometric mean radius, \bar{r} , where

$$\bar{r} = \sqrt{r_1 r_2} \quad (\text{Eq 4-9})$$

Figure 4-3 shows the variation of mean shear stress with the rotational speed of the Couette for different gap widths, for an outer bowl radius (r_2) of 50.8 mm. The range of shear stresses achievable for a given range of rotation speed progressively narrows with increasing gap widths (Figure 4-3). For example, the mean shear stress at 1200 rpm is around 100 N/m² for an annular gap width of 0.625 mm but only 19.5 N/m² for a 2 mm gap. In addition, the variation in shear stress with radial position in the annular gap increases for larger gap widths. For instance, the actual shear stress at r_1 and r_2 differed from the mean values at \bar{r} by only 0.8% for a 0.4 mm gap width, compared to 4% for a 2 mm gap width. Thus, a small gap width would give a uniform stress distribution across the gap with a wider range of mean shear stress achievable for a given range of rotation speeds. However, the gap width must be large enough to allow the carrot cultures to be loaded easily and to avoid excessive collision of the cell aggregates with the viscometer walls. It is also difficult to accurately machine for very small gap widths.

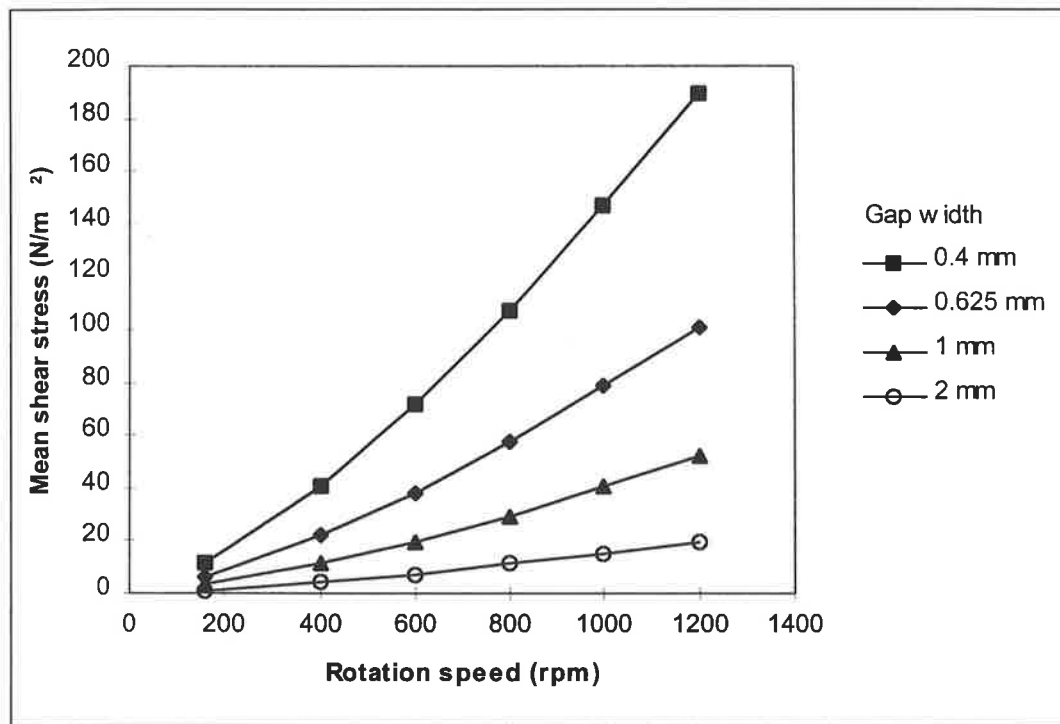


Figure 4-3: Variation of mean shear stress with the rotational speed of the outer bowl in Couette viscometers of different gap widths.

4.4 Flow stability

The stability of a fluid contained between concentric rotating cylinders had been investigated by Taylor (1936). He found that when the inner cylinder (the bob) rotates and the outer cylinder (the cup or bowl) is stationary, the flow becomes unstable above a critical Reynolds number. This is caused by the larger centrifugal force of the layers of fluid adjacent to the inner rotating cylinder compared to the outer fluid layers. This creates a centrifugal force field that produces vortices in the fluid layers, which have been termed “Taylor vortices” (e.g. Tran-Son-Tay, 1993). At even higher rotational speeds, turbulent flow occurs. On the other hand, when only the outer cylinder rotates, Taylor vortices do not form and laminar flow is strongly stabilised by the centrifugal forces (Bird *et al.*, 1960). The critical Reynolds number at which turbulence sets in for the latter case is also significantly higher (Taylor, 1936). Thus, rotating the outer cylinder in the Couette allows a wider range of rotational speeds to be used while still maintaining a stable laminar flow regime.

The critical Reynolds number for Couette flow can be determined from empirical charts reported by Taylor (1936). These charts are expressed in dimensionless forms

and were determined using a wide range of fluids. For a given gap width to bowl radius ratio (i.e. w / r_2), the chart specifies the critical Reynolds number, defined as

$$Re_{crit} = \frac{Uw\rho}{\mu_{app}} \quad (Eq\ 4-10)$$

where

$$U = \text{tangential velocity} = 2 \pi N_s r_2;$$

$$w = \text{gap width} = 0.625 \times 10^{-3} \text{ m};$$

$$\rho = \text{fluid density} = 1005 \text{ kg/m}^3 \text{ (for cell density of 0.05 g FW/ml);}$$

$$\mu_{app} = \text{apparent viscosity} = \tau / \dot{\gamma};$$

$$N_s = \text{rotational speed (rps)}$$

Although the pre-screened carrot cultures were found to behave more like a power-law fluid, a power-law relationship would make Equation 4-4 implicit in the variable N . Thus, to simplify calculations, the fluid was approximated as a Newtonian fluid with viscosity of 0.0036 Pa s (see Section 4.1.1). Figure 4-4 shows the variation of critical speeds with gap widths (using the same outer bowl radius as in Figure 4-3, i.e. $r_2 = 50.8$ mm) for fluids of different viscosities. A higher apparent viscosity would result in a higher critical rotation speed. The critical speed drops as the gap width is progressively increased. The critical speed for a gap width of 0.625 mm was approximately 2030 rpm for a fluid viscosity of 0.0036 Pa s. However, the rotational speed required to attain a shear stress of 100 N/m² is only ~1190 rpm for that gap width. Thus, a gap width of around 0.6 mm was selected for the shear viscometer as it provides a good range of shear stress (6 to 100 N/m²) within the laminar flow regime.

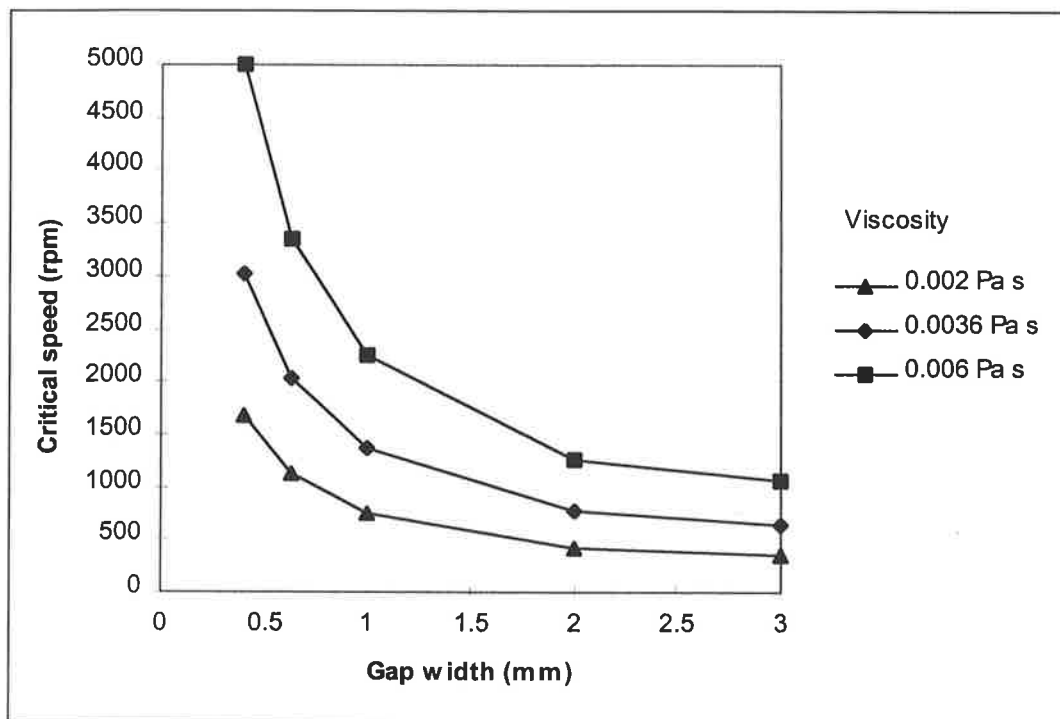


Figure 4-4: Variation of critical speed with Couette gap width for different apparent viscosities.

4.5 Oxygen transfer

4.5.1 Introduction

Plant and animal cells require oxygen to obtain metabolic energy (e.g. ATP) needed to drive a variety of vital cellular functions. Oxygen limitation of plant cells has been shown to have adverse effects on cell growth and differentiation (Kessell and Carr, 1972; Tate and Payne, 1991, and references therein). Compared to other essential culture nutrients (e.g. sucrose or glucose, inorganic salts), the solubility of oxygen in water is limited (about 0.256 mM at room temperature). Therefore, the provision of adequate oxygen to suspension cultured plant cells is vital. The following section examines if a conventional Couette-type viscometer for shear testing on carrot cells would provide sufficient oxygenation.

The oxygen uptake rate (OUR) of plant cells varies between different species. Payne *et al.* (1987) reviewed the specific OUR of various species of plant cells reported in the literature and found that the specific OUR ranges from 0.03 mmol O₂/h -g dry wt for tobacco cells to 3.6 mmol O₂/h -g dry wt for sugar cane. Pepin *et al.* (1995) has also surveyed OUR for plant cells presented in the literature and found that specific OURs typically ranged from 0.25 to 1.0 mmol O₂/h -g dry wt. It is envisaged that carrot cultures tested in the Couette viscometer for this work would have a cell density of at least 0.005 g dry wt/ml. If we assume a mid range value of specific OUR reported in the literature, say 0.33 mmol O₂/h -g dry wt, this would imply an oxygen uptake rate of 0.0017 mmol O₂/h -ml in the Couette viscometer. The carrot cell line used in this work has been provided by the Australian Commonwealth Scientific & Industrial Research Organisation (CSIRO) and they have recommended a growth temperature of 27°C. The saturation concentration for dissolved oxygen at this temperature in pure water is 0.256 mM or 0.000256 mmol/ml. Based on the value of the oxygen uptake rate estimated above and excluding mass transfer from the free surface at the top of the annular gap, all of the oxygen present in the Couette viscometer would be consumed within 10 minutes. Of course, realistically, it would take longer than 10 minutes as the OUR of the plant cells would diminish as oxygen was depleted, and oxygen would be replenished via mass transfer into the annulus from the air at the top of the annular gap. However, shear tests performed in this study are expected to have a similar or greater

duration than those performed in a Couette viscometer by Rosenberg (1989) which had a maximum duration of one hour. Therefore, this simple calculation suggests that the Couette-type viscometer may not provide sufficient oxygenation for the shear testing that is proposed.

To resolve this uncertainty, a more detailed mathematical model was used to simulate the oxygen transfer and consumption in the annular gap of a Couette viscometer. The model, the method of solution and predictions of dissolved oxygen concentrations in the viscometer made by simulation are detailed in the following sections.

4.5.2 Mathematical model

In the case where oxygen diffuses into the annulus from the air at the top of the annular gap, it can be assumed that the oxygen concentration in the annular gap is independent of radial (r) and angular position (θ) and is only a function of depth or axial position (z), as depicted in Figure 4-5. Consider a differential element of fluid, ∂z , in the annular gap. A mass balance on oxygen, assuming constant fluid density, for the differential element is:

$$N_{O_2} A_a \Big|_z + R_{O_2} A_a \cdot \partial z = N_{O_2} A_a \Big|_{z+\partial z} + \frac{\partial(c_{O_2} A_a \cdot \partial z)}{\partial t} \quad (\text{Eq 4-11})$$

where,

N_{O_2} = Axial mass flux of oxygen ($\text{mmol/m}^2 \cdot \text{s}$);

A_a = Cross-sectional area of the annular gap (m^2);

R_{O_2} = Volumetric generation or consumption of oxygen by plant cells ($\text{mmol/m}^3 \cdot \text{s}$);

c_{O_2} = Dissolved oxygen concentration (mmol/m^3);

t = Time (s)

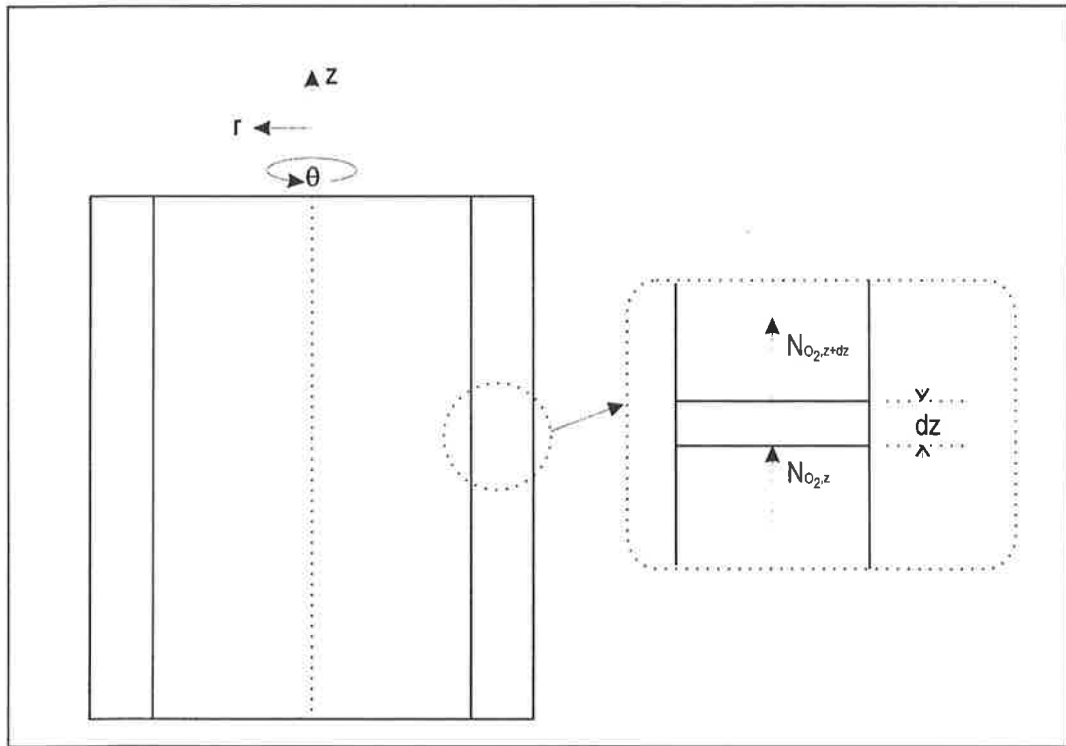


Figure 4-5: Schematic diagram of oxygen transfer in annular gap of the Couette viscometer.

Equation 4-11 above can be rearranged to yield:

$$-\frac{\partial N_{O_2}}{\partial z} + R_{O_2} = \frac{\partial c_{O_2}}{\partial t} \quad (\text{Eq 4-12})$$

From Fick's first law of diffusion, the molar flux of oxygen diffusion in the axial direction can be described by:

$$N_{O_2} = -D_{O_2} \frac{\partial c_{O_2}}{\partial z} \quad (\text{Eq 4-13})$$

where,

D_{O_2} = Diffusion coefficient for oxygen in water (m^2/s);

The diffusion coefficient for oxygen in water may be assumed to be invariant with oxygen concentration. It is also assumed that the oxygen diffusion rate in the axial direction is not enhanced by the tangential laminar fluid flow in the annulus.

Substituting Equation 4-13 into Equation 4-12 gives:

$$D_{O_2} \frac{\partial^2 c_{O_2}}{\partial z^2} + R_{O_2} = \frac{\partial c_{O_2}}{\partial t} \quad (\text{Eq 4-14})$$

Equation 4-14 describes the time-variant spatial distribution (in the axial direction) of dissolved oxygen concentration in the annular gap. The initial and boundary conditions that apply to Equation 4-14 for the shear test conditions would be:

$$\text{I.C. } t = 0: \quad c_{O_2} = c_{O_2} \Big|_{t=0}$$

$$\text{B.C. } z = L:$$

$$-D_{O_2} \frac{\partial c_{O_2}}{\partial z} \Big|_{z=L} = \frac{k_{O_2}}{R \cdot T} (p_{O_2,b} - p_{O_2} \Big|_{z=L}) = \frac{k_{O_2}}{H \cdot R \cdot T} (c_{O_2,b} - c_{O_2} \Big|_{z=L})$$

$$z = 0:$$

$$-D_{O_2} \frac{\partial c_{O_2}}{\partial z} \Big|_{z=0} = 0$$

where,

$z = L$ represents the top of the annulus, a free surface exposed to air (m);

$z = 0$ represents the base of the annulus, a solid surface wall (m);

$c_{O_2}|_{t=0}$ is the initial dissolved oxygen concentration in the annulus, assumed to have the same value irrespective of axial position (mmol/m³);

$\left. \frac{\partial c_{O_2}}{\partial z} \right|_{z=L}$ is the dissolved oxygen concentration gradient at the air-liquid interface at the top of the annulus;

k_{O_2} is the mass transfer coefficient for oxygen on the air-side (m/s);

$p_{O_2,b}$ is the air-side oxygen partial pressure (Pa);

$p_{O_2}|_{z=L}$ is the oxygen partial pressure at the air-liquid interface at the top of the annulus (Pa);

H is the Henry's law constant for oxygen in water (mmol/m³·Pa)

R is the universal gas constant (J/K·mol)

T is the temperature (K)

c_b is the saturated concentration of dissolved oxygen equilibrated (Henry's law) with oxygen in air at partial pressure $p_{O_2,b}$;

$c_{O_2}|_{z=L}$ is the concentration of dissolved oxygen equilibrated (Henry's law) with oxygen in air at partial pressure $p_{O_2}|_{z=L}$ (mmol/m³);

$\left. \frac{\partial c_{O_2}}{\partial z} \right|_{z=0}$ is the dissolved oxygen concentration gradient at the solid wall at the base of the annulus;

It is common practice to describe the substrate consumption term of cellular organisms in suspended cultures by Monod-type kinetics (Bailey and Ollis, 1986). A similar approach for the consumption term, R_{O_2} , in Equation 4-14 will be assumed for the purpose of this analysis:

$$R_{O_2} = -q_{O_2, \max} \frac{c_{O_2}}{K_{O_2} + c_{O_2}} X \quad (\text{Eq 4-15})$$

where,

$q_{O_2, \max}$ = Maximum specific oxygen consumption rate of the carrot cells
(mmol O₂ /g (cell wt)·s);

K_{O_2} = Monod coefficient for oxygen (mmol/m³) ;

X = Cell concentration (g/m³)

Equations 4-14 and 4-15 constitute the mathematical model that will be used to simulate the dissolved oxygen concentration in the annular gap of the Couette viscometer under shear testing conditions. For convenience of solution and analysis, the equations and the initial and boundary conditions can be transformed into a partially dimensionless format, as follows:

$$\bar{D} \frac{\partial^2 \bar{c}}{\partial \bar{z}^2} + \bar{R} = \frac{\partial \bar{c}}{\partial t} \quad (\text{Eq 4-16})$$

$$\bar{R} = -\bar{q} \frac{\bar{c}}{\bar{K} + \bar{c}} X \quad (\text{Eq 4-17})$$

$$\text{I.C. } t = 0: \quad \bar{c} = \bar{c}|_{t=0}$$

$$\text{B.C. } \bar{z} = 1: \quad -\bar{D} \frac{\partial \bar{c}}{\partial \bar{z}} \Big|_{\bar{z}=1} = \bar{k}(\bar{c}_b - \bar{c}|_{\bar{z}=1})$$

$$\bar{z} = 0: \quad -\bar{D} \frac{\partial \bar{c}}{\partial \bar{z}} \Big|_{\bar{z}=0} = 0$$

where,

$$\bar{c} = \frac{c_{O_2}}{c_s};$$

c_s = Arbitrarily selected concentration value used to non-dimensionlise c_{O_2} ;

$$\bar{c}_b = \frac{c_b}{c_s};$$

$$\bar{D} = \frac{D_{O_2}}{L^2};$$

$$\bar{R} = \frac{R_{O_2}}{c_s};$$

$$\bar{K} = \frac{K_{O_2}}{c_s};$$

$$\bar{k} = \frac{k_{O_2}}{H \cdot R \cdot T \cdot L};$$

$$\bar{q} = \frac{q_{O_2, \max}}{c_s}$$

4.5.3 Model solution - Numerical solution strategy

Equation 4-16 is a partial differential equation with a non-linear term represented by Equation 4-17. An analytical solution is not possible, instead it must be solved numerically.

To achieve this, Equation 4-15 was transformed to a system of ordinary differential equations by discretisation of the spatial coordinate using a finite element method: orthogonal collocation. This method involves approximating the spatial distribution of dissolved oxygen in the annular gap using interpolatory polynomials. (The orthogonal collocation technique is a well established and widely applied method. Finlayson (1972) provides an excellent exposition and examples of its application.) The same symmetrical polynomials described by Finlayson (1972) were employed. Collocation points, which are the roots of the polynomials, were deduced from tables listed in Stroud

and Secret (1966). The resulting system of ordinary differential equations are summarised as follows.

$$\bar{D} \sum_{k=1}^{N+1} M_{i,k} \bar{c}_k + \bar{R}_i = \frac{\partial \bar{c}_i}{\partial t}, i = 1, 2, \dots, N+1 \quad (\text{Eq 4-18})$$

where,

N = Number of internal collocation points;

M = The same as matrix B defined by Finlayson (1972).

Note that the ordinary differential equation in Equation 4-18 for $l = N+1$, which is the collocation point at the top of the annular gap, can be disregarded since the value of the dissolved oxygen concentration can be obtained from the boundary condition at $\bar{z} = 1$:

$$\bar{c}|_{\bar{z}=1} = \frac{\bar{k}/\bar{D} \bar{c}_b + \sum_{j=1}^N A_{N+1,j} \bar{c}_j}{A_{N+1,N+1} + \bar{k}/\bar{D}} \quad (\text{Eq 4-19})$$

where,

A = The same matrix defined by Finlayson (1972).

The system of ordinary differential equations in Equation 4-18 for $l = 1$ to N , in conjunction with Equation 4-19, can then be integrated to obtain the concentration profiles in the annular gap at various exposure periods.

The numerical solution strategy for the model was encoded as a Mathcad 5+ (Mathsoft Inc., Cambridge, MA) simulation file using a standard fourth order Runge-Kutta library algorithm for integration of the ordinary differential equations.

4.5.4 Model parameters

The principal parameters of the model described by Equations 4-6 and 4-7 and the values that were assumed for simulation in following sections are summarised in Table 4-2. Brief notes on how these values were established or calculated are discussed below.

It has already been established that a gap width of approximately 600 μm is desirable for the Couette viscometer (see Section 4.4). To provide sufficient volume of cell culture for assay purposes after shear exposures, at least 15 ml is needed. Thus, the depth of the annulus should be approximately 6 cm.

A typical value for the diffusion coefficient for oxygen in pure water is around $2.25 \times 10^{-5} \text{ cm}^2/\text{s}$ (Bailey and Ollis, 1986). Bailey and Ollis (1986) noted that the actual oxygen diffusion coefficient in cell cultures is usually less than in pure water. As the cell concentrations that would be present during shear testing is low, a value of $2 \times 10^{-5} \text{ cm}^2/\text{s}$ was used for the simulation.

The solubility of dissolved oxygen in pure water at 27°C , the temperature at which shear testing is likely to be performed, is 0.256 mmol/l. This value was assumed for the initial dissolved oxygen concentration in the annulus, $c_{\text{O}_2}|_{t=0}$. It would also therefore be the dissolved oxygen concentration in equilibrium with oxygen in air, c_b . This value was additionally used as the concentration value to non-dimensionlise the model equations, c_s .

The mid range value of 0.33 mmol/hr·g (dry wt) for oxygen uptake rate assumed earlier for the preliminary calculation was also applied to model simulations.

Kessel (1972) has investigated the critical oxygen concentration, where growth becomes oxygen limited, for carrot cells. He found that the critical concentration was 0.04 mM or 16% air saturation. Based on the results of Cho and Wang (1990) the Monod coefficient was assumed to be 10% of saturation for the purpose of this analysis.

No published value or method for directly calculating the mass transfer coefficient from a stationary gas to a fluid in a rotating annulus could be found. Instead, the mass transfer coefficient was estimated from generic correlations presented in Foust *et al.*

(1980) for gas-phase mass transfer to laminar and turbulent fluid flowing over wetted walls and plates. A bowl diameter of approximately 10 cm and rotational speed of 1200 rpm were assumed to calculate the velocity of the fluid in the annulus.

Standard physical and transport properties for oxygen in air and dissolved in water at ambient temperatures were used for other parameters.

Table 4-2: Principal model parameters and assumed values for model simulation of a conventional Couette viscometer.

Parameter	Symbol	Assumed Value
Length (Annulus Depth)	L	6 cm
Oxygen Diffusivity -Culture Broth	D_{O_2}	$2 \times 10^{-9} \text{ m}^2/\text{s}$
Dimensionalising Oxygen Concentration	c_s	0.256 mmol/l
Maximum Specific Oxygen Consumption Rate	$q_{O_2, \max}$	0.33 mmol/hr·g (dry wt)
Plant Cell Concentration	X	0.005 g (dry wt.)/ml
Monod coefficient	K_{O_2}	0.026 mmol/l
Saturated dissolved oxygen concentration in equilibrium with oxygen in air at T = 300K	c_b	0.256 mmol/l
Mass transfer coefficient	k_{O_2}	0.161 m/s
Henry's law constant	H	$1.199 \times 10^{-5} \text{ mmol/l} \cdot \text{Pa}$
Initial oxygen concentration	$c_{O_2} \Big _{t=0}$	0.256 mmol/l

4.5.5 Simulation results

To establish the optimal numerical parameters for the model, a sequence of simulations were performed using the model parameters at various numbers of internal collocation points. The results are summarised in Figure 4-6, which depicts the spatial concentration profile for dissolved oxygen at a simulation time of 1800 seconds.

Figure 4-6 suggests that more than 9 internal collocation points would be needed to obtain a perfectly converged numerical solution for the simulation. However, the numerical solution is stable and sufficiently converged at 9 collocation points to establish the behaviour of the system.

Figure 4-7 shows the variation in concentration profiles in the annulus with time (from 0 to 3600 seconds) as simulated by the model using 9 internal collocation points. It suggests that the dissolved oxygen will drop below the critical concentration (16 % saturation) within 12 minutes even with mass transfer from air above the annular gap. This result is almost identical to the preliminary calculation, and strongly suggests that adequate oxygenation might not be available in the Couette viscometer to maintain viable carrot cell cultures. Furthermore, inspection of the concentration profile at $\bar{z} = 1$ indicates that the dissolved oxygen concentration is at or just below its saturated level at the top of the annulus during the entire simulation. This suggests that improved oxygenation could not be achieved by increasing the mass transfer rate – there is simply not enough surface area for sufficient mass transfer to take place to replenish the oxygen that would be consumed by the plant cells in the annulus.

This raises grave concerns that the conventional Couette viscometer design, modelled in this section, would not be suitable for shear-testing of carrot cells. Thus, an alternative viscometer design is considered in the next section.

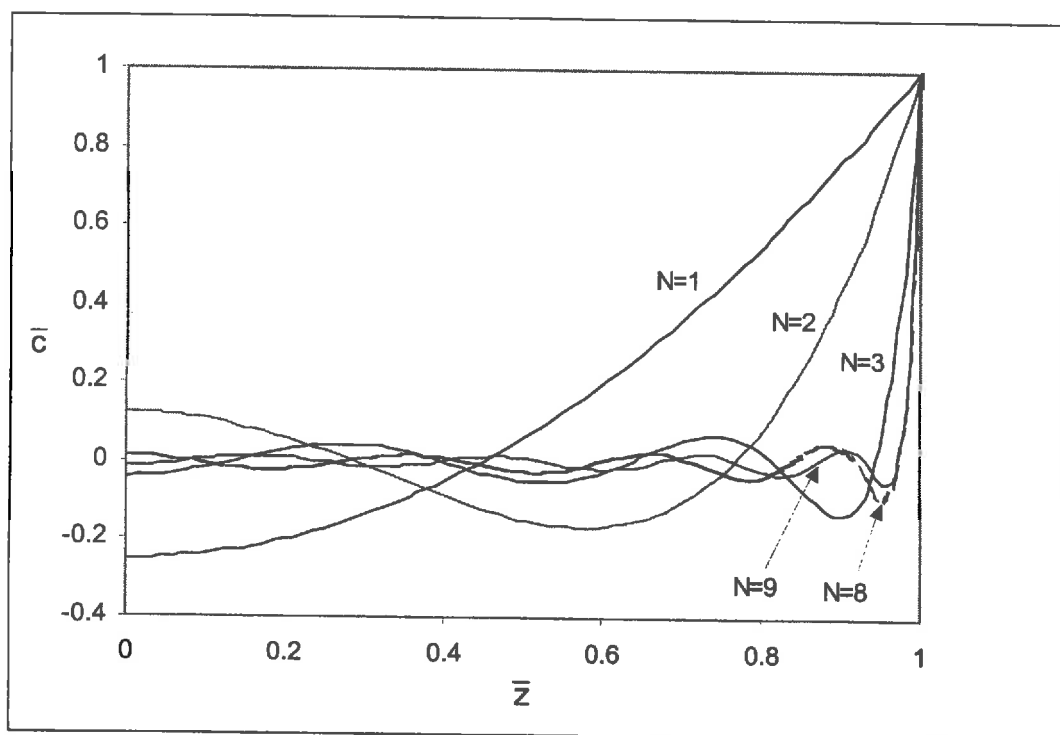


Figure 4-6: Variation in model solution with number of internal collocation points, N at a simulation time of 1800 s.

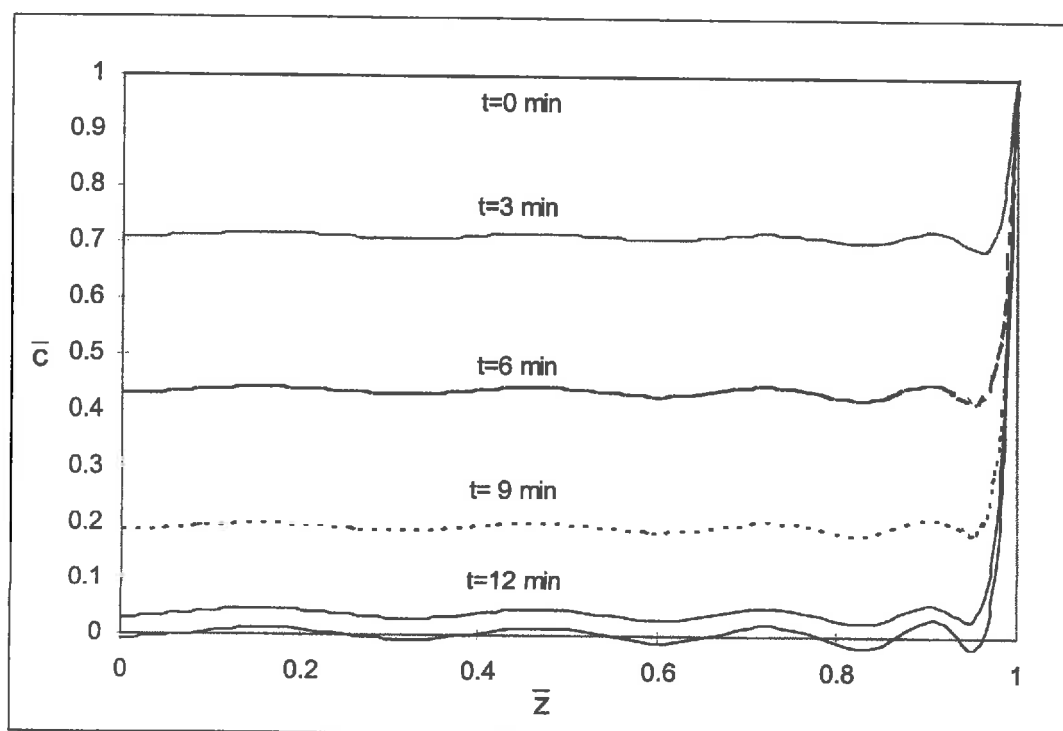


Figure 4-7: Simulated variation in dissolved oxygen concentration axial profile with time, $N=9$, conventional Couette design.

4.5.6 *Alternative viscometer design*

One way of overcoming the problem identified above with the current viscometer design would be to increase the surface area in contact with air available for re-oxygenation of the viscometer annulus. This could be achieved by making the surfaces of either the bowl or the bob permeable to oxygen in some way. For instance, a number of polymers are known to be oxygen-permeable, such as silicone rubber and polyethylene, and are also impermeable to water, making them ideal for shearing of liquid cultures. However, most of these polymers are difficult to machine and would not be strong enough to withstand the vigorous forces that would be exerted on them when the bowl is rotated at speeds of up to 1000 rpm. This problem could be overcome by using a porous material, for example, ceramic. This material could be easily machined, would be rigid enough to withstand the mechanical forces during rotation, and could also be lined with the oxygen-permeable polymer so that it faced the annular gap to allow for oxygen permeability.

Preliminary investigations of whether such a construction was feasible were undertaken. It was discovered that a porous ceramic bowl lined with a smooth and consistent layer of silicone rubber spun cast onto the inner surface could be easily constructed. The thickness of the silicone rubber was approximately 1 mm.

To determine whether such a design could provide sufficient oxygenation of the annulus, the mathematical model developed earlier was revised to simulate the radial concentration profile in the annulus that would be produced in an oxygen-permeable bowl. In this situation, mass transfer from the free surface at the top of the annulus should not be important and only mass transfer through the oxygen-permeable bowl needs to be considered. Furthermore, the small gap width proposed (600 μm) relative to the likely bowl diameter (~ 10 cm) means that radial variations will be insignificant. This enables the problem to be treated as a one-dimensional system, similar to the previous model, but with slightly different boundary conditions. Equations 4-16 and 4-17 still apply; with the exception that z is now used to represent radial direction instead of axial direction. The initial condition is also unchanged, as is the boundary condition at $\bar{z} = 0$, the solid surface of the bob. However, a new boundary condition is required at $\bar{z} = 1$, which is the oxygen-permeable surface of the bowl. This new boundary condition is:

$$\text{B.C. } \bar{z} = 1: \quad -\bar{D} \frac{\partial \bar{c}}{\partial \bar{z}} \bigg|_{\bar{z}=1} = -\bar{D}_s \frac{(\bar{c}_b - \bar{c}|_{\bar{z}=1})}{\Delta x}$$

where,

$\bar{D}_s = \eta \frac{D_s}{H \cdot R \cdot T \cdot L}$ = Partially dimensionless oxygen diffusion coefficient in the oxygen-permeable surface silicone layer;

Δx = Dimensionless thickness of the silicone rubber;

η = Porosity of the ceramic bowl, which reduces the mass transfer surface area

All other parameters remain the same except where they are re-defined to suit the re-orientation of the coordinate system.

This boundary condition assumes that the concentration gradient in the annulus at the silicon surface is equal to the concentration gradient caused by mass transfer from the air at the porous ceramic bowl-silicone interface through the silicon rubber. In this respect, it is assumed that gas-phase diffusion of oxygen would be sufficiently rapid to avoid any mass-transfer limitations in the voids of the ceramic bowl, and thus the oxygen concentration at the ceramic bowl-silicone interface would be the same as that in air.

Table 4-3 contains the values of existing model parameters where modified and the new parameters assumed for simulation. The diffusion coefficient for oxygen in silicone was reported in Charati and Stern (1998). Again, it is assumed that the diffusivity of oxygen in water (D_{O_2}) for diffusion in the radial direction is not affected by the tangential laminar fluid flow and centripetal forces. The same numerical strategy was applied to solve the model.

Table 4-3: Principal model parameters and assumed values for model simulation of alternative Couette viscometer.

Parameter	Symbol	Assumed Value
Gap Width	L	600 μm
Oxygen diffusivity in silicone rubber	D_s	$4.1 \times 10^{-9} \text{ m}^2/\text{s}$
Ceramic bowl porosity	η	0.3
Silicone Rubber Thickness	Δx	1200 μm

Figure 4-8 presents the model simulations for different numbers of internal collocation points at a simulation time of 1800 seconds. The figure shows that the solution obtained was identical for both one and two internal collocation points. This suggests that a stable and converged numerical solution for the problem only requires one internal collocation point.

Figure 4-9 shows the variation in radial dissolved oxygen concentration profiles in the annulus with time from 0 to 3600 seconds predicted by simulation of the model at 2 internal collocation points. The figure suggests that the dissolved oxygen will drop quickly, but reach a steady state within 3 minutes, where re-oxygenation through the oxygen-permeable wall of the bowl would match the rate of oxygen consumption by the plant cells.

The model simulations suggest that the Couette viscometer with oxygen-permeable walls would be able to provide sufficient oxygenation of the cells during shear testing. However, some of the values for the model parameters used in the simulation had to be approximated as no accurate values were published. To resolve this uncertainty, the conclusions derived from the modelling study will be experimentally tested later by constructing two viscometer bowls: one with oxygen-permeable walls and another with oxygen-impermeable, stainless steel walls, and measuring the dissolved oxygen concentration of carrot cultures in the annular gap after a given period. The results of this comparison will be presented in Chapter 7.

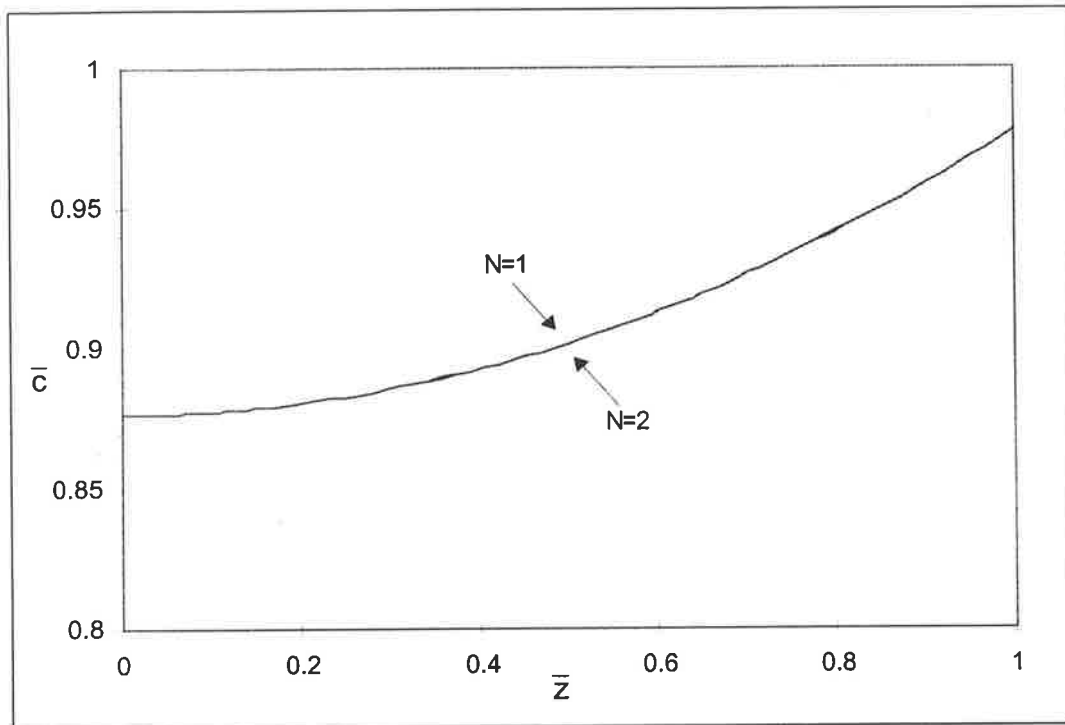


Figure 4-8: Variation in model solution with number of internal collocation points for the oxygen-permeable Couette viscometer at a simulation time of 1800 s.

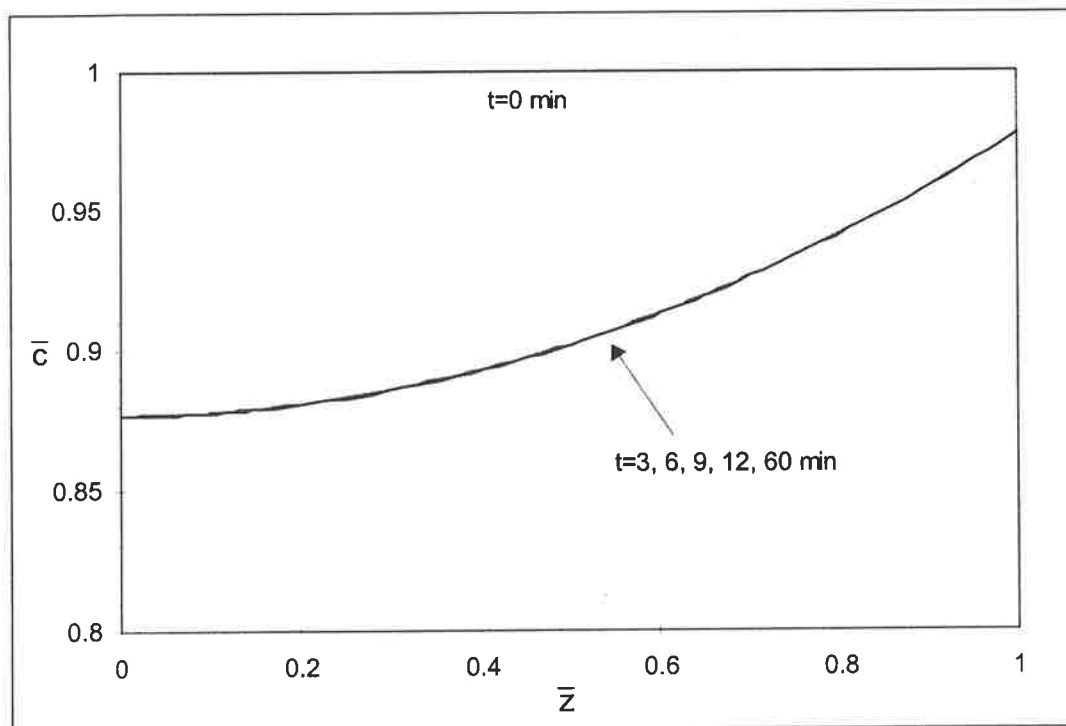


Figure 4-9: Simulated variation in dissolved oxygen concentration radial profile with time, $N=9$, oxygen-permeable Couette viscometer.

4.6 Temperature control

Temperature control is another important aspect of the viscometer design. Temperature not only affects the rheological properties of the culture fluid, which in turn affects the shear stress and rate, it can also have a direct impact on the physiological state of the plant cells. Various means of temperature control have been used in commercial viscometers (Whorlow, 1992), including air thermostat, liquid thermostat, electrical heating and Peltier heating/cooling. Taking into account the ease of construction and the fact that the operating temperature for this study was close to ambient, an air thermostat method was deemed adequate for this study. A Perspex ring was constructed to enclose the viscometer cylinders in a thermostat-controlled environment. The temperature of the air circulating around the viscometer cylinders can be maintained at a pre-set temperature by forced convection heating through a heater-fan connected to a PID temperature controller. Preliminary calculations to estimate the temperature rise due to shearing were carried out and are described below.

Assuming that the temperature rise is sufficiently small that the viscosity of the fluid is not significantly changed, the viscous energy dissipated per unit volume per second (ϵ_v) is given by

$$\epsilon_v = \tau \dot{\gamma} \quad (\text{Eq 4-20})$$

where τ is the shear stress and $\dot{\gamma}$ is the shear rate (Whorlow, 1992). If the annular gap is much smaller than the radius (i.e. gap/radius $\ll 1$), the heat transfer situation in the annular gap can be approximated by a pair of parallel plates, as illustrated in Figure 4-10.

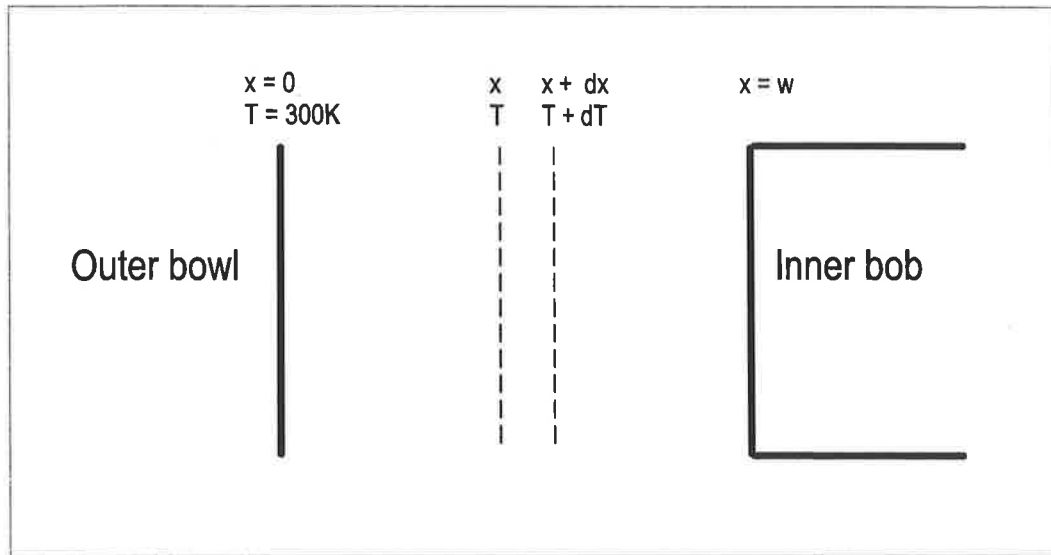


Figure 4-10: Schematic of heat transfer across viscometer gap.

A heat balance across the gap gives

$$-k' \left. \frac{dT}{dx} \right|_x + k' \left. \frac{dT}{dx} \right|_{x+\delta x} = k' \frac{d^2T}{dx^2} \delta x \quad (\text{Eq 4-21})$$

where k' is the thermal conductivity of the fluid = 0.61 W / m K (for water)

and T is the temperature (K).

At steady state,

$$k' \frac{d^2T}{dx^2} = -\tau \dot{\gamma} \quad (\text{Eq 4-22})$$

assuming that fluid flow across the planes of constant velocity is negligible for laminar flow conditions.

In addition, assume that the thermal resistance of the outer bowl is negligible compared to the fluid. In practice, the outer bowl and rotor can be allowed to attain

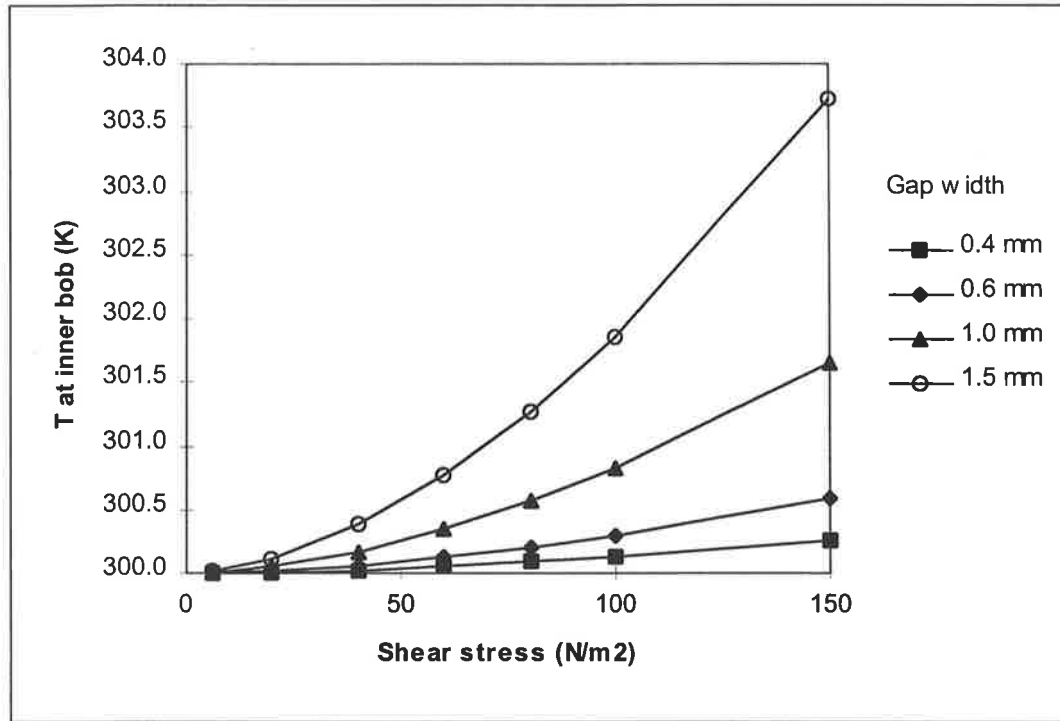


Figure 4-11: Variation of temperature at surface of inner bob with average shear stress for different gap widths.

thermal equilibrium with the surrounding air before the culture is loaded into the viscometer gap. Equation 4-7 can be integrated using the following boundary conditions

B.C.1 $x = 0$: $T = 27^\circ\text{C}$ or 300 K (outer bowl maintained at 27°C)

B.C.2 $x = w$: $\frac{dT}{dx} = 0$ (thermal equilibrium at the inner cylinder)

Thus, integrating Equation 4-7 gives

$$T = \frac{\tau\dot{\gamma}}{2k'}x(2w - x) + 300 \quad (\text{Eq 4-23})$$

Figure 4-11 illustrates the variation in temperature at the surface of the inner bob with the applied shear stress for different gap widths. The figure shows that the temperature rise due to shearing at the maximum shear stress used in this study (100 N/m^2) was less than 0.5°C for gap widths around 0.6 mm . From a study of the effect of temperature on

ion channel activity, a temperature change of at least 2 °C was required to cause any observable change in ion channel activity (Ding and Pickard, 1993b). Hence, changes in the biological response of the cells sheared in the viscometer are more likely to be due to the hydrodynamic shear stress, than to temperature effects. However, shear-induced temperature fluctuations in the micro-environment around each cell aggregate cannot be ruled out. Nevertheless, such temperature fluctuations in the micro-environment would also occur in any shear device, including bioreactors.

4.7 Sterility

Sterile operation is required so that the sheared cultures can be assayed for regrowth. Moreover, removal of pathogenic contaminants will reduce the likelihood of unwanted biological responses induced by pathogen attack of the plant cells. The most convenient method of sterilising equipment is autoclaving. Therefore, materials of construction must be selected to withstand the autoclaving treatment. The inner bob and top cover of the Couette was constructed from autoclaveable stainless steel. Although the porous ceramic bowl and silicone polymer can withstand a limited amount of autoclaving, it was thought that repeated autoclaving might affect the porosity and strength of the ceramic material. Therefore, an alternative method of sterilising the outer ceramic bowl had to be used. Careful washing of the inner surface of the outer bowl with 95% ethanol, inside a laminar flow cabinet, was found to be adequate. The inner silicone-coated surface of the outer bowl and the stainless steel base was sterilised with two washes of 95% ethanol, followed by multiple washes with sterile carrot medium prior to use. The bowl was then placed in a laminar flow cabinet to dry for at least 30 min. In addition, the entire shear viscometer set up was compact enough to fit into a standard laminar flow cabinet, and aseptic techniques were used throughout the shear testing procedure.

4.8 Description of apparatus

Figure 4-12 shows a photograph of the oxygen-permeable Couette viscometer along with a schematic diagram of the viscometer bowl-bob section. The dimensions of the viscometer inner bob and outer bowl are given in Table 4-4.

The outer bowl consisted of a stainless steel base with a pulley wheel coupled to a variable speed motor assembly. A pulley-belt system was used to extend the maximum rotation speed of the bowl to 1200 rpm. The sidewall of the outer bowl was constructed from porous ceramic material. To create an oxygen-permeable, smooth surface on the inner face of the ceramic bowl, a thin layer of air-cured silicone polymer (Dow Corning) was first applied to the surface and allowed to cure completely. Next, a layer of semi-cured silicone polymer (RTV, Dow Corning) was spun coated onto the first layer to form a smooth finish. The inner bob and top lid were constructed from stainless steel.

The base of the outer bowl assembly rested on a thin layer of Teflon to reduce friction. Guideposts helped to keep the inner bob stationary and the bowl-bob assembly stable while spinning.

The fully cured silicone polymer did not appear to be toxic to the carrot cells. Silicone polymer tubings are commonly used in bioreactor cultivations of plant, animal and microbial cells. Carrot cells exposed to the silicone polymer continued to grow normally when plated on agar medium, and showed similar properties in terms of mitochondrial activity and oxygen uptake rate compared to shake flask cultures. This can be seen, in passing, in the results presented in Chapter 7 for low shear stresses.

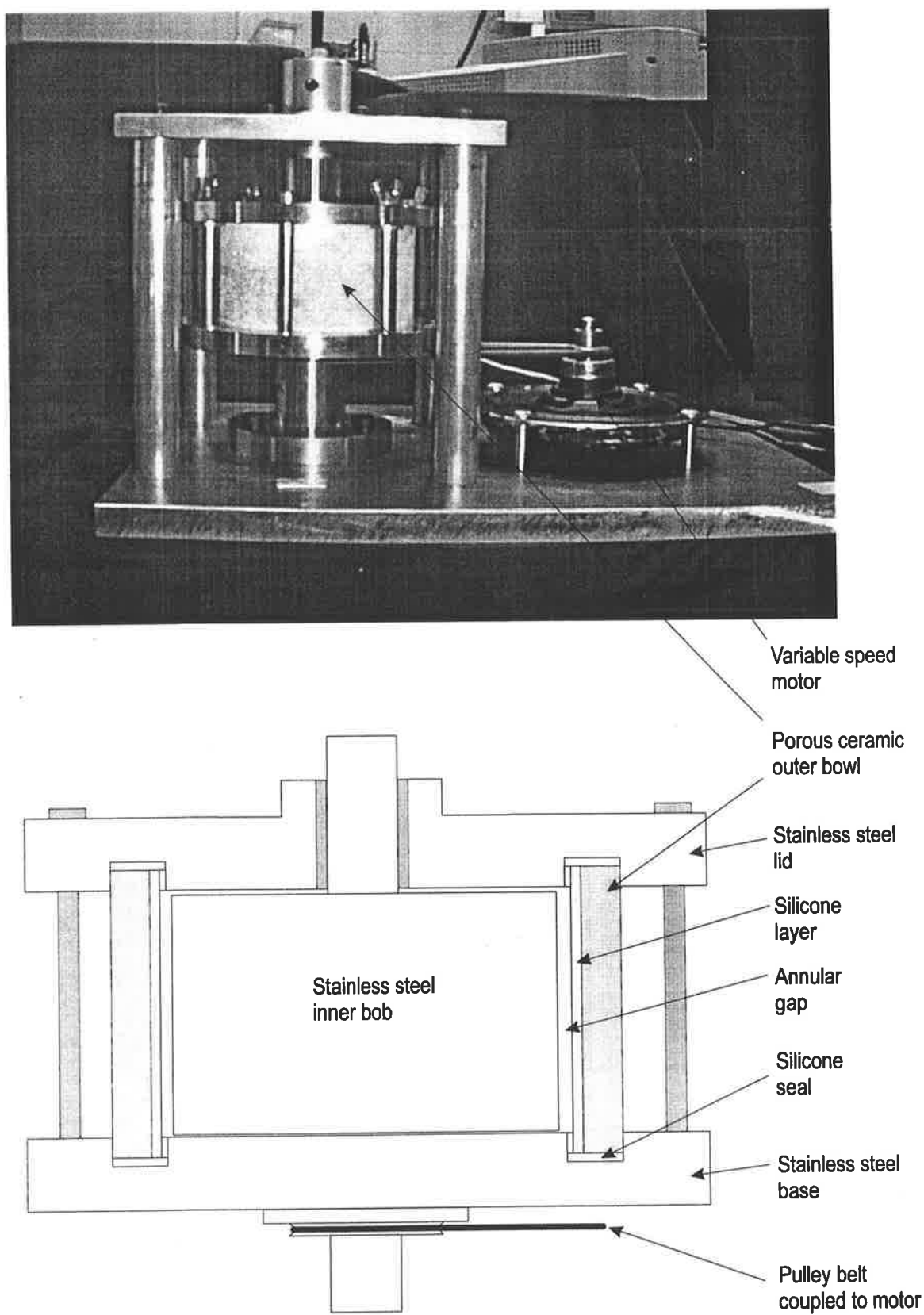


Figure 4-12: Photograph of oxygen-permeable Couette viscometer and schematic of inner bob-outer bowl section.

Table 4-4: Dimensions of oxygen-permeable Couette viscometer.

<i>Outer ceramic bowl (with silicone polymer layer)</i>	
Inner diameter	101.6 ± 0.23 mm
Outer diameter	122.6 ± 0.19 mm
Height	63.1 ± 0.22 mm
Thickness of silicone layer	1.2 mm
<i>Inner bob</i>	
Outer diameter	100.3 ± 0.04 mm
Gap width	0.625 mm

CHAPTER 5

EXPERIMENTAL METHODS

5.1 Cell culture and medium

The suspension cultures of *Daucus carota* (wild type) and callus cultures of *Nicotiana plumbaginifolia* were a gift from Commonwealth Scientific and Industrial Research Organisation (Sydney, Australia). Tobacco suspension cultures were initiated by transferring the callus to liquid medium. Both suspension cultures were maintained in 250 ml Erlenmeyer flasks containing 50 ml of medium and incubated in the dark at 27°C on a gyratory shaker at 100 rpm. The flasks had cotton bungs to allow oxygen permeation into the flasks. The carrot cultures were subcultured every 2 weeks using a 1:9 seed culture to fresh medium volume ratio (i.e. 5 ml of 14-day culture was inoculated into 45 ml of fresh medium), while the tobacco cultures were subcultured every week using a 1:3 volume ratio.

The wild carrot medium includes 0.5 mg/l 2,4-dichlorophenoxyacetic acid (2,4-D), 3 mg/l thiamine and 20 g/l sucrose. The full formulation of the carrot medium can be found in Appendix A. The pH of the medium was adjusted to 5.4 with 0.1M potassium hydroxide before autoclaving at 121°C for 20 minutes. The tobacco medium contains 2 mg/l 2,4-D, 0.05 mg/l kinetin and 30g/l sucrose, pH adjusted to 5.8 before autoclaving. All chemicals used in the medium, with the exception of sucrose, were of “plant cell culture tested” grade and were obtained from Sigma (St. Louis, MO). The sucrose used was of common table sugar grade. MilliQ water was used in all medium preparation.

Callus cultures of the carrot cells were also maintained at 27°C in the dark on agar medium. The agar medium is similar to the liquid medium used for suspension cultures except for the inclusion of 10 g/l agar (Oxoid bacteriological agar No. 1). The callus cultures were used as a back up to re-initiate the suspension cultures in case the suspension cultures became contaminated.

5.2 Chemicals

Stock solutions of verapamil, W7 and NPPB were prepared by dissolving in dimethyl sulfoxide, DMSO (plant-culture tested grade) and stored at -20°C for no longer than 3 months. Precautions were taken to limit exposure of verapamil to light. The final concentration of DMSO in the test cultures was less than 0.03% (v/v) and was not expected to affect the cells at that low concentration based on preliminary observations and other published results (for example, Jones and Mitchell, 1989). Stock solutions of ruthenium red were prepared by dissolving in MilliQ water and stored at -20°C. Stock solutions of the blockers/inhibitors were divided into small aliquots in microcentrifuge tubes and the amount required for experimentation defrosted just prior to use to avoid repeated thawing/freezing of the solutions. The stock solutions of the channel blockers were filter-sterilised through a 0.22 µm syringe filter into sterile microcentrifuge tubes during preparation. They were not sterilised again prior to addition into the shear-testing samples as the volume added was relatively minute. Stock solutions of the uncoupler, carbonyl cyanide p-trifluoromethoxyphenylhydrazone (FCCP) were prepared in 95% ethanol (analytical grade) and stored at 4°C. All chemicals were purchased from Sigma, except for ethanol, which was purchased from BDH (Australia).

5.3 Viscometer shear tests

5.3.1 Sample preparation

Thirteen to fourteen day old (late exponential growth phase) carrot cultures were pre-screened to aggregate sizes below 263 µm using stainless steel mesh (Sigma) and the cell density adjusted to approximately 0.05 g (fresh wt)/ml by re-suspension in fresh culture medium prior to shear testing. The sieving procedure was conducted in a laminar flow hood using aseptic techniques. All pipetting was carried out with sterile, wide-bore pipettes.

5.3.2 Shear tests in viscometer

For the preliminary investigations presented in Section 7.5, 17 ml of pre-screened carrot cultures were sheared at rotational speeds between 160 and 1190 rpm for periods of up to 8 h. The rotational speed and shearing period for each run was randomly

chosen. Duplicate runs of some tests were conducted at each speed and shearing period for verification purposes.

The inner bob and top lid were autoclaved before each shear run. The silicone-coated surface of the outer bowl was sterilised by ethanol washes as described in Section 4.7. The Perspex air-heater enclosure was also swabbed with 95% ethanol and left to dry inside the laminar flow cabinet. The viscometer bowl and bob and the Perspex air-heater enclosure were then assembled inside the laminar flow cabinet. The air-heater was set to 27°C and the viscometer bowl assembly left to stand for about 15 min to allow the bowl to get close to the surrounding air temperature. The pre-screened carrot cultures were then pipetted into the annular gap of the viscometer using wide-bore pipettes. The time taken to load the cell culture into the viscometer and secure the top lid was approximately 2 mins. During shear tests, pre-screened carrot cultures were maintained in 250 ml Erlenmeyer flasks on a shaker table at 100 rpm and 27°C as controls.

After each shear run, the viscometer was disassembled inside the laminar flow cabinet and samples of the sheared and control cultures were taken for measurement of coupled and uncoupled OUR, regrowth potential, mitochondrial activity and membrane integrity. The remainder of the sheared culture was transferred from the viscometer to a 250 ml Erlenmeyer flask maintained at 100 rpm, 27°C. Further samples of sheared and control cultures were taken after 30, 60 and 120 min and measurements of OUR performed. The maximum value of coupled OUR and average value of uncoupled OUR observed during this 2 h period were recorded.

For the factorial design experiments presented in Chapter 8, various combinations of ion channel blockers or calmodulin inhibitor were added to the test cultures prior to shearing, according to the experimental plan described in Chapter 6. The chemicals were added to the pre-screened cultures and allowed to incubate in shake flasks (27°C, 100 rpm, dark) for approximately 15 mins before loading into the shear viscometer. The cultures were then sheared at either 600 (38 N/m²) or 1200 rpm (100 N/m²) for an hour. At the same time, 20 ml of the pre-screened carrot culture with no blocker treatment was kept in a 250 ml shake flask at 100 rpm, 27°C, in the dark. This is referred to as "Control - " in Chapter 8. At the same time, 20 ml of pre-screened culture, treated with

the same chemicals as the sheared cells, was maintained in a separate 250 ml shake flask at 100 rpm, 27°C in the dark. This is referred to as “Control +”. The order of the factorial runs was randomised. After shearing, the mitochondrial activity, membrane integrity and OUR of both the sheared and control cultures were analyzed in the same manner as for the preliminary investigation experiments, except that OUR measurements were taken at 0, 30 and 90 mins after cessation of shearing.

The concentrations of blockers used in this study was based on typical values found in the literature and are listed in Table 5-1.

Table 5-1: Concentration and function of blockers used in factorial experiment

Chemical	Function	Concentration	Reference
W7	Inhibits calmodulin, a calcium-binding protein	30 μ M	(Snedden <i>et al.</i> , 1995; Takeda <i>et al.</i> , 1998)
Ruthenium red	Blocks mitochondrial and endoplasmic reticulum Ca^{2+} channels	100 μ M	(Haley <i>et al.</i> , 1995)
Verapamil	Blocks voltage-operated Ca^{2+} channels in the plasmamembrane	10 μ M	(Castañeda and Pérez, 1996; Takeda <i>et al.</i> , 1998)
NPPB	Blocks Cl^- channels in the plasmamembrane	20 μ M	(Schroeder <i>et al.</i> , 1993)

5.3.3 Biological assays

5.3.3.1 Mitochondrial activity

Mitochondrial activity was determined by the triphenyl tetrazolium chloride (TTC) assay described by Towill and Mazur (1975). Four ml of TTC solution (6 g/l, pH 9.2) was added to 2 ml samples of carrot culture and incubated in the dark for 18 h at room temperature. TTC concentration, pH and incubation time for the assay had previously been optimised according to the technique proposed by Towill and Mazur (1975). After the incubation period, the cells in each sample were harvested and the formazan

extracted with 95% (v/v) ethanol until the cells were colourless. Formazan extraction took around 1.5 to 2 h in a 60°C water bath. The cells were then removed by centrifugation and the absorbance of the supernatant measured at 485 nm. The absorbance per g (fresh wt) of extracted cells was determined.

5.3.3.2 Membrane integrity

Membrane integrity was determined by fluorescein diacetate (FDA) staining (Widholm, 1972). FDA diffuses into the cells where it is hydrolysed by esterase enzymes into the fluorescent compound, fluorescein. Only live cells with an intact membrane will fluoresce under UV light. Samples of carrot culture were examined under a microscope (at 100X magnification) and the number of fluorescent cells in a particular field of view was determined by digital image analysis using the public domain Scion Image program (US National Institute of Health). This was then expressed as a proportion of the total cells in the field of view, evaluated from brightfield micrographs. At least 6 randomly chosen fields of view were observed for each sample and the mean proportion calculated.

5.3.3.3 Dissolved oxygen measurement & calculation of oxygen uptake rate

DO was measured using a Rank oxygen electrode, Model 10 Dissolved Oxygen system (Rank Brothers, Cambridge, UK) which operates by oxygen polarography. The electrode was attached to the base of a 3 ml Perspex sample chamber, separated from the solution in the chamber by a thin, O₂-permeable polyethylene membrane. The sample chamber was maintained at 25°C by a re-circulating water bath. Prior to testing, the electrode was calibrated against air-saturated medium.

Carrot cultures were pipetted into the sample chamber and the chamber capped with a Perspex plug. Precaution was taken to ensure no air bubbles were trapped in the sample chamber. After a steady rate of respiration was established, 25 µl 1M sucrose was added to the sample chamber through a small injection port in the cap to ensure sufficient substrate. DO was recorded for approximately 6 min. Coupled OUR was calculated from the rate of decline in DO (Zhang *et al.* 1999).

A 1 μ L aliquot of 0.5 mM FCCP, an uncoupling agent, was then added to the sample chamber. Uncoupled OUR was calculated from the rate of decline in DO over the following 6 min.

5.3.3.4 Regrowth ability

The ability of the carrot cells to regrow after shear exposure was assessed by a method adapted from the agarose bead assay described by Steinbrenner *et al.* (1989). Wild carrot medium supplemented with 0.02 g/ml agarose (Type VII, gelling temperature < 30°C, Sigma) was autoclaved and maintained at approximately 35°C in a water bath. Five ml of the agarose medium was mixed with an equal volume of carrot culture (sheared or control) in a sterile beaker maintained at approximately 35°C. Using aseptic techniques, ten 100 μ L droplets of the cell-agarose mixture was then carefully pipetted into a sterile polystyrene Petri dish and allowed to solidify at room temperature for an hour. At least 2 petri dishes containing 10 beads each were prepared from each culture sample. A piece of grided transparent overlay was adhered to the base of the Petri dish and each bead in the dish was numbered. The solidified agarose-cell beads were then covered with 5 ml of cell free medium containing equal proportions of conditioned and fresh medium (ie. 50% fresh medium + 50% conditioned medium). Conditioned medium refers to the cell free supernatant obtained after centrifugation of the 14-day culture. The lid was replaced onto each Petri dish and sealed with oxygen-permeable parafilm (Nesco, Japan). Each agarose bead was then examined under an inverted microscope and images of the cell aggregates were captured onto a computer using the Ulead Photo Express program (Ulead systems, CA). The position of the captured image relative to the grided overlay and the angle of focus was also recorded. The plates were subsequently incubated in the dark at 27°C. The same cell aggregates were then re-examined after 4-7 days. The number and size of cell aggregates in each digital image was determined using the Scion Image program. The plates were further kept at 27°C and after 2-3 weeks checked for callus formation. As both the shear exposure and assay procedure were conducted in a laminar flow cabinet under aseptic conditions, contamination of the plates was minimal and antibiotics were not required.

5.3.3.5 Precautions to limit variability in assay results

Preliminary experiments indicate that the results from the TTC assay had a larger degree of variability compared to the other assays. The following measures were taken to improve the reproducibility of the TTC results.

- Preliminary experiments suggested that pre-sieving of the cultures prior to shear testing improved the reproducibility of the TTC results (data not shown). This could be due to mass transfer limitations encountered in the larger cell aggregates. In this study, the carrot cultures were pre-screened to remove aggregates larger than 263 μm . This size was selected based on the size-distribution of the un-sieved carrot culture so that at least 50 % of the cells from the neat culture would be sieved through. A smaller mesh size would mean that an impractically large volume of culture would need to be sieved to obtain sufficient sample for shear testing. Furthermore, removing the larger aggregates would also reduce the likelihood that the cells would be subjected to grinding by the Couette walls. The choice of cell density of 0.05 g (FW)/ml was based on Rosenberg's work (1989). This cell density was found to be low enough to yield a suitable volume of <263 μm cell aggregates and high enough to give consistent results for the TTC assay.
- After pre-sieving, the cells were re-suspended in fresh medium before shear testing or maintaining as control culture. This ensured that there was sufficient substrate present during shear-testing and that the pH of the test culture was maintained close to 5.4.
- The TTC absorbance/g (fresh weight) readings of the control cells were monitored for each shear run. Runs in which the control readings were significantly different from the normal range were considered outliers and not included for analysis. The carrot cell line used in this study had TTC readings ranging from 15 to 20 absorbance units/g for the control (cultures maintained in a shake flask at 27°C, 100 rpm, in the dark).
- Only cells in the late exponential part of the growth cycle (days 13 to 14) were used for shear testing. Preliminary tests suggested that the TTC readings of late exponential cells were less variable compared to early exponential cells (data not shown). Furthermore, Hooker *et al.* (1989) found that cultured plant cells in the late

exponential growth phase were more susceptible to shear damage compared to the early exponential, lag or late stationary phases, thus suggesting that monitoring of shear sensitivity would be most critical for cells in the late exponential growth phase.

5.4 Patch-clamping

5.4.1 Protoplast isolation for patch-clamping

The procedure for protoplast isolation was adapted from the method used by Terry *et al.* (1991). Protoplasts were prepared from seven day old cultures of *D. carota* and *N. plumbaginifolia*. Attempts at isolating healthy protoplasts from late exponential phase (13-14 day) carrot cultures were not successful, probably because the cell wall was thicker in the older cultures. Other workers have also found that protoplasts were more readily obtained from cultures in the early to mid-exponential growth phase (Fairley, 1990). About 1 g (fresh weight) of cells was harvested by centrifugation. 10 ml of cellulase/pectolyase solution was added to the cells and incubated at 30°C in the dark for 2 h in a shaker-water bath. The cellulase/pectolyase solution consisted of 500 mM sorbitol, 5 mM 2-[N-morpholino]ethane-sulfonic acid (MES), 1 mM CaCl₂, 0.5% w/v polyvinylpyrrolidone (PVP-40), 0.5% w/v bovine serum albumin (BSA, fraction V), 0.8% w/v cellulase (Onozuka RS, Yakult Honsha, Tokyo) and 0.08% w/v pectolyase, pH 5.5. A further 10 ml of cellulase solution was then added and the cells incubated for a further 1 h. The cellulase solution was similar to the cellulase/pectolyase solution except for the exclusion of pectolyase and a higher pH of 5.8. The digest was filtered through fine muslin, centrifuged at 60g for 5 min at 4°C and the pellet resuspended in 5 ml of ice-cold 500 mM sucrose, 5 mM MES, 1 mM CaCl₂, pH 6.0. On top of this was layered 2 ml of 400 mM sucrose, 100 mM sorbitol, 5 mM MES and 1 mM CaCl₂, pH 6.0, followed by a 1 ml-layer of 500 mM sorbitol, 5 mM MES, 1mM CaCl₂, pH 6.0. The tube containing the sucrose gradient was centrifuged at 200g for 5 min, after which the clean protoplasts were collected with a plastic pipette from the interface between the top two layers. The final wash involved mixing the protoplasts with 5 ml of the top gradient solution, spinning at 60g for 5 min and resuspending in 2 ml of the top gradient solution. Throughout the protoplasting procedure, the protoplasts were maintained at 4°C to delay cell wall re-synthesis. The protoplasts were kept on ice and used within

6 h. Only plastic apparatus was used after the digestion step as the protoplasts tended to stick to glass.

All chemicals used were obtained from Sigma unless otherwise indicated.

5.4.2 Solutions for patch-clamping

The solutions used for patch-clamping was adapted from Falke *et al.*(1988). The bath solution contained (in mM): 5 KCl, 10 CaCl₂, 400 mannitol, 5 MES, pH adjusted to 5.8 with tris(hydroxymethyl)aminomethane (Tris). The pipette solution contained (in mM): 200 KCl, 10 CaCl₂, 60 mannitol, 5 MES, pH adjusted to 5.8 with Tris. All solutions were filtered through a 0.22 μ M syringe filter (Millipore) before use.

5.4.3 Patch formation and clamping

A diagram of the main components of the patch-clamp set-up is shown in Figure 5-1.

The patch clamp technique was invented by Neher and Sakmann, for which they received the Nobel prize in 1991. Subsequent improvements to the technique were described in the seminal paper by the inventors and co-workers (Hamill *et al.*, 1981). In this technique, a small glass micropipette (patch pipette) is pressed against the cell membrane. By applying gentle suction, a small patch of the membrane forms a tight seal against the glass pipette, with resistances of above 10 gigaohms, known as “giga-seals”. The high resistance seal significantly reduces the background noise and allows currents from single or small groups of channels on the membrane to be recorded. It

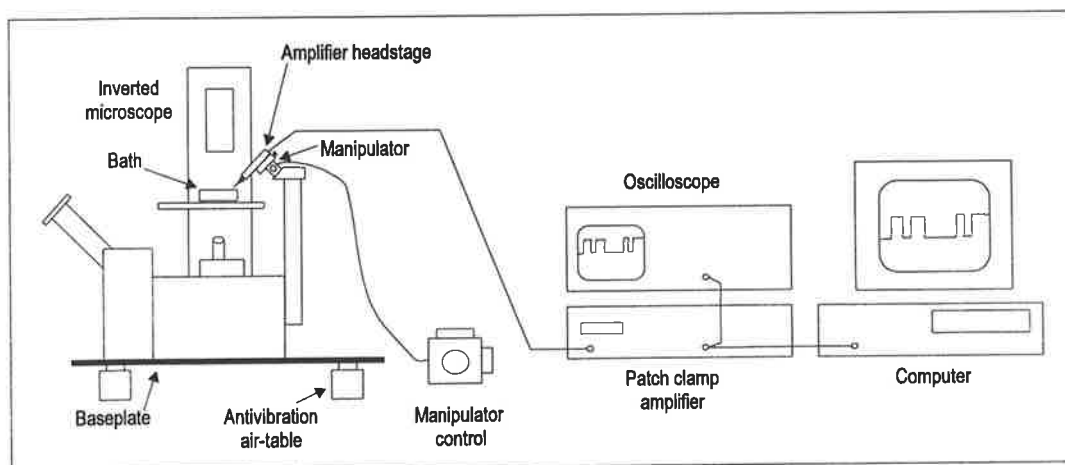


Figure 5-1: Main components of patch-clamp set-up

also enables the current or voltage across the patch of membrane to be controlled or “clamped”.

Protoplasts were transferred to a purpose-built Perspex bath chamber and allowed to settle and adhere to the glass base. The glass base was cleaned with MilliQ water and methanol prior to use to promote adherence of protoplasts. The solution in the bath chamber was earthed via a Ag/AgCl bath electrode attached to the grounding point of the patch-clamp amplifier.

Patch pipettes were pulled from borosilicate glass blanks (Clark Electromedical, Reading, UK) on a two-stage pipette puller (Narishige, Japan). They were coated near the tip with Sylguard (Dow Corning) to reduce the capacitance of the pipette wall and thus reduce noise and capacitive transients. The pipette tip was fire-polished just before use by placing near a heated filament for a few seconds. Pipettes for cell-attached and detached patches were usually polished to a pipette resistance of about 25 M Ω (measured in the bath solution). The pipettes were back-filled with pipette solution through a plastic syringe and gently tapped to remove any air bubbles before attaching to the pipette holder. A silver wire coated with AgCl₂ provided the electrical connection from the pipette solution to the recording equipment. The patch pipettes were then gently manipulated towards the surface of the protoplast until they just touched. Gentle and prolonged suction was then applied and the pipette potential clamped at about -20mV to promote sealing of the membrane to the pipette tip. If the sealing was successful, the seal resistance would rapidly rise to greater than 2 G Ω . Unfortunately, only about 20% of all approaches of pipette to protoplast resulted in a satisfactory seal. In a majority of approaches, the protoplast would not seal to a high enough resistance to allow single channel recordings. Calcofluor (Sigma) staining did not reveal any cell wall debris on the surface of the protoplasts, and FDA staining showed that the majority of the protoplasts obtained had intact membranes. Fairley (1990) reported similar difficulties in patch-clamping suspension cultured corn cells. The reason why some cell lines are more amenable to patch-clamping than others is still unknown, although it has been postulated that the lipid/protein composition of the membrane and interaction with the cytoskeleton may be important factors (Fairley, 1990).

When the patch pipette first seals against the protoplast, the configuration is known as “cell-attached”. To obtain an “inside-out” excised patch, where the cytoplasmic (inside) face of the plasma membrane is exposed to the bath solution, the pipette was gently manipulated away from the protoplast until the patch of membrane attached to the pipette tip tears away from the rest of the protoplast.

Suction was applied through the side port of the pipette holder through a rubber tube connected to a syringe and water manometer. This method enabled a quick, but not immediate, change in the pipette pressure to activate possible stretch-sensitive channels in the membrane.

5.4.4 Data acquisition and analysis

The patch-clamp amplifier used was a Axopatch 200B (Axon Instruments, Foster City, CA). Signals from the amplifier were monitored on an oscilloscope (Gould, Essex, UK) and also digitised via a Digidata 1200 series interface (Axon). The digitised signals were captured on computer hard disk by means of the Fetchex or Clampex programs and analysed using the Fetchan or Clampfit programs, included in the pClamp6 software suite (Axon).

CHAPTER 6

FACTORIAL DESIGN AND STATISTICAL ANALYSIS METHODS

In this work, we wish to investigate the effects of the ion channel blockers and calmodulin inhibitor on the biological responses of carrot cell cultures to fluid shear stresses as well as the interactions between these effects and the prevailing shear level. The factorial experimental design was used in this work as it enables both the main effects and the interactions between a large number of factors on the system response to be determined in a single, statistically-verifiable experimental plan. The alternative one-factor-at-a-time experimental plan cannot be used to evaluate interactions. The factorial design is also more efficient than one-factor-at-a-time experiments, i.e. the design assists in the selection of run conditions so that fewer runs are required, compared to one-factor-at-a-time experiments, to obtain a similar amount of information. In this chapter, the terminology used in factorial experimental designs will be defined and the statistical analysis techniques used to analyse the factorial experiment results (presented in Chapter 8) will be explained.

6.1 Definitions

The *main effect* of a factor (say A) is the difference between the average response at the high level of A and the average response at the low level of A. The magnitude and sign of this value indicates how a particular factor influences the response of the system over all conditions of the other factors.

In some cases, the effect of a factor on the final response may depend significantly on the level of one or more of the other factors. A factorial designed experiment has the useful property of enabling the *interaction* between various factors to be easily quantified. The interaction between the factors can often provide a more accurate description of the impact of various factors on the system than the main effect alone. Indeed, in some cases, a significant interaction between the factors may mask the main effect of a particular factor.

Table 6-1: System response at various levels of dummy factors A and B.

	B _{low}	B _{high}
A _{low}	20	40
A _{high}	50	12

For example, consider the data shown in Table 6-1. The main effect of A is calculated as

$$A = \frac{50 + 12}{2} - \frac{20 + 40}{2} = 1$$

The magnitude of the main effect of A seems rather small and might lead to the erroneous conclusion that factor A does not have a significant impact on the system. However, if the interaction between factors A and B is taken into account, a more accurate conclusion emerges. The interaction between A and B is calculated as follows:

$$\begin{aligned}
 AB &= \frac{1}{2} [\text{Effect of A at high level of B} - \text{Effect of A at low level of B}] \\
 &= \frac{1}{2} [(12 - 40) - (50 - 20)] \\
 &= -29
 \end{aligned}$$

There is clearly a significant interaction between factors A and B. It is now evident that factor A does have a significant impact on the system, but the effect is strongly dependent on the level of factor B. This point is illustrated in a plot of the response data against factor A for both levels of factor B (Figure 6-1). The lack of parallelism between the lines is an indication of significant interaction between the factors. Graphs such as Figure 6-1 are helpful for interpreting and illustrating significant interactions when used in conjunction with the statistical techniques to be described in Section 6.3 to analyse the experimental data. This example highlights the importance of making conclusions based on both the main effects and the interactions rather than relying on main effects alone. This point is often overlooked in one-factor-at-a-time experimental designs.

An algorithm has been devised by Yates (1937) for calculating the main effects, interactions and the sum of squares for a 2^k factorial experiment. This algorithm helps to simplify the mathematical procedure for calculating the effects. An example of the application of Yates' algorithm to the coupled OUR experimental data from this work is given in Appendix B.

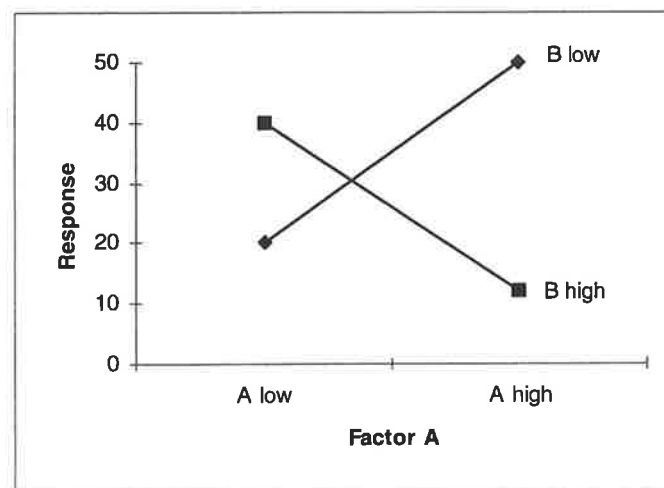


Figure 6-1: Plot of response data for Table 1 example

6.2 The half-fraction factorial design, 2^{5-1}

In this work, there are five factors of interest: the shear level and the four blockers/inhibitor. A 2^5 full factorial design (Table 6-2) would require 32 *successful* experimental runs, taking into account that some runs would need to be repeated due to contamination or the poor physiological state of a particular flask of cell culture. An experimental plan that lasts over an extended period should be avoided as the plant cell culture may undergo mutation over the period due to small, unavoidable fluctuations in the cultivation conditions. To overcome this problem, a half-fraction of the full factorial design was adopted in this study (ie. a 2^{5-1} design). This design assumes that three-factor and higher interactions are negligible compared to the main effects and two-factor interactions. This assumption is known as the “sparsity of effects principle” and is commonly applied in experimental plans where a large number of factors are examined (Daniel, 1976; Montgomery, 1991).

The 2^{5-1} design was constructed from the full 2^5 design by using the generator $E = -ABCD$. Thus, the right-most column of signs, corresponding to the shear level in Table 6-3, was derived by multiplying the signs in the four previous columns, and then reversing the sign of the result. This design is known as a resolution V design and avoids any main effects or two-factor interactions from being aliased with each other (Montgomery, 1991). However, each main effect is aliased with a four-factor interaction, and each two-factor interaction is aliased with a three-factor interaction. For example, when we estimate the main effect of A, we are really estimating A - BCDE. But by appealing to the sparsity of effects principle, the main effect of A is likely to dominate over the four-factor interaction of BCDE. Similarly, the two-factor interaction (eg. AB) is likely to dominate over the three-factor interaction CDE with which it is aliased. The resolution V design is the highest resolution possible for a factorial design with five factors and allows estimates of effects to be determined with the least restrictive assumptions while economising on the number of runs.

Table 6-2: A full 2^5 factorial design

	A	B	C	D	E
1	-1	-1	-1	-1	-1
2	1	-1	-1	-1	-1
3	-1	1	-1	-1	-1
4	1	1	-1	-1	-1
5	-1	-1	1	-1	-1
6	1	-1	1	-1	-1
7	-1	1	1	-1	-1
8	1	1	1	-1	-1
9	-1	-1	-1	1	-1
10	1	-1	-1	1	-1
11	-1	1	-1	1	-1
12	1	1	-1	1	-1
13	-1	-1	1	1	-1
14	1	-1	1	1	-1
15	-1	1	1	1	-1
16	1	1	1	1	-1
17	-1	-1	-1	-1	1
18	1	-1	-1	-1	1
19	-1	1	-1	-1	1
20	1	1	-1	-1	1
21	-1	-1	1	-1	1
22	1	-1	1	-1	1
23	-1	1	1	-1	1
24	1	1	1	-1	1
25	-1	-1	-1	1	1
26	1	-1	-1	1	1
27	-1	1	-1	1	1
28	1	1	-1	1	1
29	-1	-1	1	1	1
30	1	-1	1	1	1
31	-1	1	1	1	1
32	1	1	1	1	1

Table 6-3: The 2^{5-1} factorial design. A “1” or “-1” corresponds to the inclusion or exclusion of the chemical, respectively, for the second to fifth columns , whereas “1” corresponds to shearing at 1200 rpm (100 N/m²) and “-1” at 600 rpm (38 N/m²) for the last column.

	A	B	C	D	E
Run code	W7	Ruthenium Red	Verapamil	NPPB	Shear level
1a	-1	-1	-1	-1	-1
7a	1	-1	-1	-1	1
8b	-1	1	-1	-1	1
4b	1	1	-1	-1	-1
3a	-1	-1	1	-1	1
5b	1	-1	1	-1	-1
6b	-1	1	1	-1	-1
2a	1	1	1	-1	1
2b	-1	-1	-1	1	1
6a	1	-1	-1	1	-1
5a	-1	1	-1	1	-1
3b	1	1	-1	1	1
4a	-1	-1	1	1	-1
8a	1	-1	1	1	1
7b	-1	1	1	1	1
1b	1	1	1	1	-1

6.3 Statistical analysis methods

6.3.1 Normal scores plot of effects

Daniel (1959) proposed a simple method to determine if effects are statistically significant in unreplicated factorial designs. He suggested plotting the estimates of the effects and interactions on normal probability paper. The effects which are negligible are normally distributed with mean zero and variance σ^2 and will tend to fall along a straight line on this plot. On the other hand, significant effects will have non-zero means and will be far from the straight line.

Normal probability paper is graph paper with the ordinate scaled so that the cumulative normal distribution plots as a straight line. Montgomery (1991) describes the method for constructing a normal probability plot of effects. The effect estimates are first arranged in ascending order and the j^{th} of the ordered data is plotted against the cumulative probability point $P_j = (j - 1/2)/N_t$. Alternatively, the ordered data can be plotted against the standardised normal score Z_j which satisfies $P_j = \Phi(Z_j)$, on the vertical axis of an ordinary graph paper. The normal score can be determined using the `NORMSINV()` statistical function in the Microsoft Excel program. The formula for calculating the normal score is

$$\text{Normal score, } Z_j = \text{NORMSINV}[(j - 3/8)/(N_t + 1/4)] \quad (\text{Eq 6-1})$$

An example of a normal scores plot of effects, taken from Montgomery (1991), is shown in Figure 6-2. In this example, 5 factors (A to E) were examined in a half-fraction 2^{5-1} factorial design. The main effects and interactions were calculated and then plotted on a normal scores plot as shown in Figure 6-2. All of the effects that lie along the line are negligible, whereas the main effects of A, B and C and the AB interaction appear to be significant. In addition to the normal scores plot of effects, the statistical significance of the effects and interactions can also be investigated through an analysis of the variance of the experimental data and the residuals. These statistical techniques are described in the following sections.

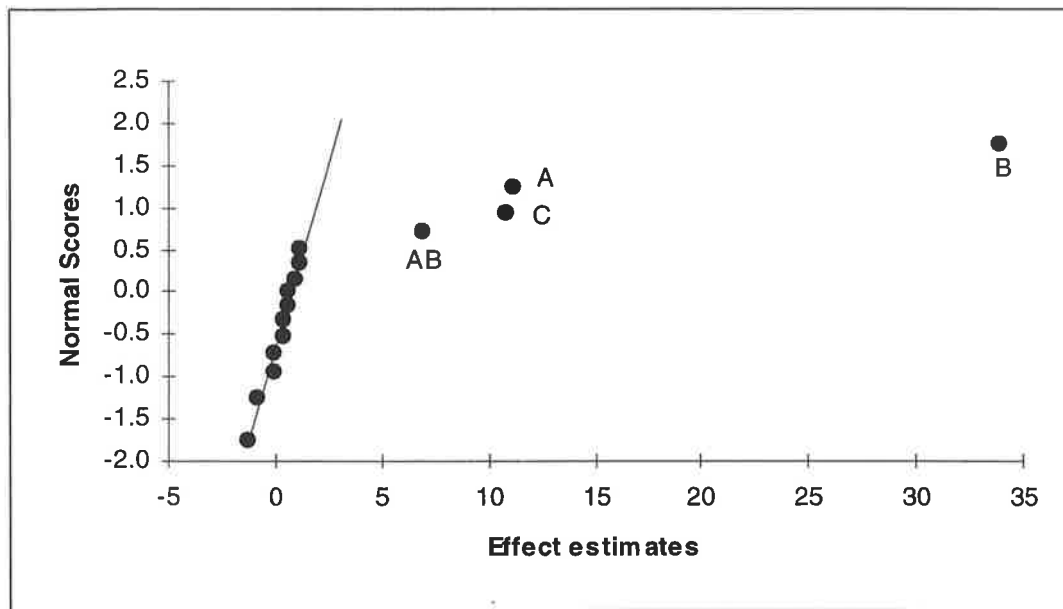


Figure 6-2: An example of a normal scores plot of effects (Montgomery, 1991)

6.3.2 Analysis of variance and F-tests

Table 6-4 summarises the analysis of variance for the same example used in Figure 6-2. The sum of squares can be obtained by following the Yate's algorithm described in Appendix B. The degrees of freedom are defined as the total number of levels of each factor minus one. Since there are only 2 levels for each factor, the degree of freedom is $2-1 = 1$. The mean square is simply the ratio of the sum of squares to the degrees of freedom. The F-test statistic is the ratio of the mean square of the main effect or interaction to the mean square of the error estimate.

In unreplicated factorial designs, an estimate of the error is usually obtained by assuming that certain higher-order interactions are negligible and combining their mean squares. However, the decision to include a particular effect in the error pool can be greatly simplified with a normal scores plot of effects. The normal scores plot provides a good indication of which effects can be safely pooled to estimate the error term. For example, Figure 6-2 suggests that all effects and interactions except for A, B, C and AB are negligible. Thus, the remaining effects can be pooled together to estimate the error. The model sum of squares calculated by adding the sum of squares for A, B, C and AB accounts for over 99% of the total variability in the response. This is a good indication that these effects dominate over the other factors. This is further reinforced by the

significantly large F-test statistic for each of these effects compared to the F-distribution (significance level = 1%).

Table 6-4: Analysis of variance for example shown in Figure 6-2.

Source of variation	Sum of squares	Degrees of freedom	Mean square	F _o
A	495.0625	1	495.0625	193.20
B	4590.0625	1	4590.0625	1791.24
C	473.0625	1	473.0625	184.61
AB	189.0625	1	189.0625	73.78
Error	28.1875	11	2.5625	
Total	5775.4375	15		

6.3.3 Analysis of residuals

The normal scores plot of effects and the analysis of variance described above help to identify the significant factors affecting the system response. Another useful diagnostic check of the conclusions from these two tests is to analyse the residuals between the response predicted from a regression model and the actual response. A regression model based on the dominant effects and interactions alone can take the form

$$\hat{y} = \beta_0 + \beta_1 x_1 + \beta_2 x_2 + \beta_3 x_1 x_2 + \dots \quad (\text{Eq 6-2})$$

where x is the coded variable for each of the effects or interactions deemed significant based on the normal scores plot and analysis of variance. x takes on the value of +1 or -1 depending on the column of signs designated in the factorial design (for example, Table 6-3). β_0 is the average response for all the factorial runs while the remaining β values are the regression coefficients defined as one-half of the corresponding factor effect estimates. The reason why it is one-half of the effect estimates is because the regression coefficient measures a unit of change in x , while the factor effect estimates are based on a two-unit change (from -1 to +1). The residuals (e) are calculated from

$$e = y - \hat{y} \quad (\text{Eq 6-3})$$

where y is the actual response and \hat{y} is the regressed value.

If the model based on the significant factors alone is adequate, the residuals should be normally distributed. This can be determined from a normal scores plot of the residuals. The points on this plot should lie reasonably close to a straight line if the residuals follow a normal distribution. Furthermore, if the model is correct and the underlying normality assumptions are satisfied, a plot of the residuals against the regressed value should be structureless. On the other hand, a discernible trend between the residuals and \hat{y} would indicate non-constant variance in the data (Montgomery, 1991).

CHAPTER 7

PRELIMINARY STUDIES

Previous studies, summarised in Chapter 2, have shown that many types of plant cells are sensitive to fluid shear stresses and exhibit a hierarchy of responses ranging from sub-lytic effects at low to moderate shear stresses, to lysis and cell death at high shear stresses. However, some plant cell lines have also been reported to be tolerant of fluid shear, though the cause of the shear tolerance is still poorly understood. In this chapter, the effects of fluid shear on the biological response of cultured carrot cells are evaluated over a range of shear conditions in shake flasks and in a novel oxygen-permeable Couette. The aims of these preliminary studies are to determine if sub-lytic effects can be observed in the carrot cultures, to quantify these effects and to determine the critical shear levels at which they occur. These results are then used to establish the bounds for the factorial experiments described in the next chapter.

Carrot cultures were cultivated in shake flasks at different shaker speeds to determine the effects of sustained shear exposure on the growth and membrane integrity of the cells.

Before shear testing in the Couette was carried out, the efficacy of the Couette design in providing sufficient oxygen to the cells was tested by measuring the dissolved oxygen level of the cultures contained in the annular gap over a period of time. The carrot cultures were then subjected to laminar shearing in the Couette over a range of shear stresses and shear exposure periods.

7.1 Comparison of growth in shake flasks at different speeds

Several flasks of carrot cell cultures were initially inoculated using 14-day (late-exponential growth phase) cultures from the same flask and grown at 100 rpm, 27°C as described in Chapter 5 up to day 3. On day 3, half of the original batch of flasks were transferred to an identical shaker operated at a higher rotational speed of 150 rpm. Samples of cell culture were taken from each batch of flasks and the fresh weight of the cells determined following washing and vacuum filtration. The wet cells were then placed in a 60°C oven for 1-2 days and the dry weight of the cells determined from the final, steady weight value.

Figure 7-1 compares the growth curves of the cultures (in terms of dry weight) at the 2 shaker speeds. The carrot cultures grown at 150 rpm showed decreased dry weight accumulation relative to the 100 rpm cultures. The average growth rate at 100 rpm, from day 4 to 16, was 0.194 d^{-1} (dry weight) compared to 0.143 d^{-1} (dry weight) at 150 rpm. Similarly, the fresh weight accumulation was lower at 150 rpm than at 100 rpm (Figure 7-2).

However, comparison of the membrane integrity of the carrot cells did not reveal any significant difference between the cultures grown at the 2 speeds. Figure 7-3 shows the percentage of cells with intact membranes, as determined by FDA staining. Although both cultures showed a mild decrease in membrane integrity over the growth period, there was little difference between the cultures at the 2 speeds.

The results demonstrate that a mild increase in hydrodynamic shear leads to a decrease in cell growth but has negligible impact on the integrity of the cell membrane. These observations agree with previous reports discussed in the literature review (see Section 2.1) and suggest that sub-lytic effects may be observed in the carrot cell culture selected for this work.

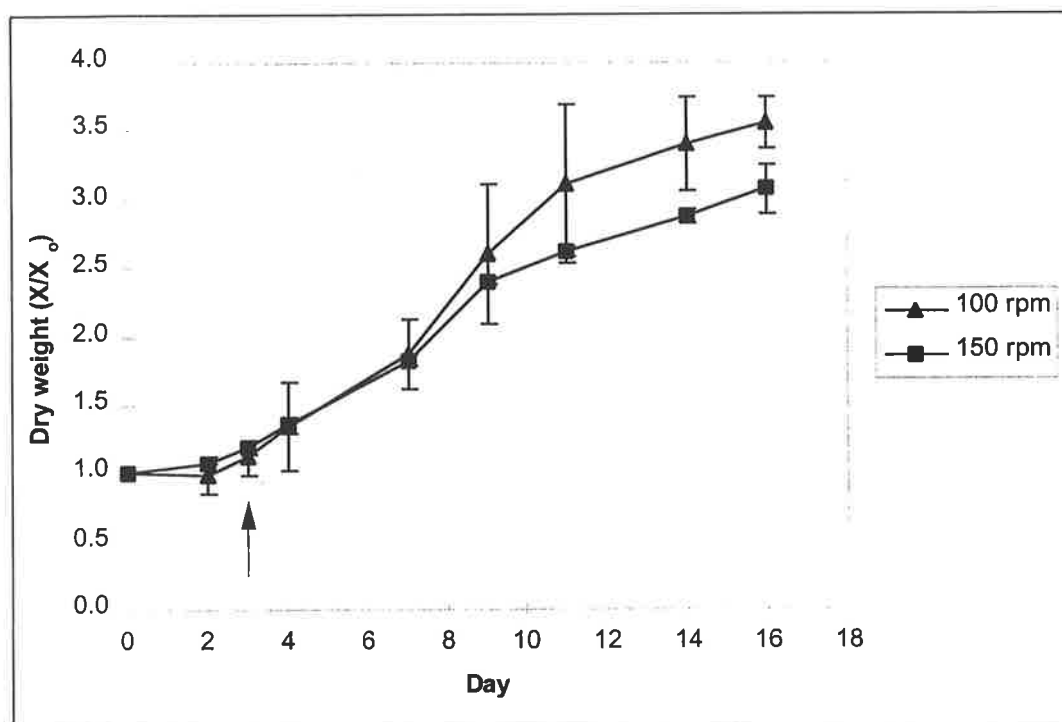


Figure 7-1: Comparison of dry weight accumulation in carrot cultures grown in shake flasks agitated at either 100 or 150 rpm. Speed increased on day 3 as indicated by the arrow. Values shown are the mean of 2 replicates. Error bars indicate standard error.

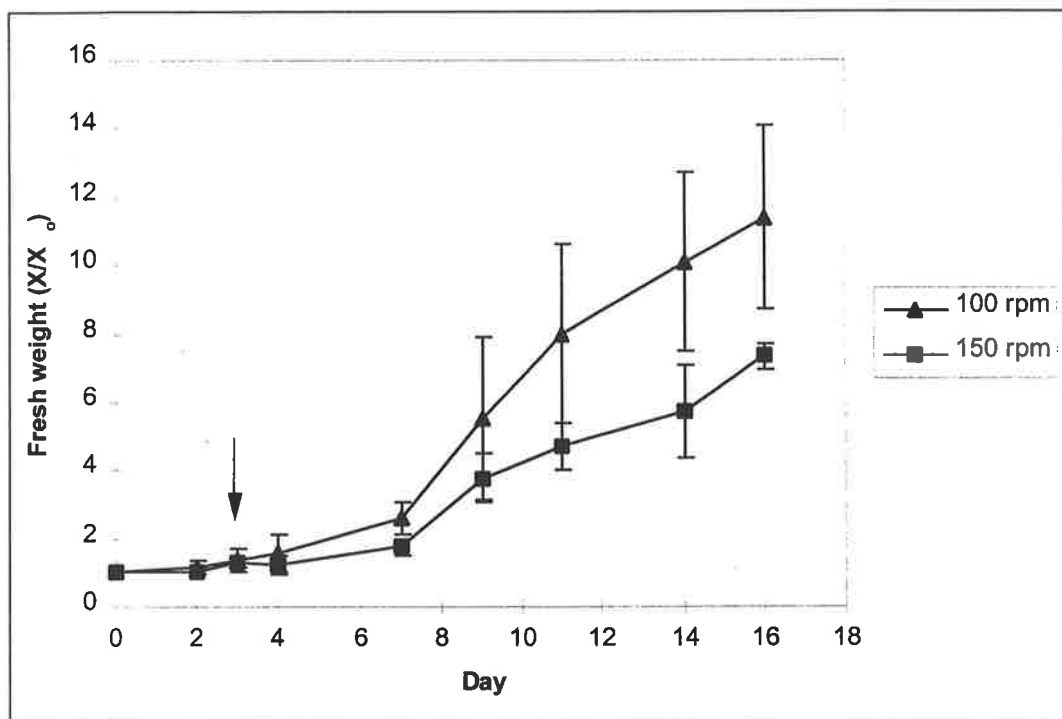


Figure 7-2: Comparison of fresh weight accumulation in carrot cultures grown in shake flasks agitated at 100 or 150 rpm. Speed increased on day 3 as indicated by the arrow. Values shown are the mean of 2 replicates. Error bars indicate standard error.

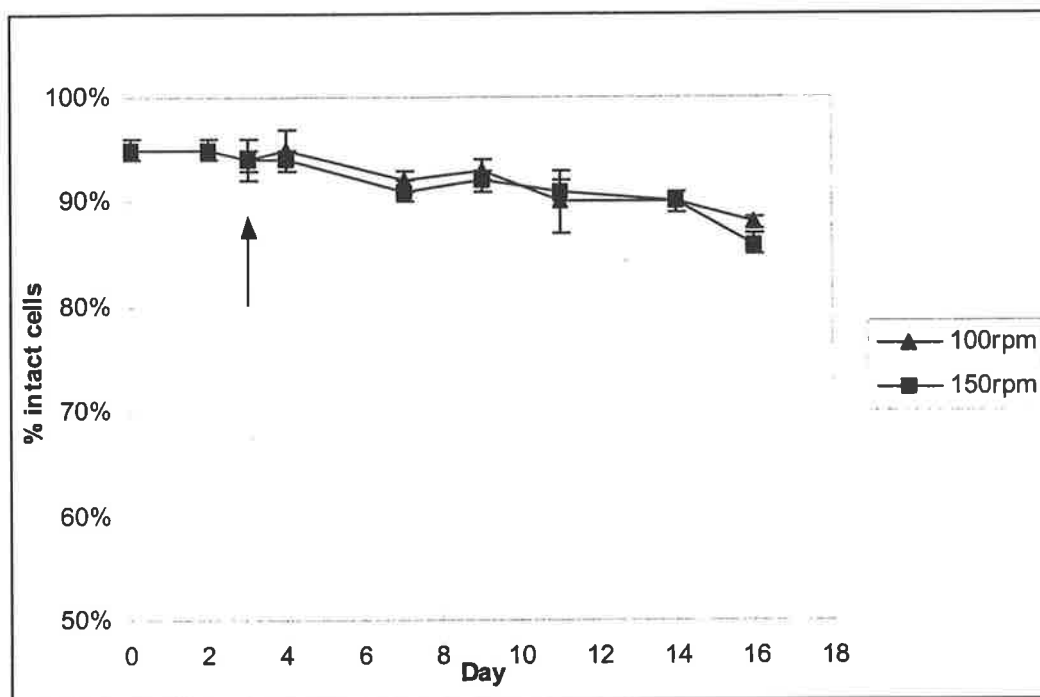


Figure 7-3: Comparison of membrane integrity in carrot cultures grown in shake flasks agitated at 100 or 150 rpm. Speed increased in day 3 as indicated by the arrow. Values shown are the mean of 2 replicates. Error bars indicate standard error.

7.2 Comparison of DO in viscometers

In Chapter 4, a finite element model of the dissolved oxygen (DO) level in a conventional Couette viscometer with a 625 μm gap width was presented. The conventional viscometer design only allowed surface aeration of the cell culture through the small area at the gap surface. The model results showed a rapid drop in the DO of plant cell cultures contained within the viscometer gap, which suggested that the rate of oxygen diffusion through the gap surface alone was insufficient to meet the oxygen requirements of the cell culture. On the other hand, the DO level in the novel Couette viscometer, which allowed diffusion of oxygen through the side wall of the viscometer bowl, was consistently higher than in the conventional viscometer.

To experimentally verify the finite element model results, the DO level in carrot cultures contained within the annular gap for periods of up to 8 h was measured in both the conventional steel bowl and the novel ceramic bowl. The same inner bob was used for both bowls. The small gap width of the viscometers made *in situ* measurements difficult as it was not possible to fit a standard DO probe into the gap. Instead, an alternative method was used to estimate the DO level of the cell cultures.

The cell cultures were loaded into the viscometer as described in Section 5.3.3. The temperature was maintained at 27°C by the temperature-controlled air-heater. After a pre-determined period, the viscometer lid and inner bob was quickly and carefully removed and the cell culture transferred into the Rank Oxygen electrode chamber described in Section 5.3.3.3. The electrode was calibrated against air-saturated medium prior to each measurement. The reading of the oxygen electrode showed an initial sharp drop as the cell culture was pipetted into the electrode chamber. The DO level immediately following this sharp drop was taken to be an estimate of the DO content of the culture after being in the viscometer gap for the pre-determined time period. A rotational speed of 500 rpm was used in these experiments. Higher speeds of rotation are expected to increase the mass transfer coefficient. Since the side wall has a larger mass transfer area compared to the top of the viscometer gap, an increase in the mass transfer coefficient would lead to a significant increase in the mass transfer rate through the side wall. On the other hand, increasing the rotational speed would have a much smaller impact on the mass transfer rate through the surface of the viscometer gap due to

the significantly smaller area. Thus, increasing rotational speeds would lead to a greater increase in the oxygen-permeable bowl than in the conventional bowl. This trend was observed in a number of trial runs at various rotational speeds.

Figure 7-4 shows the DO level in the cell culture after various times in the viscometer gap. As predicted by the finite element model, the DO level of the cell culture in the ceramic bowl was consistently higher than in the steel bowl and remained above 90% saturation for up to 8 h. On the other hand, the DO level of the cell culture in the steel bowl showed a rapid drop followed by a gradual decline to about 10% saturation after 8 h, which is below the critical DO level of 16% saturation reported for carrot cells (Kessell and Carr, 1972). The change in the rate of DO decline for the cell culture in the steel viscometer bowl could be an indication of altered cell metabolism due to anaerobic conditions. The occurrence of anaerobic conditions in annular gap of the conventional viscometer may lead to confusion in the interpretation of the effects due to hydrodynamic shear.

The finite element model suggests a more rapid drop in DO within the steel bowl (Figure 4-7) than observed in the experimental results (Figure 7-4). The difference is likely to be due to the crudeness of the method employed to estimate the DO level of the cell culture contained in the viscometer gap. Nevertheless, the trend of the results is consistent with the model predictions.

These results demonstrate that the oxygen-permeable viscometer will provide sufficient oxygenation of the cell culture for test periods of at least 8 h. Thus, changes observed in the biological response of the cells after shear exposure should not be influenced by mass transfer limitations, but would be due to hydrodynamic shear.

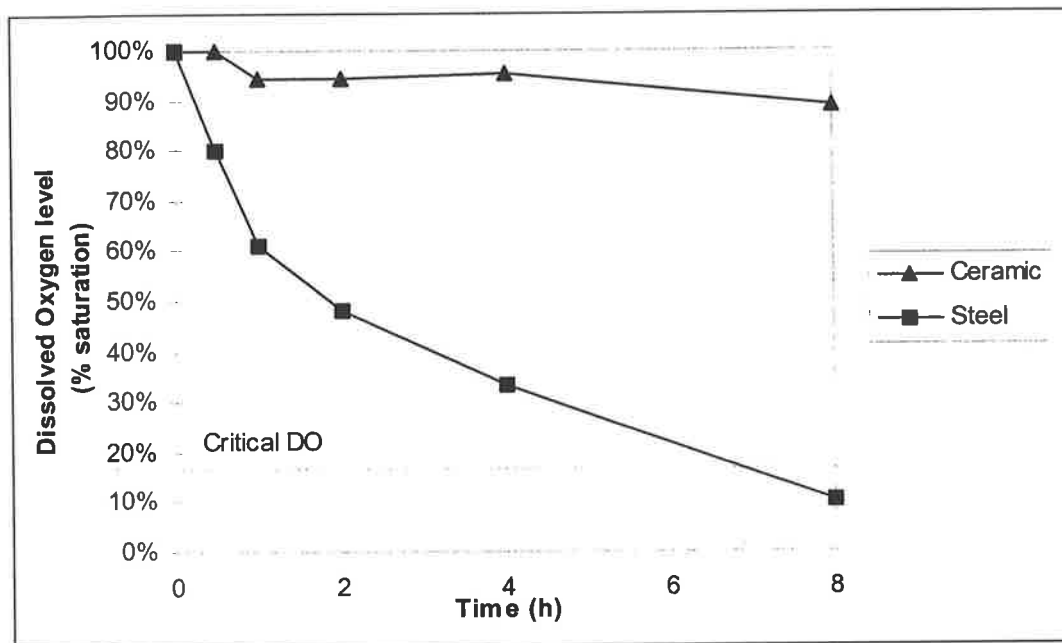


Figure 7-4: Comparison of cell suspension DO level in viscometer with oxygen-impermeable steel bowl and oxygen-permeable ceramic bowl. Viscometer gap width is approximately 1000 μm and 600 μm for the steel and ceramic bowls, respectively.

7.3 Shear tests in the oxygen-permeable viscometer

7.3.1 Effect of shear on biological response

The range of experimental values for the biological indicators: coupled and uncoupled OUR, mitochondrial activity and membrane integrity, observed in the controls (day 13-14 cultures in shake flasks at 100 rpm) during shear tests are summarised in Table 7-1.

Table 7-1: Range of values observed for biological indicators in controls during shear tests.

Biological indicator	Range
Mitochondrial activity (Abs / g fresh wt)	15-19
Uncoupled OUR ($\mu\text{mol O}_2$ / min g fresh wt)	0.31-0.54
Coupled OUR ($\mu\text{mol O}_2$ / min g fresh wt)	0.17-0.38
Membrane integrity (% fluorescent cells)	86-96

Exposure to hydrodynamic shear stress in the oxygen-permeable Couette changes each of these biological activities from their control levels. For example, Figure 7-5 shows the effect of hydrodynamic shearing at 57 N/m^2 for periods of up to 8 h on the absolute values of mitochondrial activity, coupled and uncoupled OUR and membrane integrity compared with their corresponding control values. To allow relative effects to be compared, each biological activity was expressed as a percentage of the corresponding control value, as shown in Figure 7-6 to 7-10.

Figure 7-6 shows the variation in relative mitochondrial activity with shear exposure at different shear stresses. The mitochondrial activity of the carrot cultures gradually fell below control levels with increased exposure to shear stress. In addition, the rate of decline became more dramatic at higher shear stresses. Similar trends were observed for the uncoupled OUR and membrane integrity, as shown in Figure 7-7 and 7-8, respectively.

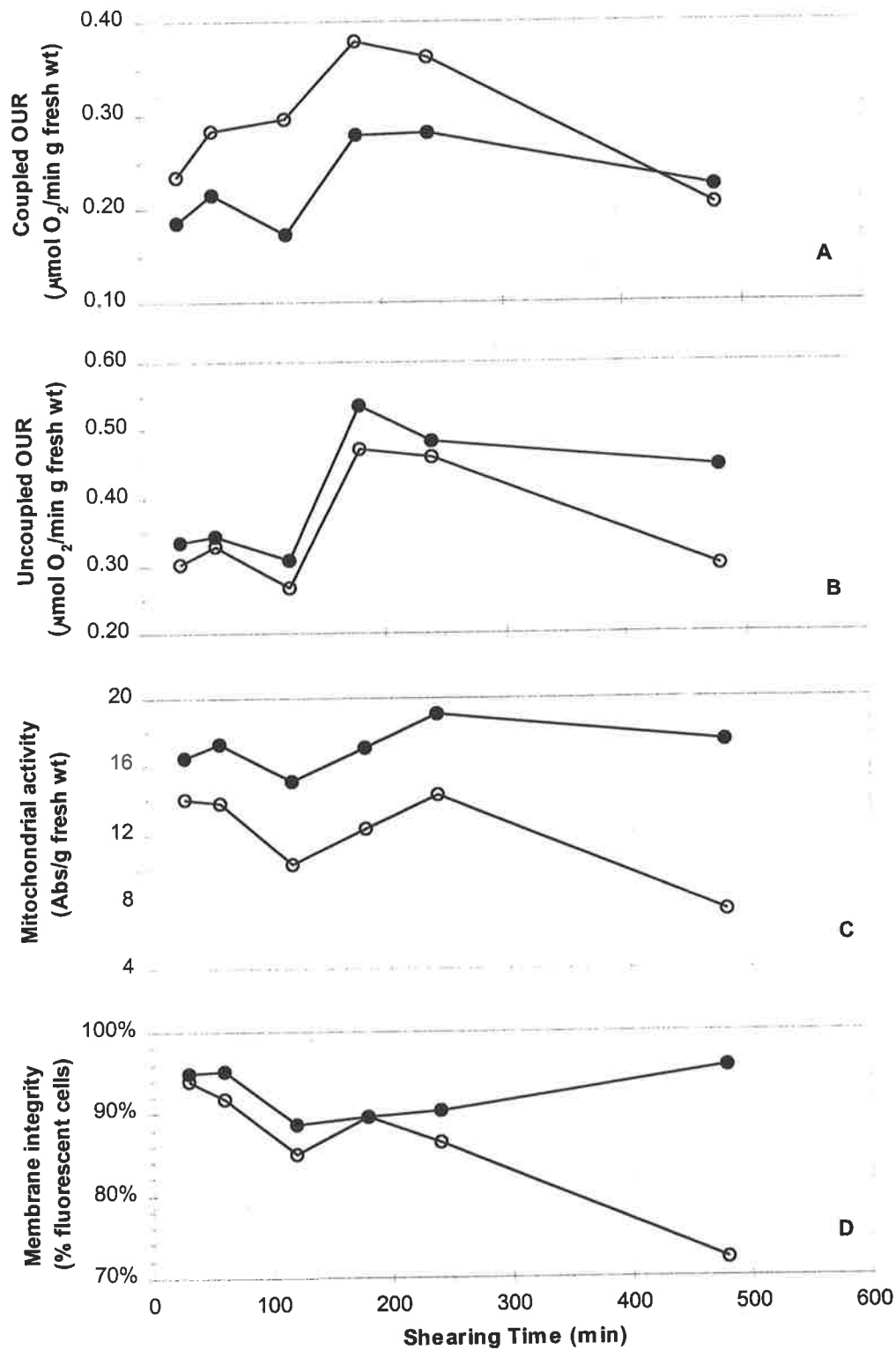


Figure 7-5: Absolute values for (A) coupled OUR, (B) uncoupled OUR, (C) mitochondrial activity and (D) membrane integrity of carrot cultures sheared at 57.3 N/m² (open circles) and controls (closed circles).

In contrast, the maximum-recorded coupled OUR (see section 5.3.2) of the viscometer-sheared cultures was stimulated above control levels by the hydrodynamic shear, as shown in Figure 7-9. At shear stresses below 22 N/m^2 , the relative coupled OUR increased and then levelled for shear exposures of up to 4 h. However, at shear stresses above 22 N/m^2 , the coupled OUR rose initially and then fell after longer periods of shearing. For instance, the coupled OUR of cells sheared at 57 N/m^2 rose to a value of about 150% of the control value after 2 h, and then dropped to about 127% after 4 h. The time taken to reach the peak value depended on the prevailing shear stress. At 74 N/m^2 , the coupled OUR peaked at about 130% after only 1 h, compared to 2 h for a shear stress of 57 N/m^2 .

The stimulation in coupled OUR at elevated shear stresses has also been reported in other plant cell cultures (e.g. Keßler *et al.*, 1997b) and will be discussed further in Section 7.4.

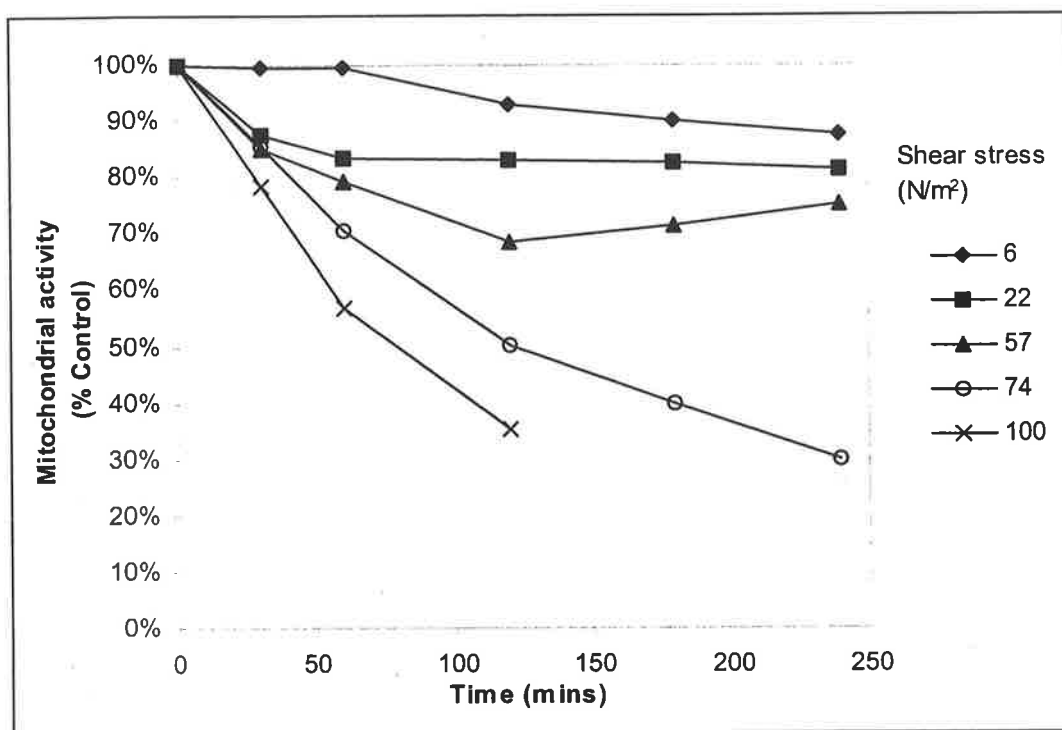


Figure 7-6: Effect of hydrodynamic shear in the oxygen-permeable viscometer on the mitochondrial activity of carrot cultures.

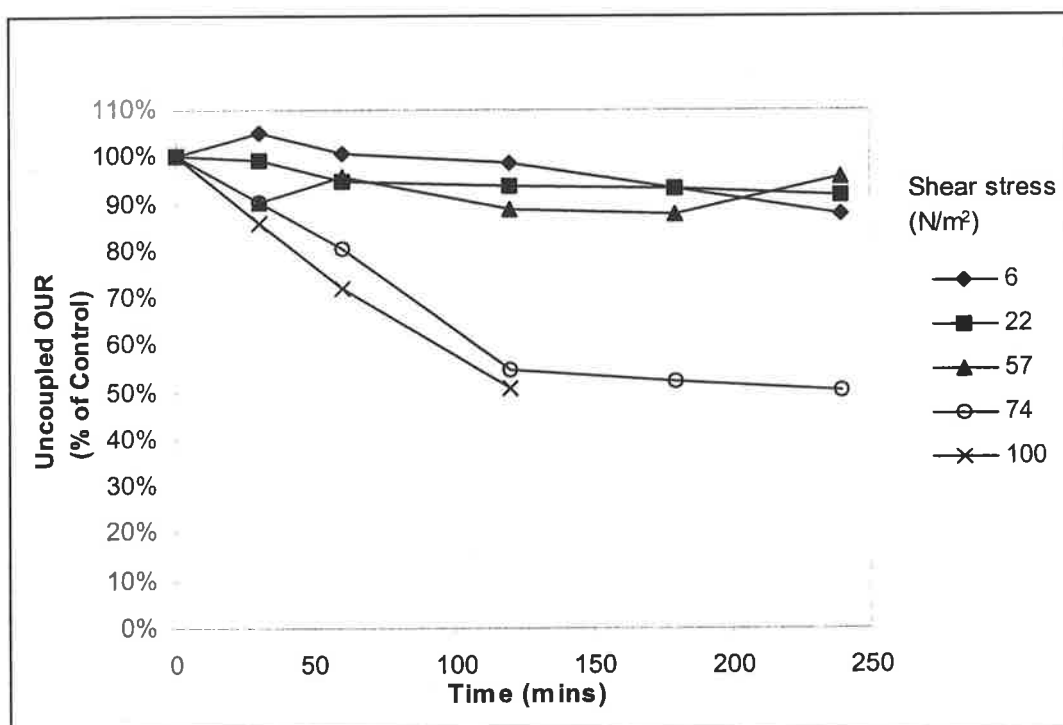


Figure 7-7: Effect of hydrodynamic shear in the oxygen-permeable viscometer on the uncoupled OUR of carrot cultures.

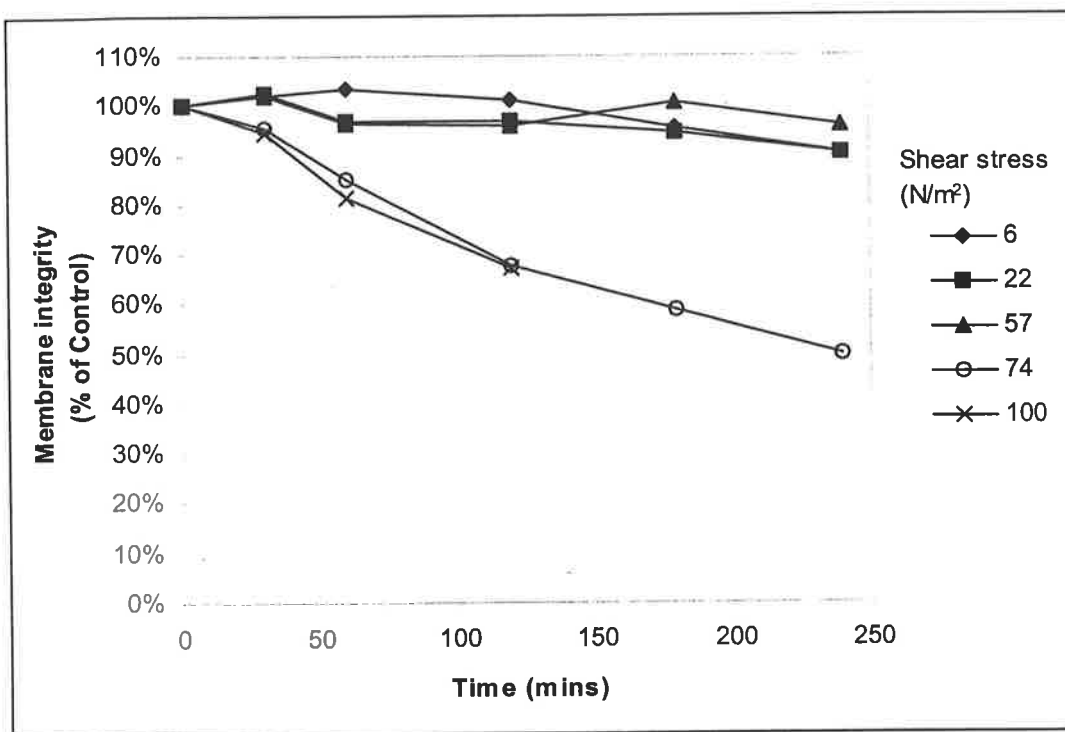


Figure 7-8: Effect of hydrodynamic shear in the oxygen-permeable viscometer on the membrane integrity of carrot cultures.

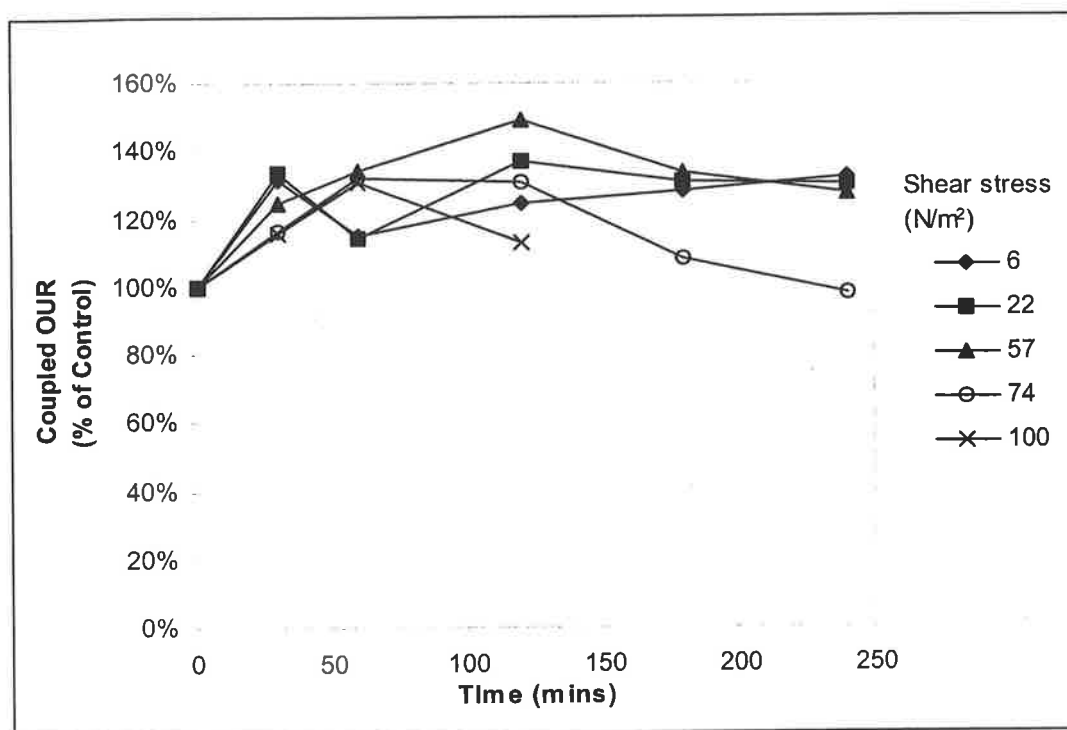


Figure 7-9: Effect of hydrodynamic shear in the oxygen-permeable viscometer on the coupled OUR of carrot cultures.

Although the relative mitochondrial activity, uncoupled OUR and membrane integrity all decreased with increased shear exposure, shearing at a particular level affects each of these biological activities to a different extent. For instance, Figure 7-10 compares the effects of shear on the relative mitochondrial activity, coupled and uncoupled OUR and membrane integrity of the cultures at a shear stress of 57 N/m^2 . The mitochondrial activity was more severely affected by the shear compared to the uncoupled OUR and membrane integrity. After 8 h, the mitochondrial activity fell to around 47% of control value. However, the membrane integrity remained around control levels for shear exposures of up to 4 h and only fell to 76% of the control value after 8 h.

The rate of change in mitochondrial activity, uncoupled OUR and membrane integrity was dependent on the prevailing shear level. At low shear stresses (e.g. 6 N/m^2), the rate of damage for these three biological activities was marginal, as illustrated in Figure 7-11. At higher shear stresses (74 N/m^2), these three activities all fell rapidly with increased exposure to shear, as shown in Figure 7-12.

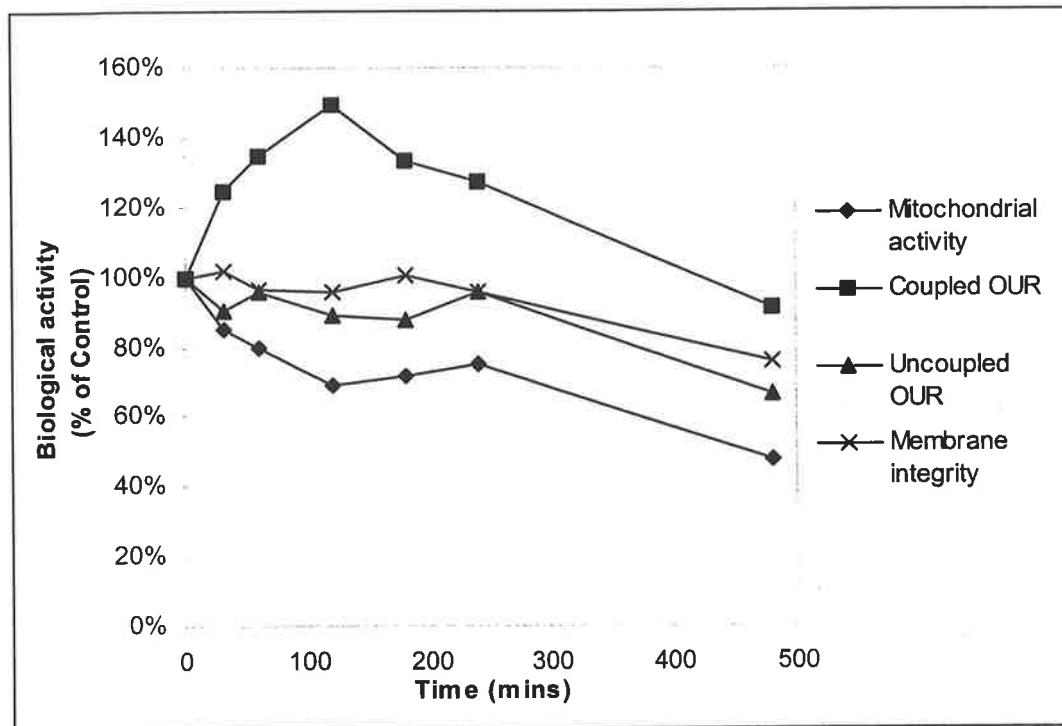


Figure 7-10: Effect of hydrodynamic shear on the biological activity of carrot cultures at a shear stress of 57 N/m².

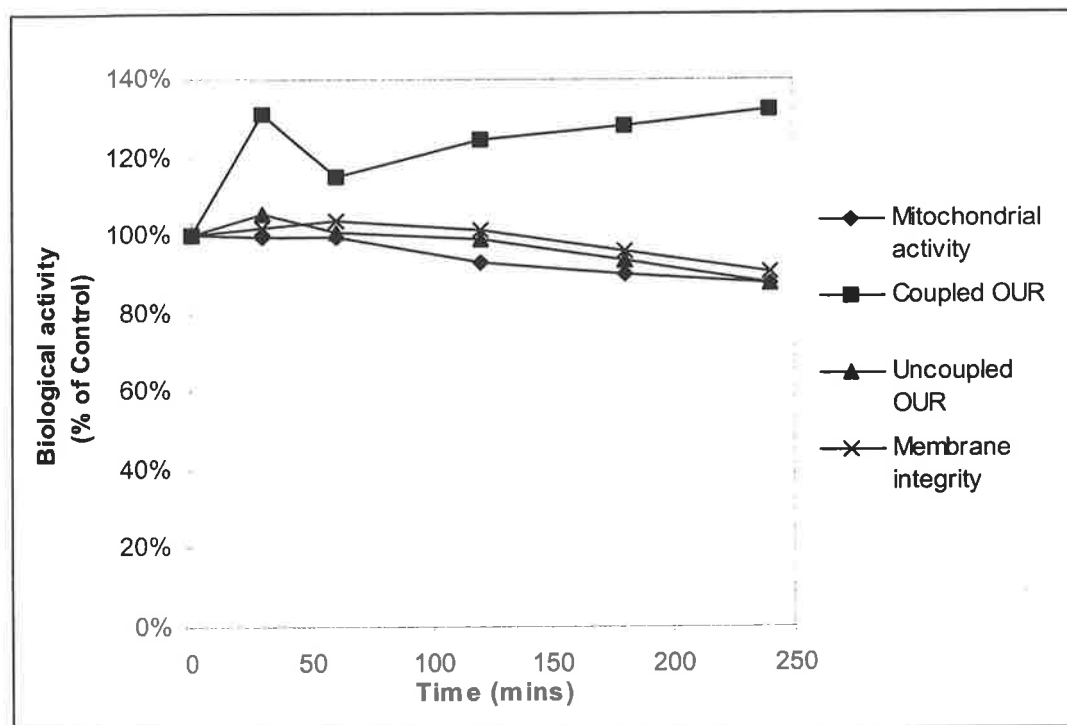


Figure 7-11: Effect of hydrodynamic shear on the biological activity of carrot cultures at a shear stress of 6 N/m².

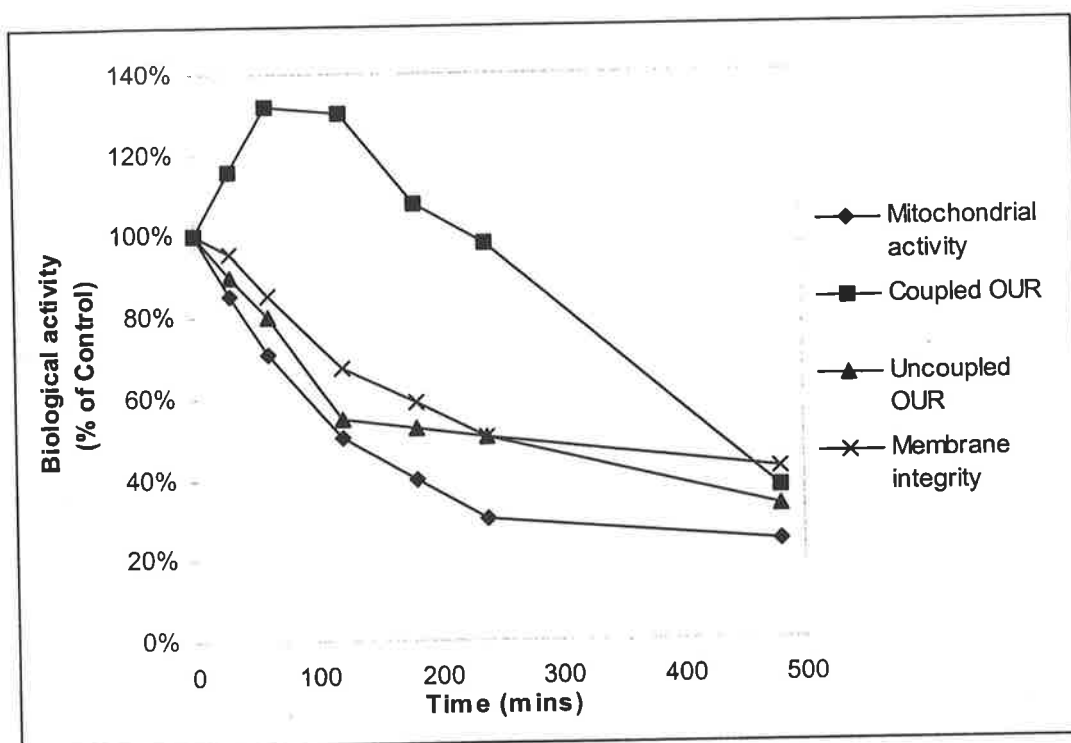


Figure 7-12: Effect of hydrodynamic shear on the biological activity of carrot cultures at a shear stress of 74 N/m^2 .

The effect of shear on the regrowth ability of the cells was also assessed. After shearing in the viscometer, the cells were immobilised in agarose beads as described in Section 5.3.3.4. Digital images of carrot cells immobilised in agarose taken on Day 0 (top image) and Day 5 (bottom image) are shown in Figure 7-13. A nominal aggregate diameter was calculated based on the projected area of each aggregate. Figure 7-14 shows the aggregate size distribution of cells immediately (i.e. Day 0) after shearing in the viscometer at 57 N/m^2 for 8 h. The cumulative frequency curve determined from the size distribution histogram is also given in Figure 7-14. Figure 7-15 compares the aggregate size distributions of the control and sheared cells at Day 0 in terms of the cumulative frequencies. As expected, a general reduction in aggregate size was observed in the sheared cells compared to the control. The same aggregates were analysed again after allowing them to re-grow in the agarose for 5 days. Figure 7-16 gives the distribution of aggregate sizes for the control and sheared cells at Day 5. There is a shift towards larger diameters for both the control and sheared cells at Day 5, indicating an increase in aggregate size due to cell division and growth. An estimate of

approximately spherical and taking the ratio of the volume at Day 5 to the initial volume (Day 0). Figure 7-17 compares the distribution of volume ratios of the aggregates between the sheared and control cells. The difference in regrowth ability between the sheared and control cells was marginal especially when compared to the other biological activities such as mitochondrial activity and oxygen uptake rate (refer to Figure 7-10). For instance, the proportion of aggregates which doubled in volume during the 5 day regrowth period was 76% and 68% for the control and sheared cultures, respectively (or, the regrowth potential of sheared cells was 88% of control value). In contrast, the mitochondrial activity and uncoupled OUR fell to 47% and 66% of their control values, respectively. The reduction in regrowth potential was comparable to that of membrane integrity (which was about 80% of control). Thus, it appeared that cells which retained their membrane integrity were able to recover and regrow normally after removing from the shear viscometer. Similar observations were made at other shear stresses and exposure times.

As the regrowth assay was inherently prone to contamination and did not appear to be as sensitive to sub-lytic levels of shear as mitochondrial activity and oxygen uptake rate, regrowth potential was not assayed in subsequent experiments.

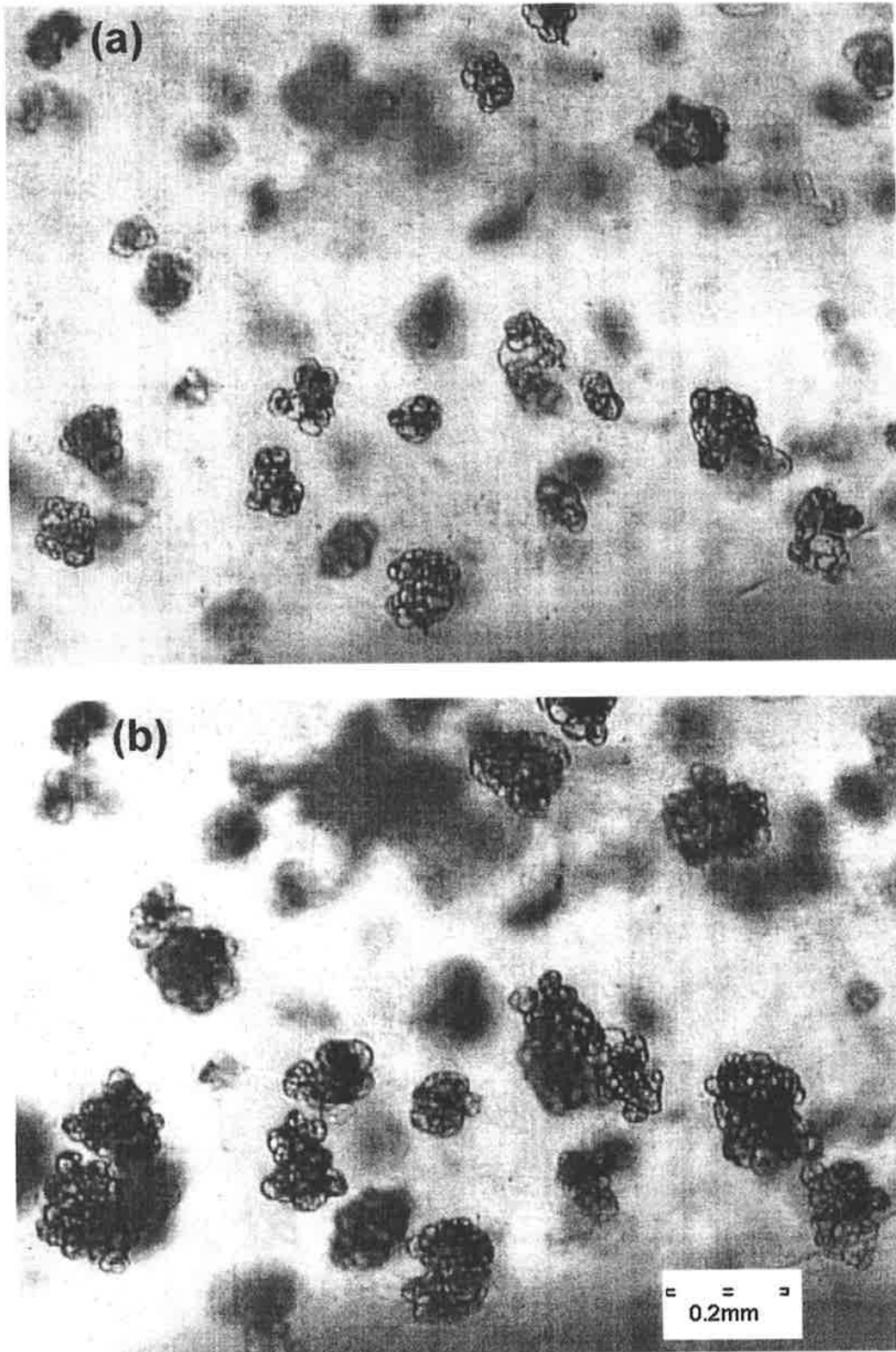


Figure 7-13: Digital images of aggregates in agarose. Images shown are of cells sheared at 57 N/m^2 for 8 h. (a) Day 0, immediately after shearing (b) Day 5. (See Section 5.3.4.4.)

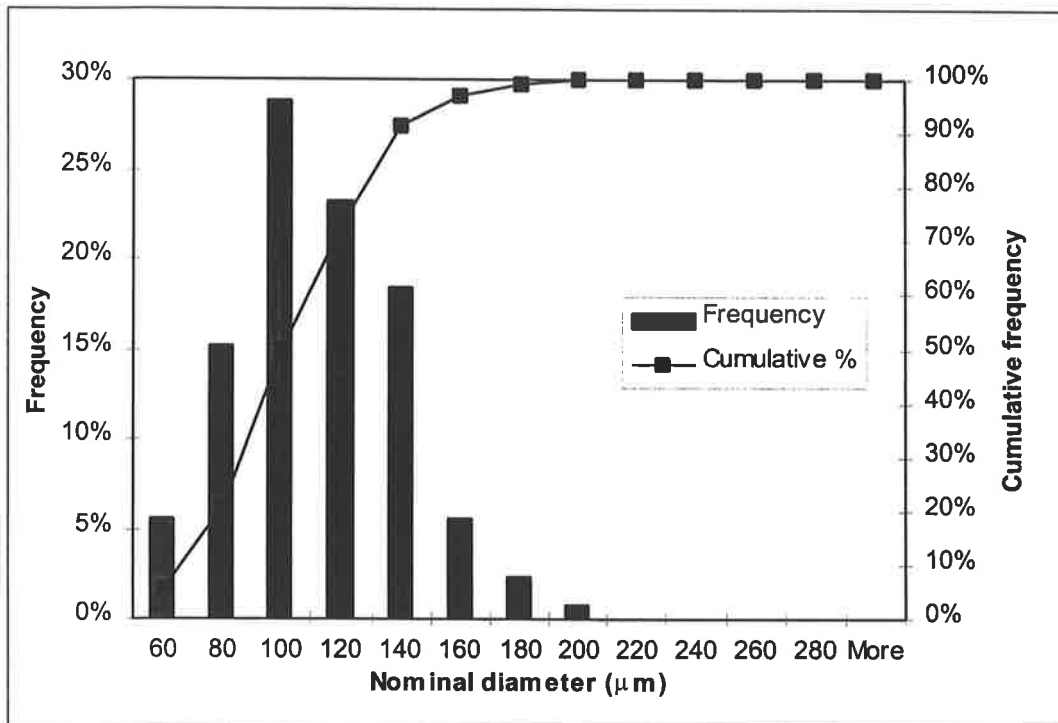


Figure 7-14: Size distribution of aggregates immediately (i.e. Day 0) after shearing at 57 N/m² for 8 h.

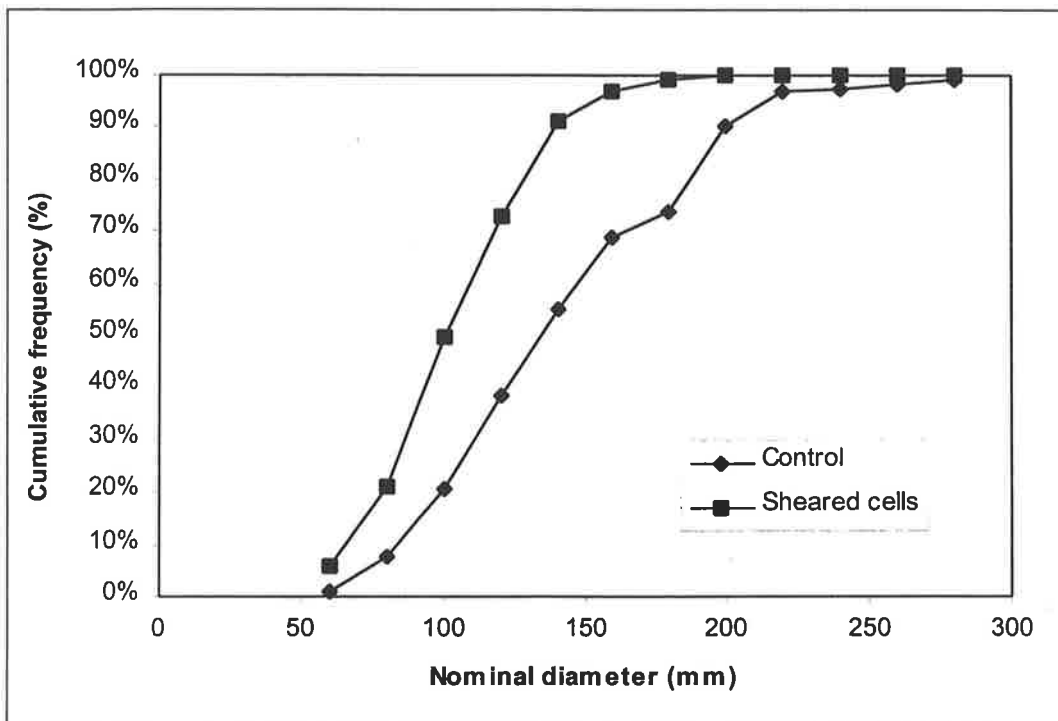


Figure 7-15: Comparison of cumulative frequencies of aggregate sizes on Day 0 for Control cells and cells sheared at 57 N/m² for 8 h.

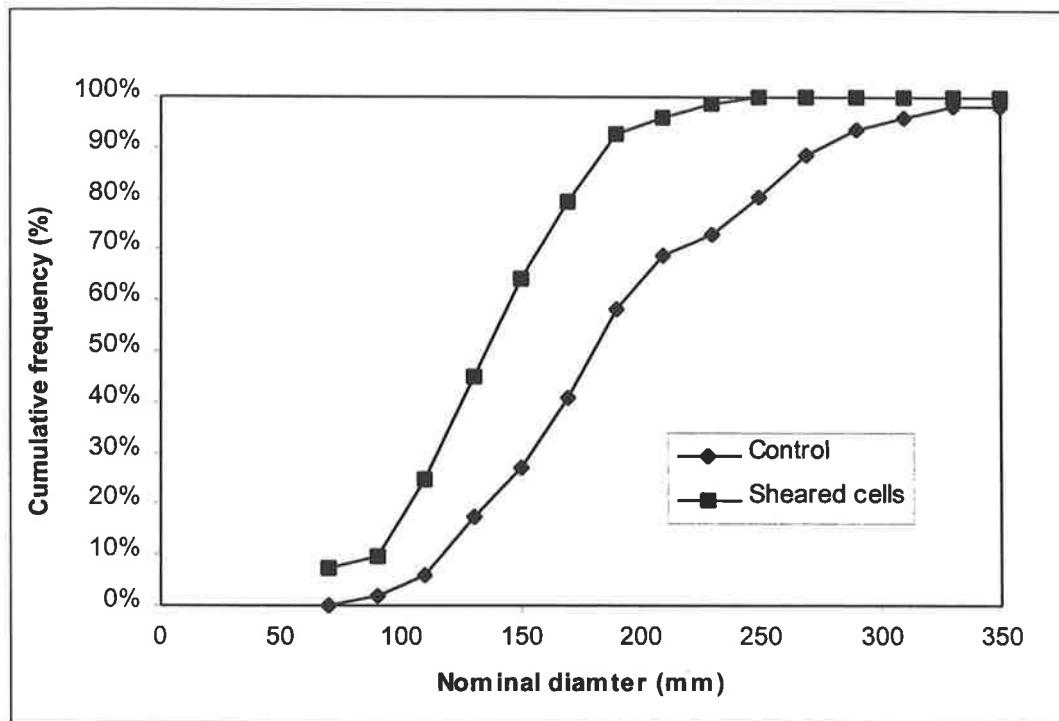


Figure 7-16: Comparison of cumulative frequencies of aggregate sizes on Day 5 for Control cells and cells sheared at 57 N/m² for 8 h.

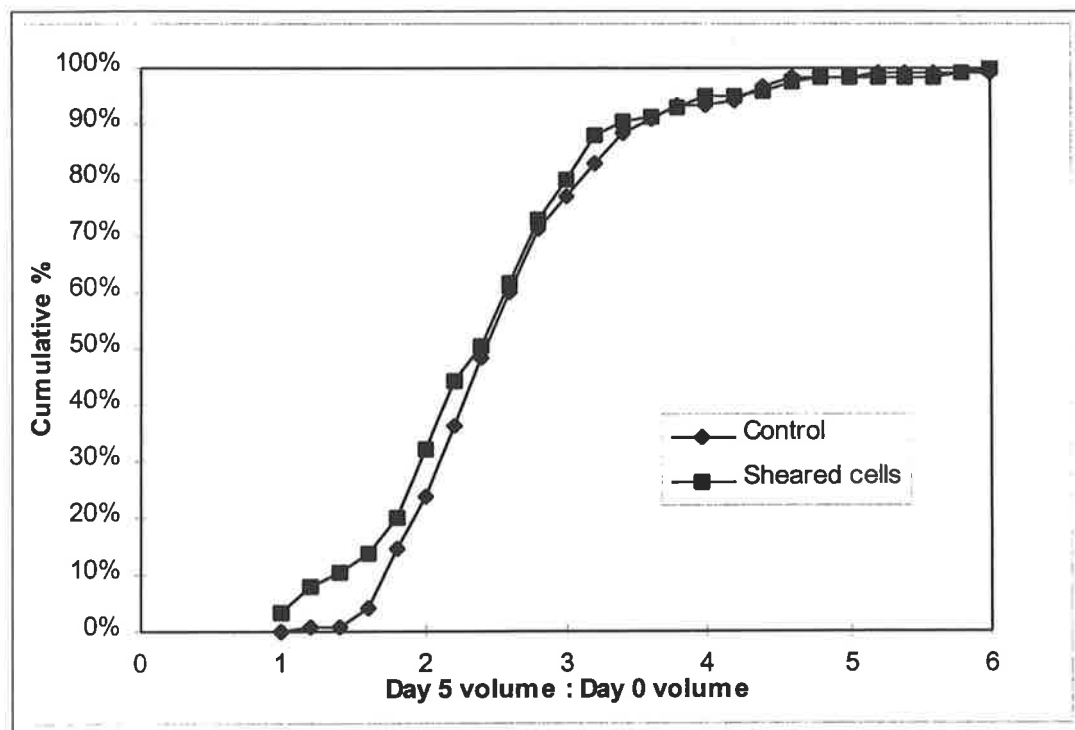


Figure 7-17: Comparison of estimated volume increase for Control cells and cells sheared at 57 N/m² for 8 h.

7.3.2 Kinetics of cell damage

The relative mitochondrial activity, uncoupled OUR and membrane integrity were all found to generally decrease with increased shear exposure, as illustrated in Figure 7-6, 7-8 and 7-9 respectively. A first-order (exponential decay) model is commonly used to model the rate at which various biological activities are damaged by shear stress (Kieran *et al.*, 1995; Rosenberg, 1989). The first-order model takes the form.

$$\frac{B}{B_0} = e^{-k_1 t} \quad (\text{Eq 7-1})$$

where B_0 and B refer to the biological activity of the control and sheared cultures respectively, t is the exposure time and k_1 is the first order rate constant. In Figure 7-18 to 7-20 a first-order model has been fitted to the relative mitochondrial activity, uncoupled OUR and membrane integrity data. The R^2 values for the proposed model are summarised in Table 7-2. In general, the proposed model appears to have a better fit to the experimental data at shear stresses of 74 N/m^2 and above. The biological response for low shear stresses tends to deviate from the proposed exponential decay model. This suggests that below a critical shear level, the rate of damage to the biological activity may not be adequately described by exponential decay.

Figure 7-21 shows the change in rate constant with the level of laminar shear stress in the viscometer. The rate of damage for each biological activity generally increases with shear stress. The rate constant for mitochondrial activity increases more rapidly than the other two, reaching a value of $1.47 \times 10^{-4} \text{ s}^{-1}$ at 100 N/m^2 . In contrast, the increase in the rate constant for membrane integrity is more gradual and only reaches $5.1 \times 10^{-5} \text{ s}^{-1}$ at 100 N/m^2 .

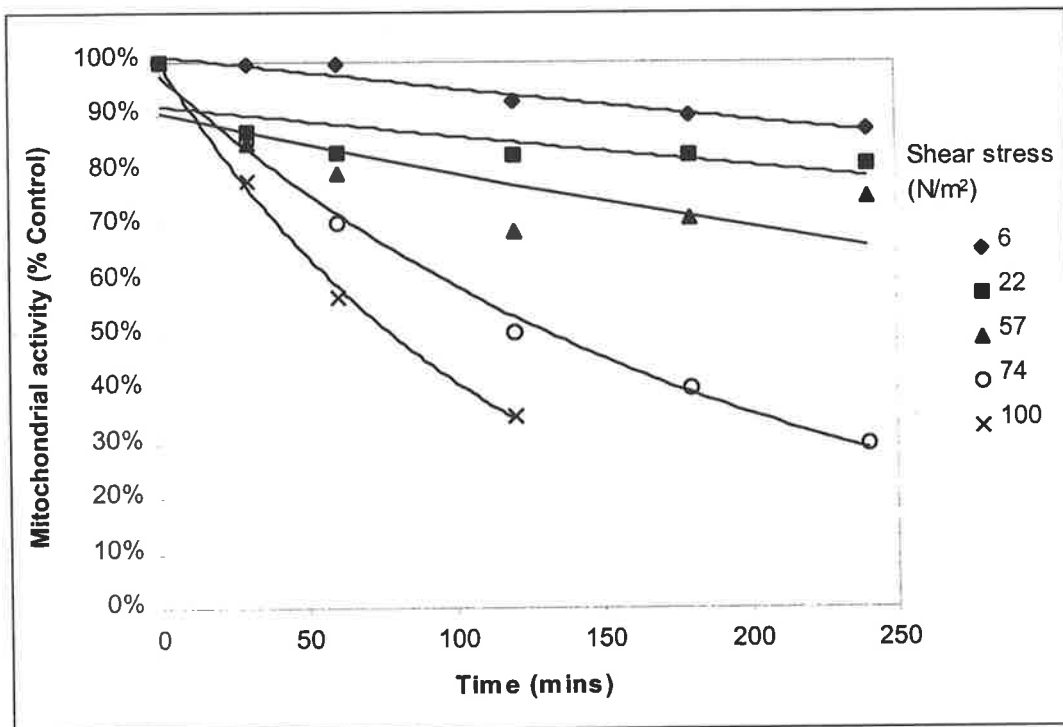


Figure 7-18: Variation of relative mitochondrial activity of sheared cells with exposure time. Lines are for first-order model fitted to the experimental data.

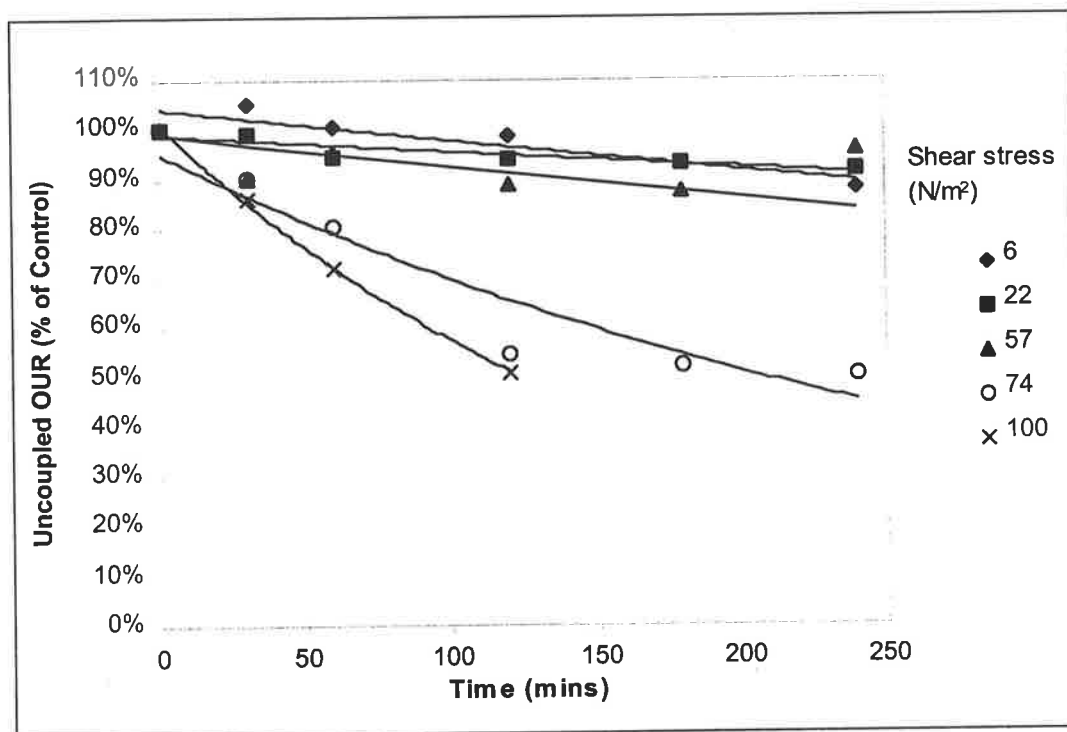


Figure 7-19: Variation of relative uncoupled OUR of sheared cells with exposure time.

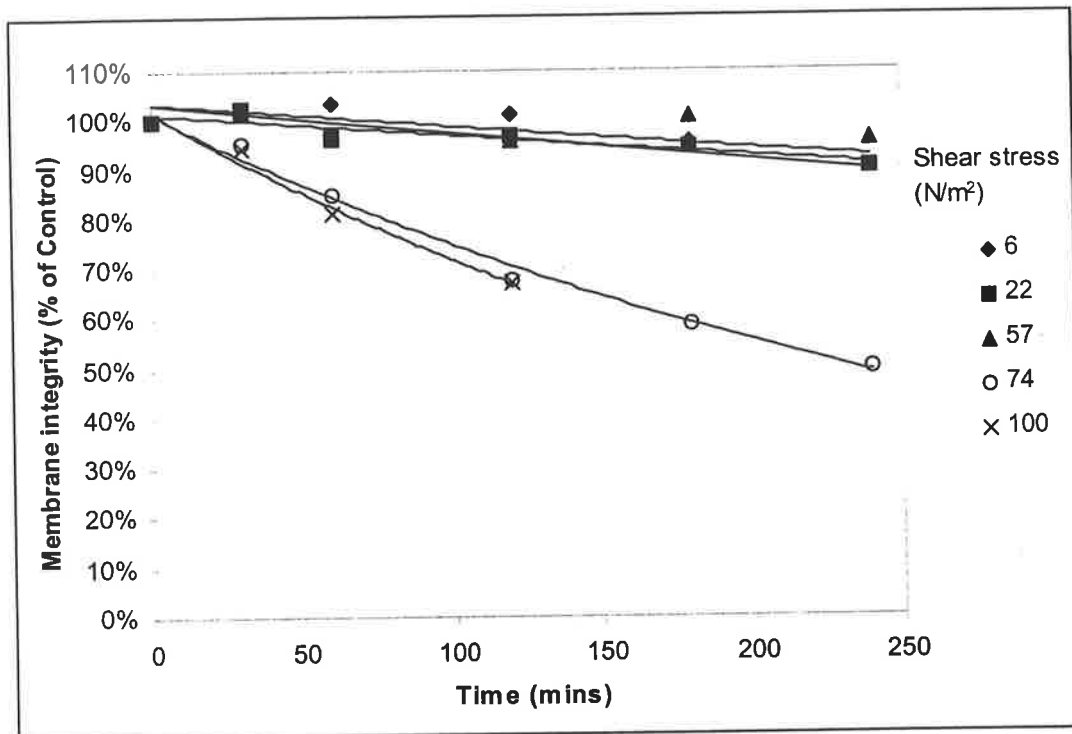


Figure 7-20: Plot of relative membrane integrity of sheared cells with exposure time. Lines are for first-order model fitted to the experimental data.

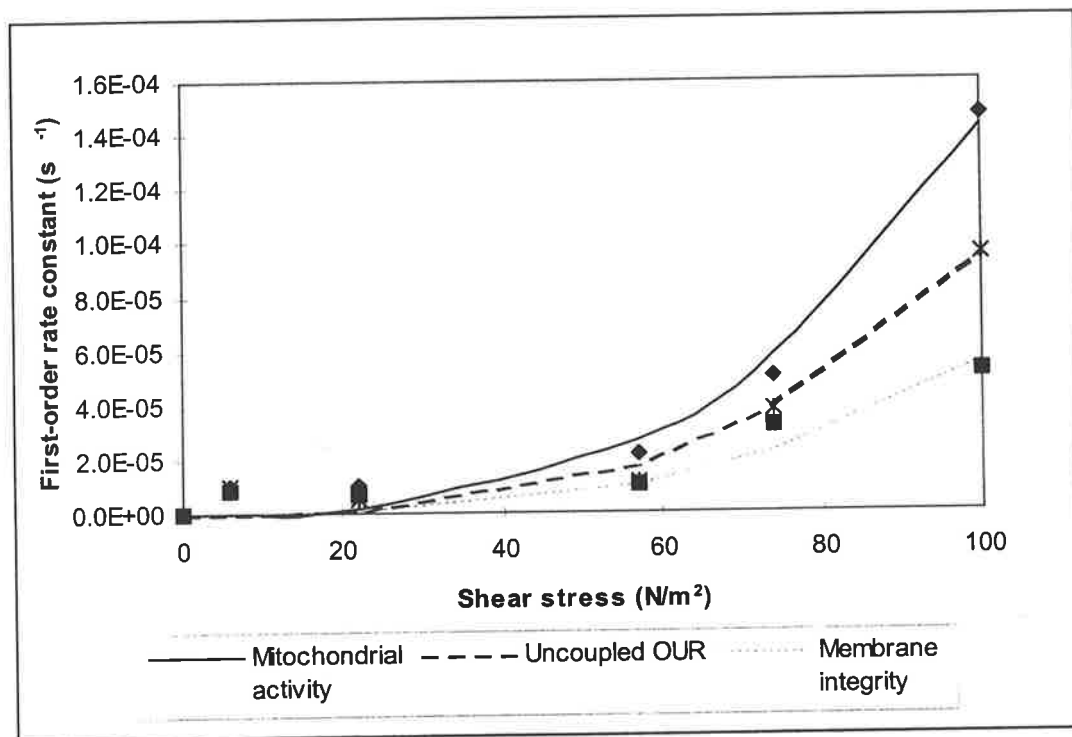


Figure 7-21: Variation of first order decay constant with average laminar shear stress for different biological activities.

Table 7-2: Correlation coefficients (R^2) for first order model of biological activity of sheared cells.

	R^2				
	6 N/m ²	22 N/m ²	57 N/m ²	74 N/m ²	100 N/m ²
Mitochondrial activity	0.96	0.56	0.86	0.99	0.99
Uncoupled OUR	0.83	0.84	0.74	0.89	0.99
Membrane integrity	0.72	0.85	0.79	0.99	0.99

7.3.3 Variation of biological activity with energy dissipation in the viscometer

Dunlop *et al.* (1994) proposed the use of cumulative energy dissipation as a common basis for comparing the effect of shear on various biological activities. This method accounts for both the intensity of the hydrodynamic shear and the exposure time. The energy dissipation rate for steady laminar flow in the Couette was derived from the total kinetic equation of motion. According to Dunlop *et al.* (1994), the rate of work performed by viscous stresses under laminar flow conditions is given by the following expression

$$\frac{\partial}{\partial x_j} (\bar{U}_i \bar{\tau}_{ij}) = \bar{\tau}_{ij} \frac{\partial}{\partial x_j} (\bar{U}_i) = \epsilon \rho \quad (\text{Eq 7-2})$$

where \bar{U}_i = time average velocity of the flow in the i^{th} direction (m/s)

$\bar{\tau}_{ij}$ = viscous shear stress due to laminar flow (N/m²)

ϵ = viscous energy dissipation rate (J/kg s)

ρ = density of the culture medium (kg/m³)

The term on the left hand side is the work performed by viscous stress, and the last term is the rate of viscous energy dissipation. The rate of viscous energy dissipation is given by the middle term, which is the product of the shear stress and shear rate. The amount of energy actually dissipated on the cells is less than the total energy dissipated in the system as the biomass occupies only a fraction ϕ of the total volume. The volume fraction of cells ϕ was estimated from fresh weight measurements assuming a biomass specific gravity of 1.0. Thus, the cumulative energy dissipated on the cells per unit volume (E) is estimated as

$$E = \epsilon_v \rho \phi t \quad (\text{Eq 7-3})$$

where t is the shear exposure time.

Using this approach, the results presented in Figure 7-6 to 7-10 can now be condensed into Figure 7-22. Lines of best fit (least squares method) were included for the uncoupled OUR, membrane integrity and coupled OUR data solely to serve as eye-guides. Exponential decay equations were used for the uncoupled OUR and membrane

integrity best fit lines, whereas a third order polynomial was used for the coupled OUR data. As with most results associated with living systems, there is considerable scatter in the data. Nevertheless, a distinction between the sensitivity of the different biological activities to the cumulative energy dissipated is apparent. The coupled OUR appeared to be the most sensitive, showing stimulation above control levels even at very low energy dissipations. The mitochondrial activity and uncoupled OUR decreased at lower energy levels than those required to damage the membrane integrity. Of these four biological activities, membrane integrity appeared to be the most insensitive to hydrodynamic shear. This will be discussed further in Section 7.5.

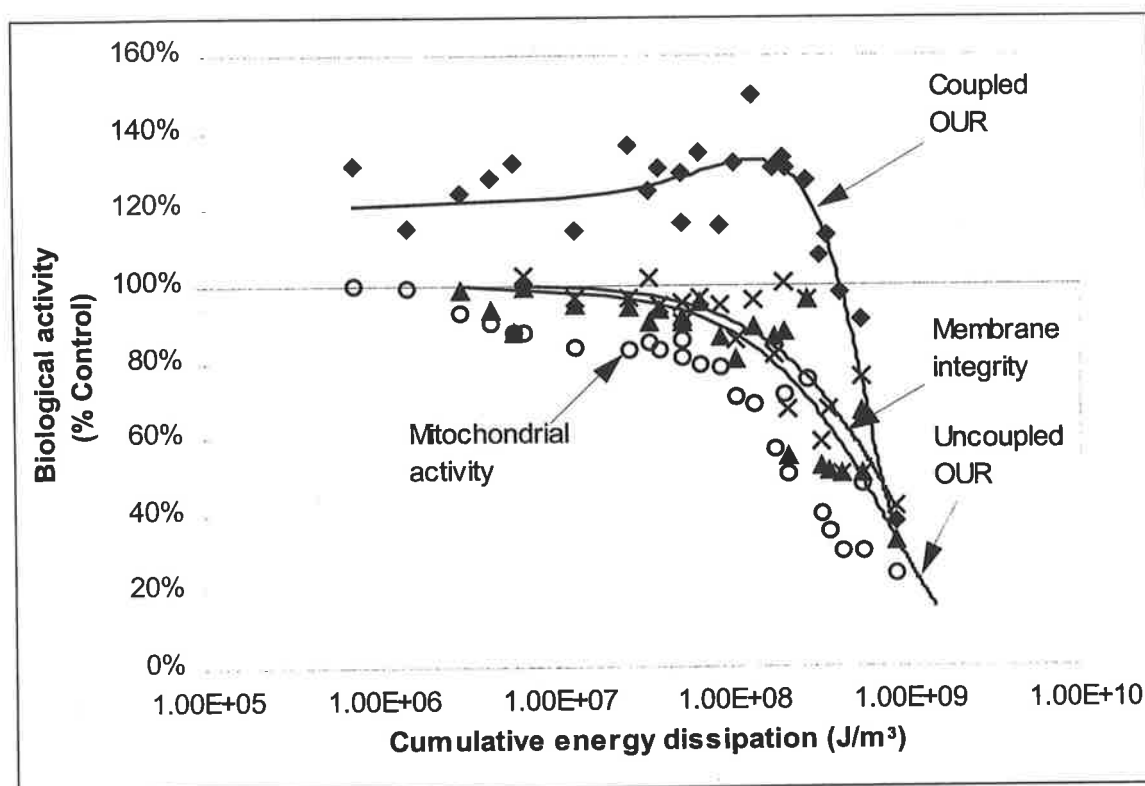


Figure 7-22: Variation of mitochondrial activity, coupled and uncoupled OUR and membrane integrity with the cumulative energy dissipated on the carrot cells in the oxygen-permeable Couette viscometer. ♦ Coupled OUR; × Membrane integrity; ▲ Uncoupled OUR; ○ Mitochondrial activity

7.3.4 *Comment on coupled OUR*

The coupled OUR of the carrot cultures was monitored for up to 2 h after removal from the shear viscometer (See Section 5.3.2). Figure 7-23 shows a typical profile of coupled OUR after the cessation of shearing. The coupled OUR of the sheared cells gradually increased relative to the control. In some cases, the coupled OUR appeared to return to the control level after reaching a peak value.

It is important to note that mild hydrodynamic shear stimulated the actual respiration rate of the cells (coupled OUR) even though the maximum achievable rate (uncoupled OUR) appeared to fall below control levels. The divergence of these 2 biological indicators is clearly seen in Figure 7-10, 7-11 and 7-12. In other words, it appeared that the sheared cells were respiring at a faster rate even when the respiratory machinery of the cells was being damaged by the shear stress. This point can also be seen by comparing the ratio of coupled to uncoupled OUR of the control cultures with the sheared cultures, as shown in Figure 7-24. The coupled/uncoupled OUR ratio of the sheared cultures was consistently higher than the control cultures. This suggests that the sheared cells utilised a higher proportion of their total respiratory capacity compared to the control cells. The ratio also appeared to vary with the prevailing shear stress level, generally rising with increasing shear stress.

It is also worth noting that the decrease in relative coupled OUR of the culture at energy dissipations above 10^8 J/m^3 corresponds approximately with energy dissipation levels where significant damage to membrane integrity of the cells was observed (refer to Figure 7-22). Since only cells with intact membranes can respire, the subsequent fall in coupled OUR of the total population of cells (which contains both damaged and intact cells) could be due to a reduction in the proportion of respiring cells, rather than a decrease in the respiratory rate of an intact cell.

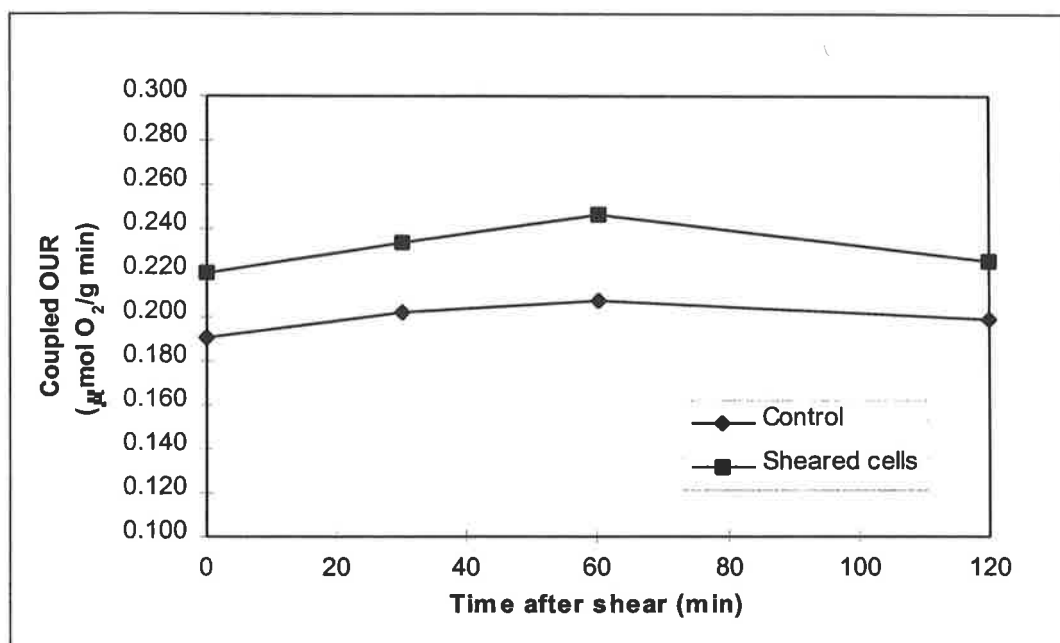


Figure 7-23: Typical profile of coupled OUR of sheared and control cells after sheared cells were removed from the viscometer. See Section 5.3.3 for experimental details.

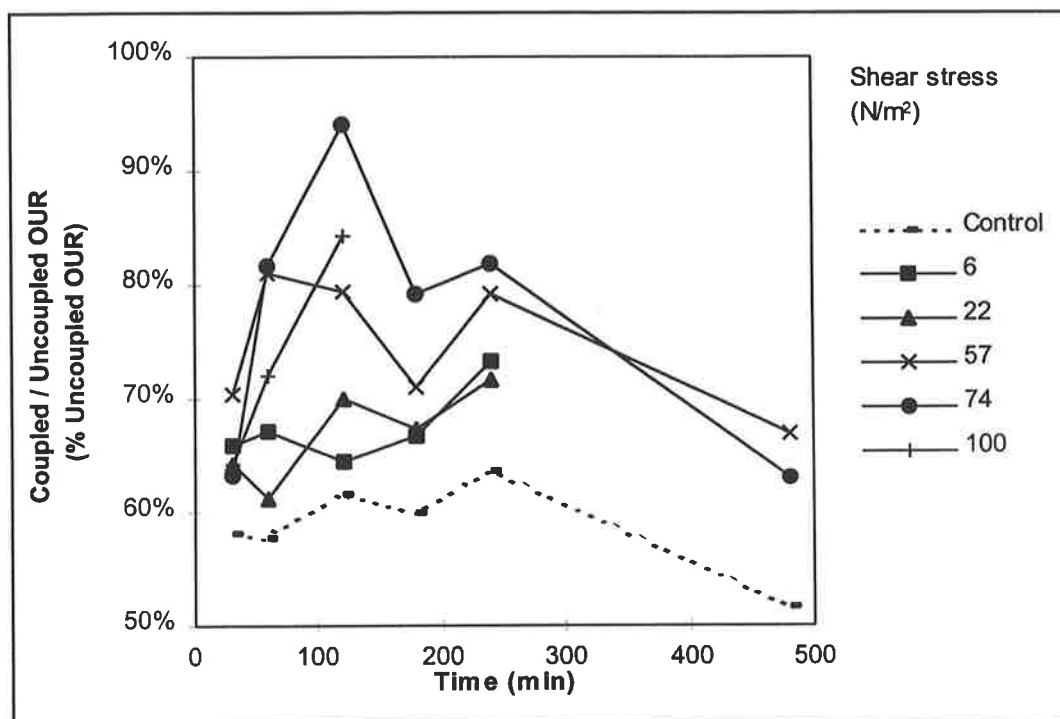


Figure 7-24: Comparison of coupled/uncoupled OUR ratio of control and sheared cultures.

7.3.5 *Correlation between mitochondrial activity and uncoupled OUR*

The mitochondrial activity and uncoupled OUR in Figure 7-10 to 7-13 display similar behaviour. A plot of the mitochondrial activity versus uncoupled OUR recorded for the shear tests is given in Figure 7-25. This plot suggests a correlation between these two biological indicators. A linear regression of the data yielded a correlation coefficient (R) of 0.92. Since both these indicators depend on the physiological state of the mitochondria and associated enzymes, it seems probable that there might be a relationship. Prompted by this observation, similar regressions were carried out between these two biological indicators and the membrane integrity. Table 7-3 summarises the correlation coefficients for the various linear regressions. The correlation between mitochondrial activity and membrane integrity appeared to be the weakest amongst the 3 cases. However, uncoupled OUR seemed to correlate equally well with mitochondrial activity and membrane integrity. Hence, based on these data alone, it is difficult to determine if the correlation between mitochondrial activity and uncoupled OUR is real or fortuitous. In the next chapter, the behaviour of these biological indicators in response to various ion channel blockers and calmodulin inhibitors will be examined. If the correlation between two biological activities is real, then they would be expected to respond similarly to each of the chemical compounds.

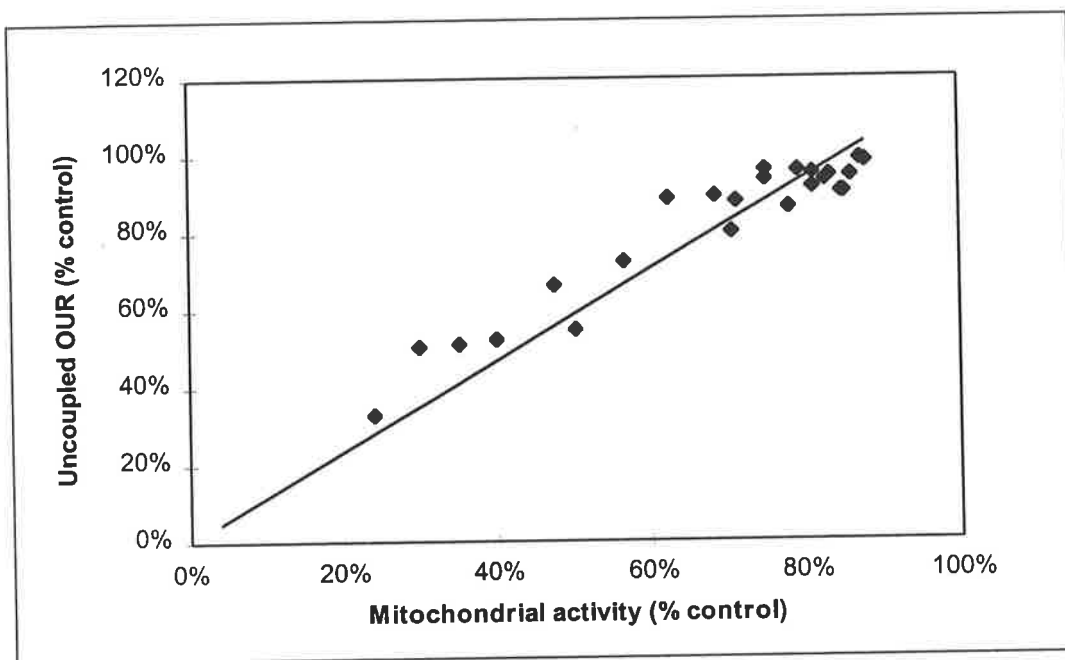


Figure 7-25: Uncoupled OUR versus mitochondrial activity for sheared cultures. Linear regression was forced through origin. $y = 0.172x$, $R^2 = 0.847$.

Table 7-3: R and R^2 values for linear regressions between mitochondrial activity, uncoupled OUR and membrane integrity. Linear regressions were forced through origin.

Correlation	R	R^2
Mitochondrial activity - Uncoupled OUR	0.920	0.847
Membrane integrity - Uncoupled OUR	0.944	0.891
Mitochondrial activity - Membrane integrity	0.805	0.648

7.4 Discussion

A variety of biological activities were found to be affected by hydrodynamic shear before significant damage to membrane integrity was observed. These sub-lytic effects included a reduction in mitochondrial activity and uncoupled OUR and a stimulation of coupled OUR (Figure 7-10 and 7-13). It is possible that the changes in these biological activities are symptoms of the growth reduction observed in shake flask cultures at high agitation rates (Figure 7-1 and 7-2). Sub-lytic effects have also been observed in a number of other plant cells, including safflower (Takeda *et al.*, 1994), eucalyptus (Takeda *et al.*, 1998), *Atropa belladonna* (Wongsamuth and Doran, 1994) and *Stizolobium hassjoo* (Chen and Huang, 2000) as well as other cultivars of carrot (Rosenberg, 1989). Measurements of the DO level in the oxygen-permeable viscometer suggest that the observed responses are unlikely to be caused by oxygen limitation or starvation as the DO level of the cultures remained above 90% saturation throughout the shear testing period (Figure 7-4). Furthermore, since the cells were re-suspended in fresh medium prior to testing, sucrose and other essential nutrients would not have been depleted during the test period. It is worth noting that oxygen depletion may be a serious problem in conventional Couette viscometers with small gap widths especially since the respiration rate of the cells appear to be stimulated by hydrodynamic shear. The results of some previous studies that used conventional oxygen-impermeable Couette viscometers (e.g. Rosenberg, 1989) may have to be re-considered in light of the present findings.

The rate of damage by shear to the mitochondrial activity, uncoupled OUR and membrane integrity could be adequately modelled by first order (exponential decay) kinetics (Figure 7-18). The model fitted the experimental data better for shear stresses above 74 N/m^2 . First order kinetics have also been found to adequately model the rate of damage by turbulent flow to membrane integrity on *Morinda citrifolia* cultures (Kieran *et al.*, 1995; MacLoughlin *et al.*, 1998). Comparison of the rate constants for the three biological indicators reveal a hierarchy in the rate of damage by fluid shear, with mitochondrial activity being most sensitive, followed by uncoupled OUR and then membrane integrity. The stimulatory effect of shear on the coupled OUR precludes the use of simple first order kinetics to model the behaviour. At present, no models have been proposed to predict the coupled OUR response to shear.

The regrowth ability of the carrot cultures appears to be less sensitive to shear than mitochondrial activity and oxygen uptake rate. The sensitivity was found to be closer to that of membrane integrity. This suggests that stressed cells which retain their membrane integrity are able to recover after removal from the high-shear environment. Scragg *et al.* (1988) made a similar observation in bioreactor cultures of *Catharanthus roseus* and *Helianthus annuus*. They found that shearing in the bioreactors affected the dry weight, aggregate size distribution and oxygen uptake of the cells but did not have a significant impact on the subsequent ability of the cells to regrow in shake flasks. Similarly, whole plants which exhibited growth retardation when mechanical stimulation was applied daily, resumed normal growth once the stimulus was removed (Jaffe, 1973). In the present study, microscopic analysis of cell aggregates previously exposed to shear was carried out by immobilising the cells in transparent agarose beads. This technique enabled the growth of selected clusters of cells to be monitored over a period of time. As shown in Figure 7-13, a majority of the cells, previously sheared at 57 N/m^2 for 8 h, clearly retained their ability to grow and divide after removal from the shear environment. At the same shear level, the mitochondrial activity, coupled and uncoupled OUR had all been significantly affected (Figure 7-10). In contrast, Rosenberg (1989) reported that regrowth ability was very sensitive to hydrodynamic shear compared to mitochondrial activity. He found that the regrowth ability of carrot cells exposed to laminar shear in a viscometer was almost completely lost before reductions in mitochondrial activity and membrane integrity were observed. At present, the reason for this difference is unclear, although it may be due to one or a combination of several factors. These factors include (i) the effect of antibiotics in the regrowth medium, (ii) differences in the regrowth assay technique or (iii) differences in the shear sensitivity of the cell lines.

No antibiotics were used in the present study to avoid placing additional selection pressure on the already shear-weakened cells. There is some evidence that certain antibiotics have adverse effects on plant growth and development (Leifert *et al.*, 1992; Sarma *et al.*, 1995).

Rosenberg (1989) based the regrowth assay on a plating technique developed by Horsch and Jones (1980). In this technique, only cell colonies which reach a size visible to the naked eye was counted as "viable". This viability criterion would be suitable if

the treatment being tested did not significantly alter the size distribution of the cell aggregates used for plating. For example, in the original article by Horsch and Jones (1980), the technique was tested on cells exposed to UV irradiation, which is unlikely to significantly affect the aggregate size distribution. However, when carrot cultures were subjected to hydrodynamic shear, a clear reduction in aggregate sizes was observed (Figure 7-15). Hence, colonies plated from sheared cultures may not reach a visible size in the same time as the control cultures, even though the sheared cells may still be actively dividing and growing. Further work is required to determine if the sensitivity of regrowth to hydrodynamic shear differs between different cell lines.

The effects of shear on the various biological activities were correlated against cumulative energy dissipation (Figure 7-22). Although there was considerable scatter in the data, the cumulative energy dissipation level at which 90% of the biological activity was maintained can be estimated. This corresponds to approximately 1×10^7 , 9×10^7 and $1.5 \times 10^8 \text{ J/m}^3$ for mitochondrial activity, uncoupled OUR and membrane integrity, respectively. The values for mitochondrial activity and membrane integrity are of the same order of magnitude as those reported by Dunlop *et al.* (1994) for carrot cells exposed to laminar shear in a viscometer. The fact that the biological activities show a good correlation with cumulative energy also suggests that the effect of shear on the measured biological activities may be cumulative. Above a critical shear stress, exposure to low shear stresses over an extended period may result in similar damage as brief exposures at higher shear stresses. Zhong *et al.* (1994) reported a similar observation for *Perilla frutescens* cultures sheared in a Couette viscometer. However, it should be noted that in bioreactor cultivations lasting for several days, culture properties will not remain constant during the growth cycle. Moreover, the sensitivity of plant cells to shear has been shown to vary between the different phases of the growth cycle (Hooker *et al.*, 1989). Nonetheless, the cumulative effect of shear may have important implications in the optimisation of conditions for bioreactor cultivations of plant cells.

The coupled OUR of carrot cells was found to be stimulated by hydrodynamic shear for cumulative energy dissipations up to $2 \times 10^8 \text{ J/m}^3$ before subsequently reducing at higher shear energies. Similar increases in the coupled OUR with shear was also reported in cultures of strawberry (Keßler *et al.*, 1997b), *C. roseus* (Scragg *et al.*, 1988) and *Nicotiana tabacum* (Ho *et al.*, 1995). In contrast, the use of uncoupled OUR as an

indicator of hydrodynamic shear damage has not been reported to date. In this study, uncoupled OUR was found to be suppressed with increased exposure to shear. Furthermore, it appears to be more sensitive to hydrodynamic shear stress than membrane integrity (Figure 7-21 and Figure 7-22), which is a commonly reported indicator for shear damage (for example Kieran *et al.*, 1995). This suggests that uncoupled OUR, along with coupled OUR, may be employed as convenient and sensitive indicators of shear damage.

There is a possibility that the increase in the coupled respiration rate of the sheared cultures could be due to the larger surface area of cell aggregates caused by aggregate break-up. However, the diverging trend between the coupled and uncoupled OUR seems to refute this explanation, as an increased surface area should lead to an increase in both OUR indicators. Keßler *et al.* (1997b) also observed an increase in the respiration rate of strawberry cells when subjected to shearing in bioreactors with different impellers. They demonstrated that impeller designs which resulted in more aggregate break-up did not cause a larger increase in oxygen uptake rate (coupled). This suggests that the shear-induced increase in coupled OUR cannot be completely attributed to aggregate break-up and is likely to be due instead to changes in cellular activity. The increase in coupled OUR of suspended plant cells resembles the stimulation in respiration rate of plant tissues or organs subjected to mechanical wounding or pathogen attack (Uritani and Asahi, 1980) and could result from similar mechanisms within the cell. In plant tissues, 'wound respiration' has been associated with higher energy requirements for wound healing and lignin formation, as well as the production of plant antibiotics to combat pathogen incursion. It is possible that suspended cell cultures similarly requires additional energy for processes such as wound healing or reinforcement of the cell wall to enable the cell to cope with the high shear environment. It is worth noting that hydrodynamic shear has been demonstrated to modify the cell wall composition and content of *C. roseus* suspension cultures (Tanaka *et al.*, 1988).

It has been suggested that factors such as culture age and cell aggregate size can affect the sensitivity of plant cells to hydrodynamic shear. For example, Hooker *et al.* (1989) demonstrated that cultures in the late exponential and early stationary phases were more susceptible to shear damage compared to cultures in the lag, early

exponential or late stationary phases. In this thesis, cell cultures in the late exponential phase (14 days) were used for shear testing. Preliminary observations of a small number of shear tests (data not shown) carried out on early-exponential phase carrot cells (7 days) appear to corroborate with Hooker's results. In addition, based on intuition, larger aggregates are more likely to be damaged by shear forces compared to smaller aggregates, as the small aggregates would be entrained harmlessly in the fluid eddies. A detailed theoretical approach would require the comparison of Kolmogoroff eddy scales with the aggregate size (for example, see Kieran *et al.* 2000). In this thesis, cell cultures were pre-screened to exclude aggregates larger than 263 μm , based on considerations to improve the reproducibility of TTC results, as well as to reduce the likelihood of aggregates being ground by the Couette walls (see Section 5.3.3.5). Further work would be required using cells for different age and aggregate sizes to establish their shear sensitivity.

Although the mechanism leading to the stress-induced increase in respiration rate is still poorly understood, it is known that the mitochondria of higher plants have a unique respiratory pathway, known as the alternative pathway, which shows increased expression in response to a wide range of environmental stresses (Vanlerberghe and McIntosh, 1997). This may have important implications for bioreactor cultivation of plant cells at high cell densities. Shear-induced stimulation in oxygen uptake rate will put additional demand to supply sufficient oxygen to the cells. This additional oxygen demand may be difficult to meet as cell densities increase towards the end of the growth phase and the culture becomes more viscous. Since plant cells have been reported to exhibit heightened shear sensitivity in the late exponential phase (Hooker *et al.*, 1989), large increases in the agitation or aeration rate may not be a viable option. Instead, limiting the adverse effects of shear on cell viability might be a more successful approach. Several studies, summarised in Chapter 2, showed that the effects of mechanical and osmotic stress on whole plants can be alleviated by ion channel blockers and calmodulin inhibitors which disrupt the ion signalling processes within plant cells. In the next chapter, the effects of these chemical compounds on the fluid shear sensitivity of the carrot cell cultures will be examined.

CHAPTER 8

RESULTS AND DISCUSSION

In the previous chapter, various sub-lytic effects were observed in carrot cultures exposed to fluid shear stresses. In particular, fluid shear was found to stimulate coupled OUR and suppress uncoupled OUR and mitochondrial activity before damage to membrane integrity was observed. In this chapter, the effects of three ion channel blockers and a calmodulin inhibitor on the biological response of carrot cells to fluid shear will be evaluated. The ability of these chemical compounds to alleviate the effects of mechanical and osmotic stress in whole plants has been highlighted in the literature review. This study aims to determine if these compounds will have similar effects on the sub-lytic response of cultured carrot cells and attempts to elucidate the mechanism leading to the sub-lytic response. Factorial-designed experiments were conducted in the oxygen-permeable Couette and in shake flasks to determine the effects of these compounds at different shear levels and the interactions between these effects. The statistical significance of the interaction effects was examined through analysis techniques outlined in Chapter 6. In addition, the effects of prolonged exposure to these compounds were investigated in shake flask cultures.

It has been suggested that membrane stretching by fluid shear forces could modulate the activity of ion channels and trigger the sub-lytic response. Hence, this chapter also describes studies using the patch-clamp to examine the behaviour of ion channels in response to stretching of the cell membrane.

In the final section, the potential application of these findings for the genetic engineering or screening of robust plant cell lines for industrial plant culture production is discussed. These results are also combined with our current understanding of the cell-signalling architecture to propose a possible mechanism by which shear stress signals are received and transduced within plant cells.

8.1 Effects of ion channel blockers and calmodulin inhibitor

8.1.1 Effects on coupled OUR

Table 8-1 summarises the response of the sheared cultures in the factorial design experiments. It shows the coupled and uncoupled OUR, mitochondrial activity and membrane integrity (expressed as % Control-) of carrot cultures sheared at either 38 N/m^2 (-1) or 100 N/m^2 (+1) for an hour. Based on the results of the viscometer runs presented in the previous chapter, these two levels of shear stress were found to induce sub-lytic effects in the late exponential carrot cultures. They are also sufficiently widespread to enable us to investigate whether the effects of the chemicals might be dependent on the level of shear stress. The combination of ion channel blockers (Ruthenium Red, Verapamil, NPPB) or calmodulin inhibitor (W7) added prior to shear exposure is also shown in Table 8-1. In each column, a plus or minus sign indicates the inclusion or exclusion of a particular chemical respectively. The concentration of each chemical was given in Table 5-1 (Chapter 5). "Control -" refers to shake flask cultures with no chemicals added (see Section 5.3.3).

Figure 8-1 and 8-2 plots the coupled OUR (% Control-) of the different runs at 38 and 100 N/m^2 respectively. A line showing the average coupled OUR level of the carrot cultures sheared without any blockers is also included in the figures for comparison. The value of this line was estimated from Figure 7-9 in Chapter 7 and verified in actual experimental runs.

Six of the runs shown in Figure 8-1 and 8-2 yielded coupled OUR responses that were at least 20% different from the response with no blockers. The 20% criterion is a general rule-of-thumb value estimated from observations of previous experimental runs involving this particular cell line and enables a rough initial estimate of significant effects. The combination of chemicals used in these 6 runs is listed in Table 8-2.

Table 8-1: Biological responses (expressed as % of the corresponding Control - response) of sheared carrot cultures in factorial design experiment

Run code	A= W7	B= Ruthenium Red	C= Verapamil	D= NPPB	E= Shear level	Response (%Control-)			
						Coupled OUR	Uncoupled OUR	Mitochondrial Activity	Membrane Integrity
1a	-1	-1	-1	-1	-1	125	97	83	93
7a	1	-1	-1	-1	1	126	86	56	90
8b	-1	1	-1	-1	1	165	97	119	87
4b	1	1	-1	-1	-1	106	82	86	88
3a	-1	-1	1	-1	1	142	84	65	82
5b	1	-1	1	-1	-1	129	92	61	94
6b	-1	1	1	-1	-1	130	89	137	93
2a	1	1	1	-1	1	124	90	92	83
2b	-1	-1	-1	1	1	159	86	81	86
6a	1	-1	-1	1	-1	123	77	86	91
5a	-1	1	-1	1	-1	125	92	111	95
3b	1	1	-1	1	1	118	61	66	76
4a	-1	-1	1	1	-1	107	82	73	90
8a	1	-1	1	1	1	105	54	52	68
7b	-1	1	1	1	1	182	93	92	80
1b	1	1	1	1	-1	110	77	81	85

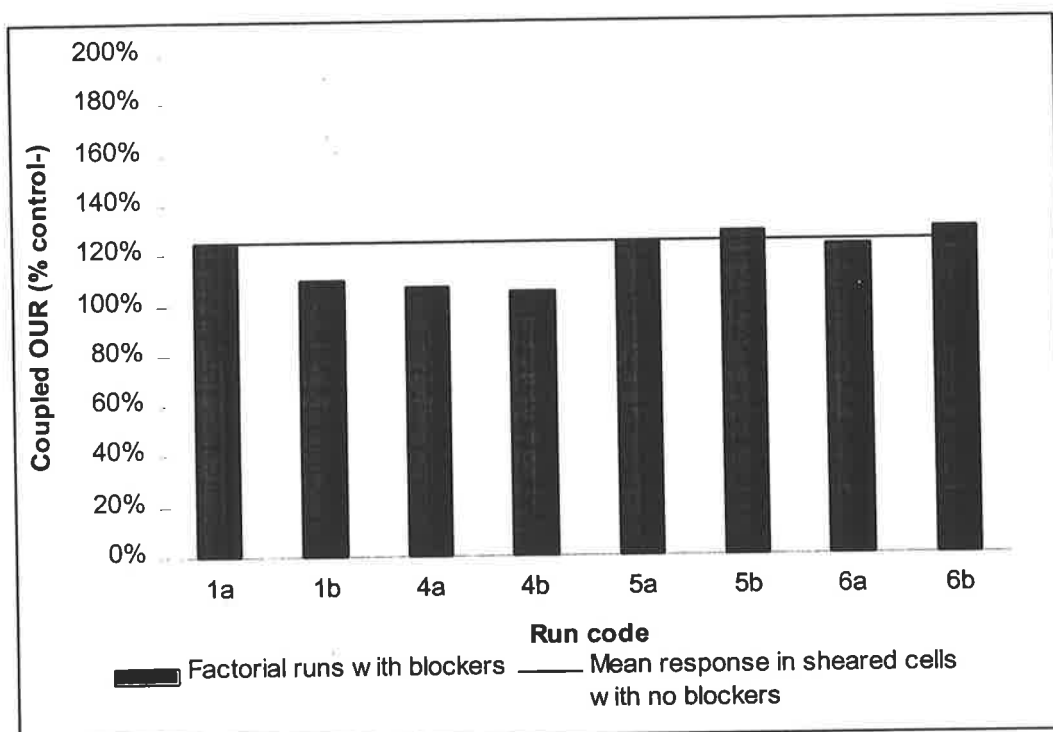


Figure 8-1: Coupled OUR of sheared cells for factorial runs at 38 N/m².

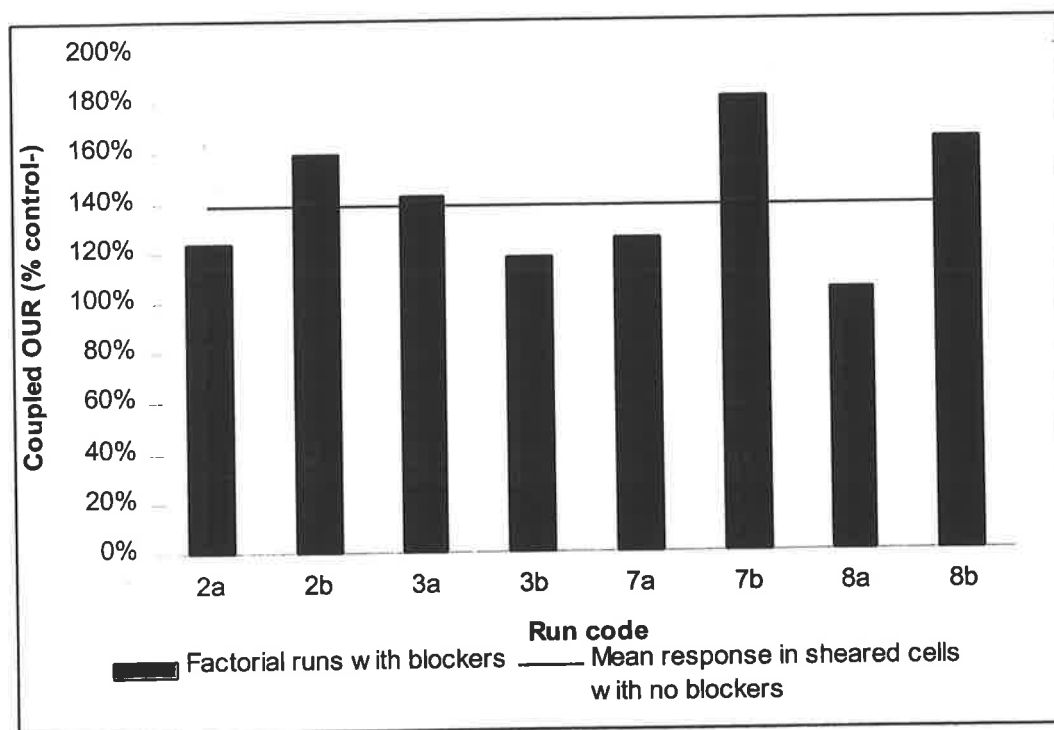


Figure 8-2: Coupled OUR of sheared cells for factorial runs at 100 N/m².

Table 8-2: Treatment combinations in the selected factorial runs. A tick indicates the inclusion of the chemical in that run. Factorial runs where the coupled OUR response of sheared cells was lower than the response when no blocker treatment was added are marked with an asterisk (*).

Run code	W7	Ruthenium	Verapamil	NPPB
		Red		
2b				✓
*3b	✓	✓		✓
*4b	✓	✓		
7b		✓	✓	✓
*8a	✓		✓	✓
8b		✓		

The three runs which yielded a coupled OUR response that was lower than when no blockers were added are marked with an asterisk (*). That is, the coupled OUR of the sheared cells was nearer to that of the control level for these 3 runs. From Table 8-2, we note that W7 was involved in all 3 of these runs. Moreover, W7 was not involved in any runs in which the coupled OUR was higher than when no blocker was added. This suggests that the effect of shear on the coupled OUR of carrot cultures may be sensitive to W7. The validity of this conclusion was tested with the statistical analysis techniques described in Section 6.3.

The definition of the *main effect* of a particular factor and the *interaction* between factors has been explained in Chapter 6. The main effect measures the influence of a particular factor on the observed response while the interaction takes into account the influence of the other variables on the main effect of a factor. The main effects, interactions and sum of squares for a factorial designed experiment can be easily calculated by applying the Yate's algorithm (1937). The application of this algorithm to the coupled OUR response is described in Appendix B. Table 8-3 summarises the main effects, interactions and sum of squares of the coupled OUR response (expressed as % Control -) for the different treatment combinations.

Section 6.3.1 described a simple method for identifying the statistically significant effects based on a normal scores plot. Figure 8-3 shows the normal scores plot of the main effects and interactions for the coupled OUR response. Effects which are negligible are normally distributed and will tend to fall along a straight line on this plot. However, significant effects will have non-zero means and will lie away from the straight line.

Table 8-3: Estimates of effects and sum of squares of the coupled OUR response of sheared cells for the factorial experiment. The letters ‘a, b, c, d, e’ refer to the effect of W7, Ruthenium red, Verapamil, NPPB and shear level respectively. The combination ‘ab’ refers to the two-factor interaction between W7 and Ruthenium red.

Actual effects with aliases	Estimated effects	Main effects / interactions (% control -)	Sum of Squares (% control -)
Average		129.7	
a-bcde	a	-24.4	23.8
b-acde	b	5.5	1.2
ab-cde	ab	-11.8	5.6
c-abde	c	-2.4	0.2
ac-bde	ac	1.2	0.1
bc-ade	bc	10.1	4.1
abc-de	-de	-3.8	0.6
d-abce	d	-2.1	0.2
ad-bce	ad	-4.8	0.9
bd-ace	bd	4.8	0.9
abd-ce	-ce	1.4	0.1
cd-abe	cd	-3.1	0.4
acd-be	-be	-8.8	3.1
bcd-ae	-ae	19.6	15.3
abcd-e	-e	-21.0	17.6

Figure 8-3 suggests that the main effects of W7 (a) and shear level (e) and the 'W7 x shear' interaction (ae) are important. As described in Chapter 6, the 2^{5-1} resolution V factorial design causes every main effect to be aliased with a four-factor interaction and every two-factor interaction to be aliased with a three-factor interaction. For example, the main effect of W7 (a) calculated is really the true main effect of W7 less the four-factor interaction of the other factors (a-bcde). Similarly, the 'W7 x shear' interaction calculated is really the three-factor interaction 'Ruthenium x Verapamil x NPPB' minus the two-factor interaction 'W7 x shear'. The alias patterns are listed in Table 8-3. However, since three-factor and higher interactions are usually negligible compared to the main effects and low-order interactions, according to the "sparsity of effects principle" (Montgomery, 1991), there is a high probability that the main effects of W7 and shear and the 'W7 x shear' two-factor interaction will dominate over their corresponding high-order aliases. The estimated effect combinations, obtained by ignoring the higher-order aliases, are also listed in Table 8-3. The validity of this assumption is checked through the statistical analysis which follows.

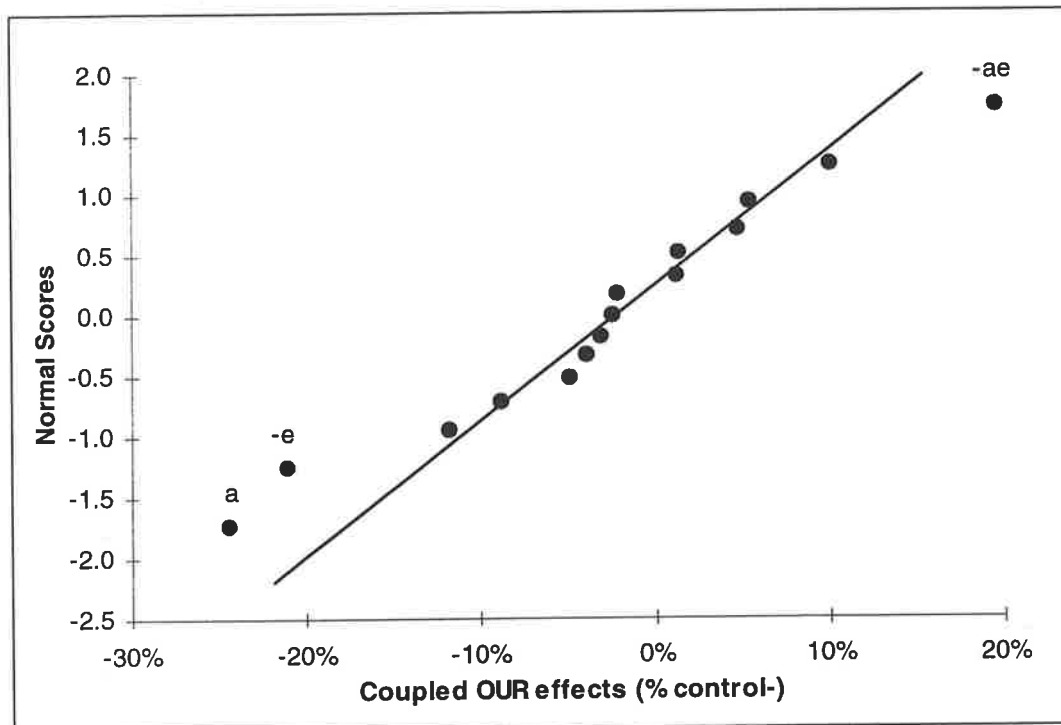


Figure 8-3: Normal scores plot of main effects and interactions of Coupled OUR response for sheared cultures. The letters 'a, b, c, d, e' refer to the effect of W7, Ruthenium red, Verapamil, NPPB and shear level respectively.

The main effects of W7 and shear are plotted in Figure 8-4. Shear had a positive effect on coupled OUR. Increasing the shear stress from 38 to 100 N/m² increased the average coupled OUR response by approximately 21% (relative to Control-) across all levels of the other factors. On the other hand, the addition of W7 reduced the coupled OUR response of the sheared cells by about 24% averaged across all levels of the other factors. Note that the coupled OUR of the sheared cells did not fall below "Control -" levels for all treatment combinations (Table 8-1).

As explained in Chapter 6, conclusions based on main effects alone can be misleading if they are involved in statistically significant interactions. Hence, we need to examine the 'W7 x shear' interaction closely. The 'W7 x shear' interaction is plotted in Figure 8-5. Increasing the shear level raised the average coupled OUR from 122% to 162% in the absence of W7 (which is a change of about 40%), compared to a change of only 1.4% in the presence of W7. This shows that addition of W7 attenuated the effect of shear on the coupled OUR response. This agrees with the hypothesis that the coupled OUR of sheared cultures is sensitive to W7.

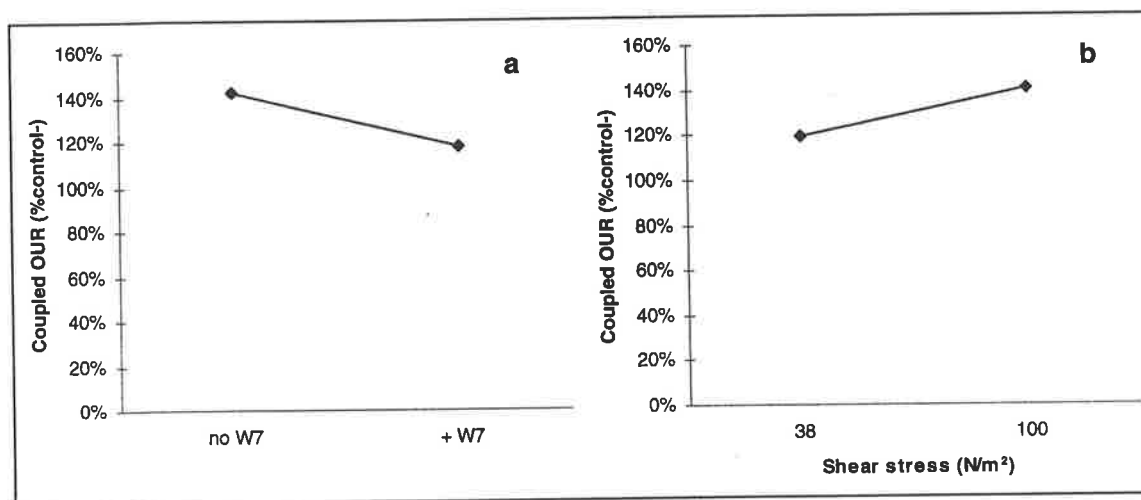


Figure 8-4: Plot of main effects on coupled OUR of sheared cells for (a) W7 and (b) shear.

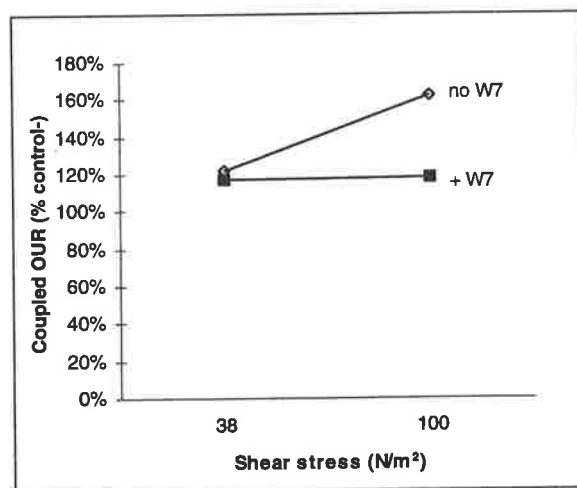


Figure 8-5: 'W7 x shear' interaction for coupled OUR of sheared cells.

Table 8-4 summarises the analysis of variance for the coupled OUR response. The model sum of squares is $SS_{\text{model}} = SS_{\text{W7}} + SS_{\text{shear}} + SS_{\text{W7} \times \text{shear}} = 56.7\%$, and this accounts for over 76% of the total variability in the coupled OUR response. In addition, the F-test for W7, shear and their interaction confirms that they are all significant at the 5% level. The error sum of squares was computed by pooling the sum of squares of the remaining main effects and of the interactions deemed to be insignificant.

Table 8-4: Analysis of variance for coupled OUR response of sheared cultures. A and E refer to W7 and shear respectively, while AE refers to the 'W7 x shear' interaction.

Source of variation	Sum of squares (% control -)	Degrees of freedom	Mean square	F-test statistic	% of Total
A	23.8	1	23.8	16.40	
E	17.6	1	17.6	12.14	
AE	15.3	1	15.3	10.54	
Error	17.4	12	1.5		
Model	56.7				76.5%
Total	74.1	15			

Residual analysis was used as a diagnostic check of the above conclusions (see Section 6.3.3). Since the only significant factors appear to be W7, shear and the 'W7 x shear' interaction, a regression model containing only these variables should theoretically fit the coupled OUR response. Montgomery (1991) suggests the following linear statistical model for residual analysis. The predicted coupled OUR (% control -), \hat{y} is given by

$$\begin{aligned}\hat{y} &= \beta_0 + \beta_a x_a + \beta_e x_e + \beta_{ae} x_{ae} \\ &= 129.7 + \left(\frac{-24.4}{2} \right) x_a + \left(\frac{21.0}{2} \right) x_e + \left(\frac{-19.6}{2} \right) x_a x_e\end{aligned}$$

where 129.7% is the average response and the coded variables x_a and x_e take on the values of +1 or -1 depending on the level of the factors W7 and shear, respectively. The regression coefficients are one-half of the corresponding factor effect estimates.

The normal scores plot of the residuals between the predicted and actual coupled OUR response is shown in Figure 8-6. The points on this plot lie reasonably close to a straight line, suggesting that the residuals are normally distributed. Furthermore, a plot of the residuals against the predicted coupled OUR response did not show any obvious trend in the variance of the residuals (Figure 8-7). These observations lend support to our proposition that W7, shear and the 'W7 x shear' interaction are the only significant factors affecting the coupled OUR response and that the underlying assumptions of the analysis are satisfied.

In the analysis above, the effect of the various chemicals on the coupled OUR of the sheared cultures was measured against the coupled OUR of untreated control cultures which were maintained in shake flasks at 100 rpm (Control-). To determine if these chemicals have similar effects on cultures not exposed to hydrodynamic shear, a parallel factorial experiment was also conducted on cells that were treated with the same combination of chemicals but not sheared in the viscometer. Instead, these cultures were maintained in shake flasks at 100 rpm (Control+). By comparing the effects of the chemicals on the viscometer-sheared cultures with that of the Control+ cultures, we can determine if these chemicals only affect shear-induced changes in cellular activity.

The normal scores plot for the main effects and interactions on the coupled OUR response of Control+ cells are shown in Figure 8-8. Note that this represents a full 2^4

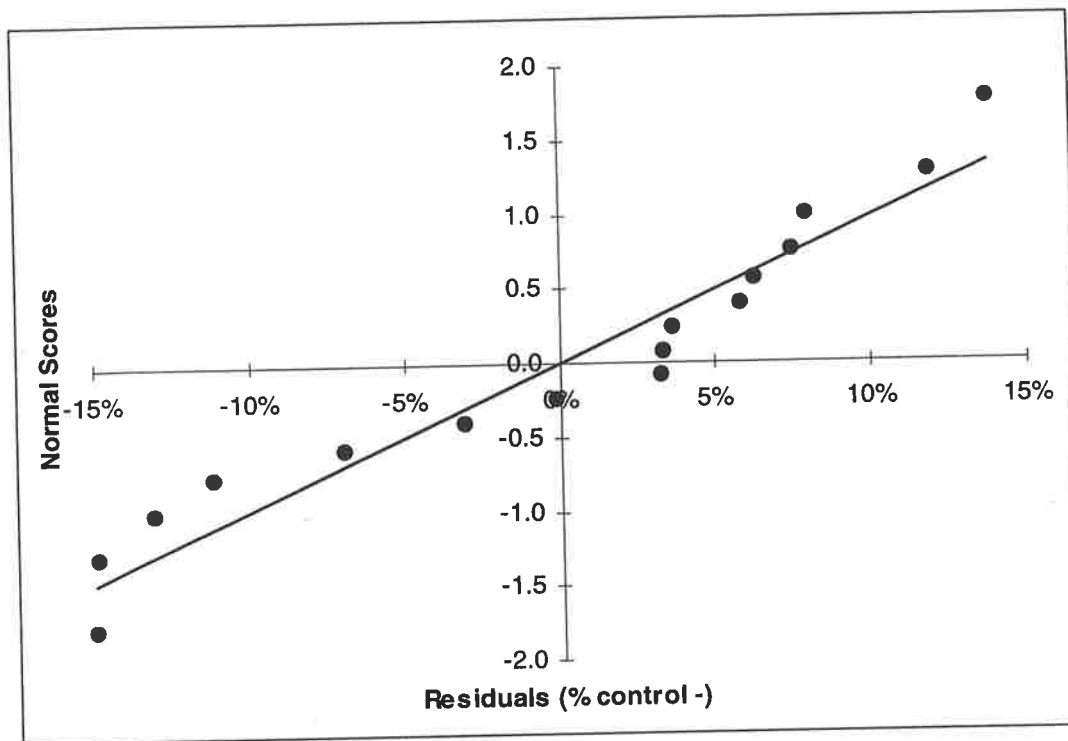


Figure 8-6: Normal scores plot of residuals between actual and predicted coupled OUR response for sheared cells.

factorial design, since shear level is not a factor, hence, the effects are not aliased with any interactions. The plot suggests that none of the effects are significant, as the data all lie along the cumulative normal distribution line. Furthermore, an analysis of variance shows that the combined sum of squares of the two largest effects in this case (i.e. the W7 x shear and the W7 x Ruthenium x NPPB interaction) account for only 35% of the total variability of the coupled OUR response (Table 8-5). Thus, it appears that the coupled OUR of un-sheared cultures is not significantly affected by any of the chemicals when exposed for up to an hour. This suggests that the reduction in the coupled OUR of sheared cultures by W7 may not be simply due to the addition of the chemical alone. Instead, there appears to be an intimate interaction between calmodulin inhibition by W7 and changes in the respiratory activity of the cells caused by hydrodynamic shear.

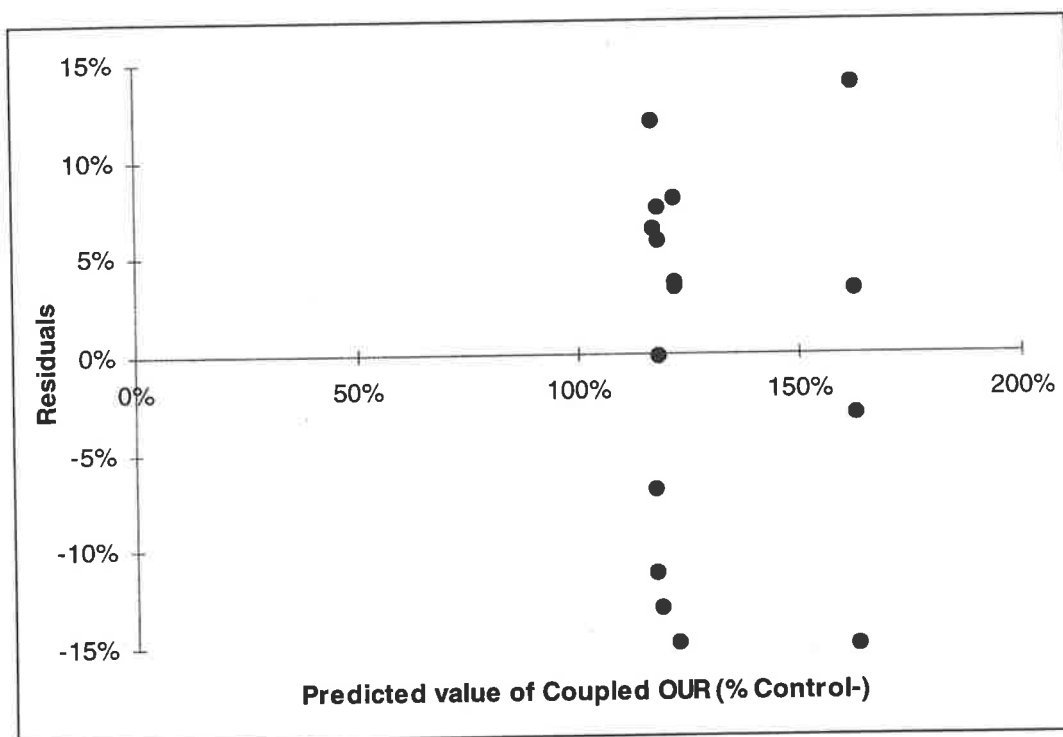


Figure 8-7: Residuals vs predicted value of coupled OUR response for sheared cells.

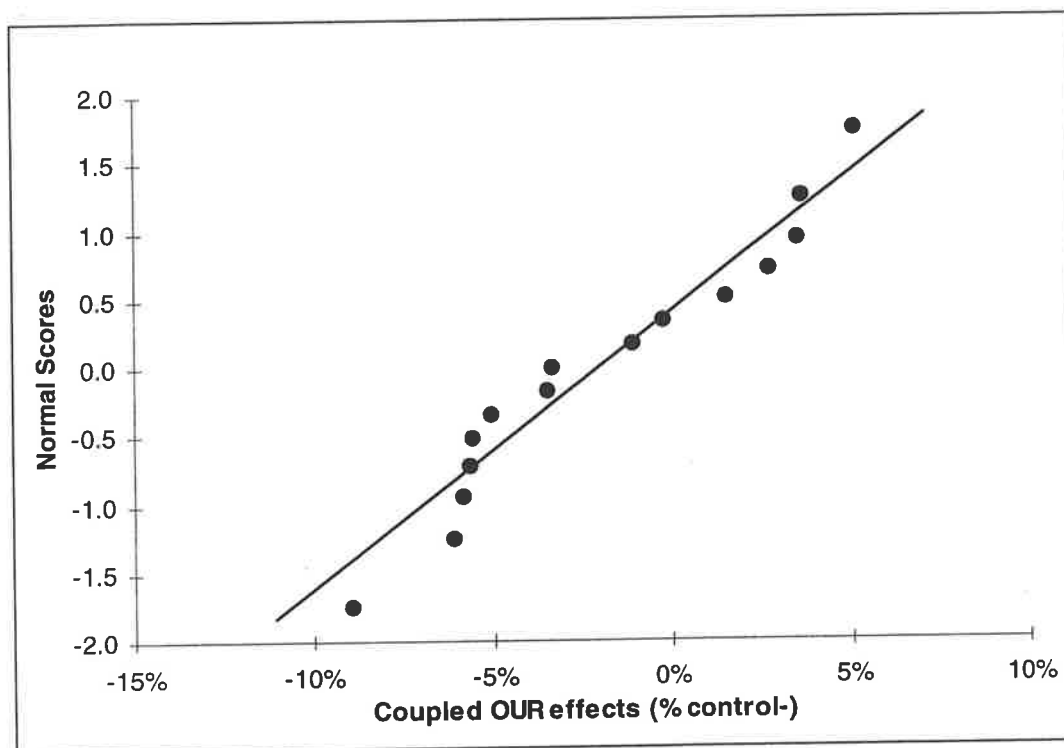


Figure 8-8: Normal scores plot of main effects and interactions of coupled OUR response for Control+ cells.

Table 8-5: Analysis of variance for coupled OUR response of Control+ cells. AD and ABD refer to the 'W7 x NPPB' two-factor interaction, and the 'W7 x Ruthenium red x NPPB' three-factor interaction, respectively.

Source of variation (% control -)	Sum of squares	Degrees of freedom	Mean square	F-test statistic	% of Total
AD	3.2	1	3.2	4.95	
ABD	1.5	1	1.5	2.29	
Residuals	8.4	13	0.6		
Model	4.7				35.8%
Total	13.1	15			

8.1.2 Effects on uncoupled OUR

The main effects and interactions for the uncoupled OUR response of the sheared cells are listed in Table 8-6. Figure 8-9 shows the normal scores plot of the main effects and interactions. This plot suggests that the main effects of W7 (a), NPPB (d) and the 'W7 x NPPB' two-factor interaction (ad) are significant. The F-test for W7, NPPB and their two-factor interaction indicates that they are significant at the 5 % level. The details of the statistical analysis can be found in Appendix C. The normal scores plot of the residuals between the predicted and actual value for each run is given in Figure 8-10. This plot suggests that the residuals are normally distributed and further supports our hypothesis that W7 and NPPB are the only significant factors. However, a plot of the residuals against the predicted uncoupled OUR response suggests that the variance in the data is not constant (Figure 8-11). Figure 8-12 shows the plot of the residuals versus each of the factors. Figure 8-12a and d suggests that runs which include W7 or NPPB tend to show a greater variability in the uncoupled OUR response compared to the other runs. That is, the presence of W7 and NPPB appears to increase the variability in the uncoupled OUR response of the sheared cells.

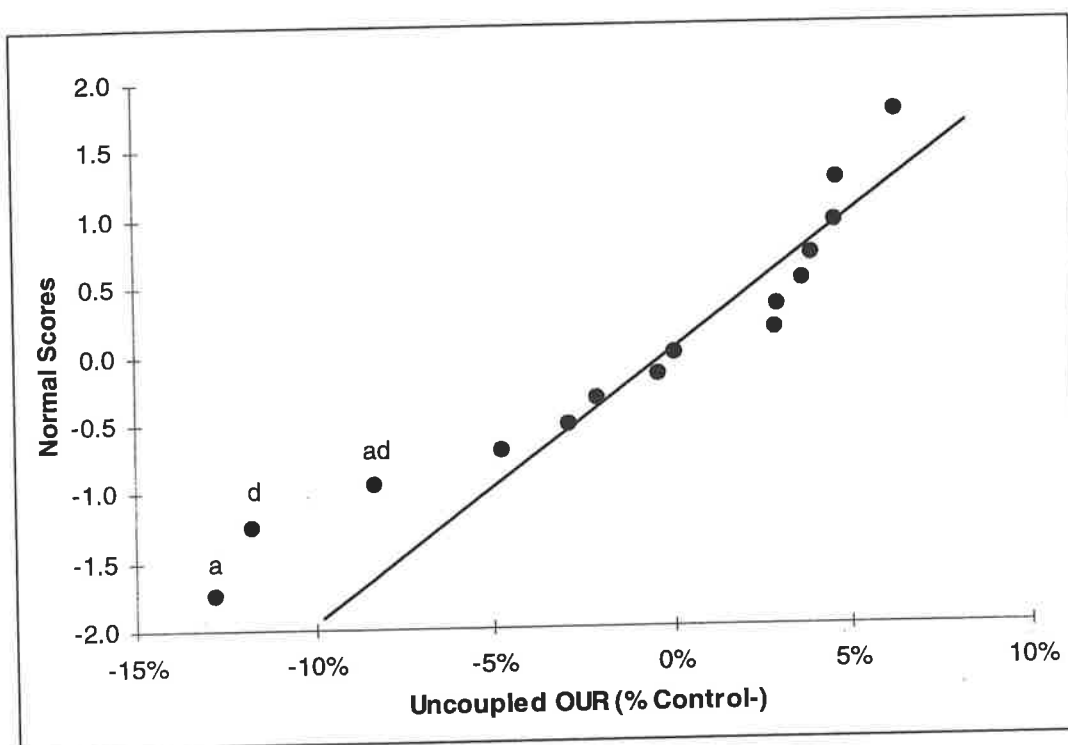


Figure 8-9: Normal scores plot of main effects and interactions of uncoupled OUR response for sheared cells. The letters 'a, b, c, d, e' refers to W7, Ruthenium red, Verapamil, NPPB and shear level respectively.

Table 8-6: Estimates of effects and sum of squares of the uncoupled OUR response of sheared cells for the factorial experiment. The letters 'a, b, c, d, e' refer to the effect of W7, Ruthenium red, Verapamil, NPPB and shear level respectively.

Estimated effects	Main effects / interactions (% control -)	Sum of Squares (% control -)
	83.7	
a	-12.8	6.6
b	3.0	0.4
ab	-2.9	0.3
c	-2.1	0.2
ac	3.7	0.6
bc	6.4	1.6
-de	4.0	0.6
d	-11.7	5.5
ad	-8.3	2.8
bd	2.9	0.3
-ce	0.1	0.0003
cd	-0.4	0.01
-be	-4.8	0.9
-ae	4.7	0.9
-e	4.7	0.9

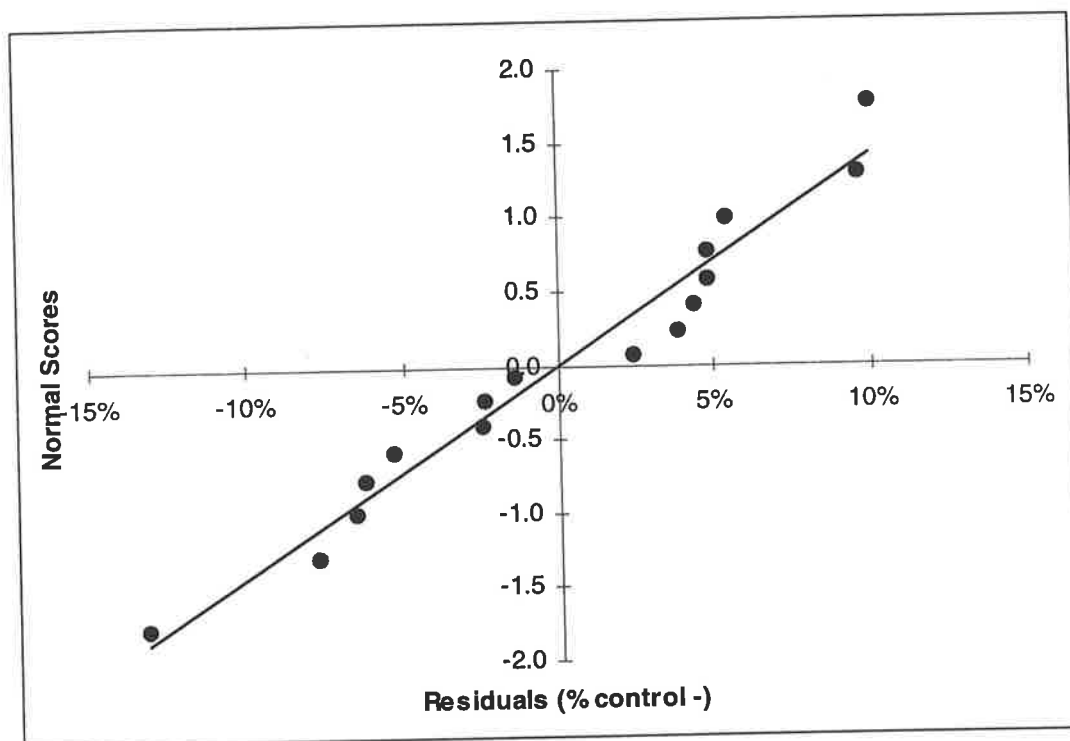


Figure 8-10: Normal scores plot for residuals of uncoupled OUR response for sheared cells

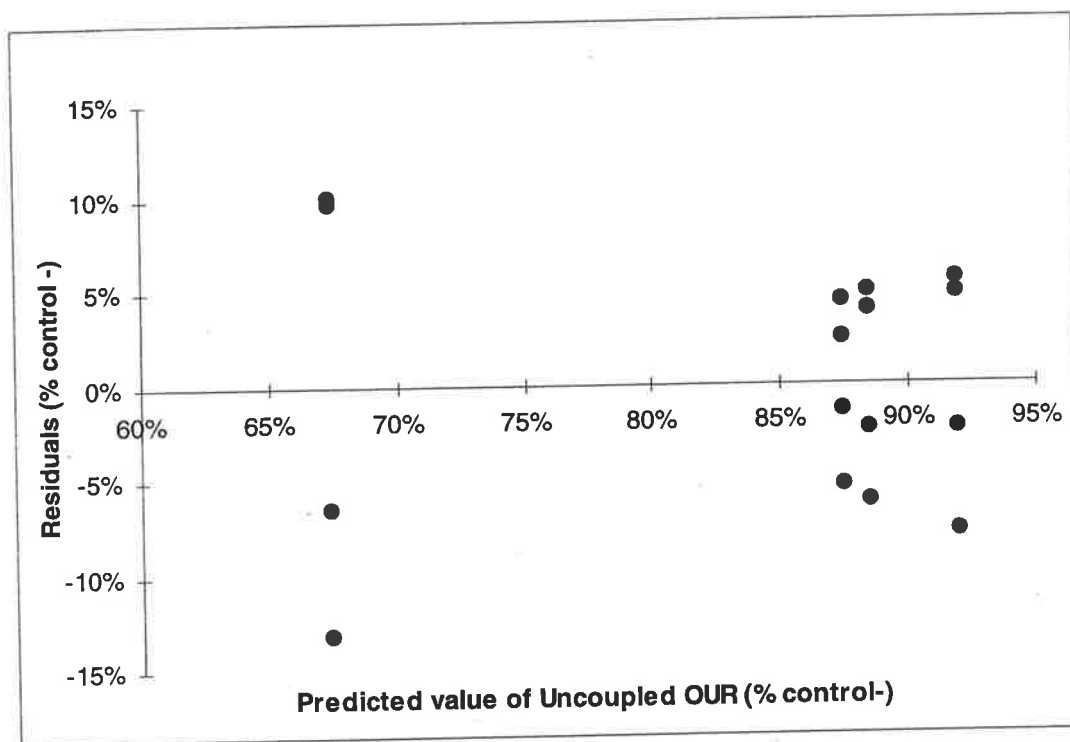


Figure 8-11: Residuals vs predicted value of uncoupled OUR for sheared cells.

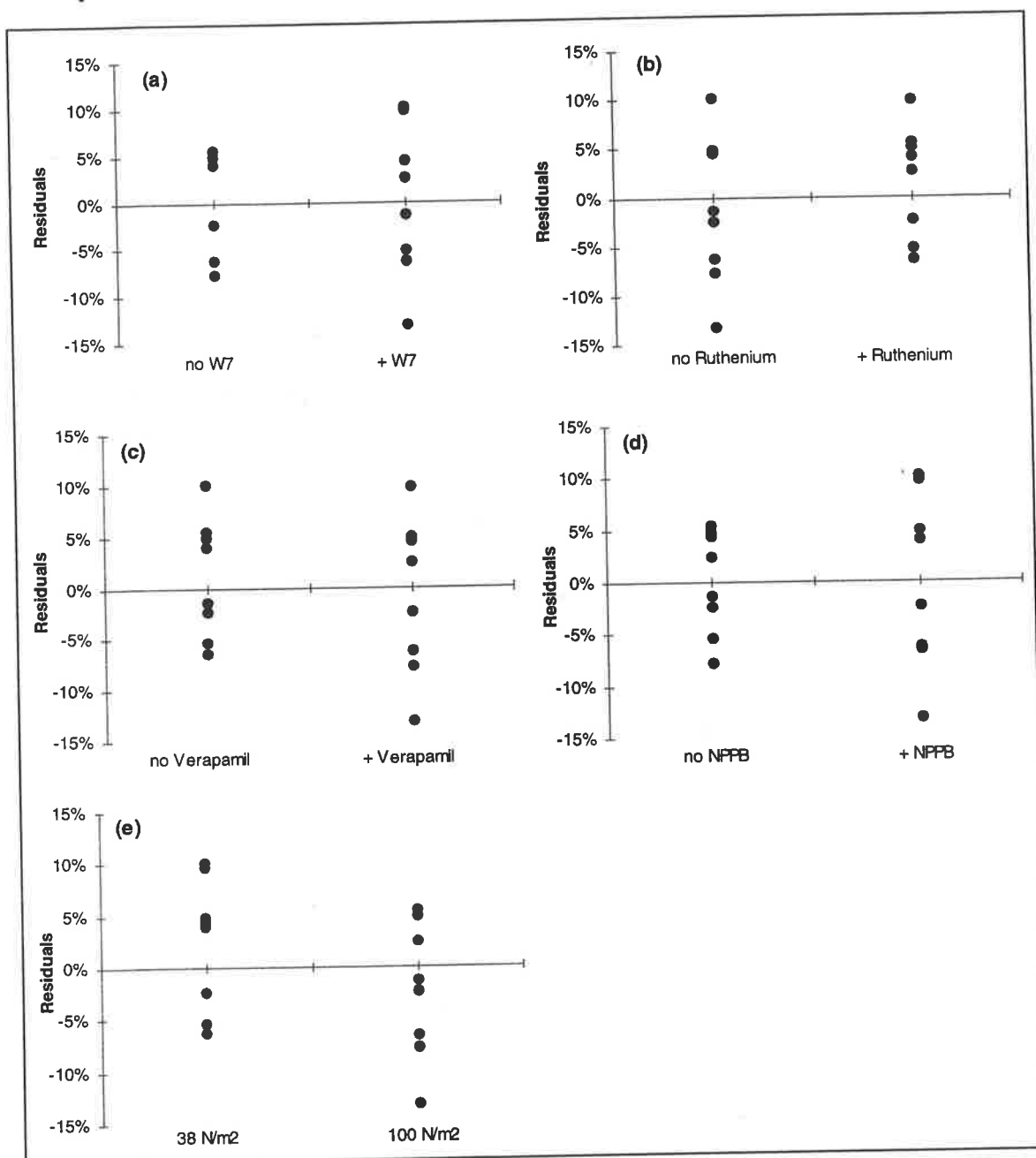


Figure 8-12: Residuals vs each of the factors for the uncoupled OUR response of sheared cells. (a) W7, (b) Ruthenium red, (c) Verapamil, (d) NPPB and (e) Shear level.

The main effects of W7 and NPPB on the uncoupled OUR response are plotted in Figure 8-13. The figure shows that both W7 and NPPB reduces the uncoupled OUR of sheared cells, relative to the Control- cells. The plot of the 'W7 x NPPB' two-factor interaction is given in Figure 8-14. In the absence of NPPB, addition of W7 lowers the average uncoupled OUR of the sheared cells by 4.5%, compared to a reduction of 21% in the presence of NPPB. That is, the negative effect of W7 on the uncoupled OUR of sheared cells is relatively mild when no NPPB is present, but becomes accentuated in the presence of NPPB.

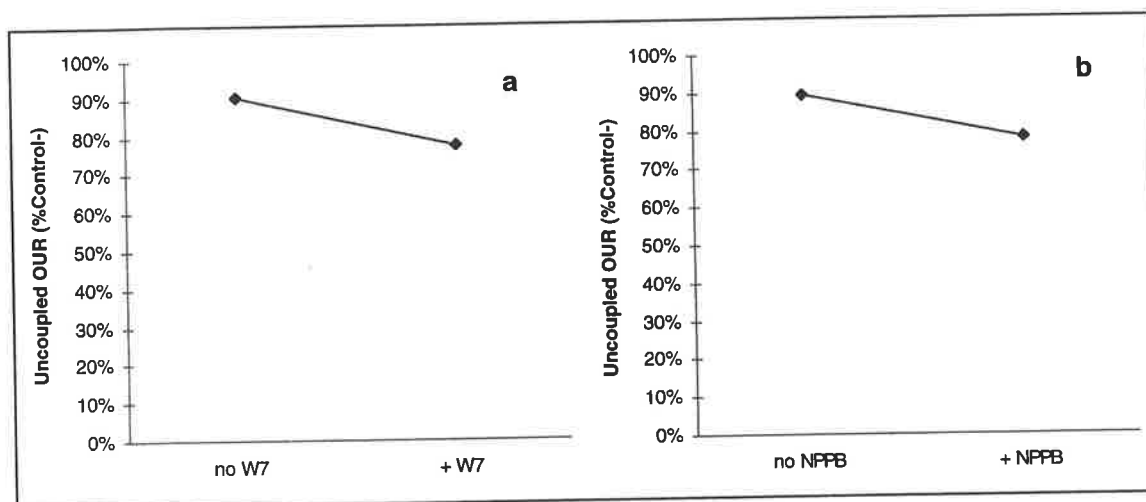


Figure 8-13: Main effects on uncoupled OUR response of sheared cells for (a) W7 and (b) NPPB.

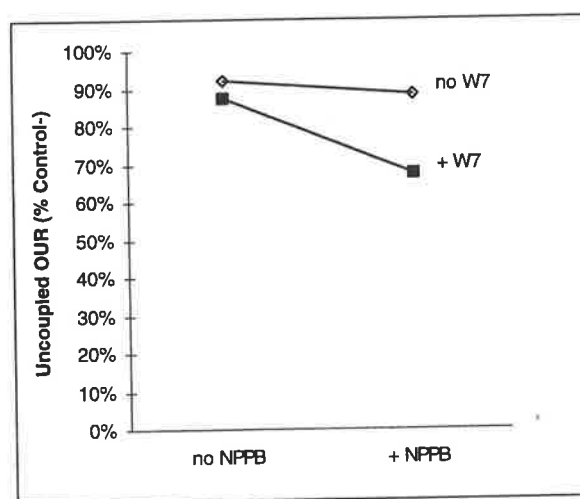


Figure 8-14: 'W7 x NPPB' interaction for uncoupled OUR of sheared cells

Figure 8-15 is the normal scores plot of the main effects and interactions on the uncoupled OUR response of Control+ cells. The only effects that appear to be significant are again the main effects of W7 (a), NPPB (d) and the 'W7 x NPPB' two-factor interaction (ad). The F-test for these effects indicates that they are all significant at the 5 % level.

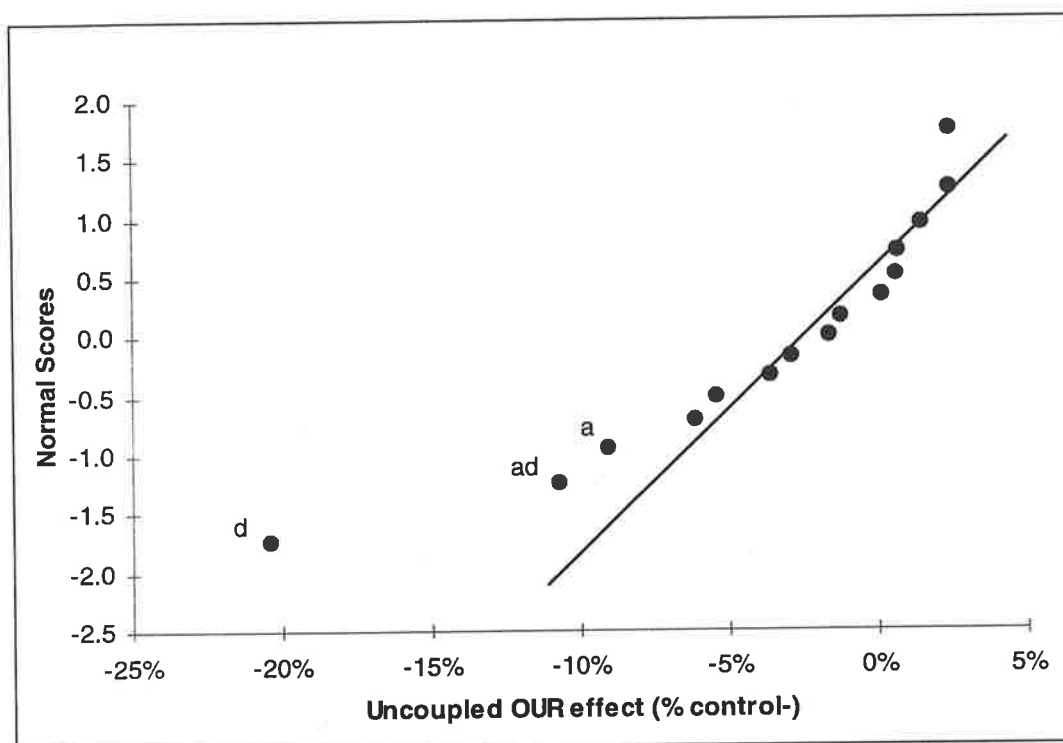


Figure 8-15: Normal scores plot of main effects and interactions of uncoupled OUR response for Control+ cells.

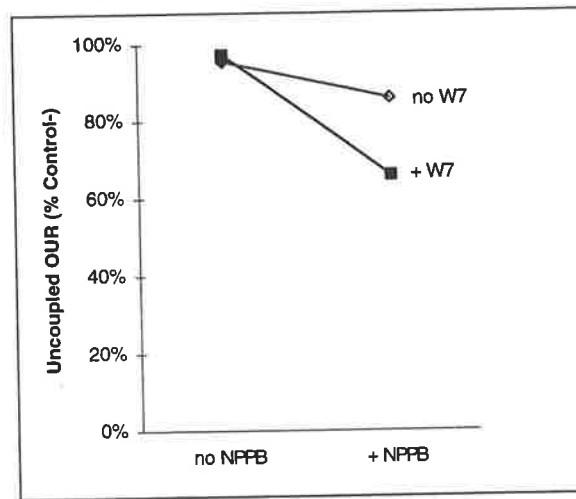


Figure 8-16: 'W7 x NPPB' interaction for uncoupled OUR of Control+ cells.

As mentioned earlier, the significant interaction between W7 and NPPB emphasises the need to examine the interaction more closely before drawing any conclusions regarding their main effects. The interaction between W7 and NPPB on Control+ cells is illustrated in Figure 8-16. The plot shows that W7 raises the average uncoupled OUR response by about 1.7% in the absence of NPPB, but lowers the response by about 20% when NPPB is present. The relative proximity of the W7 main effect to the cumulative normal distribution line in Figure 8-15 compared to the main effect of NPPB and the 'W7 x NPPB' two-factor interaction reflects the relatively small effect which W7 has on the uncoupled OUR of Control+ cells.

Thus, NPPB and W7 appear to have a significant influence on the uncoupled OUR of both the sheared and Control+ cells. However, the effect of W7 is relatively mild in the absence of NPPB. Addition of W7 without NPPB causes a mild decrease in the average uncoupled OUR of sheared cells (Figure 8-14) and slightly increases it in Control+ cells (Figure 8-16). The combination of W7 and NPPB seems particularly detrimental to the uncoupled OUR response of both sheared and Control+ cultures.

8.1.3 *Effects on mitochondrial activity*

The main effects and interactions on the mitochondrial activity of sheared cells are listed in Table 8-7. Figure 8-17 is the normal scores plot of these effects. This figure suggests the main effects of W7 (a) and ruthenium red (b) are significant. An F-test confirms that the main effects of W7 and ruthenium red are significant at the 5% level. Analysis of the residuals also supports the underlying normality assumptions and the significance of these 2 main effects.

The main effects of W7 and ruthenium red on the mitochondrial activity of sheared cells are illustrated in Figure 8-18. Treatment with W7 tends to reduce the average mitochondrial activity of sheared carrot cells by about 23%. On the other hand, addition of ruthenium red increases the mitochondrial activity of the sheared cells by an average value of 29%.

Table 8-7: Estimates of effects and sum of squares of the mitochondrial activity response of sheared cells for the factorial experiment. The letters 'a, b, c, d, e' refer to the effect of W7, Ruthenium red, Verapamil, NPPB and shear level, respectively.

Estimated effects	Main effects / interactions (% control -)	Sum of Squares (% control -)
	83.7	
a	-22.5	20.3
b	28.6	32.8
ab	-10.8	4.7
c	-4.5	0.8
ac	2.4	0.2
bc	9.3	3.5
-de	3.1	0.4
d	-7.1	2.0
ad	4.8	0.9
bd	-14.0	7.8
-ce	0.9	0.03
cd	-6.8	1.9
-be	-0.3	0.004
-ae	0.2	0.001
-e	11.9	5.7

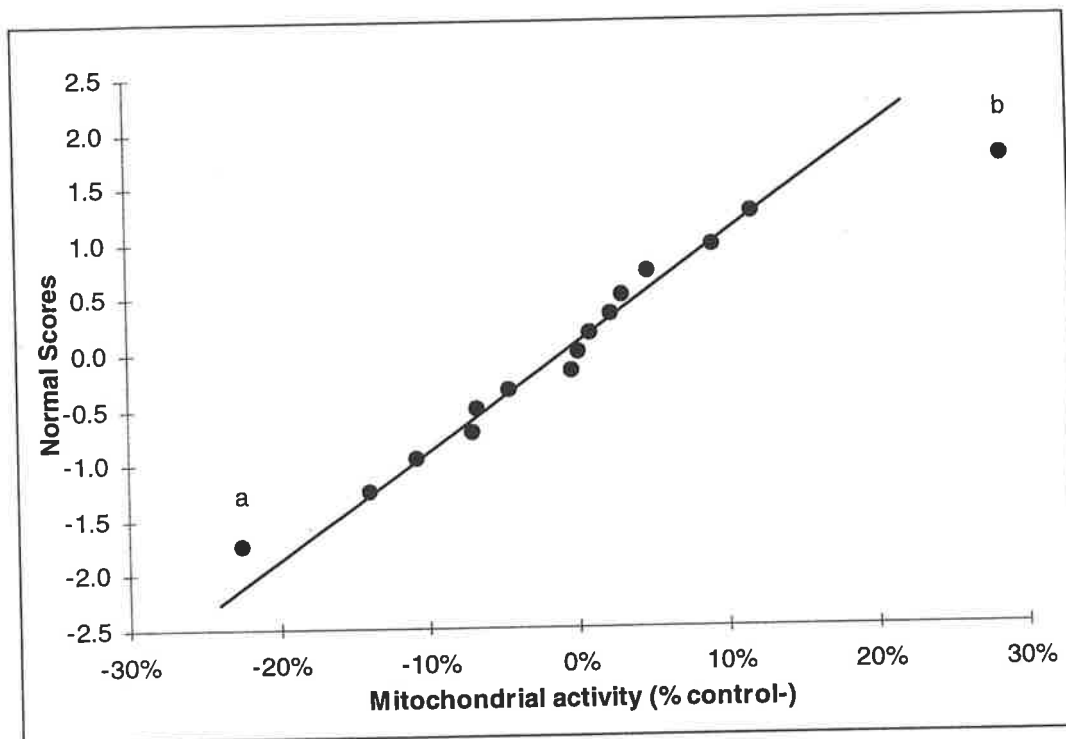


Figure 8-17: Normal scores plot for mitochondrial activity effects. The letters 'a, b, c, d, e' refer to the effect of W7, Ruthenium red, Verapamil, NPPB and shear level, respectively.

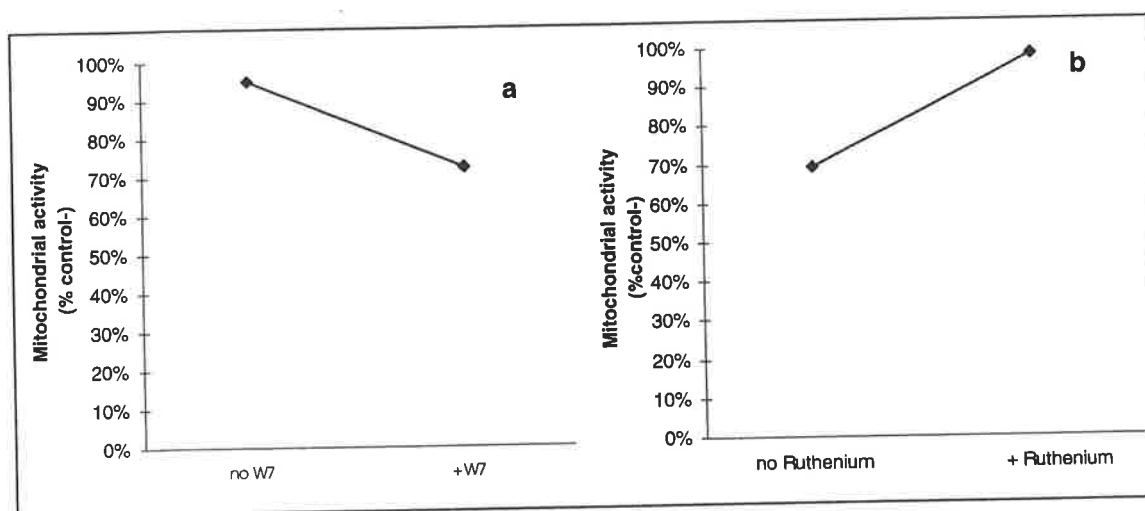


Figure 8-18: Main effects on mitochondrial activity of sheared cells for (a) W7 and (b) Ruthenium red.

The normal scores plot for the effects on mitochondrial activity of Control+ cells is shown in Figure 8-19. The plot suggests that only the main effect of W7 (a) is significant. An F-test of the W7 main effect shows that it is significant at the 5% level.

The main effect of W7 is illustrated in Figure 8-20a and indicates that addition of W7 tends to reduce the mitochondrial activity of carrot cells by about 30%. Hence, it is possible that the negative effect of W7 on the mitochondrial activity of carrot cultures sheared in the viscometer could be due to the addition of the blocker alone and not influenced by the shear exposure. On the other hand, the effect of ruthenium red does not appear to be significant in Control+ cells. Addition of ruthenium red raises the mitochondrial activity by only 1% in the Control+ cells (Figure 8-20b). Thus, ruthenium red tends to increase the mitochondrial activity of the sheared cells, but does not have a significant effect on unsheared cells exposed to the chemical for the same period.

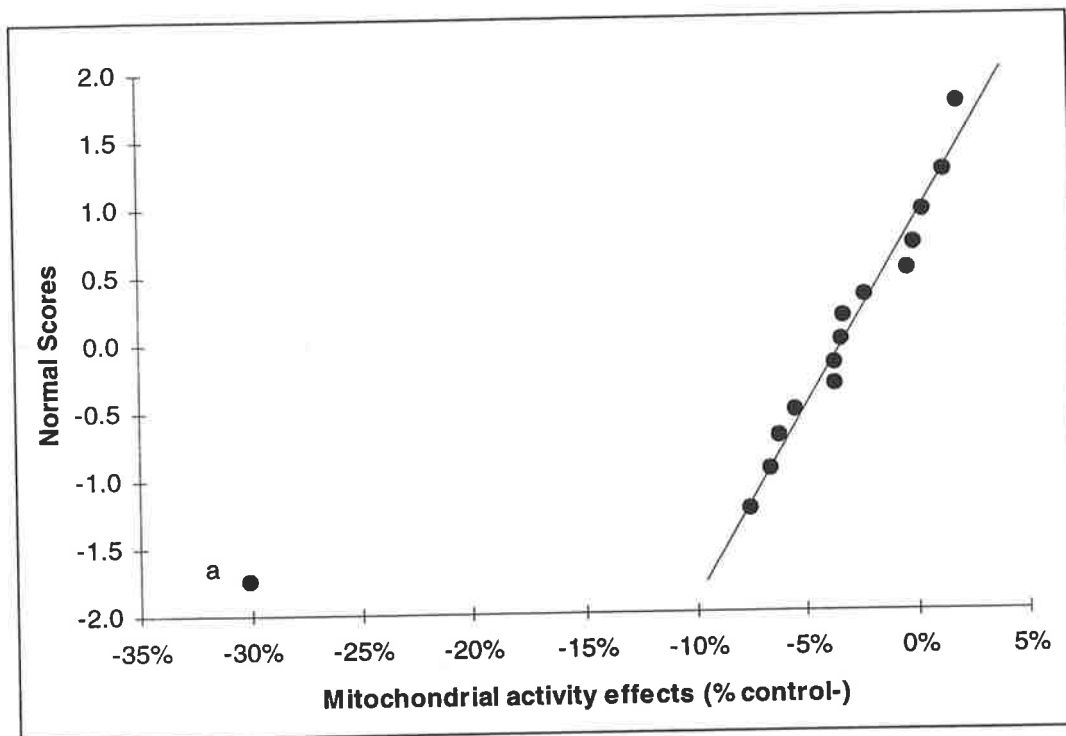


Figure 8-19: Normal scores plot of main effects and interactions of mitochondrial activity response for Control+ cells. The letter 'a' refers to W7.

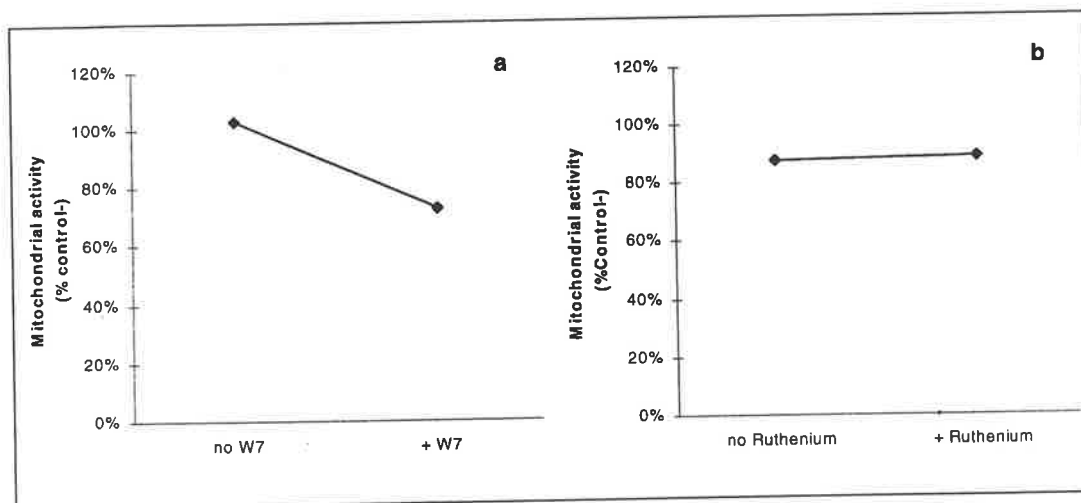


Figure 8-20: Main effect on mitochondrial activity of Control+ cells for (a) W7 and (b) Ruthenium red.

8.1.4 Effects on membrane integrity

Table 8-8 lists the main effects and interactions for the membrane integrity of the sheared cultures. Figure 8-21 shows the normal scores plot for the main effects and interactions. The only significant effect is that of shear level (denoted by letter 'e' in Figure 8-21). An F-test shows that the main effect of shear level is significant at the 5% level. Increasing the shear stress from 38 to 100 N/m² results in a modest decrease in membrane integrity by an average value of 9.7% (Figure 8-22).

A similar statistical analysis of the response of Control+ cells suggests that none of the chemicals studied had a significant impact on the membrane integrity of cells maintained in shake flasks. This is illustrated by the normal scores plot of effects for Control+ cells (Figure 8-23).

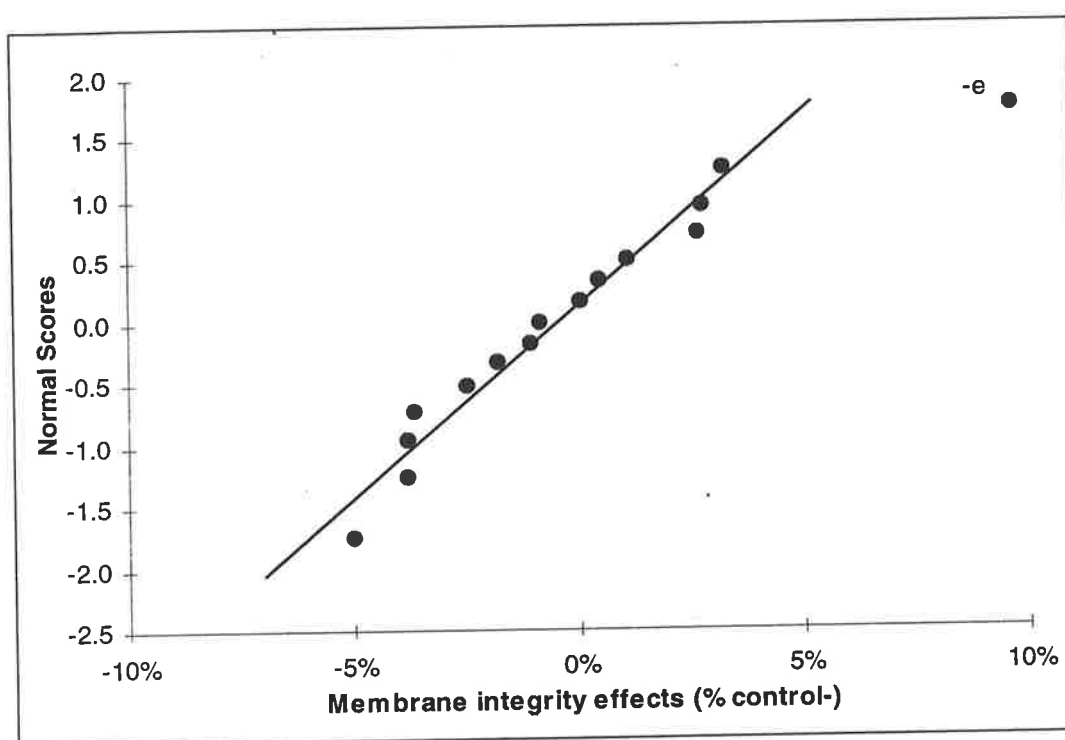


Figure 8-21: Normal scores plot of main effects and interactions of membrane integrity response for sheared cell. Letter 'e' refers to the main effect of shear level.

Table 8-8: Estimates of effects and sum of squares of the membrane integrity response of sheared cells for the factorial experiment. The letters 'a, b, c, d, e' refer to the effect of W7, Ruthenium red, Verapamil, NPPB and shear level, respectively.

Estimated effects	Main effects / interactions (% control -)	Sum of Squares (% control -)
	86.3	
a	-3.8	0.6
b	-0.8	0.03
ab	-1.8	0.1
c	-3.6	0.5
ac	0.1	0.0002
bc	2.8	0.3
-de	3.3	0.4
d	-5.0	1.0
ad	-3.8	0.6
bd	1.1	0.05
-ce	2.7	0.3
cd	-2.5	0.2
-be	-1.1	0.04
-ae	0.5	0.01
-e	9.7	3.8

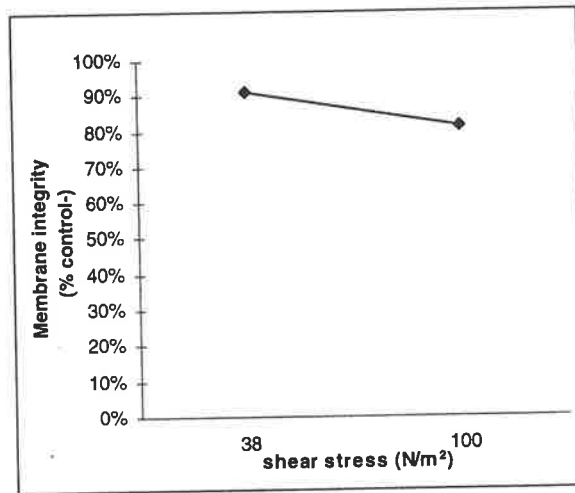


Figure 8-22: Plot of main effect on membrane integrity of sheared cells for shear level

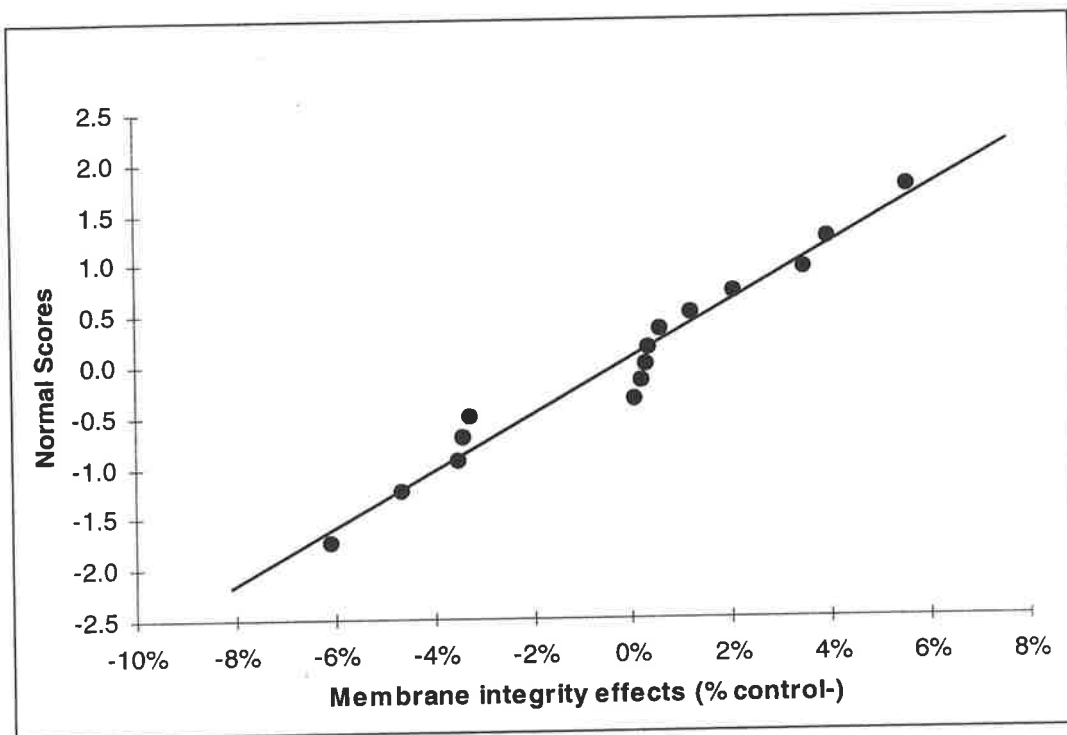


Figure 8-23: Normal scores plot of main effects and interactions of membrane integrity response for Control+ cells.

8.1.5 Summary of effects for factorial experiments

Table 8-9 summarises the results of the factorial design experiments.

The calmodulin inhibitor, W7, was found to have a statistically significant effect on the coupled OUR of carrot cells sheared in a viscometer at either 38 or 100 N/m². The interaction between the effect of W7 and the prevailing shear level on the coupled OUR response was also statistically significant. W7 attenuated the shear-induced increase in the coupled OUR of cells sheared in the viscometer but did not have a significant impact on the coupled OUR of cells maintained in the low-shear shake flasks (Control+).

W7 was found to have a statistically significant effect on the uncoupled OUR and mitochondrial activity of both the sheared cells and the shake flask cultures. There did not appear to be any significant interaction between W7 and the prevailing shear level for these two responses.

The 2-factor interaction between ruthenium red and the shear level was not significant for the mitochondrial activity response of the sheared cells. However, there was a difference between the effect of this chemical on sheared cells and Control+ cells. Ruthenium red caused a statistically significant increase in the mitochondrial activity of cells sheared in the viscometer. But the same treatment did not have a significant influence on shake flask cultures.

The Cl⁻ channel blocker, NPPB, decreased the uncoupled OUR of both sheared and shake flask cultures. There was also a significant interaction between the effects of NPPB and W7. The combination of NPPB and W7 led to a larger decrease in uncoupled OUR than each of these chemicals alone. However, there was no significant interaction between the effect of NPPB and the prevailing shear level for any of the responses.

Verapamil, a blocker of voltage-operated Ca²⁺ channels, did not have a significant effect on any of the responses. The membrane integrity was also not affected by any of the chemicals.

The divergence between the uncoupled OUR and mitochondrial activity of sheared cells in response to ruthenium red treatment is in contrast to the suggested correlation between these two responses based on the viscometer run results presented in the

previous chapter (see Section 7.3.5). However, the other chemical treatments gave similar trends for these two responses. It is unclear if the correlation between these two responses might be real. However, the relative insensitivity of membrane integrity to any of the chemicals is a strong indication that the correlation between uncoupled OUR and membrane integrity is fortuitous.

Table 8-9: Summary of factorial experiment results. Cells were sheared in the viscometer (38 or 100 N/m²) or maintained in shake flasks (100 rpm) for 1 h. The abbreviation 'n.e.' denotes no significant effect (5% level of significance).

	W7	Ruthenium red	Verapamil	NPPB
<i>Sheared cells</i>				
Coupled OUR	Decrease - interact with shear level	n.e.	n.e.	n.e.
Uncoupled OUR	Decrease - interact with NPPB	n.e.	n.e.	Decrease - interact with W7
Mitochondrial activity	Decrease	Increase	n.e.	n.e.
Membrane integrity	n.e.	n.e.	n.e.	n.e.
<i>Shake flask (Control+)</i>				
Coupled OUR	n.e.	n.e.	n.e.	n.e.
Uncoupled OUR	NPPB absent - mild increase NPPB present - decrease	n.e.	n.e.	Decrease - interact with W7
Mitochondrial activity	Decrease	n.e.	n.e.	n.e.
Membrane integrity	n.e.	n.e.	n.e.	n.e.

8.1.6 Effects of long-term exposure

To investigate the effects of extended exposure of the carrot cells to the chemical compounds, each compound was added to shake flasks containing 14-day carrot cultures and agitated at either 100 or 150 rpm for 24 h. The cultures were then assayed for mitochondrial activity as described in Section 5.3.3.1.

Figure 8-24 shows the average mitochondrial activity of the carrot cells. Exposure to ruthenium red for 24 h significantly reduced the mitochondrial activity of the cells compared to the controls with no blocker treatment. At an agitation speed of 150 rpm, verapamil also caused a significant reduction in mitochondrial activity compared to the corresponding control, but the reduction caused by ruthenium red was larger than that due to verapamil. Exposure to W7 or NPPB for 24 h appeared to decrease the mitochondrial activity slightly, but the reduction was not statistically significant at the 5% level. These results suggest that addition of ruthenium red into industrial plant cell cultures to alleviate sub-lytic shear effects is not advisable, even though ruthenium red

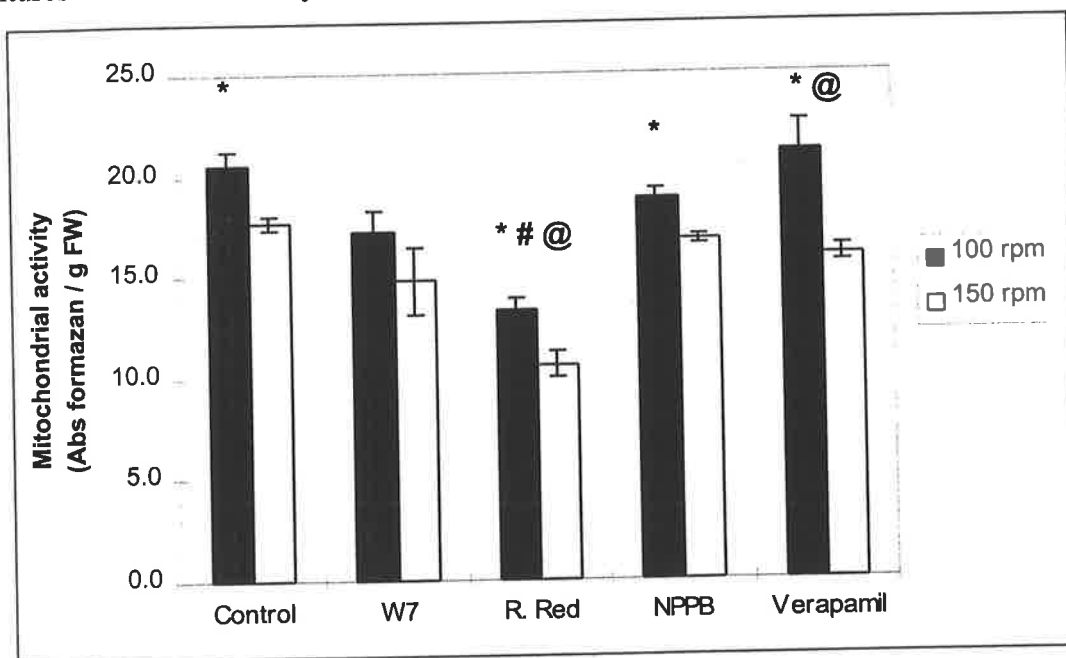


Figure 8-24: Mitochondrial activity of 14 day carrot cultures after shearing at 100 or 150 rpm for 24 h. Values shown are the mean of 2 replicates. Error bars indicate standard error. * = significant difference between 100 and 150 rpm. # = significant difference between control and blockers at 100 rpm. @ = significant difference between control and blockers at 150 rpm. $\alpha = 0.05$ for all 2-sample t-tests.

was found to attenuate the shear-induced reduction in mitochondrial activity for short exposure periods (Section 8.1.3).

The factorial experiments indicated that addition of W7 reduced the effect of shear on the coupled OUR of carrot cells, raising the possibility that W7 might be added to industrial plant cultures to alleviate the effects of fluid shear stress on the biological response of suspension cultured plant cells. Exposure of the carrot cells to W7 for 24 h did not appear to have a significant effect on the mitochondrial activity. To investigate if extended exposure to W7 might have toxic effects on cell growth, different concentrations of W7 were added to shake flask cultures cultivated at 100 rpm, 27°C in the dark and the growth monitored over 16 days. Figure 8-25 shows the change in fresh weight of the cultures. W7 had negligible effect on cell growth at concentrations below 30 μM , but inhibited growth at 60 μM .

The implications of these results for industrial plant culturing will be discussed further in Section 8.3.2.

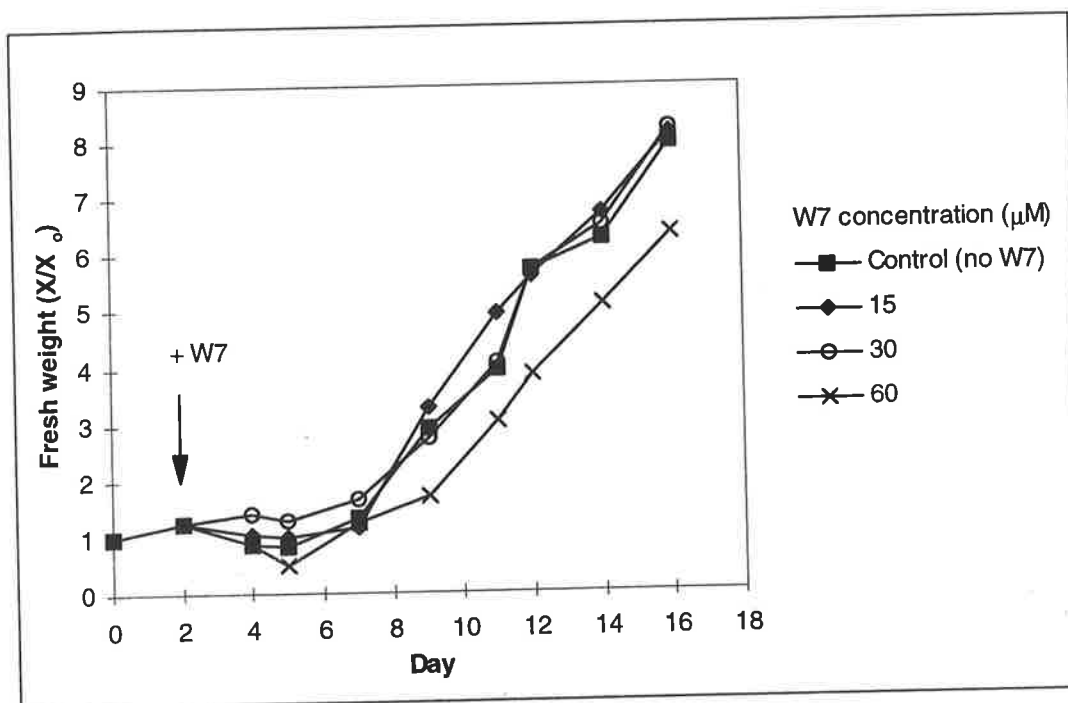


Figure 8-25: Effect of W7 dosage on growth of carrot cells in shake flasks (100 rpm, 27°C). Filter-sterilised W7 was added on day 2 as indicated by the arrow.

8.2 Patch-clamp investigations

The activity of ion channels in the cell membrane of suspension cultured carrot cells was investigated by the patch-clamp technique. Figure 8-26 shows the typical current profiles for carrot protoplasts clamped at various voltages. The respective amplitude histograms determined from the current recordings are also shown. As the ion channels flicker between the 'closed' and 'open' states, distinct changes in the current levels are observed. Furthermore, as the voltage at the tip of the pipette was lowered from 0 mV to -40 mV, the magnitude of the current jumps between 'open' and 'closed' states increased accordingly. This increase in current is reflected in the increasing separation between the peaks in the respective amplitude histograms. This behaviour is typical of ion channels (e.g. Hamill *et al.*, 1981), since movement of ions through the channels is driven by passive diffusion along the electrochemical gradient.

By measuring the amplitude of the channel currents as the membrane potential is clamped at different voltages, a current-voltage (I/V) curve may be determined. However, a more efficient method for determining the I/V curve is to apply a continuous linear voltage ramp to the channel when it is open. The same ramp is then repeated when the channel is closed, and the difference between the two current traces represents the I/V curve of the channel (Figure 8-27). The I/V curve in Figure 8-27b suggests that the current reverses at a voltage of approximately 25 mV. The I/V curve in Figure 8-27b is for a recording in the cell-attached configuration (see Section 5.4.3), which means that the whole protoplast is attached to the pipette tip. In this configuration, only the concentration of ions on the side of the cell membrane facing the pipette solution is known precisely. The ion concentration on the cytoplasmic face of the membrane is unknown. To overcome this problem, a patch of the cell membrane was excised from the remainder of the cell with the pipette still attached to the membrane, forming an 'inside-out' configuration (see Section 5.4.3). When this is done, the cytoplasmic face of the membrane is exposed to the bath solution for which the ion concentrations are known. Figure 8-28 shows a typical I/V curve for carrot protoplasts in the 'inside-out' configuration.

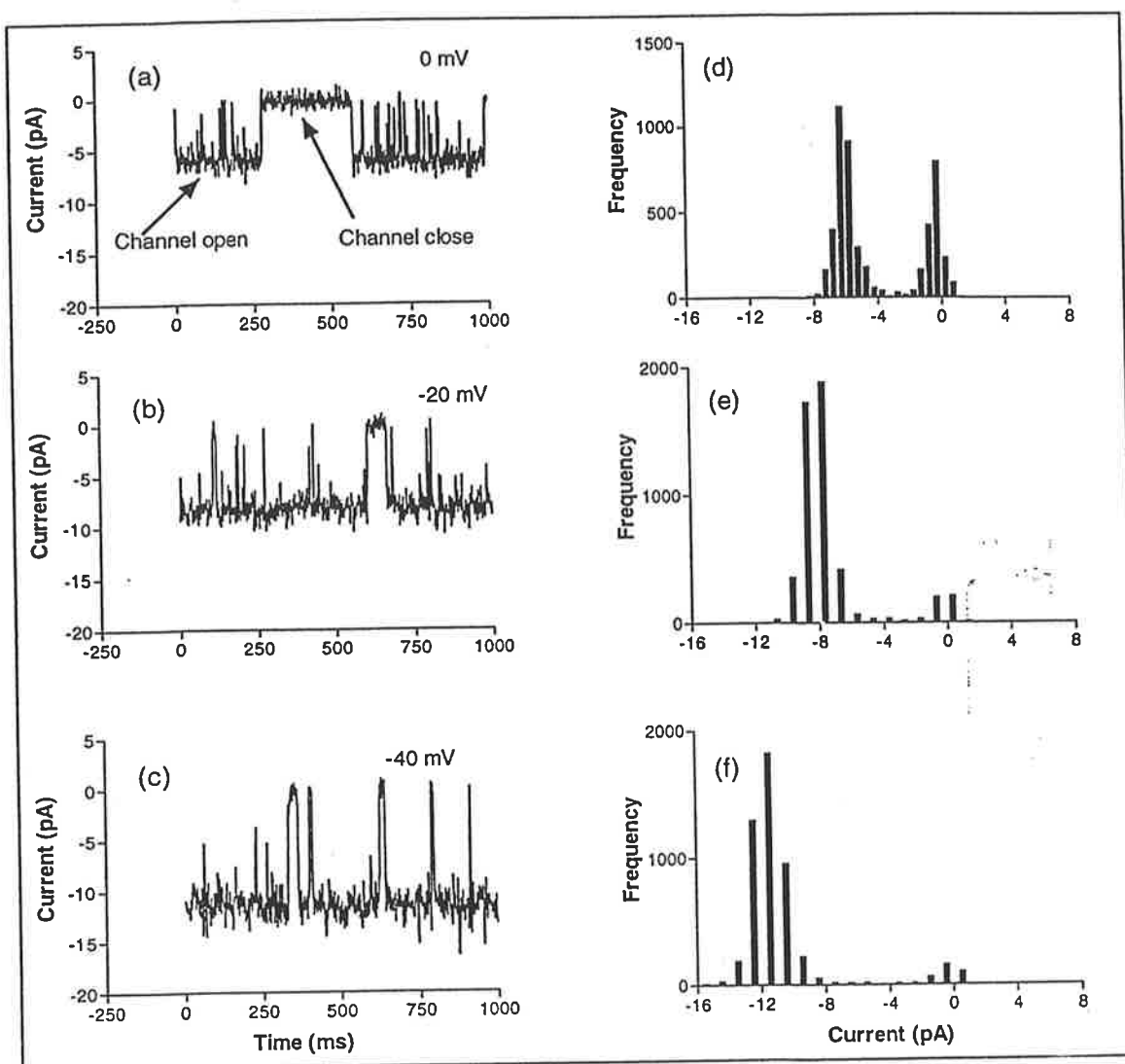


Figure 8-26: (a) to (c) Current-time profiles for carrot protoplasts, cell attached configuration, clamped at 0, -20 and -40 mV respectively. (d) to (f) are the respective current amplitude histograms.

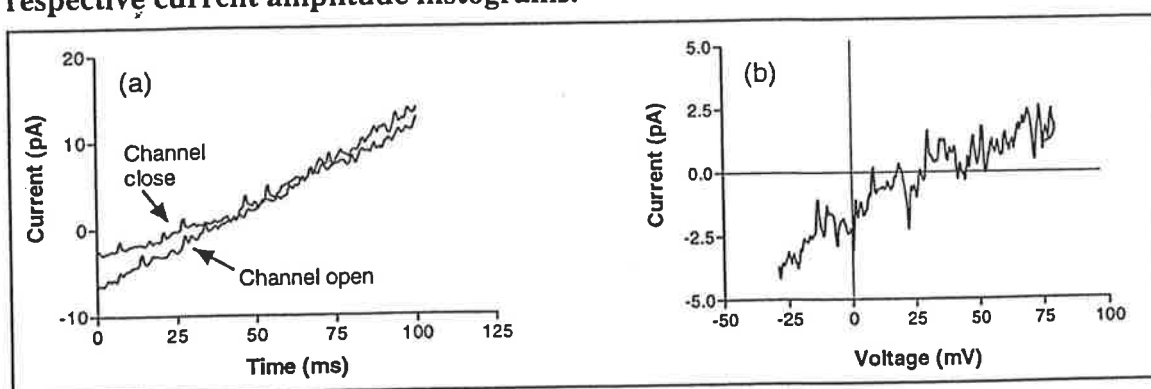


Figure 8-27: (a) Current-time profile for carrot, cell attached configuration, as a voltage ramp from -25mV to 75 mV was applied. (b) Corresponding current-voltage (I/V) curve derived from difference between open and close current traces.

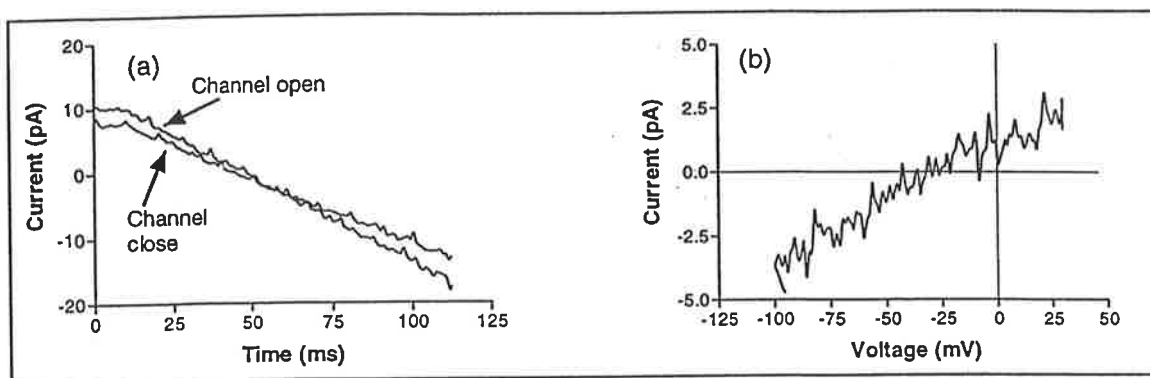


Figure 8-28: (a) Current-time profile for carrot, inside-out configuration, as a voltage ramp from -100 mV to 30 mV was applied. (b) Corresponding current-voltage (I/V) curve derived from difference between open and close current traces.

The Nernst potential for the ions is calculated from the formula

$$E_x = \frac{RT}{zF} \ln \frac{[X]_{outside}}{[X]_{inside}} \quad (\text{Eq 8-1})$$

where R = gas constant = 8.314 J/K mol

T = absolute temperature (K)

z = charge number

F = Faraday constant = 96500 C/mol

The Nernst potential for the major ions in solution are shown in Table 8-10:

Table 8-10: Nernst potential for various ions.

Ions	Concentration in pipette (mM)	Concentration in bath (mM)	Nernst potential (mV)
K^+	200	5	+ 92.9
Ca^{2+}	10	10	0
Cl^-	220	25	-54.8

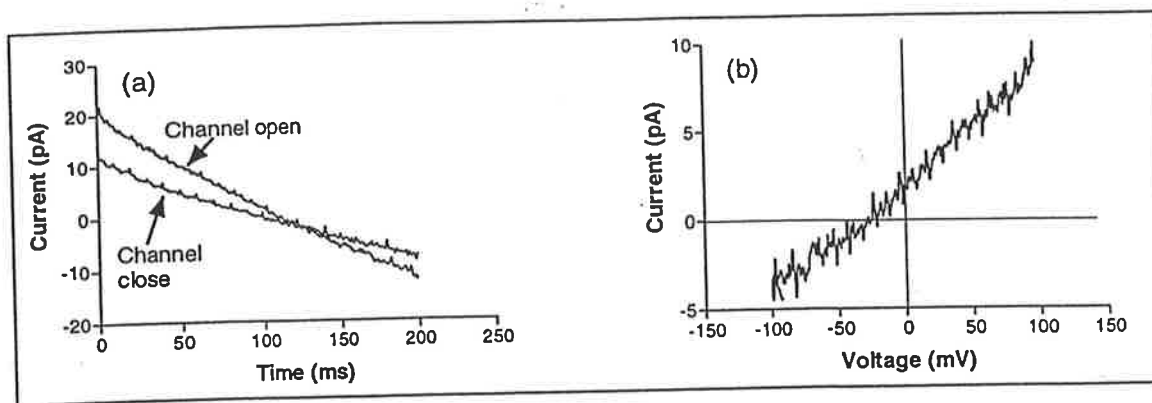


Figure 8-29: (a) Current-time profile for *Nicotiana plumbaginifolia*, inside-out configuration, as a voltage ramp from -100 mV to 100 mV was applied. (b) Corresponding current-voltage (I/V) curve derived from difference between open and close current traces.

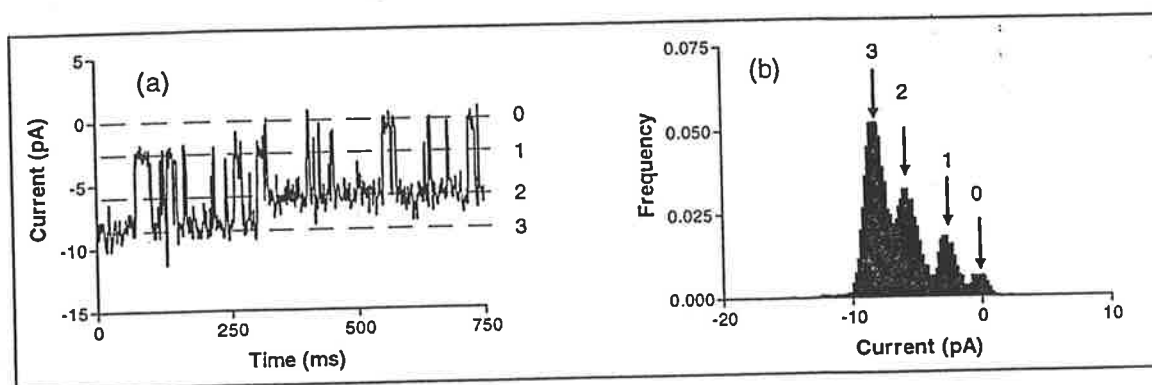


Figure 8-30: Multiple channels in a single patch. (a) Current-time profile. (b) Amplitude histogram. Carrot protoplast, cell attached, clamped at 0mV.

Figure 8-28b suggests that the reversal potential is closest to the Nernst potential for Cl^- ions, suggesting that the channel is likely to be a Cl^- channel. A Cl^- channel is also consistent with the results of the cell-attached recordings, based on estimates of the ion concentrations within the cells and a typical resting membrane potential value of -200 mV (Ward *et al.*, 1995). A similar channel was also found on protoplasts from cultured *Nicotiana plumbaginifolia* cells, as shown in Figure 8-29.

While a majority of the patches from carrot protoplasts only contained the Cl^- channel identified above, some patches contained a second channel of smaller conductance, as shown in Figure 8-30. As the difference in the current jumps are not equal (for example, compare the amplitude change between level 3 and 2 and that

between levels 3 and 1), it is unlikely to be the same channel. However, as the second channel appeared only infrequently, its identity could not be determined.

The mechanosensitive behaviour of the channel was examined by increasing the suction applied through the patch-clamp pipette. Suction, regulated by a valve and syringe, was applied through the side port of the pipette holder and was measured with a water manometer connected to the suction line. Unfortunately, no significant difference in ion channel activity was observed for the different suction pressures on the patches tested, as shown in Figure 8-31. It is possible that the channel is indeed sensitive to membrane stretching, but the channel accommodates to the higher pressure faster than the pressure can be increased, so that the transient change in channel activity cannot be detected with the current set up. However, we do not expect this to be likely, as stretch-sensitive channels reported in other plant cells usually show rapid, continuous activity when suction is applied, with the activity abating only when suction is released (Ding and Pickard, 1993a). It should also be noted that in the work reported here, application of suction often resulted in the loss of the patch seal. Thus, the mechanosensitivity of the Cl^- channel could only be tested on a small number of membrane patches. The difficulty in obtaining stable high resistance seals when patch-clamping suspension cultured plant cells has also been reported by other researchers (Fairley, 1990).

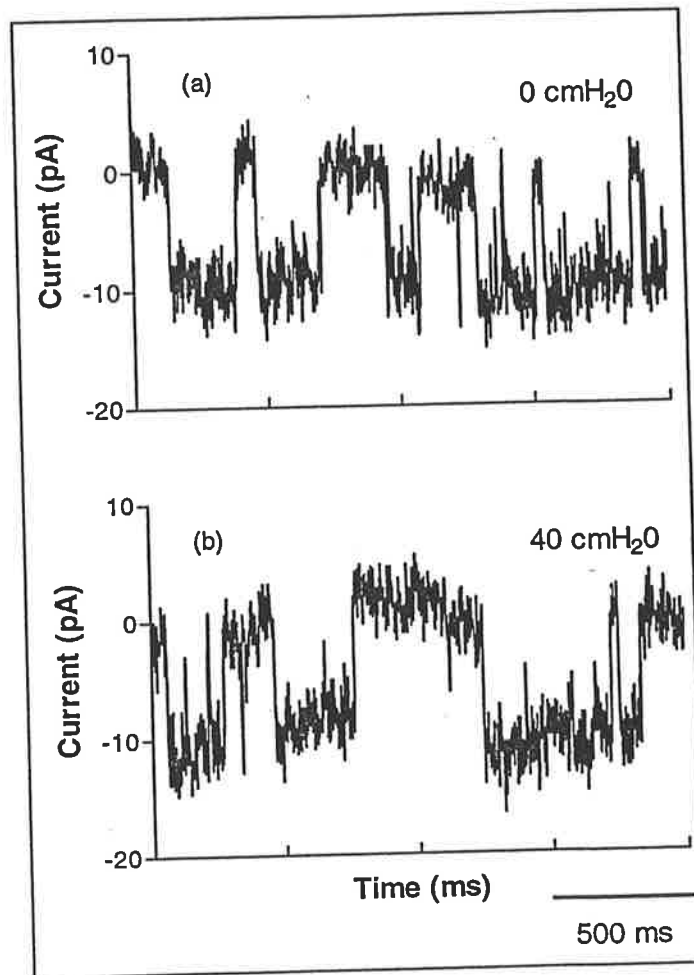


Figure 8-31: Effect of increased suction pressure on channel activity of carrot protoplasts in the cell attached configuration. (a) no suction applied. (b) 40 cmH₂O suction applied through pipette tip.

8.3 Discussion

8.3.1 Effects of ion-signalling disruption on biological response to shear

The aim of this study was to investigate if disrupting the ion-signalling process through ion channel blockers or calmodulin inhibitors will alleviate the effects of fluid shear stress on the biological response of suspension cultured plant cells. In the previous chapter, we saw how the coupled and uncoupled OUR and mitochondrial activity of carrot cells were affected by laminar shear stress before regrowth potential and membrane integrity, suggesting that the former three biological activities are indicators of the sub-lytic response. In this chapter, factorial-designed experimentation was carried out to determine the effect of different chemicals on these sub-lytic response indicators.

Figure 8-5 and Table 8-9 show that W7, a potent inhibitor of the Ca^{2+} -binding protein, calmodulin (Hidaka *et al.*, 1981), reduced the effect of shear on the coupled OUR of carrot cells. Calmodulin is a 16.7-16.8 kDa protein which acts as the primary intracellular receptor for Ca^{2+} in plant cells and is a multi-functional regulator of protein activity (Zielinski, 1998). It has been implicated in the growth-inhibition of whole plants following mechanical stress (Jones and Mitchell, 1989), and shows increased expression in a wide variety of plants which have been mechanically stimulated (Botella and Arteca, 1994; Braam and Davis, 1990; Galaud *et al.*, 1993; Takezawa *et al.*, 1995). Inhibition of calmodulin has been found to partially suppress the growth-inhibition of soybean plants following mechanical stress (Jones and Mitchell, 1989) and to attenuate the reduction in NAD(P)H of eucalyptus cultures sheared in bioreactors (Takeda *et al.*, 1998). The results of this thesis suggest that the stimulatory effect of shear on the respiratory activity of cultured plant cells may be mediated by calmodulin. Cellular respiration is a fundamental activity responsible for providing the energy needed to drive a variety of cellular processes (Alberts *et al.*, 1994c). It is, therefore, conceivable that the effect of shear on respiration through a calmodulin-mediated pathway could, in turn, trigger an array of changes in cellular activity that culminates in reduced growth and productivity of the culture. Alternatively, it has been speculated that mild stress may cause metabolic energy to be preferentially channelled towards critical activities

which reinforce the ability of the cell to withstand the environmental stress while sacrificing growth-related functions (Reuzeau *et al.*, 1997).

Since calmodulin requires the binding of Ca^{2+} to be activated, a role for Ca^{2+} as a signalling molecule in the transduction pathway is suggested. Figure 8-18b and Table 8-9 show that application of ruthenium red eliminated the effect of shear on the mitochondrial activity of viscometer sheared cells but had no significant effect on the mitochondrial activity of cells subjected to low fluid shear (Control+). Since, ruthenium red is a putative blocker of intracellular Ca^{2+} channels (Knight *et al.*, 1992, and references therein), the factorial experiment results suggest an intracellular Ca^{2+} source for the Ca^{2+} -mediated sub-lytic response. This observation is similar to that reported by Knight *et al.* (1992) for *N. plumbaginifolia* seedlings subjected to wind-induced plant motion. The authors found that wind-induced plant motion caused an immediate increase in the cytosolic Ca^{2+} concentration of tobacco plants. Application of ruthenium red abolished the wind-induced Ca^{2+} increase. They also found that blockers of stretch-activated channels and plasma-membrane Ca^{2+} -channels did not have any effect on the wind response. Knight *et al.* (1992) proposed that an internal group of microfilaments or microtubules could be responsible for sensing the cell deformation caused by the wind motion. These sensing elements are in turn coupled to the intracellular calcium source (Knight *et al.*, 1992). Various intracellular organelles within the plant cell are known to act as stores of Ca^{2+} that can be released into the cytoplasm when the appropriate stimulus is received. These organelles include the endoplasmic reticulum, vacuole and mitochondria (Hepler and Wayne, 1985). A stretch-activated channel thought to be involved in osmotic regulation has been reported in red beet vacuoles (Alexandre and Lassalles, 1991). However, that channel was found to show no strong cation/anion selectivity. A similar mechanism may operate in cultured plant cells subjected to hydrodynamic shear forces. Microfilaments and microtubules form part of the cytoskeleton of the cell which pervades throughout the cytoplasm (Alberts *et al.*, 1994b). The cytoskeleton and integrins are known to play crucial roles in converting mechanical signals into biochemical responses in animal cells (Ingber, 1997). It has been postulated that similar structures may be responsible for transducing mechanical signals in plant cells (Pont-Lezica *et al.*, 1993; Reuzeau *et al.*, 1997; Reuzeau and Pont-Lezica, 1995).

NPPB was found to be detrimental to the uncoupled OUR of carrot cells in the viscometer and in shake flasks. The effect was exacerbated when the calmodulin was inhibited by W7 at the same time (Figure 8-14 and Figure 8-16). The effect of NPPB on the uncoupled OUR was observed in both sheared and shake flask cultures, and no significant interaction between the NPPB effect and the prevailing shear level was observed (Table 8-9 and Figure 8-9). This indicates that the effect of NPPB on uncoupled OUR may not be associated with any shear-induced changes on the biological response of the carrot cells. However, the literature provides some evidence which supports the role of Cl^- channels in cell signalling and osmoregulation (Barbier-Brygoo *et al.*, 2000). Falke *et al.* (1988) reported a stretch-activated Cl^- channel in tobacco cells which have been suggested to play an osmoregulatory role. In the present study, at least two ion channels have been found on the plasma membrane of cultured carrot cells (Figure 8-30). One of the channels is likely to be a Cl^- channel (Figure 8-28), but the other channel could not be identified. Unfortunately, stretch-activated behaviour could not be demonstrated for the Cl^- channel. Thus, the involvement of Cl^- channels in mediating the sub-lytic response to shear does not appear to be supported by the results of the present study.

Verapamil, a blocker of voltage operated Ca^{2+} channels, of up to 10 μM concentration was found to have no significant effect on any of the response indicators (Table 8-9). This is consistent with the results of Legue *et al.* (1997) who found that touch-stimulated increases in the cytoplasmic Ca^{2+} concentration of *Arabidopsis* roots could not be suppressed by verapamil, but were inhibited by ruthenium red. In contrast, Takeda *et al.* (1998) found that 0.1 to 1 μM verapamil suppressed the reduction in NAD(P)H of eucalyptus cultures sheared in a bioreactor. The difference in response could be related to species specific behaviour. It is possible that verapamil is effective in blocking Ca^{2+} channels in eucalyptus cells but not in the carrot cell line used in this study. Alternatively, it could indicate that shear stress activates more than one signalling pathway in plant cells which, in turn, target different cellular activities. Therefore, blocking the voltage-operated Ca^{2+} channel may affect NAD(P)H levels but not any of the biological indicators monitored in this study. Further work using a variety of plant cell species and response indicators to compare differences in the shear-induced response between species will be required.

The results of the factorial design experiments suggest that the sub-lytic response to hydrodynamic shear may be more complicated than originally anticipated. For instance, while calmodulin inhibition by W7 was effective in reducing the effect of shear on the coupled OUR, it did not prevent the reduction in uncoupled OUR and mitochondrial activity. Similarly, ruthenium red had a significant effect on the mitochondrial activity of sheared cells but not on the coupled and uncoupled OUR. This highlights the complex nature of the signalling pathways. Other types of environmental stimuli are also known to have highly-involved signalling pathways (Bush, 1995). Much more progress needs to be made in our understanding of Ca^{2+} -calmodulin signalling in plant cells before we can identify the reasons for the observed variations in the effect of the chemical compounds between the different biological indicators. Nevertheless, these results demonstrate that disruption of the ion-signalling process could lead to alleviation of the effects of fluid shear on the biological response of suspension cultured plant cells. This is a key step towards developing a novel approach for overcoming the shear sensitivity of plant cell cultures. Previous approaches have focused on modified impeller designs (Hooker *et al.*, 1990; Leckie *et al.*, 1991) or novel bioreactor configurations (Sun and Linden, 1999) in an effort to reduce shear levels without compromising mixing and mass transfer. While these studies report some degree of success, the results are usually highly dependent on the particular plant cell species and bioreactor set-up. Furthermore, shear-induced stimulation in the coupled respiration rate could lead to oxygen deficiency effects if aeration/mixing rates are inadequate. Efforts to develop shear tolerance in selected cell lines by modifying culture maintenance procedures have also been reported (Allan *et al.*, 1988). However, there is no clear understanding of how shear tolerance develops in the reported cell line and it is not known if similar procedures can be used on other cell lines.

The present work proposes a less empirical approach to overcoming shear sensitivity in plant cell cultures. Future work may elucidate the molecular mechanisms that cause shear sensitivity or tolerance in a particular cell line (e.g. through a Ca^{2+} -calmodulin mediated pathway). Such knowledge can then be incorporated into rapid high-throughput screening programs for robust plant cell lines or to genetically engineer cell lines that are tolerant to hydrodynamic shear. These ideas are discussed in the following sections. A similar approach is being developed in animal cell cultures with

some measure of success (Tey *et al.*, 2000). As shear effects have the potential to reduce the productivity of plant cultures, alleviation of the effects of sub-lytic shear sensitivity could lead to significant improvements in culture productivity.

8.3.2 Implications for industrial plant cell culturing

The results of this work suggest several implications for the industrial cultivation of plant cells for the production of plant-derived bioproducts.

Previous attempts at bioreactor cultivation of plant cell cultures have focused on reducing shear levels to avoid cell lysis or damage to membrane integrity. However, the results from this work and other recent reports demonstrate that a wide array of cellular functions are affected at levels of shear well below those required to cause physical damage to membrane integrity or cell lysis. These sub-lytic effects include changes to critical cell functions such as (i) actual and maximal respiration rate, (ii) mitochondrial activity (reported in this thesis), (iii) ATP utilisation (Takeda *et al.*, 1998), (iv) cell cycle activity (Yanpaisan *et al.*, 1998) and (v) population dynamics (Yanpaisan *et al.*, 1998). It is entirely conceivable that these sub-lytic changes in cellular activity will have a profound impact on cell growth and secondary metabolite production. This proposition is strengthened by the fact that similar responses have been observed in whole plants and tissues following mechanical stimulation accompanied by a reduction in plant growth and modification in development (Mitchell, 1996). Since the main aim of industrial plant culturing is to optimise both biomass and metabolite production, induction of sub-lytic effects which lead to reduction of metabolic energy or arrest of the active growth phase is clearly undesirable. Thus, alleviation of sub-lytic effects has the potential to significantly boost the performance of industrial cultivation of plant cells.

The results of the factorial design experiment suggests that disruption of the Ca^{2+} -calmodulin signalling pathway through a Ca^{2+} -channel blocker (ruthenium red) or calmodulin inhibitor (W7) could lead to alleviation of certain sub-lytic effects. Inclusion of ruthenium red into the culture medium of industrial bioreactor cultures is an unlikely option as exposure to ruthenium red for 24 h was found to significantly decrease the mitochondrial activity of carrot cultures (Figure 8-24). On the other hand, exposure to W7 for 24 h resulted in only a minor decrease (not significant at 5% level) in mitochondrial activity (Figure 8-24). Figure 8-25 shows that W7 had negligible

effect on cell growth at concentrations below 30 μM , but inhibited growth at 60 μM . This suggests that direct addition of W7 to bioreactor cultures may be possible, although subsequent removal from the culture media downstream of the bioreactor may have to be considered.

The concentrations of the chemical compounds employed in this study were based on typical values previously found to alleviate the effects of mechanical and osmotic stress in whole plants and tissues (see Table 5-1). It may be possible to adjust the concentrations of these compounds to reduce the toxic effects of long-term exposure while maintaining their protective effects against fluid shear. Further work will be required to determine the optimal concentrations of the chemical compounds. Alternatively, it may be possible to use non-toxic analogues of these chemical compounds, which will have the same protective effects but with no or reduced levels of toxicity.

A more feasible approach to the alleviation of the negative effects of sub-lytic shear sensitivity could be to screen for cell lines that show reduced sensitivity in the Ca^{2+} -calmodulin signalling pathway. For instance, the screening of mutants altered in Ca^{2+} channel activity showing modified sensitivity to Ca^{2+} channel blockers should be explored. Alternatively, various cell lines can be screened for mutants which show under-expression of calmodulin proteins and there is already evidence which suggest that the latter approach may be possible. Braam and Davis (1990) have identified five genes in *Arabidopsis* plants which are rapidly up-regulated in expression when stimulated by rain, wind and touch. The authors have identified three of the genes as calmodulin and calmodulin-related genes. A fourth gene was later found to encode for a cell wall-modifying enzyme, xyloglucan endotransglycosylase (Xu *et al.*, 1995). Since that study, a number of other researchers have identified touch-sensitive genes coding for calmodulin or calmodulin-related proteins in a variety of other plant species (Botella and Arteca, 1994; Galaud *et al.*, 1993; Ito *et al.*, 1995; Oh *et al.*, 1996; Takezawa *et al.*, 1995). It would be worth investigating if naturally-occurring or genetically-engineered mutants containing a defect on the touch-sensitive calmodulin gene would be tolerant to hydrodynamic shear stress. Alternatively, cell lines which have been reported to be shear tolerant (for example, Allan *et al.*, 1988) could be subjected to Northern blot analysis to determine their shear-induced calmodulin expression behaviour compared to

other cell lines within the same species. It is possible that sensitive indicators of shear stress effects in plant cell cultures could be obtained by placing reporter gene sequences or the green fluorescent protein (GFP) under the control of the promoter of the touch-sensitive calmodulin genes. Hydrodynamic shear could also be used as a 'switching mechanism' by placing enzymes required from the production of a desired metabolite under the control of the promoter of the touch-sensitive calmodulin gene. The desired enzymes could then be stimulated under defined shearing conditions.

Ding and Pickard (1993b) demonstrated that the stretch-activated Ca^{2+} channel identified on the plasma-membrane of onion epidermal cells was sensitive to temperature and pH. Although in the present study, the Cl^- channels found in the plasma membrane of the carrot cells did not appear to be sensitive to membrane stretch, temperature and pH could still have a significant impact on the activity of this channel or of other ion channels involved in the signalling pathway for hydrodynamic shear stress. This could account for the influence of culture maintenance conditions on the shear sensitivity of a particular cell line suggested by Meijer (1989). There is also a possibility that mutant cell lines with altered channel sensitivity could be more tolerant of fluctuations in culture conditions. Clearly, this would be a desirable characteristic for industrial plant cell culturing.

8.3.3 Possible mechanism for perception and response to fluid shear by plant cells

The results of this work suggest the main features of a mechanistic model describing how plant cells sense and respond to hydrodynamic shear:

- Shear exposure studies in the viscometer and shake flasks showed that mild levels of hydrodynamic shear can lead to a reduction in biomass accumulation and modifications to an array of biological activities before cell lysis or damage to membrane integrity occurs. This suggests that cells possess structures which allow them to sense sub-lytic levels of fluid shear, amplify the signals and transduce them into biochemical reactions. As the cell wall is the outermost structure of the cell, hydrodynamic shear will impact upon it first. The cell wall consists of a network of tough cellulose microfibrils embedded in a highly cross-linked matrix of polysaccharides (mainly pectins and hemicellulose) and glycoproteins (Alberts *et al.*, 1994a). The cellulose microfibrils are the stress-bearing structures of the cell wall. Hence, most of the hydrodynamic stress exerted on the cell must be borne by the cellulose network. Pont-Lezica *et al.* (1993) proposed that wall-to-membrane linkers (WMLs) transmit the stress from the cell wall to the plasma membrane and presented evidence for the existence of WMLs in onion epidermal cells. The WMLs are then thought to attach to specific transmembrane linkers (TMLs) in the plasma membrane. These TMLs resemble the integrins found in the membranes of animal cells (Ingber, 1991). Integrin-like proteins and other transmembrane linking proteins in plant cells have been reported (Wyatt and Carpita, 1993). The TMLs are, in turn, attached to cytoskeletal elements which pervade throughout the cytoplasm. The cytoskeleton in animal cells is fairly well established and known to consist of microfilaments, intermediate filaments and microtubules (Alberts *et al.*, 1994b). The components of the cytoskeleton in plant cells is still being actively studied, and there is evidence which strongly suggest that similar structures also exist in plant cells (Reuzeau and Pont-Lezica, 1995). The involvement of the extracellular matrix - plasma membrane - cytoskeleton continuum as mechanical transducers is well established in animal cells (Ingber, 1997; Wang *et al.*, 1993) while evidence of a similar mechanism in plant cells (with the extracellular matrix being equivalent to the cell wall) is emerging (Reuzeau and Pont-Lezica, 1995).

- The increase in mitochondrial activity of sheared cells by ruthenium red suggests that an intracellular source of Ca^{2+} might be involved in the signalling pathway induced by fluid shear. The vacuole, which can occupy more than 90% of the cell volume, is a major source of Ca^{2+} (White, 2000). Other internal Ca^{2+} stores include the mitochondria and endoplasmic reticulum (Hepler and Wayne, 1985). The internal Ca^{2+} stores could be activated through the action of the cytoskeleton tugging at the organelle membrane. Alternatively, Ca^{2+} induced Ca^{2+} -release channels have been found on plant vacuoles (White, 2000). Hence, an initial rise in cytosolic Ca^{2+} concentration could induce Ca^{2+} efflux from the vacuole, thus propagating and amplifying the initial signal. The initial Ca^{2+} signal could have originated from stretch-activated channels on the plasma membrane, similar to those reported in onion cells (Ding and Pickard, 1993a). The cytosolic Ca^{2+} concentration is subsequently restored to resting levels through Ca^{2+} ATPases and antiporters (Bush, 1995). In this work, patch clamp recordings found at least two ion channels on the plasma membrane of carrot cells. One of the channels is likely to be a Cl^- channel, while the other remains unidentified. The involvement of Cl^- channels in initiating Ca^{2+} signalling could occur through depolarisation of the cell through Cl^- efflux (Ward *et al.*, 1995). The resting membrane potential of a plant cell is normally negative, ranging from -140 to -200 mV (Ward *et al.*, 1995). Depolarisation refers to a rise in the membrane potential of the cell towards more positive potentials. Cl^- channel-mediated depolarisation can, in turn, trigger the activation of voltage-dependent Ca^{2+} channels that allow Ca^{2+} influx into the cytoplasm. However, we have been unable to detect effects of verapamil (a blocker of voltage-operated Ca^{2+} channels) on the sub-lytic response. Further patch-clamp investigations will be required to deduce the mechanism for Ca^{2+} release.
- The involvement of calmodulin in mediating the biological response of carrot cells to fluid shear is suggested by the reduction in the effect of shear on coupled OUR by the calmodulin inhibitor, W7. A simple pathway for Ca^{2+} -mediated signalling through calmodulin may be as follows: Ca^{2+} enters the cytoplasm in response to a signal (in this case, hydrodynamic stress) where it binds with calmodulin to form a Ca^{2+} -CaM complex. The Ca^{2+} -CaM complex, in turn, binds with different target proteins, thus activating them and resulting in a physiological response. The actual

pathway is likely to be much more complicated, with various feedback mechanisms. For instance, Ca^{2+} concentration is known to show spatial and temporal fluctuations in the cytoplasm which increases its complexity of action (Bush, 1995). The expression of calmodulin in the cytoplasm also varies in response to the stimuli and the binding of Ca^{2+} to calmodulin is modulated by the presence of the target protein (Zielinski, 1998). Zielinski (1998) reviews some of the target proteins that have been shown to be regulated by the Ca^{2+} -CaM complex in plant cells. The list includes a wide variety of enzymes, transport proteins and cytoskeletal elements as well as a plant homolog of the multi-functional CaM-dependent protein kinase found in animal cells. It is worth noting that an important protein kinase, phosphokinase C (PKC), has been implicated as a vital mediator of hydrodynamic shear-induced cytochrome P450IA1 activity in cultured human hepatoma cells (Mufti and Shuler, 1996). Further research in this area will undoubtedly uncover many more important CaM-dependent target proteins.

The main features of the mechanistic model discussed above are illustrated in the schematic shown in Figure 8-32. Further experimentation will be required to test and refine the proposed model.

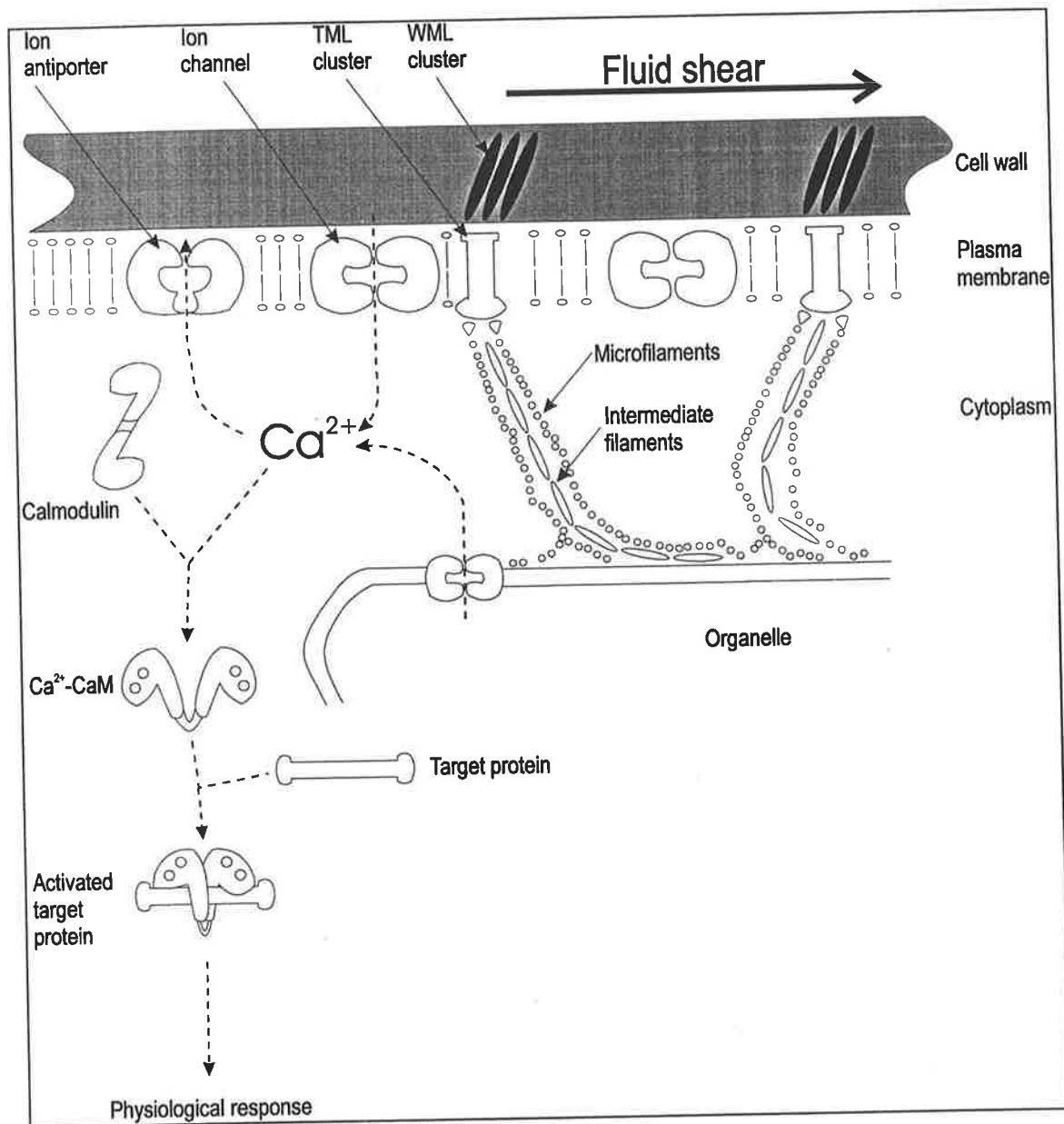


Figure 8-32: Schematic of proposed model for reception and transduction of fluid shear stimuli in plant cells. CaM refers to calmodulin. WML refers to wall-to-membrane linkers. TML refers to transmembrane-linkers.

CHAPTER 9

CONCLUSIONS

The aim of this work was to determine if disruption of the ion-signalling process in plant cells through ion channel blockers and calmodulin inhibitors may alleviate the sub-lytic effects of fluid shear stress in suspension cultured plant cells, since these chemical compounds have previously been shown to alleviate the effects of mechanical and osmotic stress in whole plants.

Preliminary investigations in shake flasks agitated at 100 and 150 rpm found that the higher shaker speed (150 rpm) reduced the growth of *Daucus carota* cultures but had no significant effect on the membrane integrity of the cells compared to the controls (100 rpm). These results demonstrate that mild, sub-lytic levels of fluid shear stresses may reduce the growth of suspension cultured plant cells, without apparent physical damage to the cell membrane.

Existing Couette viscometer designs were found to be unsatisfactory for shear-testing of living biological samples because they could not provide sufficient oxygenation and so a novel Couette viscometer with O₂-permeable walls was designed with the aid of mathematical modelling. Finite element modelling, supported by observations of dissolved oxygen (DO) levels, demonstrated that the DO level in the oxygen-permeable Couette remained above 90% of saturation throughout the shear exposure period (up to 8 h). It also showed that the oxygen-permeable Couette provided better oxygenation of the cell cultures than a conventional Couette of similar gap width. These results suggest that previous work using conventional Couettes may have to be reconsidered in light of the potential oxygen deficiency problem in these devices.

Shear-testing of the carrot cultures in the oxygen-permeable Couette for laminar shear stresses between 6 and 100 N/m² showed that the mitochondrial activity, coupled and uncoupled OUR of the carrot cultures were affected by elevated shear stresses

before significant damage to membrane integrity was observed. The mitochondrial activity, uncoupled OUR and membrane integrity all decreased with increased shear exposure. First-order decay models described the rate of damage of these three biological activities and the rate constants were found to increase with increasing shear stress. On the other hand, coupled OUR was stimulated above control levels by low to moderate shear exposures and only fell below control levels when there was significant damage to the membrane integrity following extended exposures to high shear stresses. The cumulative energy dissipation level at which 90% of the biological activity was retained was found to be 1×10^7 , 9×10^7 and 1.5×10^8 J/m³ for mitochondrial activity, uncoupled OUR and membrane integrity, respectively.

Factorial experiments designed to establish the effects of ion channel blockers and a calmodulin inhibitor on the biological response of suspension cultured carrot cells found that W7 (calmodulin inhibitor) and ruthenium red (intracellular Ca²⁺ channel blocker) had statistically significant effects (5% level) on the coupled OUR and mitochondrial activity of the viscometer-sheared cultures respectively but not on shake flask cultures. Increasing the shear stress in the viscometer from 38 to 100 N/m² resulted in a coupled OUR increase of 40% in the absence of W7, but of only 1% when W7 was present. Addition of ruthenium red increased the mitochondrial activity of viscometer sheared cultures by 29% but had no significant effect on shake flask cultures for exposures of 1 h. However, longer exposures (24 h) of the shake flask cultures to ruthenium red reduced the mitochondrial activity. Taken together, these results suggest that disruption of the ion-signalling pathway with ruthenium red or W7 would lead to an attenuation of certain sub-lytic effects. It also indicates that the signalling pathway for hydrodynamic shear stresses is likely to be mediated by Ca²⁺ and calmodulin. However, it is unclear why W7 and ruthenium red did not have uniform effects on all the biological indicators. Direct addition of these chemical compounds into large-scale plant culture medium is unlikely to be an acceptable solution as the effects of these compounds on other biological functions are still unknown and there is evidence to suggest that extended exposure to some of these compounds is detrimental to certain cellular functions. We recognised early in the work that Ca²⁺ based signalling may not be the only mechanism for transducing a mechanical signal into a biological response. Given the pervading presence of environmental stress in the life of a plant, it would be typical of biological

processes for plant cells to utilise several alternate pathways to respond to an environmental assault.

Patch-clamp investigations carried out on the cultured carrot cells identified at least two ion channels on the plasma membrane. One of the channels is likely to be a Cl^- channel, however, mechanosensitive behaviour could not be detected for this channel. The identity of the other channels could not be determined due to their infrequent appearance in the membrane patches that gave a sufficiently good seal to permit patch-clamp recordings to be made.

Recommendations for further research into the involvement of Ca^{2+} and calmodulin in the shear sensitive response of plant cells have been discussed in the previous chapter. These included shear testing of mutant plant cell lines with altered channel activity or calmodulin expression and quantification of calmodulin expression in response to a range of fluid shear stresses. In addition, different concentrations of the ion channel blockers and calmodulin inhibitor studied in this work could be tested. The effect of other ion-channel blockers and regulatory protein inhibitors as well as other chemical compounds which affect cell-signalling (e.g. cytoskeleton disruptors) should also be investigated for their effects on biological response to fluid shear stress. Further advances in our understanding of the signal transduction pathway in plant cells will be required before we can fully elucidate the mechanism by which these chemical compounds affect the sub-lytic response. The generality of the results from this work should also be extended using different plant cell species, with special emphasis on cell lines that produce industrially important bio-products. Further work using a variety of shear devices, including bioreactors, will be required to examine the sub-lytic response of plant cells in turbulent and mixed shear fields.

The results of this thesis suggest the need and potential benefits of understanding the underlying genetic expression patterns in plant cells in response to hydrodynamic shear stresses. To this end, the completed genomic sequence of the model plant, *Arabidopsis thaliana*, coupled with new molecular genetic techniques, such as DNA microarrays, which allow the study of genome-wide expression patterns of cells exposed to a variety of conditions, would be of immense value.

Early approaches to industrial plant cell culturing have been mainly empirical and based on microbial fermentation technology. These attempts have met with limited success due to several unique features of cultured plant cells, such as their sensitivity to hydrodynamic shear stresses. In this thesis, a novel approach to overcome sub-lytic shear sensitivity in plant cell cultures, based on the disruption of the ion-signalling process within the cell, was investigated and the results appear to be encouraging. In contrast to plant cell systems, industrial mammalian cell culturing has been much more successful, partly because it has benefited considerably from knowledge gained from medical-based research into mammalian cell biology and cell signalling. Similar knowledge for plant cell systems is currently fragmentary but is beginning to emerge. A combination of engineering and biology-based approaches will be required for progress in the field of industrial plant cell culturing. Previous attempts to overcome the shear sensitivity of plant cells have centred on designing low-shear bioreactors for shear sensitive cell cultures. This thesis suggests that, alternatively, it may be possible to engineer robust plant cell lines that would be suited to the high-shear environment of industrial bioreactors. Quantitative studies, such as the one presented in this thesis, which seeks to elucidate the biological mechanism for the cell response to fluid shear stresses will be helpful in this regard.

APPENDIX A

WILD CARROT MEDIUM FORMULATION

Table A-1: Formulation of wild carrot medium

Compound	Mass (g / 1 L of medium)
NH ₄ Cl	0.54
MgSO ₄ .7H ₂ O	0.185
MnSO ₄ .H ₂ O	0.07
KH ₂ PO ₄	0.068
ZnSO ₄ .7H ₂ O	0.04
H ₃ BO ₃	0.024
CaCl ₂ .2H ₂ O	0.225
KI	0.38 x 10 ⁻³
CuSO ₄ .5H ₂ O	0.015 x 10 ⁻³
NaMoO ₄ .2H ₂ O	0.014 x 10 ⁻³
FeNaEDTA	18.25 x 10 ⁻³
KNO ₃	4
Thiamine.HCl	3 x 10 ⁻³
2,4-D	0.5 x 10 ⁻³
Sucrose	20

APPENDIX B

YATE'S ALGORITHM

Table B-1: Yate's algorithm for the Coupled OUR (% control-) data

A = W7	B = Ruthenium red	C = Verapamil	D = NPPB	E = Shear level	Treatment combination	Coupled OUR (% control-)	(I)	(II)	(III)	(IV)	Effect	Estimate of effect (% control-)	Sum of Squares (% control-)
-1	-1	-1	-1	-1	(1)	125	251	522	1046	2075	average	129.7	
1	-1	-1	-1	1	a(e)	126	271	524	1029	-195	a-bcde	-24.4	23.8
-1	1	-1	-1	1	b(e)	165	271	526	-78	44	b-acde	5.5	1.2
1	1	-1	-1	-1	ab	106	254	504	-117	-94	ab-cde	-11.8	5.6
-1	-1	1	-1	1	c(e)	142	282	-59	3	-19	c-abde	-2.4	0.2
1	-1	1	-1	-1	ac	129	243	-19	41	10	ac-bde	1.2	0.1
-1	1	1	-1	-1	bc	130	212	-43	-53	81	bc-ade	10.1	4.1
1	1	1	-1	1	abc(e)	124	292	-74	-42	-31	abc-de	-3.8	0.6
-1	-1	-1	1	1	d(e)	159	1	20	3	-17	d-abce	-2.1	0.2
1	-1	-1	1	-1	ad	123	-60	-17	-22	-39	ad-bce	-4.8	0.9
-1	1	-1	1	-1	bd	125	-13	-39	40	38	bd-ace	4.8	0.9
1	1	-1	1	1	abd(e)	118	-6	80	-31	11	abd-ce	1.4	0.1
-1	-1	1	1	-1	cd	107	-36	-61	-38	-25	cd-abe	-3.1	0.4
1	-1	1	1	1	acd(e)	105	-7	8	119	-71	acd-be	-8.8	3.1
-1	1	1	1	1	bcd(e)	182	-2	29	69	156	bcd-ae	19.6	15.3
1	1	1	1	-1	abcd	110	-72	-71	-99	-168	abcd-e	-21.0	17.6

Table B-1 shows the application for Yate's algorithm to estimate the main effects, interactions and sum of squares for the coupled OUR (% control -). The treatment combinations are written down in the order shown, known as the "standard order". The first half of column (I) is obtained by adding the coupled OUR responses in adjacent pairs. The second half of column (I) is obtained by taking the difference between the second entry in each of the pairs in the coupled OUR response column and the first entry. For example, in column (I), the first entry $251 = 125 + 126$, for the ninth entry $1 = 126 - 125$, and so on.

Column (II) is calculated from column (I) in the same way that column (I) is calculated from the coupled OUR response column. Similarly, column (III) is obtained from column (II). In general, a 2^k design would require k columns. A half-fraction 2^{5-1} factorial design would be analysed by initially considering the data as having been obtained from a full factorial in 4 variables. The actual effects estimated are then identified by multiplying the treatment combinations in the full 2^4 design by the generator of the 2^{5-1} fractional factorial (ie. $I = -ABCDE$). For example, multiplying the treatment combination for the second entry a (for the full 2^4 design) with the generator (of the 2^{5-1} fractional factorial) would yield $-bcde$, following the algebraic rule that a square of a factor equals 1 (ie. $a^2 = 1$). Thus the actual effect being estimated in the second entry is $a-bcde$ since A and $BCDE$ are aliases. The estimate of the effect is obtained by dividing column (IV) by $2^{4-1} = 8$, except for the first row corresponding to the average response, which is divided by $2^4 = 16$. For example, the effect for $a-bcde = -195 / 8 = -24.4$, while the average response is $2075 / 16 = 129.7$. Finally, the sums of squares for the effects are obtained by squaring the entries in column (IV) and dividing by 2^4 . A more detailed description of Yate's algorithm can be found in Montgomery (1991). The effects and interactions for the mitochondrial activity, uncoupled OUR and membrane integrity were calculated in a similar way.

APPENDIX C

STATISTICAL ANALYSIS OF FACTORIAL DESIGN EXPERIMENT RESULTS

Uncoupled OUR

Table C-1 shows the analysis of variance for the uncoupled OUR response for the viscometer-sheared cells. The F-test for W7, NPPB and their two-factor interaction indicates that they are significant at the 5 % level.

Table C-1: Analysis of variance for uncoupled OUR response of sheared cultures. A and D refers to W7 and NPPB respectively, while AD refers to the 'W7 X NPPB' interaction

Source of variation	Sum of squares (% of control -)	Degrees of freedom	Mean square	F-test statistic
A	6.6	1	6.6	11.78
D	5.5	1	5.5	9.90
AD	2.8	1	2.8	4.94
Error	6.7	12	0.6	
Model	14.8			
Total	21.5	15		

Residual analysis for the uncoupled OUR response was presented in the main text (Chapter 8). Table C-2 shows the analysis of variance for the uncoupled OUR response of the Control+ cells. The F-test for W7, NPPB and their two-factor interaction indicates that they are significant at the 5 % level.

Table C-2: Analysis of variance for uncoupled OUR response of Control+ cultures.
A and D refers to W7 and NPPB respectively, while AD refers to the 'W7 X NPPB' interaction

Source of variation	Sum of squares (% control -)	Degrees of freedom	Mean squares	F-test statistic
D	16.7	1	16.7	46.77
AD	4.6	1	4.6	12.88
A	3.3	1	3.3	9.15
Error	4.3	12	0.4	
Total	28.9	15		

Mitochondrial activity

Table C-3 summarises the variance analysis for the mitochondrial activity of viscometer-sheared cells. The F-test for the main effects of W7 and ruthenium red indicates that they are significant at the 5 % level.

Table C-3: Analysis of variance for mitochondrial activity response of sheared cultures. A and B refers to W7 and ruthenium red, respectively.

Source of variation	Sum of squares (% control -)	Degrees of freedom	Mean square	F-test statistic
B	32.8	1	32.8	15.27
A	20.3	1	20.3	9.46
Error	22.2	13	1.9	
Model	58.8			
Total	81.0	15		

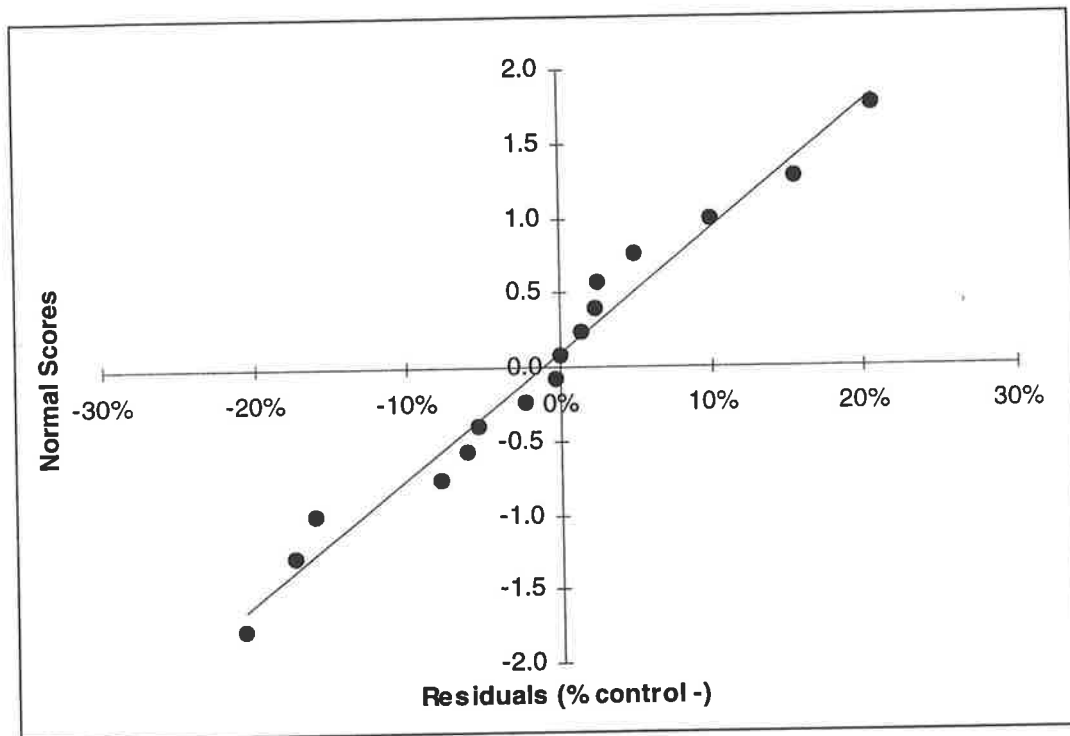


Figure C-1: Normal scores plot for residuals of mitochondrial activity response for sheared cells.

To carry out residual analysis, the following linear regression model to predict the mitochondrial activity was used:

$$\hat{y} = 83.7 + \left(\frac{-22.5}{2} \right) x_a + \left(\frac{28.6}{2} \right) x_b$$

where 83.7% is the average response, and x_a and x_b are the coded variables for W7 and ruthenium red respectively and take on the value of +1 or -1 depending on the column of signs in Table 8-1. A normal scores plot of the residuals between the predicted and actual mitochondrial activity is given in Figure C-1. The residuals appear to be normally distributed, lending support to the proposition that W7 and ruthenium red are the only significant factors.

Table C-4 shows the variance analysis for the mitochondrial activity of Control+ cells. An F-test of the main effect of W7 showed that it was significant at the 5% level.

Table C-4: Analysis of variance for mitochondrial activity response of Control+ cultures.

Source of variation	Sum of squares (% control -)	Degrees of freedom	Mean Square	F-test statistic
W7	36.3	1	36.3	56.81
Error	8.9	14	0.6	
Model	36.3			
Total	45.2	15		

Membrane integrity

Table C-5 summarises the variance analysis for the membrane integrity of the viscometer-sheared cultures. The sum of squares corresponding to the shear factor alone accounts for nearly half of the total variability of the system. An F-test for the main effect of the shear level shows that it is significant at the 5% level.

Table C-5: Analysis of variance for membrane integrity response of sheared cultures.

Source of variation	Sum of squares (% control-)	Degrees of freedom	Mean square	F-test statistic
Shear	3.8	1	3.8	12.53
Error	4.2	14	0.3	
Total	8.0	15		

The model equation used to carry out residual analysis of the membrane integrity data was

$$\hat{y} = 86.2 + \left(\frac{-9.7}{2} \right) x_e$$

where 86.2 is the average response and x_e is the coded variable for shear and takes the value of +1 or -1 depending on the column of signs in Table 8-1. The residuals were

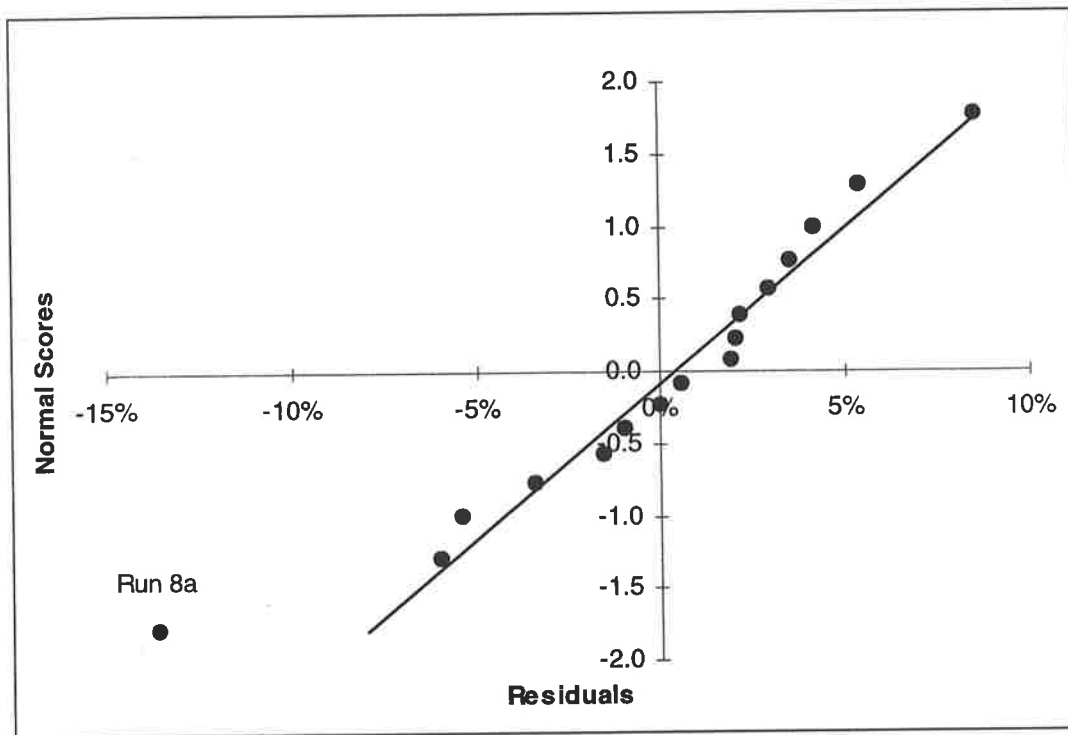


Figure C-2: Normal scores plot for residuals of membrane integrity response for sheared cells.

calculated by taking the difference between the model and actual values, and the normal scores plot for the residuals is shown in Figure C-2.

Apart from run 8a, the remaining residuals appear to lie along a straight line. The response for run 8a could be a maverick value due to experimental error.

APPENDIX D

PUBLICATIONS LIST

- 1) Wong V, Williams DRG, Colby C and Saint DA (2000) "Correlation of O₂ uptake rate and mitochondrial activity in carrot cell cultures exposed to laminar fluid shear", *Biotechnol. Lett.*, **20**(24), 1919-1924.
- 2) Wong V, Williams DRG and Colby C (2000) "Design and testing of novel oxygen-permeable viscometer for studying shear effects on plant cultures", In: European Symposium on Biochemical Engineering Science, Copenhagen, Sept 10-13.
- 3) Wong V, Williams DRG, Colby C, Dunlop EH and Saint DA (2000) "Mild hydrodynamic shear effects on *Daucus carota* cells in shake flask cultures", In: 15th Australasian Biotechnology Conference, Brisbane, July 2-6.

NOMENCLATURE

		<u>Equation</u>	<u>Units</u>
A_a	Cross-sectional area of annular gap	4-11	m^2
A	Matrix defined by Finlayson (1972)	4-19	-
B	Biological activity	7-1	-
c_{O_2}	Dissolved oxygen concentration	4-11	$mmol/m^3$
D_{O_2}	Diffusion coefficient for oxygen in water	4-13	m^2/s
e	Residual between predicted and actual value	6-3	-
E	Cumulative energy dissipated	7-3	J/m^3
E_x	Nernst potential of ion X	8-1	V
F	Faraday constant	8-1	C/mol
G	Torque	4-2	N
H	Henry's law constant	B.C. for 4-14	$mmol/m^3 \cdot Pa$
j	Order of data	6-1	-
k	Power law parameter	4-1	-
k'	Thermal conductivity	4-6	W/m K
k_1	First order rate constant	7-1	1/s
k_{O_2}	Mass transfer coefficient for oxygen on the air-side	B.C. for 4-14	m/s
K_{O_2}	Monod coefficient for oxygen	4-15	$mmol/m^3$
M	Matrix defined by Finlayson (1972)	4-18	-
n	Power law parameter	4-1	-
N	Number of internal collocation points	4-18	-
N_s	Rotation speed	4-10	rps

		<u>Equation</u>	<u>Units</u>
N_{O_2}	Axial mass flux of oxygen	4-11	mmol/m ² ·s
N_t	Total number of data points	6-1	-
p_{O_2}	Partial pressure of oxygen	B.C. for 4-14	Pa
$q_{O_2,max}$	Maximum specific oxygen consumption rate	4-15	mmol/g·s
r	Radial distance	4-2	m
r_1	Radius of inner bob	4-7	m
r_2	Radius of outer bowl	4-7	m
\bar{r}	Geometric mean radius	4-9	m
R	Gas constant	8-1	J/K mol
R_{O_2}	Volumetric generation or consumption of oxygen by plant cells	4-11	mmol/m ³ ·s
Re_{crit}	Critical Reynolds number	4-10	-
T	Temperature	4-21, 8-1	K
t	Shear exposure time	4-11, 7-1	s
U	Tangential velocity	4-10	m/s
\bar{U}_i	Time average velocity of the flow in the i^{th} direction	7-2	m/s
w	Gap width	4-23	m
X	Cell concentration	4-15	g/m ³
x	Distance from outer bowl	4-23	m
x	Coded variable for linear regression model	6-2	-
$[X]$	Concentration of ion X	8-1	mM
\hat{y}	Predicted (regressed) value	6-2	-
z	Charge number	8-1	-

		<u>Equation</u>	<u>Units</u>
Z_j	Normal score	6-1	-
z	Axial position	4-11	m

Greek symbols

β	Linear regression coefficient	6-2	-
$\dot{\gamma}$	Shear rate	4-1	1/s
$\bar{\tau}_{ij}$	Viscous shear stress due to laminar flow	7-2	N/m ²
τ	Shear stress	4-1	N/m ²
Ω	Angular velocity	4-2	rad/s
ρ	Fluid density	4-10,7-2	kg/m ³
ε_v	Viscous energy dissipation rate per unit volume	4-20	J/m ³ s
ε	Viscous energy dissipation rate per unit mass	7-2	J/kg s
η	Porosity of ceramic bowl		-
φ	Volume fraction of cells	7-3	-
μ_{app}	Apparent viscosity	4-10	Pa s
θ	Angular position		rad

Subscripts

- a W7
- b Ruthenium red
- c Verapamil
- d NPPB
- e Shear level
- o Control

REFERENCES

- Alberts, B., Bray, D., Lewis, J., Raff, M., Roberts, K. and Watson, J. D. (1994a) Cell junctions, cell adhesion, and the extracellular matrix. In: *Molecular biology of the cell*. 3rd edn: New York, Garland Publishing Inc. 949-1009.
- Alberts, B., Bray, D., Lewis, J., Raff, M., Roberts, K. and Watson, J. D. (1994b) The Cytoskeleton. In: *Molecular Biology of the Cell*. 3rd edn: New York, Garland Publishing. 787-861.
- Alberts, B., Bray, D., Lewis, J., Raff, M., Roberts, K. and Watson, J. D. (1994c) Energy Conversion: Mitochondria and Chloroplasts. In: *Molecular Biology of the cell*. 3rd edn: New York, Garland Publishing Inc. 653-720.
- Alexandre, J. and Lassalles, J.-P. (1991) Hydrostatic and osmotic pressure activated channel in plant vacuole. *Biophys. J.*, **60**: 1326-1336.
- Allan, E. J., Scragg, A. H. and Pugh, K. J. (1988) Cell suspension culture of *Picrasma quassioides*: the development of a rapidly growing, shear resistant cell line capable of Quassin formation. *Plant Physiol.*, **132**: 176-183.
- Aloi, L. E. and Cherry, R. S. (1996) Cellular response to agitation characterized by energy dissipation at the impeller tip. *Chem. Eng. Sci.*, **51**: (9) 1523-1529.
- Al-Rubeai, M., Singh, R. P., Goldman, M. H. and Emery, A. N. (1995) Death mechanisms of animal cells in conditions of intensive agitation. *Biotech. Bioeng.*, **45**: 463-472.
- Barbier-Brygoo, H., Vinauger, M., Colcombet, J., Ephritikhine, G., Frachisse, J.-M. and Maurel, C. (2000) Anion channels in higher plants: functional characterization, molecular structure and physiological role. *Biochim. Biophys. Acta*, **1465**: 199-218.
- Bailey, J. E. and Ollis, D. F. (1986). *Biochemical Engineering Fundamentals*. 2nd edn, New York, McGraw-Hill.
- Bird, R. B., Stewart, W. E. and Lightfoot, E. N. (1960) The equations of change for isothermal systems. In: *Transport Phenomena*: New York, John Wiley & Sons. 94-95.

- Botella, J. R. and Arteca, R. N. (1994) Differential expression of two calmodulin genes in response to physical and chemical stimuli. *Plant Mol. Biol.*, **24**: 757-766.
- Braam, J. and Davis, R. W. (1990) Rain-, wind- and touch-induced expression of calmodulin and calmodulin-related genes in Arabidopsis. *Cell*, **60**: 357-364.
- Bush, D. S. (1995) Calcium regulation in plant cells and its role in signalling. *Annu. Rev. Plant Physiol. Plant Mol. Biol.*, **46**: 95-122.
- Castañeda, P. and Pérez, L. M. (1996) Calcium ions promote the response of *Citrus limon* against fungal elicitors or wounding. *Phytochemistry*, **42**: (3) 595-598.
- Cazalé, A. C., Rouet-Mayer, M. A., Barbier-Brygoo, H., Mathieu, Y. and Laurière, C. (1998) Oxidative burst and hypoosmotic stress in tobacco cell suspensions. *Plant Physiol.*, **116**: 659-669.
- Charati, S. G. and Stern, S. A. (1998) Diffusion of gases in silicone polymers: Molecular dynamics simulations. *Macromolecules*, **31**: 5529-5535.
- Chen, S. Y. and Huang, S. Y. (2000) Shear stress effects on cell growth and L-Dopa production by suspension culture of *Stizolobium hassjoo* cells in an agitated bioreactor. *Bioprocess Eng.*, **22**: 5-12.
- Cho, M. H. and Wang, S. S. (1990) Practical method for estimating oxygen kinetic and metabolic parameters. *Biotechnol. Prog.*, **6**: 164-167.
- Cormier, F., Brion, F., Do, C. B. and Moresoli, C. (1996) Development of process strategies for anthocyanin-based food colorant production using *Vitis vinifera* cell cultures. In: F. DiCosmo and M. Misawa, (Eds.). *Plant Cell Culture Secondary Metabolism: Toward Industrial Application*: Boca Raton, CRC Press Inc., 167-185.
- Cosgrove, D. J. and Hedrich, R. (1991) Stretch-activated chloride, potassium and calcium channels coexisting in plasma membranes of guard cells of *Vicia faba* L. *Planta*, **186**: 143-153.
- Curtin, M. E. (1983) Harvesting profitable products from plant tissue culture. *Bio/technology*, **1**: 649-657.

- Daniel, C. (1959) Use of half-normal plots in interpreting factorial two level experiments. *Technometrics*, **1**: 311-342.
- Daniel, C. (1976). Applications of Statistics to Industrial Experimentation, New York, Wiley.
- Ding, J. P. and Pickard, B. G. (1993a) Mechanosensory calcium-selective cation channels in epidermal cells. *The Plant Journal*, **3**: (1) 83-110.
- Ding, J. P. and Pickard, B. G. (1993b) Modulation of mechanosensitive calcium-selective cation channels by temperature. *The Plant Journal*, **3**: (5) 713-720.
- Ding, J. P., Badot, P.-M. and Pickard, B. G. (1993) Aluminium and hydrogen ions inhibit a mechanosensory calcium-selective cation channel. *Aust. J. Plant Physiol.*, **20**: 771-778.
- Doran, P. M. (1993) Design of reactors for plant cells and organs. *Adv. Biochem. Eng. Biotechnol.*, **48**: 117-168.
- Dunlop, E. H., Namdev, P. K. and Rosenberg, M. Z. (1994) Effect of fluid shear forces on plant cell suspensions. *Chem. Eng. Sci.*, **49**: (14) 2263-2276.
- Fairley, K. (1990), Currents Through Ion Channels in Plant Cell Membranes, PhD, The University of Sydney.
- Falke, L. C., Edwards, K. L., Pickard, B. G. and Misler, S. (1988) A stretch-activated anion channel in tobacco protoplasts. *FEBS letters*, **237**: 141-144.
- Finlayson, B. A. (1972). The Method of Weighted Residuals and Variational Principles, New York, Academic Press.
- Foust, A., Wenzel, L., Clump, C., Maus, L. and Anderson, L. (1980). Principles of Unit Operations. 2nd edn, New York, John Wiley & Sons.
- Frangos, J. A., McIntire, L. V. and Eskin, S. G. (1988) Shear stress induced stimulation of mammalian cell metabolism. *Biotechnol. Bioeng.*, **32**: 1053-1060.
- Galaud, J.-P., Lareyre, J.-J. and Boyer, N. (1993) Isolation, sequencing and analysis of the expression of Bryonia calmodulin after mechanical perturbation. *Plant Mol. Biol.*, **23**: 839-846.

- Haley, A., Russell, A. J., Wood, N., Allan, A. C., Knight, M., Campbell, A. K. and Trewavas, A. J. (1995) Effects of mechanical signaling on plant cell cytosolic calcium. *Proc. Natl. Acad. Sci. USA*, **92**: (10) 4124-4128.
- Hamill, O. P., Marty, A., Neher, E., Sakmann, B. and Sigworth, F. J. (1981) Improved patch-clamp techniques for high-resolution current recording from cells and cell-free membrane patches. *Pflügers Archiv*, **391**: 85-100.
- Hegarty, P. K., Smart, H. J., Scragg, A. H. and Fowler, M. W. (1986) The aeration of *Catharanthus roseus* L.G. Don suspension cultures in airlift bioreactors: The inhibitory effect at high aeration rates on culture growth. *J. Exp. Bot.*, **37**: (185) 1911-1920.
- Hepler, P. K. and Wayne, R. O. (1985) Calcium and plant development. *Ann. Rev. Plant Physiol.*, **36**: 397-439.
- Hidaka, H., Sasaki, Y., Tanaka, T., Endo, T., Ohno, S., Fujii, Y. and Nagata, T. (1981) N-(6-Aminohexyl)-5-chloro-1-naphthalenesulfonamide, a calmodulin antagonist, inhibits cell proliferation. *Proc. Natl. Acad. Sci. USA*, **78**: (7) 4354-4357.
- Ho, C.-H., Henderson, K. A. and Rorrer, G. L. (1995) Cell damage and oxygen mass transfer during cultivation of *Nicotiana tabacum* in a stirred-tank bioreactor. *Biotechnol. Prog.*, **11**: 140-145.
- Hooker, B. S., Lee, J. M. and An, G. (1989) Response of plant tissue culture to a high shear environment. *Enzyme Microb. Technol.*, **11**: 484-490.
- Hooker, B. S., Lee, J. M. and An, G. (1990) Cultivation of plant cells in a stirred tank: effect of impeller design. *Biotechnol. Bioeng.*, **35**: 296-304.
- Horsch, R. B. and Jones, G. E. (1980) A double filter paper technique for plating cultured plant cells. *In Vitro*, **16**: (2) 103-108.
- Hua, J., Erickson, L. E., Yiin, T.-Y. and Glasgow, L. A. (1993) A review of the effects of shear and interfacial phenomena on cell viability. *Crit. Rev. Biotechnol.*, **13**: (4) 305-328.
- Ingber, D. (1991) Integrins as mechanochemical transducers. *Current Opinion in Cell Biology*, **3**: 841-848.

- Ingber, D. E. (1997) Tensegrity: The architectural basis of cellular mechanotransduction. *Annual review of physiology*, **59**: 575-599.
- Ito, T., Hirano, M., Akama, K., Shimura, Y. and Okada, K. (1995) Touch-inducible genes for calmodulin and a calmodulin-related protein are located in tandem on a chromosome of *Arabidopsis thaliana*. *Plant Cell Physiol.*, **36**: (7) 1369-1373.
- Jaffe, M. J. (1973) Thigmomorphogenesis: The response of plant growth and development to mechanical stimulation. *Planta*, **114**: 143-157.
- Jones, R. S. and Mitchell, C. A. (1989) Calcium ion involvement in growth inhibition of mechanically stressed soybean (*Glycine max*) seedlings. *Physiol. Plant.*, **76**: 598-602.
- Joshi, J. B., Elias, C. B. and Patole, M. S. (1996) Role of hydrodynamic shear in the cultivation of animal, plant and microbial cells. *The Chemical Engineering Journal*, **62**: 121-141.
- Kessell, R. H. J. and Carr, A. H. (1972) The effect of dissolved oxygen concentration on growth and differentiation of carrot (*Daucus carota*) tissue. *J. Exp. Botany*, **23**: (77) 996-1007.
- Keßler, M. and Furusaki, S. (1997) Unsuitability of 2,3,5-Triphenyl-2H-tetrazolium chloride (TTC) as a viability assay for plant cells in suspension. *J. Chem. Eng. Jap.*, **30**: (4) 718-723.
- Keßler, M., Bye, Ø. and Furusaki, S. (1997a) Loss of viability correlates with altered acid phosphatase activity in suspended strawberry cell fractions after excessive agitation. *Biotechnol. Lett.*, **19**: (6) 545-548.
- Keßler, M., ten Hoopen, H. J. G., Heijnen, J. J. and Furusaki, S. (1997b) O₂ uptake rate measurements as a novel tool to study shear effects on suspended strawberry cells. *Biotechnol. Tech.*, **11**: (7) 507-510.
- Kieran, P. M., MacLoughlin, P. F. and Malone, D. M. (1997) Plant cell suspension cultures: some engineering considerations. *J. Biotech.*, **59**: 39-52.
- Kieran, P. M., Malone, D. M. and MacLoughlin, P. F. (2000) Effects of hydrodynamic and interfacial forces on plant cell suspension systems. *Adv. Biochem. Eng. Biotechnol.*, **67**: 139-177.

- Kieran, P. M., O'Donnell, H. J., Malone, D. M. and MacLoughlin, P. F. (1995) Fluid shear effects on suspension cultures of *Morinda citrifolia*. *Biotechnol. Bioeng.*, **45**: 415-425.
- Knight, M. R., Smith, S. N. and Trewavas, A. J. (1992) Wind-induced plant motion immediately increases cytosolic calcium. *Proc. Natl. Acad. Sci. USA*, **89**: 4967-4971.
- Leckie, F., Scragg, A. H. and Cliffe, K. R. (1991) Effect of bioreactor design and agitator speed on the growth and alkaloid accumulation by cultures of *Catharanthus roseus*. *Enzyme Microb. Technol.*, **13**: 296-305.
- Leckie, F., Scraggs, A. H. and Cliffe, K. R. (1991) Effect of impeller design and speed on the large-scale cultivation of suspension cultures of *Catharanthus roseus*. *Enzyme Microb. Technol.*, **13**: 801-810.
- Legué, V., Blancaflor, E., Wymer, C., Perbal, G., Fantin, D. and Gilroy, S. (1997) Cytoplasmic free Ca^{2+} in *Arabidopsis* roots changes in response to touch but not gravity. *Plant Physiol.*, **114**: (3) 789-800.
- Leifert, C., Camotta, H. and Waites, W. M. (1992) Effect of combinations of antibiotics on micropropagated *Clematis Delphinium*, *Hosta*, *Iris* and *Photinia*. *Plant Cell Tiss. Org. Cult.*, **29**: 153-160.
- Low, P. S. and Merida, J. R. (1996) The oxidative burst in plant defense: Function and signal transduction. *Physiologia plantarum*, **96**: 533-542.
- Lynch, T. M. and Lintilhac, P. M. (1997) Mechanical signals in plant development: A new method for single cell studies. *Dev. Biol.*, **181**: 246-256.
- MacLoughlin, P. F., Malone, D. M., Murtagh, J. T. and Kieran, P. M. (1998) The effects of turbulent jet flows on plant cell suspension cultures. *Biotechnol. Bioeng.*, **58**: (6) 595-604.
- Mandels, M. (1972) The culture of plant cells. *Adv. Biochem. Eng.*, **2**: 201-215.
- Markx, G. H., ten Hoopen, H. J. G., Meijer, J. J. and Vinke, K. L. (1991) Dielectric spectroscopy as a novel and convenient tool for the study of the shear sensitivity of plant cells in suspension culture. *J. Biotech.*, **19**: 145-158.

- McCabe, P. F., Levine, A., Meijer, P.-J., Tapon, N. A. and Pennell, R. I. (1997) A programmed cell death pathway activated in carrot cells cultured at low cell density. *The Plant Journal*, **12**: (2) 267-280.
- Meijer, J. (1989), Effects of hydrodynamic and chemical/osmotic stress on plant cells in a stirred bioreactor, PhD, Delft University of Technology.
- Meijer, J. J., ten Hoopen, H. J. G., Luyben, K. C. A. M. and Libbenga, K. R. (1993) Effects of hydrodynamic stress on cultured plant cells: A literature survey. *Enzyme Microb. Technol.*, **15**: 234-238.
- Meijer, J. J., ten Hoopen, H. J. G., van Gameren, Y. M., Luyben, K. C. A. M. and Libbenga, K. R. (1994) Effects of hydrodynamic stress on the growth of plant cells in batch and continuous culture. *Enzyme Microb. Technol.*, **16**: 467-477.
- Merchuk, J. C. (1991) Shear effects on suspended cells. *Adv. Biochem. Eng. Biotechnol.*, **44**: 65-95.
- Millward, H. R., Bellhouse, B. J. and Sobey, I. J. (1996) The vortex wave membrane bioreactor: hydrodynamics and mass transfer. *Chem. Eng. J. Biochem. Eng. J.*, **62**: 175-181.
- Millward, H. R., Bellhouse, B. J., Nicholson, A. M., Beeton, S., Jenkins, N. and Knowles, C. J. (1994) Mammalian cell damage in a novel membrane bioreactor. *Biotechnol. Bioeng.*, **43**: 899-906.
- Mitchell, C. A. (1996) Recent advances in plant response to mechanical stress: theory and application. *HortScience*, **31**: (1) 31-35.
- Montgomery, D. C. (1991). Design and Analysis of Experiments. 3rd edn, New York, John Wiley & Sons.
- Mufti, N. A. and Shuler, M. L. (1995) Induction of cytochrome P-450IA1 activity in response to sublethal stresses in microcarrier-attached Hep G2 cells. *Biotechnol. Prog.*, **11**: 659-663.
- Mufti, N. A. and Shuler, M. L. (1996) Possible role of Arachidonic Acid in stress-induced cytochrome P450IA1 activity. *Biotechnol. Prog.*, **12**: 847-854.

- Mufti, N. A., Bleckwenn, N. A., Babish, J. G. and Shuler, M. L. (1995) Possible involvement of the Ah receptor in the induction of cytochrome P-450IA1 under conditions of hydrodynamic shear in microcarrier-attached hepatoma cell lines. *Biochem. Biophys. Res. Commun.*, **208**: (1) 144-152.
- Namdev, P. K. and Dunlop, E. H. (1995) Shear sensitivity of plant cells in suspensions: Present and future. *Appl. Biochem. Biotechnol.*, **54**: 109-131.
- Nollert, M. U., Diamond, S. L. and McIntire, L. V. (1991) Hydrodynamic shear stress and mass transport modulation of endothelial cell metabolism. *Biotechnol. Bioeng.*, **38**: 588-602.
- Oh, S.-A., Kwak, J. M., Kwun, I. L. and Nam, H. G. (1996) Rapid and transient induction of calmodulin-encoding gene(s) of *Brassica napus* by touch stimulus. *Plant Cell Rep.*, **15**: 586-590.
- Pan, Z.-W., Wang, H.-Q. and Zhong, J.-J. (2000) Scale-up study on suspension cultures of *Taxus chinensis* cells for production of taxane diterpene. *Enzyme Microb. Tech.*, **27**: 714-723.
- Papoutsakis, E. T. (1991) Fluid-mechanical damage of animal cells in bioreactors. *Trends Biotechnol.*, **9**: 427-437.
- Payne, G. F., Shuler, M. L. and Brodelius, P. (1987) Large scale plant cell culture. In: B. K. Lydersen, (Ed.). *Large Scale Cell Culture Technology*: Munich, Hanser Publishers. 195-229.
- Payne, G., Bringi, V., Prince, C. and Shuler, M. L. (1991) The quest for commercial production of chemicals from plant cell culture. In: *Plant cell and tissue culture in liquid systems*: Munich, Hanser Publishers. 1-10.
- Pepin, M. F., Archambault, J., Chavarie, C. and Cormier, F. (1995) Growth kinetics of *Vitis vinifera* cell suspension cultures: 1. Shake flask cultures. *Biotechnol. Bioeng.*, **47**: 131-138.
- Pont-Lezica, R. F., McNally, J. G. and Pickard, B. G. (1993) Wall-to-membrane linkers in onion epidermis: some hypotheses. *Plant, Cell and Environment*, **16**: 111-123.

- Prokop, A. and Bajpai, R. K. (1992) The sensitivity of biocatalysts to hydrodynamic shear stress. *Adv. Appl. Microb.*, **37**: 165-232.
- Reuzeau, C. and Pont-Lezica, R. F. (1995) Comparing plant and animal extracellular matrix-cytoskeleton connections-are they alike? *Protoplasma*, **186**: 113-121.
- Reuzeau, C., McNally, J. G. and Pickard, B. G. (1997) The endomembrane sheath: A key structure for understanding the plant cell? *Protoplasma*, **200**: 1-9.
- Rodriguez-Monroy, M. and Galindo, E. (1999) Broth rheology, growth and metabolite production of *Beta vulgaris* suspension culture: A comparative study between cultures grown in shake flasks and in a stirred tank. *Enzyme Microb. Technol.*, **24**: 687-693.
- Rosenberg, M. Z. (1989), The hydrodynamic shear sensitivity of suspension cultured plant cells, PhD, Washington University.
- Sarma, K. S., Evans, N. E. and Selby, C. (1995) Effect of carbenicillin and cefotaxime on somatic embryogenesis of Sitka spruce (*Picea sitchensis* (Bong.) Carr.). *J. Exp. Bot.*, **46**: (292) 1779-1781.
- Schreck, S., Dornenburg, H. and Knorr, D. (1996) Evaluation of hydrogen peroxide production in tomato (*Lycopersicon esculentum*) suspension cultures as a stress reaction to high pressure treatment. *Food Biotechnology*, **10**: (2) 163-171.
- Schroeder, J. I. and Thuleau, P. (1991) Ca^{2+} channels in higher plant cells. *The Plant Cell*, **3**: 555-559.
- Schroeder, J. I., Schmidt, C. and Sheaffer, J. (1993) Identification of high-affinity slow anion channel blockers and evidence for stomatal regulation by slow anion channels in guard cells. *The Plant Cell*, **5**: 1831-1841.
- Scragg, A. H. (1995) The problems associated with high biomass levels in plant cell suspensions. *Plant Cell Tissue Organ Cult.*, **43**: 163-170.
- Scragg, A. H., Allan, E. J. and Leckie, F. (1988) Effect of shear on the viability of plant cell suspensions. *Enzyme Microb. Technol.*, **10**: 361-367.

- Singh, G. and Curtis, W. R. (1994) Reactor design for plant cell suspension culture. In: P. D. Shargool and T. T. Ngo, (Eds.). *Biotechnological Applications of Plant Cultures*: Boca Raton, CRC. 151-183.
- Snedden, W. A., Tzahi, A., Fromm, H. and Shelp, B. J. (1995) Calcium/Calmodulin activation of soybean glutamate decarboxylase. *Plant Physiol.*, **108**: 543-549.
- Steinbrenner, B., Schroeder, R., Knoop, B. and Beiderbeck, R. (1989) Viability factors in plant cell suspension cultures - A novel bioassay. *J. Plant Physiol.*, **134**: 582-585.
- Steward, N., Martin, R., Engasser, J. M. and Goergen, J. L. (1999) Determination of growth and lysis kinetics in plant cell suspension cultures from the measurement of esterase release. *Biotechnol. Bioeng.*, **66**: (2) 114-120.
- Stroud, A. H. and Secrest, D. (1966). *Gaussian Quadrature Formulas*, New Jersey, Prentice-Hall Inc.
- Sun, X. and Linden, J. C. (1999) Shear stress effects on plant cell suspension cultures in a rotating wall vessel bioreactor. *J. Ind. Microbiol. Biotechnol.*, **22**: 44-47.
- Takahashi, K., Isobe, M., Knight, M. R., Trewavas, A. J. and Muto, S. (1997) Hypoosmotic shock induces increases in cytosolic Ca^{2+} in tobacco suspension-culture cells. *Plant Physiol.*, **113**: 587-594.
- Takeda, T., Kitagawa, T., Takeuchi, Y., Seki, M. and Furusaki, S. (1998) Metabolic responses of plant cell culture to hydrodynamic stress. *Can. J. Chem. Eng.*, **76**: 267-275.
- Takeda, T., Seki, M. and Furusaki, S. (1994) Hydrodynamic damage of cultured cells of *Carthamus tinctorius* in a stirred tank reactor. *J. Chem. Eng. Jap.*, **27**: (4) 466-471.
- Takezawa, D., Lui, Z. H., An, G. and Poovaiah, B. W. (1995) Calmodulin gene family in potato: developmental and touch-induced expression of the mRNA encoding a novel isoform. *Plant Mol. Biol.*, **27**: 693-703.
- Tanaka, H., Semba, H., Jitsufuchi, T. and Harada, H. (1988) The effect of physical stress on plant cells in suspension cultures. *Biotechnol. Lett.*, **10**: (7) 485-490.

- Tate, J. L. and Payne, G. F. (1991) Plant cell growth under different levels of oxygen and carbon dioxide. *Plant Cell Reports*, **10**: 22-25.
- Taylor, G. I. (1936) Fluid friction between rotating cylinders I - Torque measurements. *Proc. Roy. Soc. A*, **157**: 546-564.
- Telewski, F. W. and Jaffe, M. J. (1986) Thigmomorphogenesis: field and laboratory studies of *Abies fraseri* in response to wind or mechanical perturbation. *Physiol. Plant.*, **66**: 211-218.
- Terry, B. R., Tyerman, S. D. and Findlay, G. P. (1991) Ion channels in the plasma membrane of *Amaranthus* protoplasts: one cation and one anion channel dominate the conductance. *J. Membrane Biol.*, **121**: 223-236.
- Tey, B. T., Singh, R. P., Piredda, L., Piacentini, M. and Al-Rubeai, M. (2000) Bcl-2 mediated suppression of apoptosis in myeloma NS0 cultures. *J. Biotechnol.*, **79**: (2) 147-159.
- Thomas, C. R., Nienow, A. W. and Dunnill, P. (1979) Action of shear on enzymes: Studies with alcohol dehydrogenase. *Biotechnol. Bioeng.*, **21**: 2263-2278.
- Thuleau, P., Graziana, A., Ranjeva, R. and Schroeder, J. I. (1993) Solubilized proteins from carrot (*Daucus carota* L.) membranes bind calcium channel blockers and form calcium-permeable ion channels. *Proc. Natl. Acad. Sci. USA*, **90**: 765-769.
- Towill, L. E. and Mazur, P. (1975) Studies on the reduction of 2,3,5-triphenyltetrazolium chloride as a viability assay for plant tissue cultures. *Can. J. Bot.*, **53**: 1097-1102.
- Tran-Son-Tay, R. (1993) Techniques for studying the effects of physical forces on mammalian cells and measuring cell mechanical properties. In: J. A. Frangos, (Ed.). *Physical Forces and the Mammalian Cell*: California, Academic Press. 1-59.
- Uritani, I. and Asahi, T. (1980) Respiration and related metabolic activity in wounded and infected tissues. In: D. D. Davies, (Ed.). *The Biochemistry of Plants: A Comprehensive Treatise*, **2**: New York, Academic Press. 463-485.
- Vanlerberghe, G. C. and McIntosh, L. (1997) Alternative oxidase: From gene to function. *Annu. Rev. Plant Physiol. Plant Mol. Biol.*, **48**: 703-734.

- Wagner, F. and Vogelmann, H. (1977) Cultivation of plant tissue cultures in bioreactors and formation of secondary metabolites. In: W. Barz, M. H. Reinhard and M. H. Zenk, (Eds.). *Plant Tissue Culture and It's Biotechnological Application*: Berlin, Springer-Verlag. 245-255.
- Wallace, W., Secor, J. and Schrader, L. E. (1984) Rapid accumulation of γ -aminobutyric acid and alanine in soybean leaves in response to an abrupt transfer to lower temperature, darkness, or mechanical manipulation. *Plant Physiol.*, **75**: 170-175.
- Wang, N., Butler, J. P. and Ingber, D. E. (1993) Mechanotransduction across the cell surface and through the cytoskeleton. *Science*, **260**: 1124-1127.
- Ward, J. M., Pei, Z. M. and Schroeder, J. I. (1995) Roles of ion channels in initiation of signal transduction in higher plants. *The Plant Cell*, **7**: 833-844.
- White, P. J. (2000) Calcium channels in higher plants. *Biochim. Biophys. Acta*, **1465**: 171-189.
- Whorlow, R. W. (1992) Rotational viscometer. In: *Rheological Techniques*. 2nd edn: England, Ellis Horwood. 101-183.
- Widholm, J. M. (1972) The use of fluorescein diacetate and phenosafranine for determining viability of cultured plant cells. *Stain Technol.*, **47**: 189-194.
- Wilkinson, W. L. (1960). *Non-Newtonian fluids: Fluid Mechanics, Mixing and Heat Transfer*, London, Pergamon Press.
- Wongsamuth, R. and Doran, P. M. (1994) Foaming and cell flotation in suspended plant cell cultures and the effect of chemical antifoams. *Biotechnol. Bioeng.*, **44**: 481-488.
- Wongsamuth, R. and Doran, P. M. (1997) The filtration properties of *Atropa belladonna* plant cell suspensions; effects of hydrodynamic shear and elevated carbon dioxide levels on culture and filtration parameters. *J. Chem. Tech. Biotechnol.*, **69**: 15-26.
- Wudtke, M. and Schugerl, K. (1987) Investigations of the influence of physical environment on the cultivation of animal cells. In: *European Society of Animal Cell Technology, the 8th meeting*, Tiberias, Israel, Butterworth & Co.: 297-315.

- Wyatt, S. E. and Carpita, N. C. (1993) The plant cytoskeleton-cell wall continuum. *Trends in cell Biology*, **3**: 413-417.
- Xu, W., Purugganan, M. M., Polisensky, D. H., Antosiewicz, D. M., Fry, S. C. and Braam, J. (1995) Arabidopsis *TCH4*, regulated by hormones and the environment, encodes a xyloglucan endotransglycosylase. *The Plant Cell*, **7**: 1555-1567.
- Yahraus, T., Chandra, S., Legendre, L. and Low, P. S. (1995) Evidence for a mechanically induced oxidative burst. *Plant Physiol.*, **109**: 1259-1266.
- Yanpaisan, W., King, N. J. C. and Doran, P. M. (1998) Analysis of cell cycle activity and population dynamics in heterogeneous plant cell suspensions using flow cytometry. *Biotechnol. Bioeng.*, **58**: (5) 515-528.
- Yates, F. (1937). Design and Analysis of Factorial Experiments, London, Imperial Bureau of Soil Sciences.
- Zhang, Q., Wiskich, J. T. and Soole, K. L. (1999) Respiratory activities in chloramphenicol-treated tobacco cells. *Physiol. Plant.*, **105**: 224-232.
- Zhong, J. J., Fujiyama, K., Seki, T. and Yoshida, T. (1994) A quantitative analysis of shear effects on cells suspension and cell culture of *Perilla frutescens* in bioreactors. *Biotechnol. Bioeng.*, **44**: 649-654.
- Zhong, J.-J., Chen, F. and Hu, W.-W. (2000) High density cultivation of *Panax notoginseng* cells in stirred bioreactors for the production of ginseng biomass and ginseng saponin. *Process Biochem.*, **35**: 491-496.
- Zielinski, R. E. (1998) Calmodulin and calmodulin-binding proteins in plants. *Annu. Rev. Plant Physiol. Plant Mol. Biol.*, **49**: 697-725.